Contract DSS EMR OST83-00212

STEAM INJECTION EXPERIMENTS IN A SCALED PHYSICAL MODEL

FINAL REPORT

(Oct. 1, 1983 - June 30, 1985)

Principal Investigator: S.M. Farouq Ali

University of Alberta
Edmonton, Alberta
T6G 2G6
(Phone:(403)432-3453)

Research Assistants: M. Proctor
M. Kasraie

(Phone:(403)432-4182)

239 pp

MAR 3 1986
MICROMEDIA

ABSTRACT

This research was directed toward a study of steam injection processes and was comprised of experiments conducted in a scaled physical model, under a wide variety of conditions.

A large part of the work was devoted to the design and construction of the scaled model apparatus used to conduct the steam injection experiments. The apparatus was designed to represent one-quarter of an eight hectare (twenty acre) five-spot pattern and was scaled based upon low pressure scaling criteria.

A number of steamflood experiments were carried out to show the use of the apparatus and the efficacy of the processes under investigation. The main target of the experimental studies was the Aberfeldy heavy oil reservoir of the Lloydminster area. This reservoir is characterized by a viscous oil (1275 mPa-s at reservoir temperature) and thin pay. Bottom water is present in parts of the reservoir. To examine the recovery potential of this reservoir, several types of runs were conducted, including continuous steamfloods in a homogeneous pack, a continuous steamflood in a bottom water pack, slug runs on a homogeneous pack, and a steamflood following a waterflood.

The cold water slug runs on the Aberfeldy model, which entailed the injection of a small volume of steam followed by the continuous injection of cold water, gave favorable results, generally better than the continuous steamflood

runs. Judging from these experiments, the steam slug process would appear to be a viable recovery technique for the Aberfeldy reservoir.

As expected, bottom water had a very detrimental effect on the efficiency of a conventional steamflood, with oil recovery in one run being one-tenth of the recovery experienced in the continuous steamflood experiments. Conducting a steamflood in an Aberfeldy model without bottom water, following a waterflood, produced a low incremental recovery of 5.9% of the original oil in place (8.1% of the waterflood residual oil saturation).

The possibility of steamflooding a conventional oil reservoir to improve the ultimate oil recovery, appears to warrant further investigation. Experiments conducted on a model of a light oil prototype yielded the highest oil recovery of all experiments carried out in this research. Recoveries of 36% of the original oil in place were predicted for a prototype thickness of eleven meters. Future experiments designed to examine the steamflood recovery response from a conventional oil reservoir should include an examination of the effect of oil saturation, since reservoirs of this type will normally be waterflooded first.

Work on a modified steam simulator was initiated. The simulator has a number of new features such as foam flow, and will be used for bottom water steamflood simulations.

FOREWARD

This final report covers the period of Oct. 1, 1983 - June 30, 1985 of the subject project. During this period, a low pressure, scaled steam injection model was designed, built, and operated, and work was initiated on a numerical simulator. Two papers were published, and a third one presented during this period, which are included in Appendix C. The work completed to date, both experimental and theoretical, has pointed the way for Phase II of this project. The emphasis will be on the development of marginal heavy oil reservoirs, such as those of Alberta and Saskatchewan, as well as light oil reservoirs, such as those of Ontario and British Columbia.

The invaluable technical assistance provided by Mr. D.K. Faurschou, and of late by Dr. Albert George is gratefully acknowledged. The kindness and understanding shown by Mr. Terry Patrick and Mr. Pat Monnelly is greatly appreciated. Thanks are also expressed to Dr. W.T. Strickland, Jr., of Husky Oil Operations Ltd., for providing information on the Aberfeldy reservoir, which served as the prototype.

Table of Contents

Chapter Page

1. INTRODUCTION 1

2. OBJECTIVES OF THIS STUDY 3

3. LITERATURE REVIEW 5

    3.1 Experimental Approaches to Steam Injection 5

        3.1.1 Unscaled Physical Models 6

        3.1.2 Scaled or Partially Scaled Physical Models 12

            3.1.2.1 High Pressure Scaled Model Studies 13

            3.1.2.2 Low Pressure Scaled Model Studies 17

            3.1.2.3 High Pressure vs. Low Pressure Scaled Models 21

        3.1.3 Studies of Thin, Bottom Water Reservoirs .23

    3.2 Agreement Between Experimental and Field Results 24

    3.3 Role of Numerical Simulation 25

4. SCALING THE STEAM DRIVE PROCESS FOR A VACUUM MODEL ..27

    4.1 Vacuum Model Scaling Parameters 27

    4.2 Designing the Aberfeldy Scaled Model 31

        4.2.1 Prototype Data 32

        4.2.2 Selection of Length Scale 33

        4.2.3 Selection of Model Production Pressure ...34

        4.2.4 Calculation of Model Differential Pressure Scaling 34

        4.2.5 Determination of Model Temperature Scaling 35

        4.2.6 Calculation of Steam Quality Required 37

        4.2.7 Calculation of Model Viscosity 38

        4.2.8 Calculation of Time Scale 38

4.2.9 Calculation of Model Permeability 39
4.2.10 Calculation of Injection and Production Rate Scales 40
4.2.11 Calculation of Water Proportion for Steam Quality 40
4.2.12 Well Scaling 43
5. EXPERIMENTAL APPARATUS AND PROCEDURE 46
5.1 Physical Model 46
5.1.1 Model Wells 49
5.1.2 Porous Media 49
5.1.3 Steam Injection System 50
5.1.4 Model Cart, Cold Storage 53
5.1.5 Data Acquisition System 55
5.1.6 Collection System 56
5.1.7 Model Fluids 59
5.1.7.1 Oil for the Aberfeldy Model 59
5.1.7.2 Materials for Heavy Oil and Light Oil Runs 61
5.2 Model Packing and Saturation 61
5.2.1 Model Packing Procedure 61
5.2.2 Model Saturation 66
5.2.2.1 Preparing the Bottom Water Model .67
5.3 Conducting the Experiments 68
5.4 Data Analysis 70
6. EXPERIMENTAL RESULTS AND DISCUSSION 71
6.1 Model Design and Operation 73
6.1.1 Operational Difficulties 76
6.2 Base Steamflood 77
6.3 Continuous Steamfloods on Aberfeldy Model 78

6.4 Steamflood Following a Waterflood 82
6.5 Steamflooding a Highly Viscous Oil 84
6.6 Light Oil Steamfloods 84
6.7 Bottom Water Steamflood 86
6.8 Steam Slug Runs 88
6.9 Hot Water Slug Run 91
7. NUMERICAL SIMULATIONS 93
7.1 Objectives 93
7.2 Model Assumptions 93
7.3 Derivation of Mass Balance Equations 94
7.3.1 Mass Balance on i 95
7.3.2 Mass Balance for Water 96
7.3.3 Other Equations 96
7.3.3.1 Surfactant 96
7.3.3.2 Nitrogen 97
7.3.3.3 Oil 97
7.3.3.4 Solution Gas 97
7.3.4 Energy Balance 97
7.4 Formulation of the Problem 99
7.4.1 Equations 99
7.4.2 Solution Method 99
7.4.3 Current Status 100
8. CONCLUSIONS 102
NOMENCLATURE 104
REFERENCES 106
APPENDIX A: Tables of Experimental Data for All Runs 111
APPENDIX B: Experimental Results Presented in Graphical Form 124

APPENDIX C: Papers Presented.

1. "Application of Thermal Recovery Techniques to Marginal Reservoirs", Proceedings of the 3rd European Meeting on Improved Oil Recovery, Rome, Italy (April 16-18, 1985).

2. "Heavy Oil Recovery in the Presence of Bottom Water", Paper presented at the 35th Annual Technical Meeting of the Petroleum Society of CIM, held in Calgary, Alberta (June 10-11, 1984).

3. SPE 13039: "Effect of Bottom Water and Gas Cap on Steam Injection Response", Presented at the 59th Annual Fall Meeting of SPE, Houston, Texas (Sept. 16-19, 1984).

List of Tables

Table Page

1 Scaling Parameters for Steam Processes 28

2 Steam Enthalpy at Various Model Pressures 42

3 Summary of Scaling Calculations for Aberfeldy Model 44

4 Prototype and Model Scaling Values 45

5 Temperature vs. Oil Viscosity for Aberfeldy Prototype Oil and Model Oil 60

6 Temperature vs. Oil Viscosity for the Heavy Oil 62

7 Temperature vs. Oil Viscosity for the Light Oil 62

8 Initial Conditions for Experiments 72

9 Experimental Data for Run #5 112

10 Experimental Data for Run #6 112

11 Experimental Data for Run #7 113

12 Experimental Data for Run #9 115

13 Experimental Data for Run #10 116

14 Experimental Data for Run #12 117

15 Experimental Data for Run #13 118

16 Experimental Data for Run #15 119

17 Experimental Data for Run #17 120

18 Experimental Data for Run #18 121

19 Experimental Data for Run #19 122

20 Experimental Data for Run #22 123

List of Figures

Figure Page

1 Schematic Diagram of Apparatus 47

2 Diagram of Model Illustrating Thermocouple Positions 51

3 Produced Fluids Collection System 57

4 Temperature-Viscosity Profile for Ideal and Actual Model Oil 63

5 Model Packing Device 65

6 Run 4, Temperature Profile at 0.25 PV Steam Injected 125

7 Run 4, Temperature Profile at 0.50 PV Steam Injected 126

8 Run 4, Temperature Profile at 0.75 PV Steam Injected 127

9 Run 4, Temperature Profile at 1.00 PV Steam Injected 128

10 Run 6, Cumulative Recovery vs. PV Injected. 129

11 Run 6, Temperature Profile at 0.25 PV Steam Injected 130

12 Run 6, Temperature Profile at 0.50 PV Steam Injected 131

13 Run 6, Temperature Profile at 0.75 PV Steam Injected 132

14 Run 6, Temperature Profile at 1.00 PV Steam Injected 133

15 Run 6, Instantaneous Oil and Water Production vs. Cumulative Injection. 134

16 Run 7C, Temperature Profile at 0.25 PV Steam Injected 135

17 Run 7C, Temperature Profile at 0.50 PV Steam Injected 136

18 Run 7C, Temperature Profile at 0.75 PV Steam Injected 137

Figure Page

19 Run 7C, Temperature Profile at 1.00 PV Steam Injected 138

20 Run 7, Cumulative Recovery vs. PV Injected. 139

21 Run 7, Instantaneous Oil/Steam Ratio vs. Cumulative Oil Production. 140

22 Run 7, Instantaneous Oil and Water Production vs. Cumulative Injection. 141

23 Run 10, Temperature Profile at 0.25 PV Steam Injected 142

24 Run 10, Temperature Profile at 0.50 PV Steam Injected 143

25 Run 10, Temperature Profile at 0.75 PV Steam Injected 144

26 Run 10, Temperature Profile at 1.00 PV Steam Injected 145

27 Run 10, Instantaneous Oil/Steam Ratio vs. Cumulative Oil Production. 146

28 Run 10, Cumulative Recovery vs. Pore Volumes Steam Injected. 147

29 Run 10, Instantaneous Oil and Water Production vs. Cumulative Injection. 148

30 Comparison of the Recovery Response of Run 6 and Run 10. 149

31 Run 9, Temperature Profile at 0.50 PV Steam Injected 150

32 Run 9, Temperature Profile at 1.00 PV Steam Injected 151

33 Run 12, Temperature Profile at 0.25 PV Steam Injected 152

34 Run 12, Temperature Profile at 0.50 PV Steam Injected 153

35 Run 12, Temperature Profile at 0.75 PV Steam Injected 154

36 Run 12, Temperature Profile at 1.00 PV Steam Injected 155

Figure Page

37 Run 12, Instantaneous Oil and Water Production vs. Cumulative Injection. 156

38 Run 12, Instantaneous Oil-Steam Ratio vs. Cumulative Oil Production. 157

39 Run 13, Temperature Profile at 0.25 PV Steam Injected 158

40 Run 13, Temperature Profile at 0.50 PV Steam Injected 159

41 Run 13, Temperature Profile at 0.75 PV Steam Injected 160

42 Run 13, Temperature Profile at 1.00 PV Steam Injected 161

43 Run 13, Instantaneous Oil-Steam Ratio vs. Cumulative Oil Production. 162

44 Run 13, Instantaneous Oil and Water Production vs. Cumulative Injection. 163

45 Comparison of the Steamflood Recovery Response of Run 12 and Run 13. 164

46 Run 15, Temperature Profile at 0.25 PV Steam Injected 165

47 Run 15, Temperature Profile at 0.50 PV Steam Injected 166

48 Run 15, Temperature Profile at 0.75 PV Steam Injected 167

49 Run 15, Temperature Profile at 1.00 PV Steam Injected 168

50 Run 15, Cumulative Oil Recovery vs. PV Steam Injected. 169

51 Run 15, Instantaneous Oil-Steam Ratio vs. Cumulative Oil Production. 170

52 Run 15, Instantaneous Oil and Water Production vs. Cumulative Injection. 171

53 Run 17, Temperature Profile at 0.25 PV Steam Injected 172

54 Run 17, Temperature Profile at Start of Cold Waterflood 173

Figure Page

55 Run 17, Temperature Profile at 0.50 PV Steam Injected 174

56 Run 17, Temperature Profile at 0.75 PV Steam Injected 175

57 Run 17, Temperature Profile at 1.00 PV Steam Injected 176

58 Run 17, Instantaneous Oil-Steam Ratio vs. Cumulative Oil Production. 177

59 Run 17, Instantaneous Oil and Water Production vs. Cumulative Injection. 178

60 Run 18, Temperature Profile at 0.25 PV Steam Injected 179

61 Run 18, Temperature Profile at Start of Cold Waterflood 180

62 Run 18, Temperature Profile at 0.50 PV Steam Injected 181

63 Run 18, Temperature Profile at 0.75 PV Steam Injected 182

64 Run 18, Temperature Profile at 1.00 PV Steam Injected 183

65 Run 18, Temperature Profile at 1.25 PV Steam Injected 184

66 Run 18, Instantaneous Oil-Steam Ratio vs. Cumulative Oil Production. 185

67 Run 18, Instantaneous Oil and Water Production vs. Cumulative Injection. 186

68 Run 19, Temperature Profile at 0.25 PV Steam Injected 187

69 Run 19, Temperature Profile at Start of Cold Waterflood 188

70 Run 19, Temperature Profile at 0.50 PV Steam Injected 189

71 Run 19, Temperature Profile at 0.75 PV Steam Injected 190

72 Run 19, Temperature Profile at 1.00 PV Steam Injected 191

Figure Page

73 Run 19, Temperature Profile at 1.25 PV Steam Injected 192

74 Run 19, Instantaneous Oil-Steam Ratio vs. Cumulative Oil Production. 193

75 Run 19, Instantaneous Oil and Water Production vs. Cumulative Injection. 194

76 Comparison of the Recovery Responses of Runs 17, 18, and 19. 195

77 Run 22, Temperature Profile at 0.25 PV Steam Injected 196

78 Run 22, Temperature Profile at 0.50 PV Steam Injected 197

79 Run 22, Temperature Profile at 0.75 PV Steam Injected 198

80 Run 22, Temperature Profile at 1.00 PV Steam Injected 199

81 Run 22, Cumulative Oil Recovery vs. PV Injected. 200

82 Run 22, Instantaneous Oil-Steam Ratio vs. Cumulative Oil Production. 201

83 Run 22, Instantaneous Oil and Water Production vs. Cumulative Injection. 202

List of Plates

Plate Page

1 Model Assembly in Inclined Position 48

2 Steam Injection System 52

3 Model Cart and Cold Storage Unit 54

4 Data Acquisition System 58

1. INTRODUCTION

Steam injection has been widely successful in North America for the recovery of heavy oil. It currently accounts for over 78% of all oil produced in the world by enhanced recovery methods[1]. The form of steam injection which has had greatest success in Canada (Cold Lake) is cyclic steam stimulation, although recoveries are limited to less than 20%.

The emphasis in this work was on steamflooding, which is normally the second stage process after cyclic steam stimulation. In California heavy oil reservoirs, steamflooding has resulted in oil recoveries of as much as 77% (San Ardo), with 55-60% being commonplace (Kern River). Steamflooding is dependent on achieving communication between injection and production wells which is more difficult to achieve in Canadian heavy oil reservoirs than in California because of low reservoir temperatures which preclude primary production and because of excessive heat losses in thin formations. However, steamflooding is now succeeding in Lloydminster reservoirs which were previously - after extensive work - considered to be unsuitable for this method of enhanced recovery.

Other studies[2,3] have shown that steamflooding may be a viable method of recovering waterflood residual oil from light oil or moderately viscous oil reservoirs. Farouq Ali[3] suggests that the product of the rock porosity and the oil saturation must be greater than 0.10 for a steamflood project to be economically successful. He lists several conventional oil fields in Alberta and Saskatchewan as possible candidates for steamflood operations based on data from the Energy Resources Conservation Board of Alberta. These fields include Acheson, Fenn-Big Valley, Golden Spike, Pembina, Red Water, Turner Valley, Wizard Lake, and Steelman.

Generally, the occurrence of bottom water and/or gas cap zones, common in Alberta and Saskatchewan heavy oil reservoirs, have been regarded as being additionally unfavorable factors in steamflood operations, leading to poor volumetric sweep efficiency. However, experience has shown that gravity drainage is an important factor in thermal in situ recovery of bitumen and heavy oil. This experience suggests ways in which the high water saturation zones (bottom water) and existing or induced gas caps may be utilized, possibly in association with steam additives, to promote cost effective steam drives in marginal reservoirs.

2. OBJECTIVES OF THIS STUDY

The principal objectives of this investigation were as follows:

1. To design and fabricate a low pressure, scaled steamflood model to simulate a selected field (Aberfeldy) in Saskatchewan with the provision of the following:
    - i. Model including injection and production equipment, and material to simulate adjacent formations.
    - ii. Facility for steam generation and steam quality control.
    - iii. Equipment for rapid cooling of the model for establishing the initial conditions in accordance with the scaling criteria.
    - iv. Facility for data acquisition, processing, and plotting.
2. To conduct a series of steamflood experiments to examine model performance under a wide variety of operating conditions, in particular the following:
    - i. Base steamflood in a model saturated with 100% water to observe temperature distributions and to refine operational procedures.
    - ii. Waterflood at room temperature and at low temperature to establish the base oil recovery.
    - iii. Continuous steamfloods in the Aberfeldy model.
    - iv. Light oil steamflood.

v. Heavy oil steamflood.

vi. Effect of production interval.

vii. Effect of bottom water on steamflood recovery.

viii. Steam slug driven by cold water.

The purpose of the above runs was to judge the model capability for a variety of experiments, and also to examine a broad range of steamfloods to determine the processes which merit a closer look in the near future.

3. LITERATURE REVIEW

Several in-depth reviews detailing the current state of steamflood technology are presented in the literature.[4,5] Farouq Ali[4] gives a comprehensive description of the theories that have been proposed to explain the mechanics of steam advance in an oil-bearing formation.

Models (both physical and numerical) have been used to gain a better understanding of the physical processes involved in a steamflood operation. Models have also been extensively employed as predictive tools to help design the best recovery program for a particular field. This chapter presents a survey of the experimental approaches to steam injection and a brief description of the types of experiments that have been conducted. The agreement between model and prototype results will also be examined. Finally, the role of numerical simulation in conjunction with physical models will be discussed.

3.1 Experimental Approaches to Steam Injection

Experiments of many types have been conducted in physical models to examine thermal recovery processes. These include straightforward steamflood studies which investigate relevant operating parameters such as steam injection rate and pressure, steam quality, pattern size and type, and reservoir thickness, to name a few. Other steam injection studies have been conducted in laboratory models to examine recovery from reservoirs with specific attributes such as bottom water, gas caps, shale breaks, extremely high oil viscosity, or with substantial waterflood residual oil saturation.

Physical models representing prototype reservoirs can be of three types: (1) scaled, (2) partially scaled, or (3) unscaled. A fully scaled model would be extremely desirable because the experimental results could be directly applied to a field situation and used to predict reservoir response to various recovery schemes. However, it is difficult to achieve an exactly scaled model. Relaxing some of the scaling criteria to give a partially scaled model may alleviate some of the scaling problems, but then the possibility exists that incomplete scaling will produce errors in the results. The other option is to forego scaling altogether and to focus on a particular aspect of the reservoir in an attempt to obtain qualitative information about a distinct recovery mechanism. The great majority of laboratory investigations have utilized this type of model, as discussed in the next section.

3.1.1 Unscaled Physical Models

Unscaled models have been used extensively in petroleum research. Typically, the materials and operating conditions for the unscaled model are chosen to represent an element of the prototype being studied, and although the models are not scaled (and thus quantitative predictions are not possible), the unscaled experiments can provide important information with respect to the processes at work in the prototype. One of the earliest laboratory studies dealing with steam injection was conducted by Willman et al.[7] This work provided much useful information on the mechanisms involved in a steamflood operation. The experiments were carried out using linear cores saturated with refined oils and crudes having varying viscosities and steam distillation properties. Of particular significance, the study obtained oil recoveries by steam injection as much as 100% greater than oil recoveries by waterflood. The improved oil recovery by steam injection was attributed to (1) thermal expansion of the oil, (2) viscosity reduction, and (3) steam distillation. The procedures used for predicting the performance of a steam drive were based on the Marx-Langenheim[8] equations and thus the same assumptions were applied. Important limitations are inherent as a result of the assumptions of frontal displacement of oil by steam and equal heat losses to cap and base rock.

Ozen and Farouq Ali[9] conducted experiments on linear, consolidated cores under isothermal conditions and found that the steam drive can be an effective process to recover waterflood residual oil. They also performed an experiment which indicated that the injection of a small volume of a light hydrocarbon such as naphtha, prior to steam injection would increase the ultimate oil recovery. Ozen and Farouq Ali[9] were among the first to study the role of heat losses in laboratory studies of steam injection.

Baker[10] conducted an experimental study of heat flow in steamflooding by using steam to displace water in a plane-radial fluid-flow model. The heat losses to the cap and base rocks were calculated using thermocouple data and it was found that heat losses were not dependent on injection rate but were a function of time alone for a given reservoir thickness and thermal diffusivity. However, he did find that the volume of the hot water zone ahead of the steam did depend on the injection rate and that this hot water zone contained a significant portion of the injected heat. Baker also reports that considerable gravity override was observed in his experiments. In a later study, again using the radial flow model, Baker[11] obtained a more detailed definition of the steam front which enabled him to provide a quantitative measure of the steam zone volume and gravity override.

El-Saleh and Farouq Ali[12] conducted an experimental study of oil recovery by a steam slug driven by a cold waterflood in a linear porous medium using several types of oil and various steam-slug sizes. They found that the steam displacement process was more efficient in the case of light oils than for heavier ones and that oil recovery increased with an increase in the steam slug size. Hong[13] and Ault, Johnson and Kamilos,[14] recently presented papers which discussed the application of a waterflood to reservoirs which have been subject to steam-drive operations. Hong's[13] work was based on numerical simulations while Ault et al[14] present actual field performance data.

Two large elemental models, used to simulate steam injection and other recovery processes as applied to the oil sands are described by Redford, Flock, Peters, and Lee.[13] One of the two models consists of a 6-inch by 6-foot steel pipe with a 1/4-inch cement lining and an outer 4-inch layer of magnesia for insulation. The model was fitted with many thermocouples and pressure transducers and used a data acquisition system for collecting all necessary information during a run. It could be packed with any oil sand of interest and inclined to represent the desired angle of dip. This model has been used extensively in many steam injection studies and is still in operation at the University of Alberta.

Redford et al[13] also described a second model which was built at the Alberta Research council. It consists of a 1.5m diameter cell equipped with an elaborate data acquisition and analysing system which includes approximately 1500 thermocouples, pressure transducers, and flow measurement devices as well as extensive control equipment. The Alberta Research Council also runs a similar, but smaller (18 inch diameter) model. It has been used for a variety of experiments employing steam and other fluids in oil sand recovery experiments and is still in use today.

Flock and Lee[14] carried out an investigation involving a steamflood displacement of a medium gravity crude oil using the 6-foot steel pipe described by Redford et al.[15] The tube was packed with unconsolidated sand from the Lloydminster field and saturated with a medium gravity crude oil. It was noted that the temperature distribution within the porous system resulting from injecting steam into a core with a waterflood residual oil saturation was similar to the temperature distribution observed when steam displaced a water saturated porous medium. The authors found agreement between their work and the work of Baker.[10,11]

Flock and Lee[14] suggest that these results indicate that steam can be used as a tertiary recovery process in medium gravity crude oil reservoirs that have been previously waterflooded. They obtained as much as a 40% increase in oil recovery by injecting steam into a previously waterflooded core. However, with the model being insulated as described above, the experimental environment was adiabatic and as such, the effects of heat losses to cap and base rock were not considered. Thus, as the authors indicate, the results obtained from these experiments must be treated with care when considering applying them to a prototype.

Farouq Ali and Abad[17] performed experiments to obtain qualitative information on the effect of three solvents injected into a three-dimensional elemental model in conjunction with steam. They found that bitumen recovery was determined by the solvent used, the volume of the solvent, and the placement of the solvent. It was found that when the solvent was injected into the producing well, followed by steam injection into the injection well, recovery was much higher than when both solvent and steam were injected into the same well. Their results indicated that smaller solvent slugs are more effective in bitumen recovery than large slugs. They suggest that an optimum combination of the solvent and steam slug sizes exists which will maximize bitumen recovery. They also found that recovery tends to increase with a decrease in steam injection rate, down to some minimum optimal rate.

Lee[18] observed results similar to those of Farouq Ali and Abad[17] from his adiabatic experiments conducted using a 6-foot linear elemental model; i.e. that sweep efficiency improved with higher injection rate and lower pressure. In addition he performed experiments to investigate the effect of reservoir dip on oil recovery and found that downdip steam injection was always more efficient than updip steam injection. He observed the downdip displacement was more piston-like whereas in the updip injection case, the upward channelling of steam left behind a substantial amount of unswept oil. In another series of experiments with the model in a horizontal position, Lee[18] compared various locations of the injection interval and found that injection into the lower portion of the tube gave better oil recovery than injection into the upper portion.

The models described thus far were essentially unscaled, elemental models. The general purpose of models of this type is to provide insight into the fluid-rock interactions under appropriate conditions of temperature, pressure, and, when additives are used, chemical environment. The limitations of these models result from the fact that they are not scaled and therefore cannot be used for quantitative prototype predictions.

3.1.2 Scaled or Partially Scaled Physical Models

A model which could accurately predict the production response of a reservoir under steam stimulation would be highly desirable. Scaled model experiments have been carried out to study the effect of variations in operational parameters such as injection rate, production pressure, slug size, completion intervals, flood pattern and size, steam additives, reservoir heterogeneities, and steam quality. These models may also be used to calibrate numerical models or provide some insight into the effects of parameters which may not be properly incorporated into a numerical simulator.

Farouq Ali and Redford[19] present a comprehensive review of the approaches used in scaling steam injection processes. They state that the design of a scaled physical model is based on the Principle of Similarity* and is characterized by the same ratios of dimensions, forces, velocities, temperature differences, and concentration differences as those occurring in the prototype.

---

*The authors refer the readers to a book by Johnstone and Thring[20] for a discussion of the Principle of Similarity.

In general, two types of scaling methods can be used to model thermal recovery processes; (1) high pressure and (2) low pressure (or vacuum). Each of these will be discussed and a comparison of the two will be made.

3.1.2.1 High Pressure Scaled Model Studies

There have been several notable studies dealing with scaling thermal recovery methods as applied to high pressure scaled models. Geertsma, Croes, and Schwarz[21] derived the dimensionless groups for scaling the displacement process involving the injection of hot water with the objective of increasing recovery from reservoirs containing viscous crudes. (They also derived the scaling groups for the conventional water drive and a solvent injection process). Pujol and Boberg[22] developed one of the best known sets of scaling criteria applicable to multidimensional steam injection. Their work has been utilized by several experimentors in scale model studies. Niko and Troost[23] derived scaling criteria for cyclic steam stimulation in a radial, two phase (oil-steam) system. Other noteworthy studies which deal with high pressure model scaling criteria include the work of Perkins and Collins[24], Demetre, Bentsen and Flock[25], Greenkorn[26], Loomis and Crowell[27], Bentsen[28], Rapoport[29], and Leverette, Lewis and True[30]. Several experimental studies have employed high pressure model scaling criteria, some of which will be discussed below.

Pursley[31] applied the Pujol-Boberg[22] scaling criteria to simulate reservoir conditions existing at Cold Lake, Alberta using several three-dimensional models. For the steam drive studies, high pressure scaled models were constructed to represent one-eighth of a five spot pattern for a prototype of thickness of 140 feet (42.7 m) and depth of 1500 feet (457.3 m). Models representing 1.25-, 10-, and 20-acre patterns were used. The prototype oil viscosity was approximately 100 000 mPa-s and in some experiments the reservoir contained a bottom water zone and/or a gas cap. The model fluids were the same as the reservoir fluids but due to the scaling criteria, the porous medium for the model was different (200 times more permeable than the prototype). The author states that the objective of the model studies was to determine if either the bottom water zone or the gas cap could be used during a steam drive operation. A water zone was created by inverting the model, scraping out a layer of oil-saturated sand, and replacing it with water saturated sand. A gas cap was installed by slowly injecting gas into the model, removing a corresponding volume of oil, and allowing the gas to distribute over the top of the model by gravity segregation. He also incorporated impermeable tight streaks in his model (when required) by placing thin sheets of silicone or concrete into the pack at appropriate positions.

With bottom water present, Pursley[31] found that recovery was significantly higher because of the tendency of the steam to override and contact a greater portion of the oil sand. He suggested that a steam drive through a bottom water zone would be feasable if good vertical permeability exists and if heating close to the base of the oil sand can be achieved. However, he found that thicker water sands had the adverse effect of significantly delaying oil production. Based on results of runs with a gas cap present, he suggested that steam injection through the gas cap may provide a better approach in cases where the oil sand is separated from the bottom water layer by an impermeable material. In other experiments, the effect of permeability was examined. Pursley[31] found that increasing the model permeability from 400 darcys to 1200 darcys had little effect on oil recovery. He also found that lowering the quality of the injected steam decreases recovery at corresponding values of steam injected, but on the basis of heat injected, the recoveries were similar. Pursley[31] also reported on experiments concerning pattern size, steam bank size, additives to steam, and tertiary wet combustion studies.

Ehrlich[32] conducted experiments in a three-dimensional model, scaled according to the Pujol-Boberg[33] scaling criteria to study steam displacement in the Wabasca Grand Rapids 'A' sand. The model represented one-quarter of a 0.2 acre five-spot pattern for a prototype reservoir with a 30-35 feet (9-10.7m) thick pay zone and with oil viscosity of approximately 5×10^4 mPa-s. Based on this study, the author found that the residual oil saturation behind a steam front is about 20% of the pore volume regardless of the initial oil saturation. He suggested that the areal sweep efficiency of a steam front is high because of the low effective steam mobility. He found that vertical sweep efficiency was low because of steam override and the oil-steam ratio is low when override occurs. Ehrlich[32] also found that the use of caustic along with steam does not improve recovery despite the success of caustic emulsifiers used as additives with hot waterfloods.

Huygen[33] used a three-dimensional, high pressure (7MPa) model packed with Berea sand to examine the steamflood recovery of eight different crudes. (The model considers only heat flow in the scaling calculations). Huygen[33] prepared a correlation using exponential curves to predict oil production and steam sweep data based on values of initial oil saturation, specific gravity, viscosity at 38 C, distillation residue at steam temperature, steam-to-oil viscosity ratio, and the viscosity ratio multiplied by the steam/water specific volume ratio. In a later study, Huygen and Lowry[34] performed experiments to study steamflooding in the presence of a bottom water zone. The bottom water was installed in their model by the same method as that used by Pursley.[31] They observed that the bottom water acted as a pressure sink which counteracted gravity segregation of the steam. They also reported that if the steam injection rate is high enough, no gravity override occurs and much of the formation is swept layer by layer, resulting in a oil recovery. However, they state that too high of an injection rate wastes steam and too low a rate promotes override, and thus, an optimum rate exists. The authors conclude that a bottom water zone provides the steam injectivity missing in immobile tar sands but soaks up heat and oil, making the process inefficient when thicker bottom water layers exist. They found that heating of the oil sand by conduction through the water layer is slow. They also observed the displacement of the heated tar to be parallel to the steam front and through the bottom water zone, rather than ahead of the steam.

Singhal[35] and Lo[36] employed Pujol-Boberg[22] scaling criteria in their scaled model study. They observed that the hot condensate zone ahead of the steam zone exhibited severe fingering and channelling which resulted in early water breakthrough but that the steam zone did not exhibit fingering. Consistent with other studies, the authors observed severe gravity override as well as underrunning of hot condensate fluid. They also report that oil recovery increased with both increased steam injection rate and with increased steam quality. They suggest, based on experimental results, that waterflooding a reservoir after steamflooding will recover as much as 5% more oil.

3.1.2.2 Low Pressure Scaled Model Studies

Scaled physical models employing vacuum scaling criteria were first proposed by Stegemeier, Laumbach, and Volek.[37] They demonstrated that materials differing from those found in the prototype reservoir can be used in the vacuum model system and that such a model can accurately predict field response. As this is the scaling method applied to the physical model used in this study, extensive details of the scaling criteria of Stegemeier et al are presented in a later chapter.

Stegemeier et al[37] report that they performed scaled experiments to design or to provide operational assistance for several of Shell's steam drive projects including Tatums[38], Coalinga[39], Slocum[40], Mt. Poso[41], Peace River[42], Yorba Linda[43] and Midway Sunset.[37] They provide results from two of their large model studies, the Mt. Poso and Midway Sunset fields, as examples of the type of information which may be derived from vacuum model studies.

The Mt. Poso study conducted by Stegemeier et al[37] included a series of about fifty experiments which demonstrated that steam layover would be a significant factor in the field, causing oil and water to be displaced downdip by gravity. They found that heating downdip improved the oil-steam ratio but that only part of the reservoir was depleted. In some runs, the effect of prototype oil saturation distribution along dip was investigated and it was found that a high oil saturation mid-dip, or especially updip, improved the displacement process over a uniform saturation distribution. The results of these experiments led the authors to recommend conditions for a successful steamflood at Mt. Poso. A study of the Midway Sunset field included experiments to compare the results of steamflooding and a steam soak process.

Prats[42] conducted numerous experiments using vacuum models employing Stegemeier et al's[37] scaling criteria. His study was focused on the Peace River, Alberta oil sand deposit where a bottom water layer exists. Five prototypes were examined and Prats concluded that each prototype reservoir required a unique operating strategy in order to obtain the optimal recovery. Many operational variables were examined including steam quality, injection rates, completion interval, pressure levels, and heat scavenging by injecting water after the steam drive. Many of the runs were conducted with a high water saturation present in the lower part of the model. This zone of high water saturation was established by creating a temperature gradient in the model (with the bottom being significantly hotter) and injecting water through selected wells with bottom completions. The injected water preferentially displaced oil from the lower layer of the model. After the desired initial oil saturation profile was established, the temperature gradient was maintained for one or two days to allow the model to reach horizontal and vertical equilibrium.

Doscher[44] constructed a vacuum model based on the scaling criteria of Stegemeier et al[37] with a slight modification. Doscher developed scaling parameters from similarities in an integral form, based on a study by Yortsos[45], rather than a differential form as used by

Stegemeier et al.[37] Doscher and Huang[44] used this model to investigate the steam drive performance in a Kern River type heavy oil field. Experiments were conducted to study the effect of injection rate, bottom water, steam quality, oil viscosity, and reservoir permeability. Based on the experiments conducted for a particular prototype, they concluded that an optimum steam injection rate exists, above and below which, performance decreases. They suggested that production rate is a linear function of steam quality, and a function of the square root of the oil viscosity at steam temperature.

Doscher and Ghassemi[47] performed experiments on the vacuum model described above[44] and determined that the viscosity of the crude oil is a very important parameter which affects the efficiency of the steam drive process. They also conducted experiments to examine the effect of reservoir thickness on the steam drive efficiency. Although little evidence is presented in the paper, they suggest the possibility of the oil-steam ratio in thin reservoirs being as high as, or even higher than in thick reservoirs. This is contrary to the prediction made by analytic models which indicate that the oil-steam ratio will vary directly as a function of reservoir thickness. It seems likely that excessive heat losses would limit the economic viability of a steam drive process in thin formations.

3.1.2.3 High Pressure vs. Low Pressure Scaled Models

Each of the two model types has distinct advantages and disadvantages. Since high pressure models often employ the same fluids as the prototype, they are considered to provide a better scaling of rock-fluid interactions such as permeability, relative permeability, capillary pressure alterations, and gravity segregation. Stegemeier et al[37] note that the Clausius-Clapeyron relation is more accurately matched at subatmospheric pressures and low temperatures, thus the modeling of temperature distribution is better in the vacuum model. This affects the viscosity distribution, internal energy distribution, and the steam zone pressure gradient, all of which are thought to be important aspects of the thermal recovery process. It is generally accepted that the vacuum model is less expensive to construct, safer to operate, and is able to turn out results quicker than the high pressure model. It is interesting to note that although Prats[42] had both types of models available to him, after considering the relative advantages and disadvantages of each, he chose to conduct his experiments in a vacuum model.

On the negative side, neither the high pressure nor the low pressure scaled model account for compressibility effects. More importantly, neither model is able to use prototype fluids or porous media if proper scaling is to be maintained. Kimber and Farouq Ali[44] found that if prototype fluids and porous media are used in a high pressure model, the geometric similarity must be distorted in the vertical dimension. This would also affect other scaling parameters. Doscher and Huang[44] point out that physical scaling fails badly when chemical reactivity, capillary pressure, or physical adsorption play important roles in the process, but they state that in the steam drive these phenomena are not important.

Prats[42] and others suggest that the main factor which may not be scaled in the vacuum model is the relative permeability. (This would also be true of the high pressure model, but to a lesser extent.) In a discussion at the Canada-Venezuala oil sands symposium of 1977[44] he stated that it is not known if the relative permeabilities are scaled and gave several factors which contribute to the problem. The most important is that it is not known how to obtain a single set of three-phase relative permeability curves which will be applicable for a given prototype reservoir under the anticipated operating conditions. In addition, he says it is not known how to make up a set of relative permeability properties for the laboratory scaled models. For these reasons, he suggests that it is not possible to determine how well or how poorly relative permeabilities are matched in the scaled models.

In general, it is believed that the high and low pressure scaled models provide a reasonable description of the phenomena involved in the steam drive process. A later section gives some examples of the ability of the scaled models to predict the field response to steam stimulation.

3.1.3 Studies of Thin, Bottom Water Reservoirs

Kasraie and Farouq Ali[38] discuss the mechanisms involved in thermal stimulation of bottom water reservoirs. Based on their survey of existing field and laboratory data, the authors conclude that a water zone thicker than about one-fifth of the oil zone would make cyclic steam stimulation uneconomical.

As mentioned in previous sections, a few experimental studies have been undertaken to examine oil recovery by steam injection into reservoirs underlain by water. However, none of these studies were directed toward reservoirs of the Alberfeldy type; i.e. thin reservoirs, often associated with relatively thick bottom water zones and/or a gas cap.

The Peace River reservoirs, modeled by Prats[42] contain a substantial oil saturation (45%) in conjunction with the "bottom water" layer; thus injection into the bottom water zone still produces an economically acceptable amount of oil. The Cold Lake reservoir studied by Pursley[31] has a pay thickness of 140 feet (42.7 m) and the Wabasca reservoir studied by Huygen and Lowry[34] has a thin bottom water zone relative to the total pay thickness. Both have viscosities in the order of 10^5 mPa-s. Thus, the results of these studies may not be representative of the Aberfeldy reservoir. Similarly, only limited work has been reported with respect to steamflooding thin oil reservoirs; (e.g. Doscher and Ghassemi[47]).

A numerical simulation study was recently reported by Singh, Malcolm, and Heidrick[51]. Their objective was to evaluate steam injection and steam injection with additives into reservoirs with bottom water. The project encompassed a number of simulations which were run to determine the effects of bottom water thickness, carbon dioxide injected along with the steam, blocking agents, and injection-production strategy. They concluded that the injection of carbon dioxide alone, followed by steam injection would result in improved production. They note that there is no data available concerning the application of additives for the thermal recovery of bitumen from reservoirs with bottom water. The results given are of a very general nature, and do not give any definite guidelines for producing bottom water reservoirs.

3.2 Agreement Between Experimental and Field Results

With regard to unscaled experiments, there is no likelihood of obtaining the same oil recovery or oil production rate as in the field. However, some studies have shown that field values of the residual oil saturation to steam are similar to laboratory values. The residual oil saturation to steam is dependent upon the the ultimate oil displacement by steam, and depends less on mass/heat transfer effects.

Stegemeier et al[37] observed excellent agreement between their scaled model studies and field responses for the Mount Poso steam drive model. They present a plot of the predicted versus the actual field performance, which demonstrates the accuracy of the scaled model. Prats[42] gives a comparison of the full-scale vs. actual response for the Peace River scaled model studies in a table and again, close agreement is observed. This is particularly interesting in the case of the Peace River study because the in situ oil viscosity is very high, while representation in the model was accomplished by a relatively light oil.

3.3 Role of Numerical Simulation

Numerical simulation of steam injection processes is at a stage where simpler situations can be simulated. The principle limitations are (1) the grid size, which limits simulation to that of an element of symmetry of a pattern, and that too, with limited definition; and (2) process representation, which means that some of the processes involved in thermal stimulation are still unclear, particularly the rock-fluid interactions. Often, unrealistic assumptions are put into a simulator to obtain a history match, for example, using a rock compressibility factor which is several orders of magnitude higher than the real compressibility ('spongy rock' effect[52]) to compensate for a parameter which is not implemented (or possibly not understood).

In spite of these deficiencies, numerical simulators can be valuable tools to complement physical model studies. They can provide fast predictions which may be used to assess the relative role of variables in a given steam process. With adequate information available for history matching, numerical simulators may be modified to provide accurate predictions of reservoir response to changes in operational strategy, thus precluding the need for physical models. However, if production data is limited or nonexistent, the use of a numerical simulator in conjunction with a scaled physical model would provide the most reliable prediction.

4. SCALING THE STEAM DRIVE PROCESS FOR A VACUUM MODEL

This chapter will outline some of the details of the scaling method which was used in this study. The assumptions underlying the scaling procedure are listed and justification is given for two of the major ones. To demonstrate the application of this scaling method, the details of the calculations used to model the Aberfeldy reservoir and the associated operating parameters will be presented.

4.1 Vacuum Model Scaling Parameters

The scaled model used in this study was designed based on the scaling rules of Stegemeier et al.[37] The scaling rules were derived by rewriting the equations governing the steam injection process into dimensionless form and then determining a set of similarity parameters by inspectional analysis. Engineering judgement was used to reduce the set of similarity parameters to a set of scaling parameters which could generally be matched between the scaled model and the field prototype. These scaling parameters are presented in Table 1 on the following page.

In the derivation of the scaling parameters, the following assumptions were made by Stegemeier et al[37]:

1. Three phases may exist consisting of an oleic phase, an aqueous phase, and a steam vapour phase (no volatile hydrocarbons).
2. There is no partitioning into or out of the oil phase

Table 1. Scaling Parameters for Steam Processes

Number	Parameter	Name of Parameter
1	$\frac{P_r}{\rho_r g_r L_r}$	Poiseuille number divided by Stokes number.
2	$\left\{\frac{f_{sr} L_{vr}}{C_r T_r} + 1\right\} \cdot A$	Modified Jacob number + 1.
3	$\frac{f_{sr} \mu_{sr} \rho_r}{\mu_r \rho_{sr}}$	Ratio of steam pressure gradient to oil pressure gradient.
4	$\frac{k_{hr} t_r}{\phi_r S_r \rho_r C_r L_r^2} \cdot A$	Fourier number or Peclet number.
5	$\frac{\phi_r S_r \mu_r L_r}{k_r \rho_r g_r t_r}$	Stokes Number
6	$\frac{w_r t_r}{\rho_r \phi_r S_r L_r^3}$	Poiseuille number divided by modified Poiseuille number.

After Stegemeier, Laumbach, and Volek[37] (dead oil).

3. Rock compressibility and thermal expansion are negligible.
4. Darcy's and Fourier's equations are valid.
5. Capillary pressure effects are negligible.
6. The system is in local thermodynamic equilibrium.
7. Kinetic energy, potential energy, and viscous dissipation energy are negligible compared with the thermal energy.
8. The enthalpy and internal energy are essentially equal for the oleic phase and for the aqueous phase, and are linear functions of the temperature.
9. The difference between the steam enthalpy and internal energy can be neglected.
10. The time rate of change of the specific steam enthalpy in the steam zone is negligible.
11. The internal energy of the rock is a linear function of the temperature.
12. The saturated steam temperature is the maximum temperature in any location.
13. Relative permeabilities depend exclusively on the saturations.
14. The residual oil saturation to steam and the connate water saturation are constant and uniform throughout the model.
15. Critical saturation for steam flow is assumed to be zero.

16. The changes in the density of the immovable water and residual oil are negligible.

In view of the above assumptions, some degree of error in the results is inevitable. In particular, strict scaling would require that the capillary pressure and the relative permeability relationships be the same functions of saturation in the model as in the prototype. In addition, a practical limitation results from the possible problems associated with finding model materials and fluids with the properties necessary to satisfy the scaling groups.

The failure to scale the capillary pressure is thought to be acceptable because of the high crude oil viscosity in the prototype reservoir. Demetre et al[25] found that in the case of large values of mobility ratio, the breakthrough recovery is only a weak function of the capillary number, provided the displacement is stable. Bentsen[28] states that the mobility ratio dominates the displacement process in a linear system and therefore it is possible to eliminate the requirement that the relative permeabilities (or their ratio) be the same in the model and in the prototype, under certain circumstances. The paper deals with a linear displacement process, but the author suggests that more complex problems may be handled in an analogous manner.

As mentioned in the literature review, Prats[41] states that the three-phase relative permeability curves applicable to the prototype under the anticipated operating conditions cannot be determined. Similarly, it is not known how to make up a set of relative permeability properties for the laboratory model. This problem makes it difficult to know whether the relative permeability relationships are scaled or are not scaled. Despite this limitation, good agreement was obtained between the model and field results, as noted above.

Aside from the arguments presented above, justification for the assumptions made in deriving the scaling rules is further (and perhaps better) provided by the agreement between laboratory model results and actual field operations. Some examples were given in the literature review.

4.2 Designing the Aberfeldy Scaled Model

Three models were built to represent the Alberfeldy prototype, one with a scaling factor of 173.2 to 1, and two with scaling factors of 400 to 1 (one of which represented a reservoir twice as thick as the other). Each model was designed to simulate one quarter of a five-spot pattern and as such, each had one injection well and one production well, at diagonally opposite corners. Because of the work involved in preparing for a run, and the cleaning necessary after a run, the smallest model was used for the preliminary runs until familiarity with the equipment was established.

The thin pay zone of the Aberfeldy reservoir requires that the scaled model representing it be very thin also, particularly for a model with a scaling factor of 400 to 1.

Thus the second small model was built with an exaggerated vertical height to give a better insight into the effects of bottom water and steam override. However, since the best predictions can be made with as large a model as is practical, the large model was used for the majority of the runs. This is the model that will be discussed in the example calculations presented in the following sections.

4.2.1 Prototype Data

The first step in designing a physical model to simulate a field system is to determine the characteristics which will be used to describe the prototype reservoir. The following values were chosen to represent the Aberfeldy prototype:

Well Spacing: 8 hectare (20 Acre), 5 spot pattern

Net Pay Thickness: 11 meters.

Gross Pay Thickness: Varies from 10 to 13 meters.

Porosity: 0.31

Permeability: 2000 md

Thermal Conductivity: 1.2 Btu/hr-ft-F (0.002077 KW/m-K)

Heat Capacity: 2.2217 KJ/Kg-K

Initial Saturation: S_o=0.75, S_g=0.02, S_w=0.23

Steamflood Residual Oil Saturation: S_{or}=0.15

Oil Viscosity: 1275mPa-s at 23.9 C, 560mPa-s at 32.2 C, 90mPa-s at 65.6 C, 12.5mPa-s at 135.0 C, and 1.29mPa-s at 301.7 C

Water Viscosity: 0.891mPa-s at 25.8 C

Gas Viscosity: 0.013mPa-s at 23.3 C and 0.016mPa-s at 134.4 C

Specific Gravity of Gas: 0.55

Initial Reservoir Pressure: 3.45 MPa

Initial Reservoir Temperature: 23.3 C

Steam Injection Pressure: 1.900 MPa

Steam Injection Rate: 100-150 m^3/day

Steam Quality: 0.70 (Actually it is 0.80 to 0.85 but a lower value was used to allow for wellbore heat loss.)

Depth of Reservoir: 522.4 m

Bottom Water: Varies from 0 to 6.9 m.

Pressure Range: The pressure range is usually bounded on the upper side by the fracture gradient of the reservoir and on the lower side by the bottomhole production pressure. For calculation purposes, a back pressure on the formation of 0.34475 MPa (50 psia) was assumed.

$$\therefore (P_p)_p = 0.34475 \text{ MPa}$$

4.2.2 Selection of Length Scale

The selection of length scale is determined by pressure-temperature relations and by constraints placed on the size of the physical model. Generally, in order to match the pressure-temperature relation for saturated steam, the scaling factor, $\gamma(L)$, should be made as small as possible and thus the model should be as large as possible.

The limits are that the model must be of a size suitable for a laboratory and small enough to ensure that the run time is not prohibitive.

In this project, the model represents 1/4 of an 8 hectare, 5-spot pattern. The model is 32 inches square (81.3 cm) and 2.5 inches (6.4 cm) thick. This gives a scaling factor of 173.2 in 3 dimensions.

$$\therefore L_p/L_m=\gamma(L)=173.2 \quad ...(1)$$

4.2.3 Selection of Model Production Pressure

For prototype pressures of the order of 50 psia (0.345 MPa) and for typical length scales, Stegemeier et al[37] state that the pressure-temperature relation at saturation can best be matched if one selects as low a value for the model production pressure as is possible. From a practical standpoint, the lowest value that can be maintained due to vacuum pump limitations and vapour pressure considerations is about 1 psia (7 kPa).

$$\therefore (P_p)_m=6.895 \text{ kPa (1 psia)}$$

4.2.4 Calculation of Model Differential Pressure Scaling

With the above value for the model production pressure chosen, model production scaling is calculated from scaling parameter (1) in Table 1.

$$\gamma(\Delta P) = \frac{(P-P_p)_p}{(P-P_p)_m} = \frac{\rho_p\ g_p\ L_p}{\rho_m\ g_m\ L_m} \quad ...(2)$$

To this point, the density ratio is the only unknown in the above equation. The first time through the scaling calculations it is necessary to assume a value of $\gamma(\rho_r)$, the density ratio, which was found to be approximately equal to 0.9, and using this, a relationship between P_m and P_p can be developed from equation (2) as follows:

$$\gamma(\Delta P) = \frac{(P-P_p)_p}{(P-P_p)_m} = (0.9)(1.0)(173.2)$$

$$P_m = (P_p)_m + 0.0064152\ P_p - 0.0064152\ (P_p)_p$$

$$P_m = 0.006895 - (0.0064152)(0.34475) + 0.0064152\ P_p$$

$$\therefore P_m = 0.004683 + 0.006415\ P_p \quad ...(3)$$

where P_m is the model pressure corresponding to a prototype pressure P_p, with P_m and P_p both in MPa. Refer to Table 4 for a tabulation of the corresponding values.

4.2.5 Determination of Model Temperature Scaling

Unlike hot water scaling for which the model temperature scaling is arbitrary, in scaling steam recovery methods, the problem becomes more complex. The dimensionless pressure-temperature relation for saturated steam is a constraint on the scaling which determines the optimum temperature scaling.

In general, in order to obtain the best match between model and prototype oil viscosity curves, the model temperature range should be made as large as possible.

As a practical limitation, the minimum initial model temperature is about 3 C. Cooling below this point may lead to difficulties due to localized freezing of model lines. Thus $(T_o)_m = 3$ C. To scale the temperature, corresponding temperatures at only one other point are required.

Stegemeier et al[37] suggest that it is best to take a value from the middle of the pressure range for finding the temperature difference ratio because most of the oil will be produced when these temperatures are significant. Also the lower part of the pressure-temperature relation for saturated steam is difficult to fit.

Using midrange prototype and model temperatures from Table 4 corresponding to a prototype pressure of 2.00 MPa yields the following value for the temperature ratio:

$$\frac{\Delta T_p}{\Delta T_m} = \frac{(T-T_o)_p}{(T-T_o)_m} = \frac{(212.42-23.30)}{(57.03-3.0)} \quad ...(4)$$

$$\frac{\Delta T_p}{\Delta T_m} = 3.5 \quad ...(5)$$

The ratio must be constant over the temperature range in order to have the proper proportion of energy stored as internal energy. If the ratio is constant, for any prototype temperature a model temperature relation can be developed as follows:

$$T_m - (T_o)_m = \frac{T_p - (T_o)_p}{3.5}$$

$$\therefore T_m = 0.286\ T_p - 3.657 \quad \ldots(6)$$

The model values calculated from the above equation are given in Table 4 and are designated T_{sc} to denote that they are calculated values.

As seen in Table 4, the calculated values, T_{sc}, do not correspond exactly to the saturated steam values, T_s. Stegemeier et al[37] state that better scaling is obtained by allowing the error to occur at the lower temperatures. They note that the portion of the pressure-temperature saturation relation which is most difficult to match is the part pertaining to low prototype pressures, which often are not encountered.

4.2.6 Calculation of Steam Quality Required

The model steam quality is determined from parameter (2) in Table 1.

$$\left(\frac{f_{sr}\ L_{vr}}{C_r\ T_r} + 1\right) * A \quad \ldots(7)$$

When $\phi\Delta S$ is not matched, and if we assume that cap and base rock heating are dominant, as is often the case in steam drive processes (particularly in thin reservoirs), 'A' takes on a value of $\phi S_r(\rho_r c_r/\rho_{cr} c_{cr})$. Thus the equation to calculate the model steam quality is given by:

$$f_{sm} = \left(\frac{C_w \Delta T}{L_v}\right)_m \left\{\left(\frac{f_s L_v}{C_w \Delta T}+1\right)_p \left[\frac{(\phi_p \Delta S_p)}{(\phi_m \Delta S_m)} . \frac{(\rho_p C_p)}{(\rho_m C_m)} . \frac{(\rho_{cm} C_{cm})}{(\rho_{cp} C_{cp})}\right] -1\right\} \quad ..(8)$$

Assume that a porosity of 0.32 is obtained in the model,

$$\therefore \phi_m = 0.32$$

and assume that, $\Delta S_m = 0.85$.

Since $\Delta S = 1 - S_{or} - S_{wc}$, and $S_{or} = 0.15$,

$$\Delta S_p = 0.62$$

Values of model steam quality at various pressures have been calculated using equation (8) and are presented in Table 4.

4.2.7 Calculation of Model Viscosity

Parameter (3) in Table 1 is used to scale the oil viscosity. From parameter (3) the following relation can be obtained:

$$\frac{\mu_{o_m}}{\mu_{o_p}} = \left[\frac{(f_{sm})}{(f_{sp})} . \frac{(\mu_{sm})}{(\mu_{sp})} . \frac{(\rho_{sp})}{(\rho_{sm})} . \frac{(\rho_{o_m})}{(\rho_{o_p})} \right] \quad ...(9)$$

Known quantities have been substituted into this equation and values of model viscosity have been calculated for various pressures. These are presented in Table 4.

4.2.8 Calculation of Time Scale

Parameter (4) of Table 1 is used to determine the time scale. Assuming that the temperature distribution is more significant in the cap and base rock than in the reservoir (as was done to determine the model steam quality), the following equation can be developed from parameter (4):

$$\frac{t_m}{t_p} = \frac{(k_{hp})}{(k_{hm})} \cdot \frac{(\rho_{cm} c_{cm})}{(\rho_{cp} c_{cp})} \cdot \left(\frac{L_m}{L_p}\right)^2 \quad \ldots(10)$$

The thermal conductivity for granite is 2.81 kcal/(m·hr·deg C).[53]

$$\therefore k_{hm} = 0.003266 \text{ KW/m·K}$$

M_p = heat capacity of the prototype is given by the following equation:

$$M_p = \phi \rho_o c_o S_o + \phi \rho_w c_w S_w + (1-\phi)(\rho_r c_r)$$

Substituting the prototype data and taking ρ_r = 2.14 g/cm³ [54] gives:

$$M_p = (\rho_r c_r)_p = 2.1803 \text{ KJ/Kg·K}$$

Similarly, the heat capacity in the model can be calculated as follows:

$$M_m = (\rho_r c_r)_m = 2.3824 \text{ KJ/Kg·K}$$

Substituting values into the time scale equation (equation (10)), the time scale can be determined:

$$t_m/t_p = 12.1836 \text{ min/year} \quad \ldots(11)$$

4.2.9 Calculation of Model Permeability

The model permeability is scaled from parameter (5) in Table 1. By modifying this parameter, the following equation can be developed:

$$\frac{k_m}{k_p} = \left[\frac{(\phi_m \Delta S_m)}{(\phi_p \Delta S_p)} \cdot \frac{(L_m)}{(L_p)} \cdot \frac{(\mu_m)}{(\mu_p)} \cdot \frac{(\rho_p)}{(\rho_m)} \cdot \frac{(t_p)}{(t_m)} \right] \quad \ldots(12)$$

Since μ_m/μ_p is a function of temperature, the expression for k_m/k_p is also temperature dependent; however, this is not permissible. Consequently, a single value for

μ_m/μ_p must be chosen. Stegemeier et al[37] state that values from the lower portion of Table 4 should be weighted most heavily. Thus for the scaling of the Aberfeldy prototype, a value corresponding to a prototype pressure of 1.00 MPa was chosen. By substituting thess values and the prototype data into equation (12), a value for the model permeability can be determined.

$$k_m = 4216.5 \text{ darcies.}$$

4.2.10 Calculation of Injection and Production Rate Scales

The injection rate and production rate are both scaled according to parameter (6) in Table 1. This parameter can be used to develop the following equation:

$$\frac{w_m}{w_p} = \left[\frac{(\rho_{om})}{(\rho_{op})} \cdot \left\{\frac{L_m}{L_p}\right\}^3 \cdot \frac{(\phi_m \Delta S_m)}{(\phi_p \Delta S_p)} \cdot \frac{(t_m)}{(t_p)} \right] \quad \text{...(13)}$$

Substituting values into equation (13) gives,

$$w_m/w_p = 9.0728 \; \frac{\text{cm}^3/\text{min}}{\text{m}^3/\text{day}} \quad \text{...(14)}$$

where the volumetric rates are at standard conditions.

Thus, to simulate an injection rate of 100 m^3/day in the prototype, the model injection rate would be 1/4 of 907.3 cc/min

4.2.11 Calculation of Water Proportion for Steam Quality

The proportion of injected water and steam must be calculated to obtain the desired model steam quality. The enthalpy rate of the two inlet streams combined must equal the required enthalpy rate of the wet steam injected into the model plus any heat losses. Thus,

$$w_{ss}h_{ss}+w_a h_a = (w_{ss}+w_a)(f_{sm}L_v+c_w\Delta T)+Q_{loss} \quad ...(15)$$

where w_s and w_a are the mass rates of flow of the superheated steam and the aqueous phase respectively; h_{ss} and h_a are the entering superheated steam enthalpy and quality control water enthalpy respectively, and Q_{loss} is the rate of heat loss.

Equation (13) can be rearranged as follows:

$$\frac{w_a}{w_{wi}} = \frac{h_{ss}-f_s L_v-c_w\Delta T-(Q_{loss}/w_{wi})}{h_{ss}-h_{wa}} \quad ...(16)$$

where w_{wi} is the total mass rate injected ($=w_{ss}+w_a$) and $h_{wa}=h_f$ at 23 C which is equal to 96.52 KJ/Kg.

Assuming that the steam temperature is 120 C, the quality control water temperature is 23 C, and $Q_{loss}=0$, the values of h_{ss} were calculated and found to vary with model pressure as shown in the table given on the following page.[55]

Using these values for h_{ss} and substituting other known values into the equation above gives values of w_a/w_{wi} at various pressures. These are tabulated in Table 4.

Table 2. Steam Enthalpy at Various Model Pressures

Model Pressure (MPa)	Steam Enthalpy (KJ/Kg)
0.006895	2726.00
0.007891	2725.92
0.01110	2725.59
0.01431	2725.25
0.01751	2724.92
0.02072	2724.59
0.02393	2724.25
0.02682	2723.95

4.2.12 Well Scaling

Direct geometric scaling of the wells is not practical for a model of this size. The 'slit well' technique presented by Stegemeier, Lambauch, and Volek[37] was used to scale the wells. The width of the slit is determined by the following equation:

$$w = 2\pi r \qquad \text{where } w = \text{slit width.} \quad \ldots(17)$$

$$r = \text{scaled radius of the well.}$$

Using the length scale of 173.2 for this model, and assuming that the prototype wells are 6 inches in diamater, the scaled diameter of the model wells would be 6/172.3 = 0.03464". With this, the width of the model well slit can be calculated.

$$w = \frac{2\pi(0.03464")}{2} = 0.1088"$$

The wells in the model have been constructed in a manner such that the injecting and producing interval may be altered with relative ease. For most of the experiments conducted in this study, the injection and production intervals were positioned in the same manner as described by Singhal.[35] For the injection well there are four slots opposite the lower portion of the well and for the production well there are eight slots over the length of the well.

Summary of Scaling Calculations for Aberfeldy Model

Length Scale: $\gamma(L) = L_p/L_m = 173.2$

Pressure Relation: $P_m = 0.004683 + 0.006415\ P_p$ (MPa)

Temperature Relation: $T_m = 0.286\ T_p - 3.657$ (C)

Time Scale: $t_m/t_p = 12.18$ min/year

Permeability: prototype = 2 darcies,
model = 4216.5 darcies

Injection and Production Rate Scales:

$$\frac{w_m}{w_p} = 9.0728\ \frac{\text{cm}^3/\text{min}}{\text{m}^3/\text{day}}$$

Table 4: Prototype and Model Scaling Values.

Prototype Values							Model Values										
P (MPa)	Ts (C)	hw (kJ/kg)	CwΔT (kJ/kg)	Lv (kJ/kg)	ρs (kg/m3)	μs (cp)	P (MPa)	Ts (C)	Tsc (C)	hw (kJ/kg)	CwΔT (kJ/kg)	Lv (kJ/kg)	ρs (kg/m3)	μs (cp)	fs	μom/μop (cp/cp)	ws/wl
3.45	241.73	1045.9	947.84	1757.9	17.2322	0.0173	0.02662	66.47	65.48	274.07	261.50	2342.59	0.17100	0.01090	0.06965	7.0195	0.8654
3.00	233.90	1008.4	910.64	1795.7	14.9970	0.0170	0.02393	63.92	63.24	264.69	252.12	2349.28	0.15110	0.01080	0.07319	7.3253	0.8827
2.50	223.99	962.11	864.33	1841.0	12.5031	0.0166	0.02072	60.77	60.40	252.80	240.23	2356.40	0.13520	0.01060	0.07750	7.2644	0.8793
2.00	212.42	908.79	811.01	1890.7	10.0371	0.0162	0.01751	57.03	57.10	238.99	226.42	2365.72	0.11290	0.01040	0.08230	7.4558	0.8776
1.50	198.32	844.89	747.11	1947.3	7.5890	0.0156	0.01431	52.84	53.06	222.12	209.55	2373.60	0.08820	0.01020	0.08792	7.8512	0.8765
1.00	179.91	762.61	665.03	2015.3	5.1430	0.0149	0.01110	47.61	47.80	200.15	187.58	2386.99	0.07816	0.01000	0.09474	6.6411	0.8758
0.50	151.86	640.23	542.45	2108.5	2.6674	0.0140	0.007891	41.15	39.77	166.61	154.04	2403.94	0.06170	0.00970	0.10440	4.9637	0.8754
0.34475	138.34	582.00	484.22	2149.7	0.5322	0.0133	0.006695	38.50	35.91	150.48	137.91	2409.19	0.04556	0.00950	0.10790	1.4290	0.8751

5. EXPERIMENTAL APPARATUS AND PROCEDURE

This chapter contains a description of the equipment and materials used in the study. Details concerning the model operation are presented including a discussion of the procedures involved in packing and saturating the model, and conducting the experiments. A schematic diagram of the apparatus used in this research is given in Figure 1 on the following page. The main components of this apparatus are the physical model, the steam injection system, the model cart and cold storage unit, and the data aquistion system.

5.1 Physical Model

Plate 1 shows the model in an inclined position with the cap and base rocks in place. A spare model is shown in front of the apparatus to illustrate what the porous media of the model was contained in.

All of the models used in this project were designed to represent one-quarter of a 281.55m x 281.55m x 11m thick five-spot pattern, with an area of 8 ha (20 acres). The model which was used for the bulk of the experiments was constructed with the dimensions of 81.28cm x 81.28cm x 6.35cm thick (32in. x 32in. x 2.5in.) which results in a three-dimensional length scale of 173.2. Since the experiments are conducted under vacuum conditions in order to satisfy the scaling groups, a severe load is induced on the large surface area of the models. Thus, it was necessary to construct the models from a strong material,

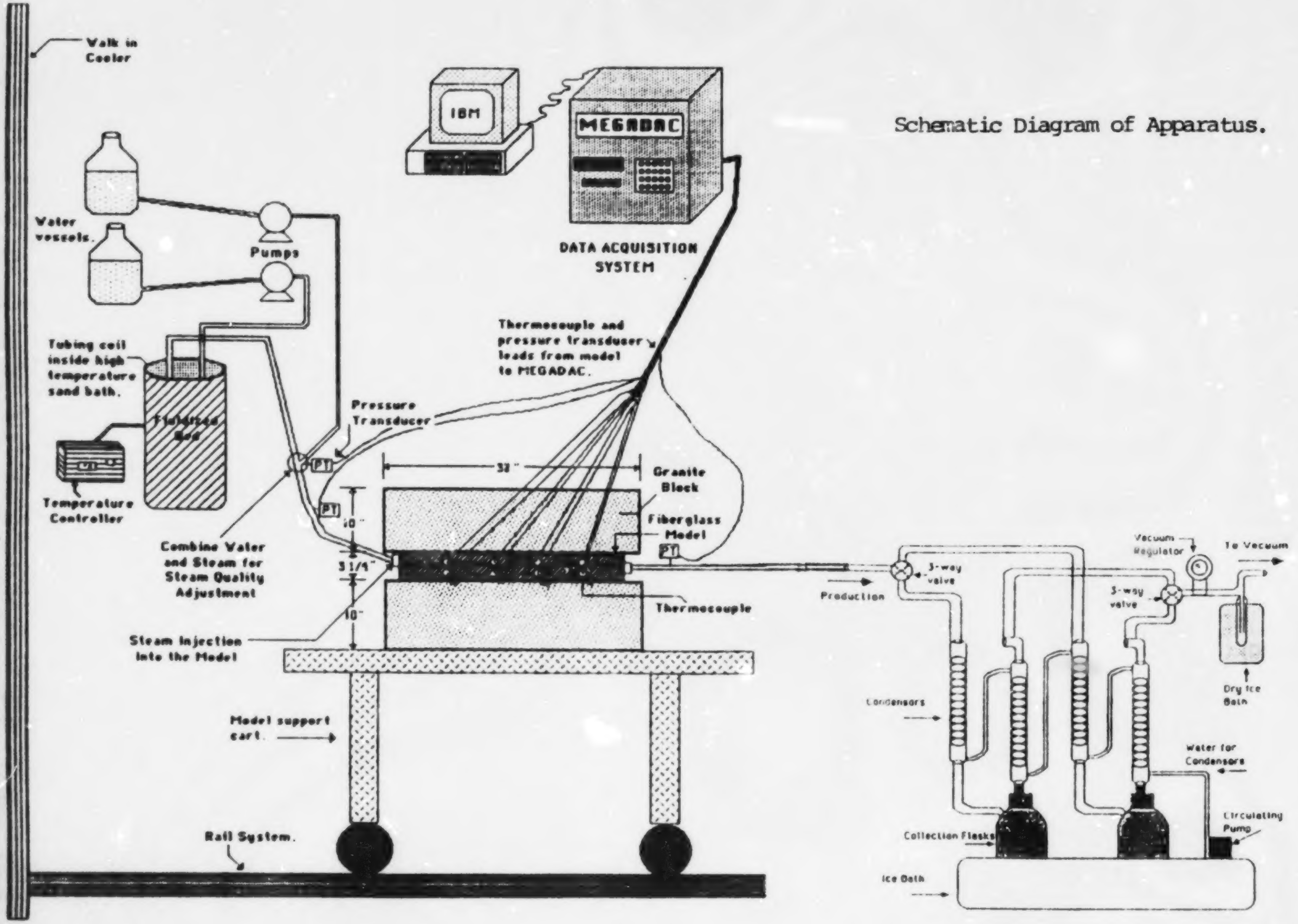
Walk in Cooler
IBM
MEGADAC
DATA ACQUISITION SYSTEM
Water vessels.
Pumps
Tubing coil inside high temperature sand bath.
Fluidized Bed
Temperature Controller
Thermocouple and pressure transducer leads from model to MEGADAC.
Pressure Transducer
PT
PT
32"
10"
3 1/4"
10"
Granite Block
Fiberglass Model
PT
Thermocouple
Combine Water and Steam for Steam Quality Adjustment
Steam Injection into the Model
Model support cart.
Rail System.
Production
3-way valve
3-way valve
Vacuum Regulator
To Vacuum
Dry Ice Bath
Condensors
Water for Condensors
Circulating Pump
Collection Flasks
Ice Bath

Schematic Diagram of Apparatus.

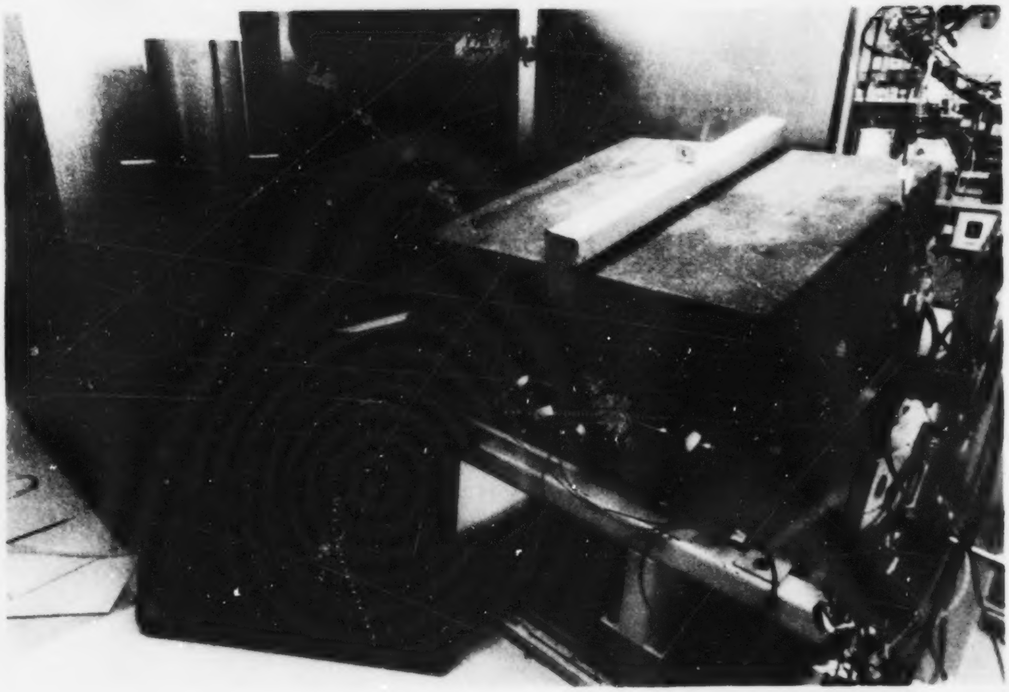

Plate 1: Model Assembly in Inclined Position.

suitable for withstanding this type of loading. Another consideration in the model construction is the heat transfer coefficient of the model material, which should be as low as possible. For these reasons, fiberglass was chosen to fabricate the model. Fiberglass is inexpensive and is also relatively easy to machine. A local company* is able to build the models according to the desired specifications.

The cap and base rocks of the model consist of granite blocks, each with the dimensions of 91.4cm x 91.4cm x 21.6cm thick (36in x 36in x 8.5in thick)†. Heat losses from the lateral boundaries of the model are minimized by applying a two inch layer of cellular neoprene to all exposed surfaces.

5.1.1 Model Wells

Important components of the model are the injection and production wells. These were constructed out of aluminum rod and set into diagonally opposite corners of the molded fiberglass model as seen in Plate 1. The wells have been designed to allow a gate device to be inserted into them which enables the experimentor to selectively choose the injection and production interval.

5.1.2 Porous Media

The scaling groups require that the model permeability be of the order of 4200 darcies. To obtain this high permeability, glass beads with a diameter of approximately 3 mm (6-8 mesh) were purchased.* Because of the high cost of these beads, it is necessary to clean them following every run so that they may be reused. A degreasing solution† is first used to remove most of the oil, then a laboratory detergent is applied by hand to the beads. The beads are dried in a five foot stainless steel tube which can be seen to the left of the cooler doorway in Plate 1.

---

*Triple M Fiberglass, 8135 Wagner Road, Edmonton, Alberta. Cost = $400 ea

†DoAll Edmonton Ltd., 9743-45th Ave., Edmonton, 436-0373.

Thirty-one thermocouples are placed within the model to measure temperatures for the purpose of recording the heat fronts through the model. A diagram is given as Figure 2 to illustrate the thermocouple positions within the model.

5.1.3 Steam Injection System

The steam used in the experiments was obtained by combining a stream of superheated steam with a stream of room temperature water. A low pressure boiler comprised of a fluidized bath** with a 100 foot (30.5 m) length of stainless steel tubing coiled inside was used to generate the superheated steam. By maintaining the superheated steam at a temperature of 120 C, the desired steam quality was obtained.

Plate 2 shows the main componenets of the steam injection system. The boiler assembly can be seen in the

---

*Canasphere Industries Ltd., 3344-58th Ave. S.E., Calgary, Alberta. Cost = $9.25/lb.

†Slik No. 5 degreaser, supplied by Baroid of Canada, Ltd., Calgary, Alta., 263-8740. Cost = $2.40/litre.

**Techne Incorporated, 3700 Brunswick Pike, Princeton, New Jersey. Cost = $5400.

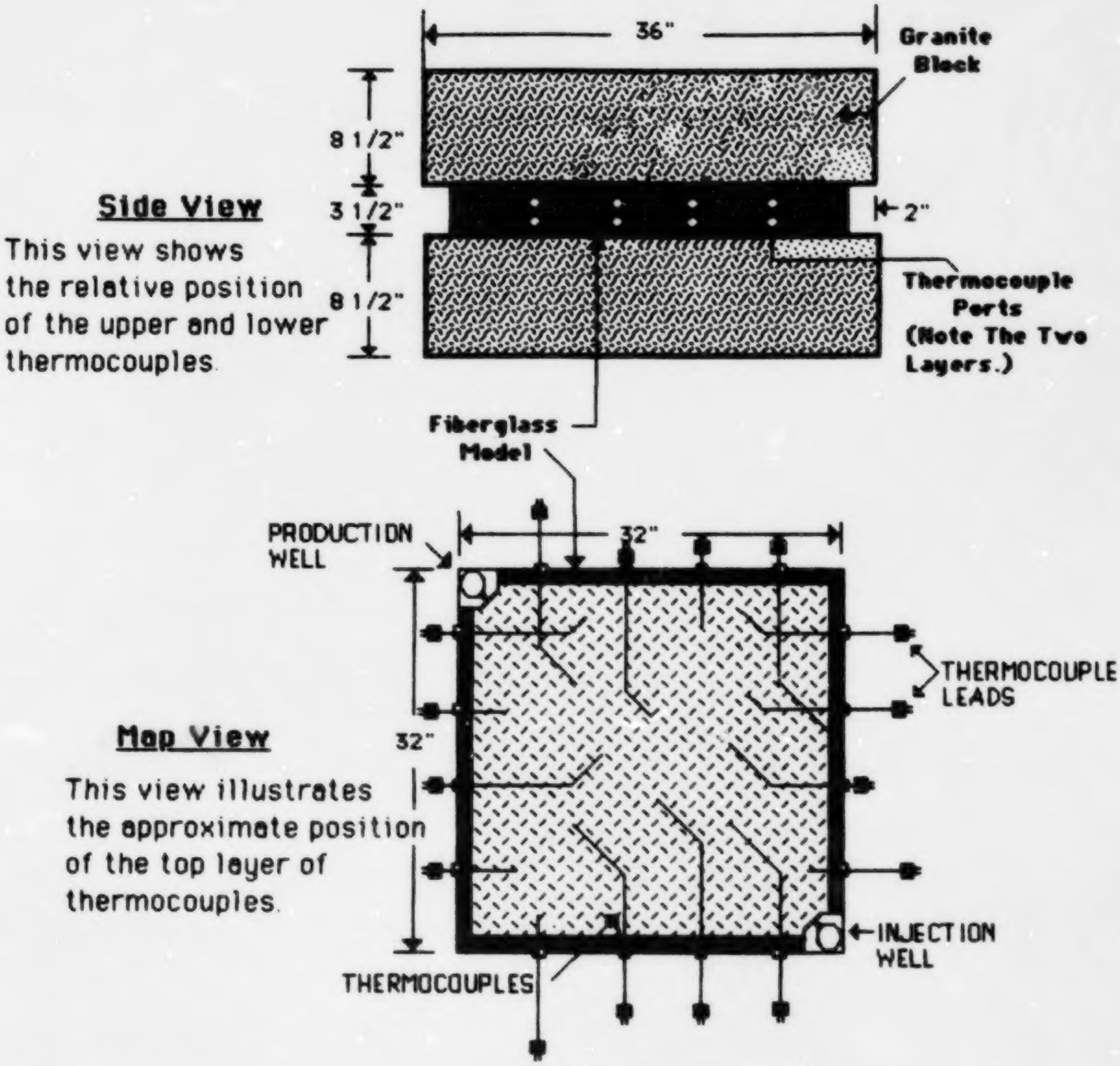

Side View

This view shows the relative position of the upper and lower thermocouples.

Map View

This view illustrates the approximate position of the top layer of thermocouples.

36"
Granite Block
8 1/2"
3 1/2"
2"
8 1/2"
Thermocouple Ports (Note The Two Layers.)
Fiberglass Model
PRODUCTION WELL
32"
32"
THERMOCOUPLE LEADS
INJECTION WELL
THERMOCOUPLES

Figure 2. Diagram of Model Illustrating Thermocouple Positions

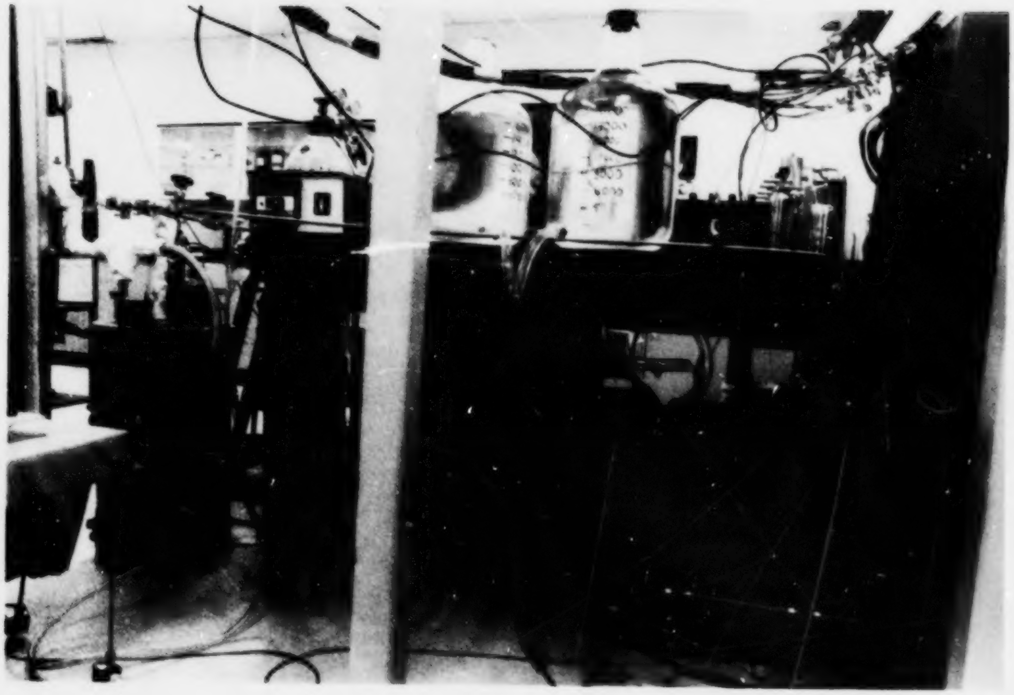

Plate 2: Steam Injection System.

left portion of the plate. The two Milroyal controlled volume pumps used to pump de-aired, distilled water to the steam generator and to the water/steam mixing point are shown on the shelf of the table in the center part of this plate. Some of the stainless steel tubing and fittings required for the steam injection system are also visible in this plate.

5.1.4 Model Cart, Cold Storage

A unique design was employed in the construction of many components of the experimental apparatus. The model support cart is a good example of this. A shaft is welded into the support area for the model and this shaft is connected by a rack and pinion to a gear box. The gear box has a tremendous mechanical advantage so that the entire 4000 pound model apparatus can be rotated with ease to improve the efficiency of the saturation process and to allow the simulation of a dipping reservoir for future runs. The cart is set on castors which roll on a track to facilitate the movement of the model in and out of the cold storage room.

A walk-in cooler was used to cool the model to the initial temperature, as required by the scaling groups. A local company* custom built and installed the 8' x 10' x 7'h walk-in cooler.

---

*Alberta Zero-Temp Industries Ltd., 11440-81st Street, Edmonton, Alberta. Cost = $5387.

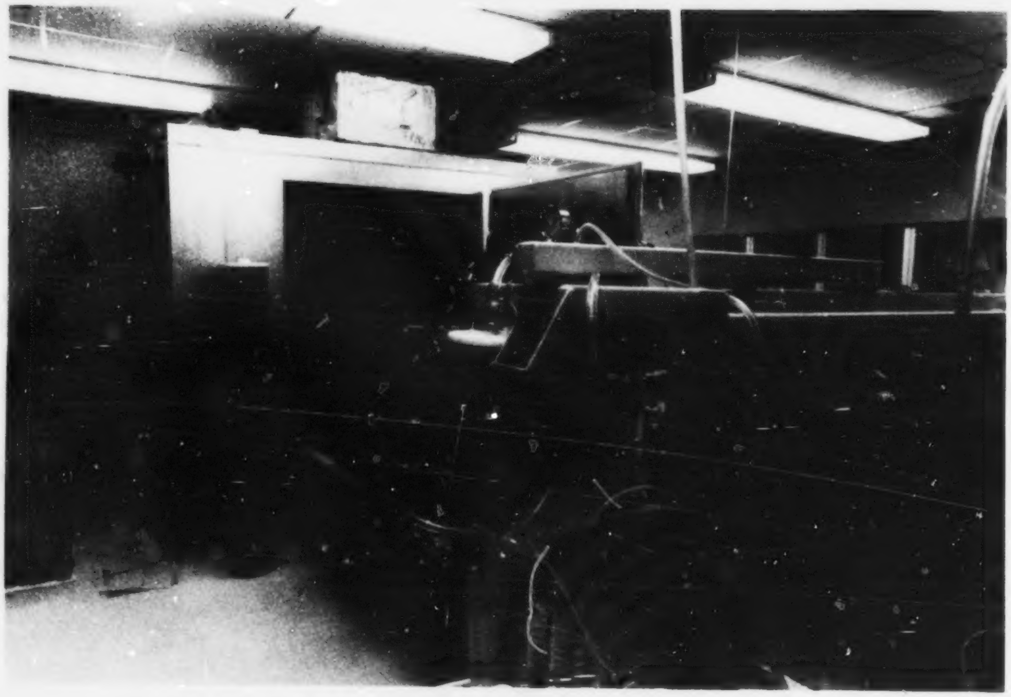

Plate 3: Model Cart and Cold Storage Unit.

Plate 3 shows the model apparatus on the cart, ready to roll into the cooler. Notice the tracks on the floor for moving the cart in and out of the cold storage. The structure shown in the foreground is used to remove the upper granite block to facilitate packing and cleaning operations.

5.1.5 Data Acquisition System

In order to obtain as much information as possible from each experiment, thermocouples* and pressure transducers† are placed in the system to measure temperature and pressure, respectively. A MEGADAC data acquisition unit from Optim Electronics Corporation** is used to collect data during the experimental runs. The MEGADAC is capable of reading up to 128 input channels and these channels can be scanned at a rate as slow as one sample per 30 minutes and as fast as 20000 samples per second. One outstanding feature of this unit is that it can be configured with an IBM Personal Computer and, using the software supplied with the MEGADAC, the IBM PC can control the data acquisition system and process the experimental results.

The IBM PC acts as an interactive interpreter between the data acquisition unit and the experimentor. It prompts the experimentor to send information to the MEGADAC which then performs the desired operation and returns the result to the IBM PC. In addition to these controlling capabilities, the software provides many other features, including graphing of results. A system with such capabilities is essential in a project of this type in which the actual run time is very short. The MEGADAC unit and the IBM PC running the OPTIM User's Software are shown in Plate 4.

---

*Thermo Electric (Canada) Ltd., 8425 Argyll Road, Edmonton, Alberta. Cost = $72.99 (TC and wire).

†Validyne Engineering Corporation, 8626 Wilbur Avenue, Northridge, California.

**Optim Electronics Corporation, Middlebrook Tech Park, 12401 Middlebrook Road, Germantown, Maryland. Cost = $26,000

5.1.6 Collection System

Operating the experiments under vacuum conditions introduces special considerations into the design of a collection system. The pore volume of the model is too large to allow the use of a single container to collect the produced fluids and very little information could be obtained from a single sample. Therefore, the system uses two flasks to collect the produced fluids and these flasks are configured so that they may be isolated from the vacuum and emptied individually. Since the pressure in the model during a run is low, considerable vapourization of the oil can be expected. For this reason, the collection system includes a series of condensors and cold traps to collect all of the produced fluids. Figure 3 shows the configuration of the collection system.

The initial production temperature is low (approximately 3 C), so in order to prevent clogging within the production lines, the early production stream was warmed by flowing hot tap water through the first series of

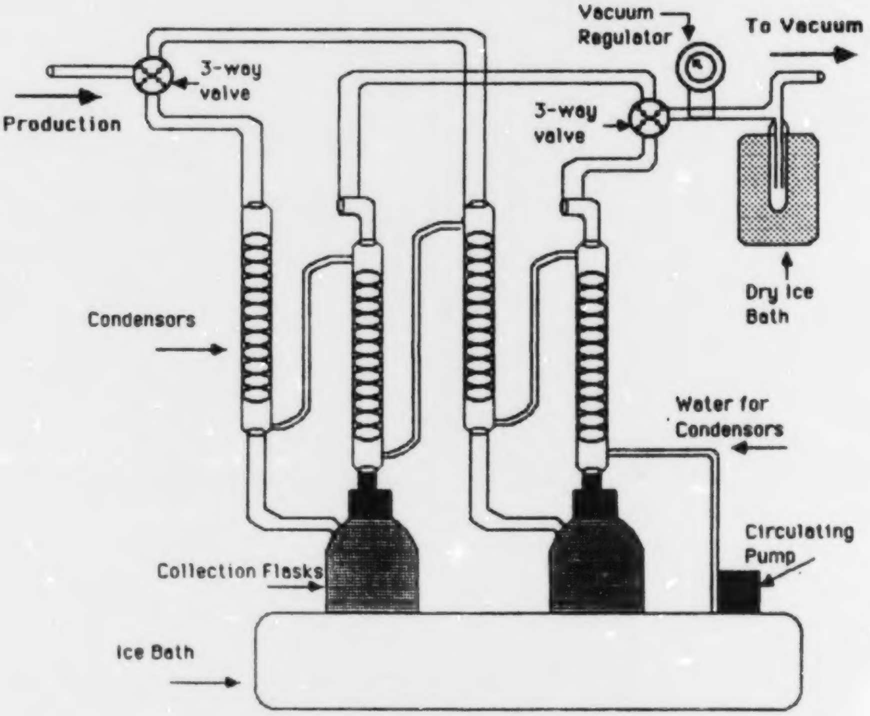
Vacuum
Regulator
To Vacuum
3-way
valve
Production
3-way
valve
Dry Ice
Bath
Condensors
Water for
Condensors
Circulating
Pump
Collection Flasks
Ice Bath

Figure 3. Produced Fluids Collection System

Plate 4: Data Aquisition System.

condensors. However, after injecting approximately half a pore volume of steam, the production temperature was considerably higher. The hot water previously running through the first series of condensors was then replaced by ice water so that the produced fluids were completely condensed.

Since the vacuum was applied through the collection system, it was expected that some of the liquid would be vapourized again, after reaching the production flasks. For this reason, another set of ice water condensors and finally a carbon dioxide cold trap were included in the collection system.

5.1.7 Model Fluids

5.1.7.1 Oil for the Aberfeldy Model

A table detailing the relationship between the required model oil viscosity and the Aberfeldy prototype oil viscosity was presented in a previous chapter as Table 4. Using values from the upper part of this table, which Stegemeier, Laumbach, and Volek[37] indicate are the most accurate, an average value of the ratio of model oil viscosity to prototype oil viscosity was found to be 7.26. If the prototype versus model temperature relation, given by equation (6), is applied to this viscosity relationship, the table of values presented in Table 5 can be obtained.

To obtain the desired temperature - viscosity profile for the model oil, a refined MCT 30 base oil, Faxam 100,

Table 5. Temperature vs. Oil Viscosity for Aberfeldy Prototype Oil and Model Oil

Prototype Temperature (C)	Prototype Oil Viscosity (mPa-s)	Model Temperature (C)	Ideal Model Oil Viscosity (mPa-s)
23.9	1275	3.2	9256.5
32.2	560	5.6	4065.6
65.6	90	15.1	653.4
135.0	12.5	35.0	90.75
301.7	1.29	82.6	9.37

supplied by Imperial Oil Limited* was used. A temperature - viscosity profile comparing the ideal curve and the curve given by the Faxam 100 oil is presented as Figure 4. The inclusion of the temperature scaling relationship creates a distortion in the ideal model oil curve which cannot be represented by a real oil. However, the Faxam 100 does provide a reasonable match.

5.1.7.2 Materials for Heavy Oil and Light Oil Runs

In addition to the Aberfeldy model experiments, runs were conducted with a higher viscosity oil (11000 mPa-s at room temperature) which represented a prototype oil with reservoir temperature oil viscosity of approximately 13000 mPa-s, and runs were conducted with a lower viscosity oil (50 mPa-s at room temperature) which represented a prototype oil with reservoir temperature oil viscosity of approximately 25 mPa-s. Tables are given on the following page indicating the temperature - viscosity relationship of both of these oil, in prototype terms.

5.2 Model Packing and Saturation

5.2.1 Model Packing Procedure

Due to the size and shape of the model used, packing methods such as tamping or vibrating are not practical. Therefore, a 'particle distributor' was employed to pack the glass

---

*McEwen's Fuels & Fertilizers Ltd., ESSO Bulk Plant Agent, 3704 92nd Ave., Edmonton, Alberta.

Table 6. Temperature vs. Oil Viscosity for the Heavy Oil

Model Temperature (C)	Ideal Model Oil Viscosity (mPa-s)	Prototype Temperature (C)	Prototype Oil Viscosity (mPa-s)
3.18	95000	23.9	13085.4
5.55	81000	32.2	11157.0
15.10	36000	65.6	4958.7
35.00	7600	135.0	1046.8
82.63	4500	301.7	619.8

Table 7. Temperature vs. Oil Viscosity for the Light Oil

Model Temperature (C)	MCT 10 Oil Viscosity (mPa-s)	Prototype Temperature (C)	Prototype Oil Viscosity (mPa-s)
3.0	185.5	23.3	25.6
11.0	96.8	51.2	13.3
32.0	33.1	124.7	4.6
49.0	17.6	184.1	2.42

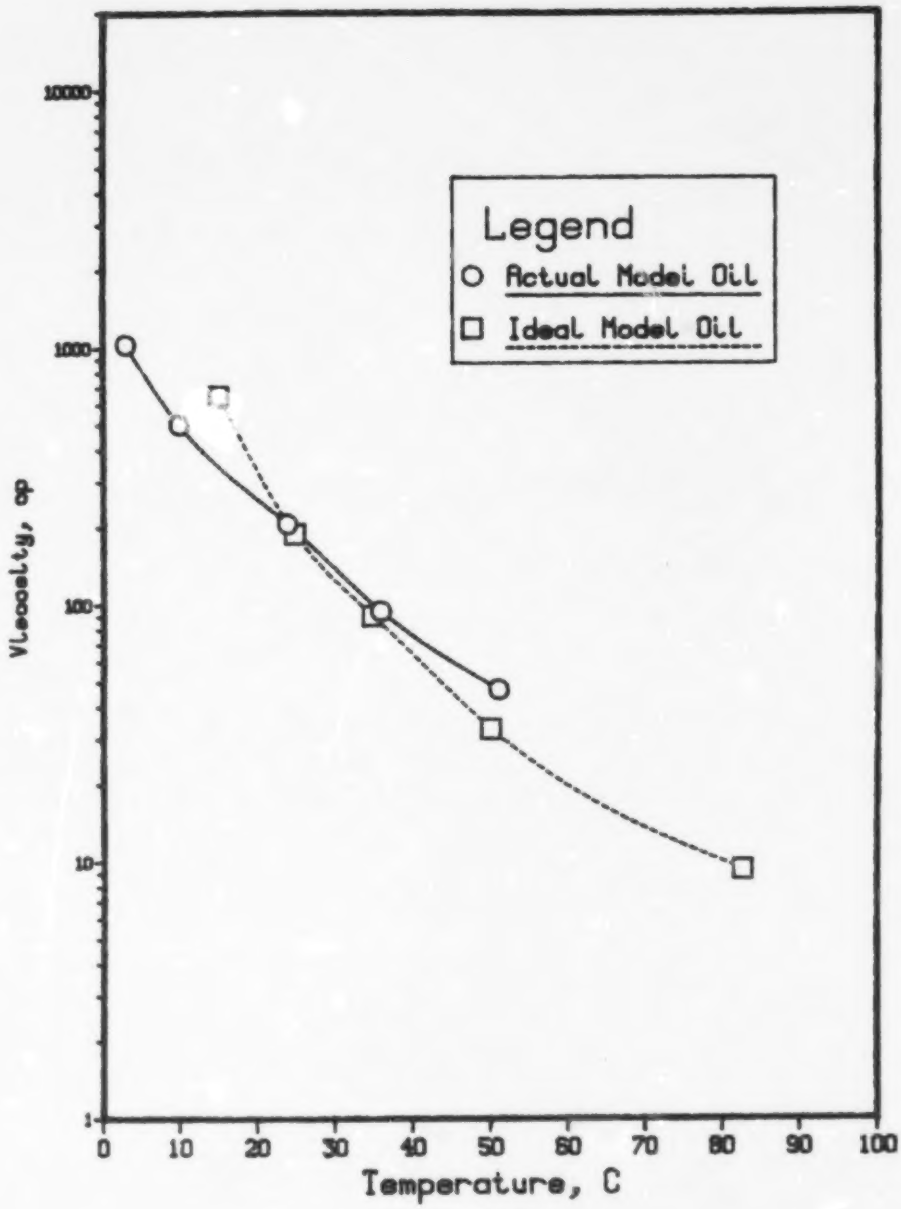

Figure 4. Temperature-Viscosity Profile for Ideal and Actual Model Oil

beads in the model. This method of packing was first proposed by Currie and Gregory[36] and later modified by the Gulf Research & Development Company as reported in a paper by Wygal.[37]

It is claimed that the particle distributor can be used to obtain packs which are mechanically stable with uniform properties throughout, and which may be accurately reproduced. The tamping and vibrating method of packing is said to create packs which are usually non-uniform or unstable.

The success of the particle distributor is a result of the beads hitting the pack singly after being evenly distributed by a set of sieves. Part of the energy of the falling bead is transferred to the surface beads which are thereby knocked into more stable positions. As the pack grows, the surface reportedly appears fluid and alive for a depth of two or three particle diameters.

The particle distributor is easily made. For this project, it was constructed using five wire mesh screens with 5/8 inch openings. The screens were enclosed in a plywood box designed to fit over the large model. A diagram of the particle distributor is given in Figure 5. The model was packed by allowing the beads to pass through a metering board onto the screens at a uniform rate. After passing a sufficient number of beads through the particle distributor and into the model, the particle distributor is removed and the excess beads are trimmed off of the model surface. The

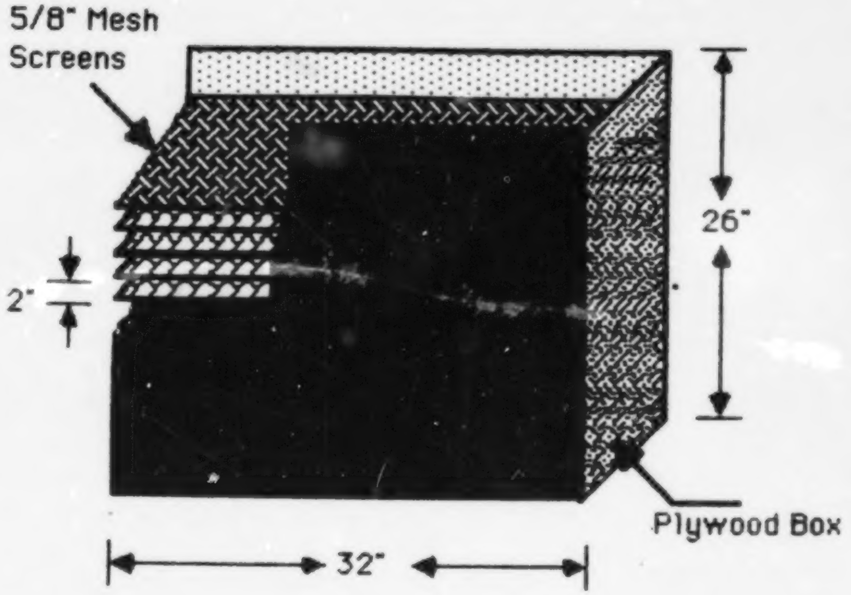
5/8" Mesh Screens
26"
2"
Plywood Box
32"

Wygal Particle Distributor

Figure 5. Model Packing Device

porosities of the bead packs were consistently of the order of 33%, with very little variation.

5.2.2 Model Saturation

After packing the model with glass beads, a Teflon sheet was placed above the model with a thin layer of silicone applied as a sealant to provide a vacuum tight seal. A rubber sheet was placed on top of the Teflon sheet to ensure that complete contact was made between the model and the upper granite block, which was then set in place above the model, and the entire apparatus was tilted.

Six large saturation ports were incorporated into the model (three on each of two opposing sides) to improve the efficiency of the saturation process. With the apparatus in a tilted position, fluids entered the model from the downdip end and thus the fluid flow into the model proceeded with a gravity stabilized front. To begin the saturation process, a deep vacuum was applied at the updip end and de-aired, distilled water was pulled into the model through the saturation ports at the downdip end. This continued until the model was completely saturated with water. The amount of water taken into the system was carefully measured and the model porosity calculated.

Valves were installed at the injection and production points. When the model was completely saturated with water, these valves were closed so that a vacuum was maintained within the model, and the water injection lines were replaced by oil injection lines. Next, oil was drawn into the model by a method similar to that described for the water. The amount of oil taken into the model was measured so that the initial oil saturation could be determined.

The above saturation procedure worked well for the Aberfeldy model oil (Faxam-100) and the light oil (MCT-10), but the heavy oil required a modification of the above procedure. It was necessary to warm the heavy oil to about 75 degees C before attempting to pull it into the model. Even then, the saturation process required ten hours, more than seven of which were needed to pull the oil into the model.

After saturation was complete, the apparatus was rolled into the cooler to bring the model to the low initial temperature required by the scaling groups. Cooling the large model to 3 C took between 24 and 36 hours.

5.2.2.1 Preparing the Bottom Water Model

Run 15 was a continuous steamflood in a bottom water model. The water layer was established by packing the lower layer of the model with beads and then introducing the volume of water necessary to create the desired bottom water thickness. The original intention was to create a layer of water one inch thick (2/5 of the reservoir thickness). An average final porosity of the bead pack was assumed to be 33% (based on the experience of previous runs). Thus the pore volume of the model would be 0.33 times 42005 cc (the total volume of the empty model) which equals 13862 cc.

Therefore, 2/5 of this was expected to make up the desired one inch bottom water layer. This volume of water was added to the packed model, and the model was placed in a level position in a freezer to freeze the bottom water into place.

To complete the saturation procedure for this run, a vacuum was applied and 9490 cc of de-aired water was pulled into the upper part of the model. Some thawing of the frozen water layer may have occurred in this step, but because the water saturation procedure was relatively quick, the amount of thawing was probably minimal. (The thawing at this point could be further reduced in future runs by saturating with ice cold water.)

Next, oil was drawn into the model to displace the liquid water. The volume of water displaced during this phase of the saturation process was 11520 cc, which indicates a significant amount of thawing occurred in the frozen layer. Calculations based on the assumption that the oil saturation in the oil zone was 92% (which was typical of many runs), indicated that the bottom water layer was 0.43 inches thick (17.2% of the total formation thickness).

5.3 Conducting the Experiments

During the time the model was cooling, other work was performed in preparation for the run. The injection bottles were filled with distilled water and a vacuum was applied to remove any gas which was trapped in the water. All injection and production lines were inspected for leaks and adjusted or replaced if necessary. The thermocouples external to the model were inspected and replaced if necessary. In addition, all of the pressure transducers were checked or calibrated prior to each run. Just before the model was taken from the cooler, the collection system was prepared by filling the upper vacuum cold trap with dry ice and obtaining hot water and ice for the condensors.

When the model apparatus had cooled to the initial temperature as dictated by the scaling calculations, it was rolled out of the cooler and the thermocouple and pressure transducer leads were attached. The data acquisition unit was monitored to ensure that all of the thermocouples and pressure transducers were functioning properly and giving reasonable readings. The injection and production lines were then attached and the steam bypass valve was opened. Steam was flowed through the bypass line until it had stablized at the temperature required for the run, typically 65 C.

With all of the preparatory work complete, the data acquisition unit was reset for the new experiment and the production and injection valves were opened simultaneously. The MEGADAC was programmed to scan each thermocouple and pressure transducer once every thirty seconds. The data was printed continuously and was also saved on the IBM hard disk drive.

The produced fluids were collected in two, 2000 cc flasks which were emptied into a series of 2000 cc graduated cylinders. In this way, instantaneous oil and water recovery could be observed as a function of each two litres of total production. Steam injection was continued until between one and a half to two pore volumes had been injected, unless problems were encountered.

5.4 Data Analysis

Following the run, a table of instantaneous and cumulative production as functions of the number of pore volumes of steam injected was prepared. Several plots were generated for each run to analyze the data. These included the following:

* A plot of cumulative recovery vs. pore volumes of steam injected.
* A plot of instantaneous oil and water recovery as a function of pore volumes of steam injected.
* A plot of instantaneous oil-steam ratio as a funtion of the cumulative oil production.
* Temperature profiles at 0.25, 0.50, 0.75, and 1.00 pore volumes of steam injected.

In addition to these plots, some plots were generated to compare the production response resulting from varying recovery schemes and experimental conditions.

6. EXPERIMENTAL RESULTS AND DISCUSSION

Twenty-two experimental runs were attempted as part of this work. The initial conditions for each of these experiments are presented in Table 8 on the following page. The successful experiments were of the following types:

1. Preliminary runs on a small model. These runs were conducted to gain familiarity with the apparatus and to ensure that all the components were operating satisfactorily.
2. Continuous steamflood conducted on model saturated with water only. This run was conducted to observe the heat flow within the model and to gain experience with the large model.
3. Continuous steamfloods conducted on the Aberfeldy model.
4. Continuous steamfloods conducted on a model designed to represent a light oil prototype.
5. Continuous steamfloods conducted on a model saturated with an oil much more viscous than the Aberfeldy model oil (9250 mPa-s at room temperature).
6. Steamflood following a waterflood. This run was conducted to examine the recovery of waterflood residual oil by steam injection and to analyze the ability of the vacuum model to simulate such a process.
7. Continuous steamflood conducted on the Aberfeldy model with a bottom water zone.
8. Cold water slug runs. These runs were conducted to examine the possibility of driving a small slug of steam

TABLE 8: INITIAL CONDITIONS FOR EXPERIMENTS

Run#	Vol Water Inj to Sat (cc)	Porosity (%)	Vol Oil Inj to Sat (cc)	Swi (%)	Soi (%)	Initial Temp. (C)	Oil Type	Run Type
1								Preliminary Run
2								Preliminary Run
3								Preliminary Run
4	13590	32.4	0.00	100.00	0.00	23.0	(Water)	Continuous Steamflood
5	14180	33.8	12300	13.26	86.74	2.5	Faxam-100	Continuous Steamflood
6	13990	33.3	12160	15.51	84.49	1.9	Faxam-100	Continuous Steamflood
7A	13040	31.0	11420	12.42	87.58	3.0	Faxam-100	Cold Waterflood
7B						23.9	Faxam-100	Room Temperature Waterflood
7C						2.7	Faxam-100	Continuous Steamflood
8	15080	35.9	*			3.0	Heavy Oil	Unsuccessful Run
9	13800	32.9	12100	12.32	87.68	4.0	Heavy Oil	Continuous Steamflood
10	12700	30.2	11680	8.00	92.00	4.0	Faxam-100	Continuous Steamflood
11	12945	30.8	11040	14.72	85.28	3.0	MCT-10	Unsuccessful Run
12	14050	33.5	12535	10.78	89.22	3.0	MCT-10	Continuous Steamflood
13	12660	30.1	11670	7.82	92.18	3.0	MCT-10	Continuous Steamflood
14	13910	33.1	12550	9.78	90.22	3.0	Faxam-100	Unsuccessful Run
15	13136	35.9	11520	12.30	87.70	3.0	Faxam-100	Steamflood on Bottom Water Model
16	13620	32.4	12730	6.53	93.47	3.0	Faxam-100	Unsuccessful Run
17	13820	32.9	12800	7.38	92.62	3.0	Faxam-100	Cold Water Slug Run
18	13880	33.0	12770	8.00	92.00	3.0	Faxam-100	Cold Water Slug Run
19	13970	33.3	12785	8.48	91.52	3.0	Faxam-100	Cold Water Slug Run
20	13510	32.1	12620	6.59	93.41	3.0	Faxam-100	Unsuccessful Run
21	13660	32.5	12890	5.64	94.36	3.0	Faxam-100	Unsuccessful Run
22	14310	34.1	11600	18.94	81.06	3.0	Faxam-100	Hot Waterflood
AVERAGE	13676	32.8	12186	10.50	89.50			

Faxam-100 represents Aberfeldy prototype. (Viscosity = 208 cp at 23 C)
Heavy Oil. (Viscosity = 9256.5 cp at 24 C)
MCT-10 represents a light oil prototype. (Viscosity = 60 cp at 23 C)

* Note: The Heavy Oil was too thick at room temperature to saturate the model.

with a continuous cold waterflood.

9. Hot water slug run. This run was conducted to determine whether steam injectivity could be improved by the initial injection of hot water.

The data analysis following each run included a table showing all of the important experimental parameters and a listing of the production as a function of steam or water injection. Plots of cumulative recovery versus pore volumes of steam injected, plots of instantaneous oil and water production as a function of cumulative injection, plots of instantaneous oil-steam ratios, and plots comparing the recoveries of several runs are also included in the data analysis. In addition, temperature profiles are presented for each run at intervals of 0.25, 0.50, 0.75, and 1.00 pore volumes of steam or water injected.

6.1 Model Design and Operation

Extensive details concerning the scaling of the steam injection process, the equipment included in the apparatus, and procedures used to conduct the experiments are presented in previous chapters. A brief summary of the model design and operation is presented in this section.

Three models were constructed for this project to represent the Alberfeldy prototype; two with scaling factors of 400 to 1 (one twice as thick as the other) and one relatively large model with a scaling factor of 173.2 to 1. Each model was designed to simulate one quarter of a five-spot pattern and as such, each had one injection well and one production well in diagonally opposite corners. The smallest model was used for the preliminary experiments (Runs 1-3) because the degree of work involved in preparing for and conducting these experiments was proportionally less than the work necessary for the larger model experiments.

Most of the experiments were conducted in the large scale model. This model has dimensions of 81.28cm x 81.28cm x 6.35cm thick (32in. x 32in. x 2.5in.) which, when used to represent the Aberfeldy prototype (20 acre pattern, 11m thick), results in a three-dimensional geometric scaling factor of 173.2. It is constructed out of molded fiberglass and is fitted with 31 thermocouples, placed in two layers within the model. Figure 2 gives a sketch of the model and indicates the position of the thermocouples within the model. The model wells were fabricated from aluminum and were designed to allow a gate device to be inserted into them so that the injection and production intervals could be selectively chosen as required.

In preparation for a run, the model was packed with 3 mm (6-8 mesh) glass beads which gave a permeability of approximately 4200 darcies. A Teflon sheet was sealed to the top of the fiberglass model with silicone and a vacuum was applied to the pack. When the silicone had set sufficiently, so that a vacuum was maintained in the model, the model pack became extremely rigid, and was ready to saturate. The model was saturated in an inclined position with the fluids entering the model from the downdip end through specially designed saturation ports. It is crucial that a vacuum be maintained during the entire saturation process.

With oil and water saturation complete, two clamping devices were attached to the model to help maintain the vacuum in the event that the internal pressure momentarily exceeded atmospheric during the run. The model was then rolled into the cold storage unit and left to cool for 24 to 36 hours. During this time, the distilled water used for the run was de-aired (and cooled if necessary). The injection pumps were calibrated and all other components of the apparatus were inspected and calibrated if required.

When the model had reached the desired inital temperature (3 C) as dictated by the scaling calculations, it was rolled out of the cooler and the thermocouple and pressure transducer leads were attached and the injection and production lines were put in place. When the steam had stabilized at the desired temperature and the data acquisition unit had been programmed for a new experiment, the run was started. For a typical steam injection run, the steam entered the model at a temperature of about 65 C and at a flow rate of 230 cc/min

The first few minutes of each run were the most critical. For a successful run, oil production was almost immediate, however, as shown in Table 8, not all runs were successful. A common problem with the runs was that the initial steam injectivity could not be attained for the flow rates dictated by the scaling criteria. In a few cases (Runs 11,14,16) this resulted in overpressuring the model to the point where even the clamping device could not maintain the vacuum seal and thus, the run was aborted. Runs 20 and 21 were spoiled when plugging of the production lines by silicone was not detected prior to the runs.

The heavy oil runs (Runs 8 and 9) posed a special problem with respect to the saturation process. Before the vacuum could successfully draw the heavy oil into the model, the oil had to be warmed to about 75 C and even then, seven hours were required to pull the oil into the model.

In general, the packing and saturation procedures were trouble-free (except for Run 8, as discussed). Table 8 shows that the porosity of the bead pack was consistently of the order of 33% and that the initial oil saturation was, in general, quite consistent. The initial temperature of the model was consistent at the model design temperature of 3 C.

6.1.1 Operational Difficulties

Since this project entailed the design and construction of the entire apparatus, several modifications were necessary in the early stages. These included improving the saturation procedure, modifying the collection system, and incorporating better data reduction techniques. However, at the completion of the preliminary runs, most of the necessary improvements had been made.

Some problems could not be remedied with as much success. As noted previously, injectivity problems at the beginning of some runs prevented the continuous injection of steam at the design flow rate. It was occasionally necessary to turn off the injection pumps while maintaining the vacuum at the production end in order to lower the pressure within the model. It is felt that these brief periods without steam injection did not significantly affect the experimental results.

The lack of precise control over the temperature of the steam generating bath posed some difficulties. The boiler was occasionally unable to maintain the necessary temperature and as a result, the steam quality may have been slightly lower than it was designed to be for a few runs. The hot water slug run did not go off as planned because the steam generator was not capable of increasing temperature during the run. The plan was to begin the run with hot water at an injection temperature of about 40 C and gradually increase the temperature to a steam temperature of 65 C.

6.2 Base Steamflood

In this experiment, the model was saturated with 100% water and steamflooded. The purpose of this run was to examine the model and overall system operation, and to observe the general pattern of flow distribution. The temperature profiles for this run at 0.25, 0.50, 0.75 and

1.00 pore volumes of steam injected are presented as Figures 6, 7, 8 and 9, respectively. Each temperature profile clearly shows the heat distribution through the model, and examining them in series illustrates the progression of the heat front.

6.3 Continuous Steamfloods on Aberfeldy Model

Runs 5,6,7,10, and 17 to 19 were steamfloods conducted on a model with all pertinent parameters designed to simulate the Aberfeldy reservoir. Run 7 involved a steamflood following a waterflood and will be discussed in a later section. Similarly, Runs 17 to 19 were designed to simulate a particular recovery scheme (cold water slug runs) and also will be discussed in a separate section.

The remaining Aberfeldy runs (Runs 5,6, and 10) were conducted with steam temperature and pressure of about 24 kPa and 65 C, respectively, and a steam quality of about 70%. The average steam flow rate was 230 cc/min and the average initial oil saturation was 87.7%. Injection for each of these three runs was into the lower half of the reservoir while the production well was opened over the entire interval. Tables 9, 10, and 13 give a summary of the important experimental parameters of each run. Table 13 also details the recovery for Run 10 as a function of pore volumes of steam injected.

Run 5 was halted prematurely when the apparatus developed a leak after about 25 minutes of steam injection

(0.45 pore volumes of steam injected). However, at this point, 6.6% of the original oil in place was recovered which is typical of the initial production response observed in the other steamflood runs. This represents an oil-steam ratio of approximately 0.13.

Figures 10 and 28 present the cumulative recovery as a function of the pore volumes of steam injected for Runs 6 and 10, respectively, and plots of instantaneous oil and water production as a function of cumulative injection are given in Figures 15 and 29 for Runs 6 and 10, respectively. These figures indicate that following breakthrough (which was observed during the experiments to be at about 0.13 pore volumes injected), the cumulative oil recovery still increases at an appreciable rate. This is probably because the steam advance at this point is irregular, and pockets of oil are recovered sporadically. If the steam zone had advanced in the classical sweep pattern (as predicted by an assumption of frontal drive), there would be very little oil production after breakthrough.

The average oil-steam ratio for Run 10, at 2.114 pore volumes of steam injected, was 0.1369. Total recovery to this point was 31.48% of the original oil in place. The total oil recovery of Run 6 was considerably lower than that of Run 10 (21.9% OOIP after injecting 2.34 pv) which is illustrated by plotting the two recovery curves together, as done in Figure 30. However, it can be seen that the initial oil production response for the two runs is similar and that the production response only begins to differ signicantly after breakthrough.

Temperature profiles for Run 6 at 0.25,0.50,0.75, and 1.00 pore volumes of steam injected are presented as Figures 11, 12, 13, and 14, respectively, and those for Run 10 at 0.25,0.50, 0.75, and 1.00 pore volumes of steam injected are presented as Figures 23, 24, 25, and 26, respectively. An examination of these temperature profiles shows an unexpected response in Run 10, relative to that of Run 6. Figure 23, for 0.25 pore volumes injected, shows that the higher isotherms are advancing faster in the lower part of the model than near the top. This is contrary to the expected trend, based on experiences with steam override. It is also quite different from the trend shown in Figure 11 for Run 6 at a similar stage of the injection process. Figures 24 and 25 for Run 10 at 0.50 and 0.75 pore volumes injected, respectively, show that this trend persists, but that although the advance is relatively uniform in the upper part of the model (almost radial), it is highly irregular in the lower part. This is typically indicative of hot water advance. With 0.75 pore volumes of steam injected, the 15 C isotherm has reached the producer in the upper layer, while in the lower layer, the 25 C isotherm has reached the producer. Upon the injection of 1.00 pore volumes of steam for Run 10, the temperature distribution in the lower layer is very irregular, but most of the formation had been heated to over 35 C.

If Run 10 involved hot water injection only at the outset, it is possible that the hot water zone would stay in the lower part of the model and that heating of the upper part of the reservoir would only be accomplished by convection. This is a reasonable possibility, especially when one considers the that the density of the water is higher than that of the oil, and that the injection well is completed over the lower half of the formation. Run 22 provides some support for this point of view in that it was designed and conducted as a hot waterflood in the initial stages of the run and its temperature profiles (given as Figures 77, 78, 79, and 80 for 0.25, 0.50, 0.75 and 1.00 pore volumes of hot water injected, respectively) show a trend similar to that of Run 10. Further details concerning Run 22 will be presented in a later section.

On the other hand, if steam was initially injected into the formation of Run 10 (as was intended), and the steam rapidly condensed, it is conceivable that the condensate would segregate and eventually develop a path for steam as well. It is possible that excessive condensation of steam led to steam channeling in Run 10. Figure 27 shows the instantaneous oil-steam ratio as a function of cumulative oil production for Run 10. It shows that the initial period of clean oil production was relatively short compared to that of other runs (see Figures 38, 43, 58, 66, and 74) which suggests that a clear cut oil bank was not formed, rather, the displacement process consisted of rapid mobilization of the in-place oil due to the unstable advance in the lower portion of the model, and displacement of the mobilized oil by steam.

6.4 Steamflood Following a Waterflood

Run 7 was comprised of a waterflood prior to a steamflood. The run was conducted with all experimental parameters designed to simulate the Aberfeldy prototype, the model oil being Faxam-100 with room temperature viscosity of 208 mPa-s. During the run, the fluids were injected into the lower half of the reservoir with water injection at approximately 100 cc/min and the subsequent steam injection at 225 cc/min The initial oil saturation was 90.4% and the model porosity was 31.0%. All pertinent experimental data for this run is presented in Table 11.

In the first part of the run, water at the same temperature as the model (3 C) was injected. After injecting 1.17 pore volumes of water, at which point 22.5% of the in-place oil had been recovered, the injected water temperature was raised to the room temperature of 23 C. The waterflood was terminated at a water/oil ratio of approximately 6, at which time the oil recovery was 26.5% and the average oil saturation in the model was 63.7%. The steamflood was started at this point.

The steamflood was continued to a cumulative pore volume of water injected equal to 2.867 (1.05 pore volumes of steam injected), at which point the cumulative oil recovery was 32.40%. The incremental oil recovery by steam was 5.9% of the original oil in place (8.1% of the waterflood residual oil saturation) which represents a very low recovery for a steamflood. Nevertheless, the temperature profiles for this steamflood given as Figures 16, 17, 18, and 19 for 0.25, 0.50, 0.75, and 1.00 pore volumes of steam injected, respectively, indicate a very uniform advance of the steam zone, again with the condensate underride dominating the steam override. Figure 20 shows the cumulative recovery of oil as a function of the injected fluid volume and indicates where the processes were altered. Figure 22 shows the instantaneous oil and water production as a function of cumulative injection. These curve show that the ultimate recovery for this run with an initially waterflooded porous medium, is similar to the recovery obtained in Run 10, and distinctly better than the recovery obtained for Run 6. It is recalled that in Run 7, 26.5% of the original oil in place was produced in the waterflood stage, with only 8.1% waterflood residual oil being recovered upon the injection of 1.05 pore volumes of steam. It is believed that the waterflood helped to create adequate injectivity for steam, but at the same time it led to an inefficient utilization of the injected steam. Figure 21 shows the instantaneous oil-steam ratio for the steamflood portion of this run which further illustrates the poor response of the reservoir to steam injection.

6.5 Steamflooding a Highly Viscous Oil

Run 9 utilized a highly viscous oil, the viscosity - temperature relation for which is given in Table 6. Steam injection was over the lower half of the model at a rate of 228.8 cc/min The initial oil saturation was 87.7 % and the model porosity was 32.9 %. Oil recovery for this run was minimal (1.7% OOIP).

Figures 31 and 32 show the temperature profiles for this run at 0.50 and 1.00 pore volumes of steam injected, respectively. It is interesting to note, that unlike the runs discussed previously, in this run the steam clearly sweeps the upper part of the model. Figure 31 shows that at 0.50 pore volumes of steam injected, the steam front in the lower part of the model lags behind the top by almost 100% (i.e. the area inside the 30 C isotherm is approximately twice that of the bottom).

6.6 Light Oil Steamfloods

Run 12 and 13 utilized a light oil (60 mPa-s at 23 C) to simulate a steamflood in a conventional oil reservoir. Tables 14 and 15 give the important experimental parameters for Runs 12 and 13, respectively, and also present a tabulation of the oil recovery for each run as a function of the volume of steam injected. In Run 12, the production well was only opened over the lower half of the formation while in Run 13 the production well was opened over the entire interval. Oil recovery after the injection of about one pore volume of steam was 29.72% for Run 12 and 29.26% for Run 13. Figures 37 and 44 show the instantaneous oil and water production as a function of the cumulative steam injected for Runs 12 and 13, respectively. A comparison of the cumulative recovery behavior for the two runs is given in Figure 45. This indicates that the production interval had very little effect on the cumulative oil recovery. The small departure in the curves is probably due to experimental error.

The temperature profiles for Run 12 at 0.25, 0.50, 0.75 and 1.00 pore volumes of steam injected are given as Figures 33, 34, 35, and 36, respectively, while those for Run 13 are given as Figures 39, 40, 41, and 42, respectively. A comparison with the previously discussed Aberfeldy model runs in which the oil viscosity was 208 mPa-s at 23 C, immediately shows the much steeper temperature fronts, as indicated by the proximity of the contours. Figure 33 shows that at 0.25 pore volumes of steam injected into the model of Run 12, the higher temperature contours at the top and the base of the model are almost coincident, however, the lower temperature contours (e.g. 20 C) advance more rapidly in the lower part of the model. Thus, there is considerable evidence of a steam front advancing in the upper part of the formation while condensate is segregating and flowing in the lower part. By the time one pore volume of steam had been injected into the model in Run 12 (Figure 36), the picture becomes more complex. It can be seen that the steam spreads areally over most of the formation, with a strong temperature profile developing near the base of the sand as well. The temperature profiles for Run 13 (Figures 39, 40, 41, and 42) are very similar to those of Run 12. The agreement between these and the cumulative recovery responses of the two runs serves to show the good reproducibility of the results.

The oil recovery for these two runs was the highest observed of all the runs which were conducted as part of this work. The oil-steam ratio for Run 12 as a function of the volume of steam injected is shown in Figure 38 and that of Run 13 in Figure 43. The two curves are similar, but higher initial production response is observed in Run 12. However, the oil-steam ratio in both cases achieves a value of approximately 0.1 at 30% oil recovery. Note that the decline in the OSR for the peak value is sharper in the case of light oils, as would be expected on the basis of a frontal drive.

6.7 Bottom Water Steamflood

One run, Run 15, was conducted with a bottom water layer in the model. The bottom water layer was installed by freezing a measured volume of water into the lower layer of the the model, which had previously been packed with beads. (Extensive details of the process are given in a previous chapter.) It is believed that the layer of water was 0.43 inches thick (17.2% of the formation thickness). All important experimental parameters, as well as a tabulation of recoveries as a function of pore volumes of steam injected, are given in Table 16.

The bottom water model was steamflooded through the water zone, with the production well open only over the top half of the formation, at an injection rate of 228.6 cc/min Figures 46, 47, 48, and 49 show the temperature profiles for this run upon the injection of 0.25, 0.50, 0.75, and 1.00 pore volumes of steam, respectively. It is clear that the injected steam advanced rapidly in the bottom water layer. Notice that the 15 and 20 C isotherms in the upper part of the sand are virtually stationary while the heat advances unevenly in the water layer. This suggests that a hot waterflood is occurring as a result of the injected steam condensing and the condensate migrating rapidly into the high conductivity water layer.

As expected, the oil recovery for this run was poor, being 3.1% of the original oil in place after injecting 1.2 pore volumes of steam as shown in Figure 50. The curve showing the instantaneous oil-steam ratio as a function of cumulative oil production is given as Figure 51. Future runs in the continuation of this research will concentrate on minimizing the deleterious effects of the bottom water zone. In spite of the poor oil recovery, this run is considered to be successful, since it showed that a bottom water layer can be created in the vacuum model (note that Prats[42] situation was very different), and that a steamflood can be conducted under such conditions. The observed behavior of the steamflood was according to expectations.

6.8 Steam Slug Runs

Runs 17,18, and 19 were designed to test the steam slug process, and to ascertain the reproducibility of such experiments. As seen in Table 8 the initial oil saturation in each of these runs was very close 92%. Tables 17, 18, and 19 present the important experimental parameters for Runs 17, 18, and 19, respectively, and also give a tabulation of the oil recovery as a function of pore volumes of steam injected.

Steam injection for these runs was terminated at the point where a sharp drop in the oil-steam ratio was observed, and then water was injected. (Refer to Figures 58, 66, and 74 for the oil-steam ratio curves for Runs 17, 18, and 19, respectively.) The water was injected at 4 C to coincide with the scaling criteria, thus the water was at a temperature similar to the initial reservoir temperature.

Consider the temperature distribution plots for Run 17, given in Figures 53, 54, 55, 56, and 57, for injection to 0.25, 0.31 (start of cold waterflood), 0.50, 0.75, and 1.00 pore volumes, respectively. At 0.25 pore volumes of steam injected, it is seen that the advance of the steam front is nearly radial but there is some underrunning of the condensate. There is an isolated 15 C zone near the producer. At the point where steam injection is terminated, and the cold waterflood is started (Figure 54), the temperature profiles for the upper part of the model still show approximately radial advance, but the lower part of the model shows very irregular heat (condensate) advance. Upon the injection of 0.50 pore volumes of water and steam (Figure 55), heat is spread over the entire area in the lower part of the formation, but the development of a heat bank in the upper part of the model still seems to follow an approximately radial pattern. Injection of water to 0.75 pore volumes (Figure 56) totally condenses the steam, while further injection to 1.00 pore volumes (Figure 57) indicates even more distortion of the isotherms.

The temperature profiles for Run 18, given as Figures 60, 61, 62, 63, 64, and 64, for the injection of 0.25, 0.30 (start of cold waterflood), 0.50, 0.75, 1.00, and 1.25 pore volumes of steam show a behavior very similar to that of Run 17. Run 18 was continued slightly longer than Run 17 and the final profile (Figure 65) shows that the heat distribution is highly asymmetrical, with a 15 C isotherm still present in the lower part of the formation. On the whole, the temperature profiles for the two runs show; (i) considerable slowdown of heat advance in the upper part of the formation with the injection of cold water and, (ii) more rapid and very uneven heat spreading in the lower part of the model. The former is symptomatic of steam condensation by the injected cold water, essentially bringing the steam zone to a halt until total condensation has occurred, while the latter is quite typical of a hot waterflood, characterized by fingering and unstable heat advance.

The temperature profiles for Run 19, are given in Figures 68, 69, 70, 71, 72, and 73, for 0.25, 0.28 (start of cold waterflood), 0.50, 0.75, 1.00, and 1.25 pore volumes of steam injected, respectively. These are sufficiently different than those of Runs 17 and 18 to show that even though the experimental conditions were identical, instabilities can play a significant role in modifying the temperature distributions in the upper and lower parts of the model. Possibly some perturbation during the steam injection stage caused early departure from radial flow, with concomitant later distortion of temperature profiles. Nevertheless, the final recovery curves for all three runs are very similar as evidenced in Figure 76. Similarities are also observed in the plots of instantaneous oil and water production as functions of cumulative injection. These plots are given as Figures 59, 67, and 75, for Runs 17, 18, and 19, respectively.

The final temperature profile of Run 19 at 1.25 pore volumes injected (Figure 73), although different from the other two runs, still shows a greater heat accumulation in the lower part of the formation than in the upper part. It could be hypothesized that the injected cold water condenses the steam zone at the top, with the condensate then dropping down and flushing out the oil.

On the whole, the steam slug process appears to be quite attractive since;

i. it yields a good oil recovery,

ii. it utilizes less steam than other variations of steam injection and thus is more economical in field operations,

iii. it promotes greater utilization of the injected heat with the injected water transporting heat from the swept zone into the colder parts downstream.

6.9 Hot Water Slug Run

Run 22 was a hot water slug run which was conducted for the purpose of determining whether steam injectivity could be improved by an initial slug of hot water. The experimental parameters and a tabulation of the recovery response for this run are presented in Table 20. The water injection rate was 230.2 cc/min into the lower half of the formation.

The run was designed to inject approximately one half of a pore volume of hot water and gradually heat up the injected fluid until it became steam. However, the steam generating system was unable to gain heat at the rate required and thus it is questionable whether steam was injected at the later stages of the run.

Figure 81 shows the recovery response of Run 22. The sudden jump in the recovery curve at the injection of 0.8

pore volumes of water, could possibly be attributed to steam injection. It is possible that, although the boiler was not hot enough to generate superheated steam, the injected hot water flashed to steam when it encountered a low enough pressure within the model. A sudden increase in oil recovery is also observed in the oil-steam ratio curve, given as Figure 82, and in the instantaneous oil and water production curve given as Figure 83.

An inspection at the temperature profiles for this run (Figures 77, 78, 79, and 80, for the injection of 0.25, 0.50, 0.75, and 1.00 pore volumes of water, respectively), shows that the heat advance is occurring very quickly in the lower part of the formation. Figure 77 shows that even upon the injection of only 0.25 pore volumes of hot water, the heated zone had advanced considerably in the lower part of the formation, while little movement occurred in the upper part. Figure 78 at 0.50 pore volumes of steam injected shows the further advance of the hot zone in the lower layer. The sweep appears to be very efficient, extending almost radially. At 0.75 pore volumes injected (Figure 79) the isotherms begin to appear slightly irregular, and this nonuniformity becomes even more pronounced upon the injection of 1.00 pore volumes (Figure 80).

NUMERICAL SIMULATION

Objectives

The purpose of this part of the research is to develop a numerical simulator of steam injection under multiphase, multicomponent flow in two-dimensions. This simulator is to have a number of new features as discussed below. This simulator will be used for

(i) simulating laboratory steamfloods;
(ii) carrying out sensitivity studies for bottom water (and gas cap) reservoirs;
(iii) examining the steamflood scaling criteria.

Model Assumptions

This model simulates three phase two-dimensional flow. We are considering five components, which are (1) water/ steam, (2) a water-soluble surfactant, (3) a non-condensable gas:nitrogen, (4) a non-volatile oil, and (5) solution gas which is soluble in the oil phase only. The three phases are assumed to have the components as indicated below:

Oleic Phase - Nonvolatile oil
Solution gas
Aqueous Phase - Water
Surfactant
Vapour Phase - Steam
Noncondensable gas (nitrogen)
Surfactant
Solution gas

The special features of the simulator will consist in the simulation of foam formation, rheology and flow in a porous medium; incomplete equilibrium between the phases; thermal upgrading of oil; and diffusion.

Derivation of Mass Balance Equations

Consider the flow of oleic, aqueous and vapour phases across an element of porous medium of cross sectional area A and length Δx. We will derive the mass balance on component i flowing in all three phases. We will carry out the derivations in one dimension but all subsequent equations will be generalized for two dimensions. We will allow for diffusional transfer by means of the following equation:

$$m_{ip} = -AD_{ip}\rho_{ip}\frac{\partial C_{ip}}{\partial x} ,$$

where m_{ip} is the mass rate of diffusion of component i in phase p, and D_{ip} is diffusional rate in one of the three phases.

$$\text{Net throughput} + \text{Net Change} = 0$$

$$(\text{Mass out} - \text{Mass in}) + (\text{Mass at}_{t+\Delta t} - \text{Mass at}_{t}) = 0$$

$$[(C_{io}\rho_o q_o)_{x+\Delta x} \quad m_{iow_{x+\Delta x}}$$

$$- (C_{io}\rho_o q_o)_x - m_{iow_x} - m_i^{*} (A\Delta x)$$

$$+ (C_{iw}\rho_w q_w)_{x+\Delta x} + m_{igo_{x+\Delta x}}$$

$$- (C_{iw}\rho_w q_w)_x - m_{igo_x}$$

$$+ (C_{ig}\rho_g q_g)_{x+\Delta x} + m_{igw_{x+\Delta x}}$$

$$- (C_{ig}\rho_g q_g)_x - m_{igw_x}] \Delta t$$

$$+ \phi A \Delta x \left[\begin{array}{ll} (S_o\rho_o C_{io})_{t+\Delta t} & - (S_o\rho_o C_{io})_t \\ (S_w\rho_w C_{iw})_{t+\Delta t} & - (S_w\rho_w C_{iw})_t \end{array} \right.$$

$$+ (S_g\rho_g C_{ig})_{t+\Delta t} - (S_g\rho_g C_{ig})_t = 0$$

$$V_{o_x} = - \frac{k\, k_{ro}}{\mu_o} \frac{\partial\, \Phi_o}{\partial_x} \qquad \text{etc.}$$

$$\nabla \left(\frac{k\, k_{ro}\, C_{io}\, \rho_o}{\mu_o}\ \nabla \Phi_o\right) + \nabla \left(\frac{k\, k_{rw}\, C_{iw}\, \rho_w}{\mu_w}\ \nabla \Phi_w\right)$$

$$+ \nabla \left(\frac{k\, k_{rg}\, C_{ig}\, \rho_g}{\mu_g}\ \nabla \Phi_g\right) + \nabla (D_{igw}\, \rho_g\, \nabla C_{ig})$$

$$+ \nabla (D_{iow}\, \rho_o\, \nabla C_{io}) + \nabla (D_{igo}\, \rho_g\, \nabla C_{ig})$$

$$+ m_i^{*} = \frac{\partial}{\partial t} [\phi\, S_o\, \rho_o\, C_{io} + \phi\, S_w\, \rho_w\, C_{iw} + \phi\, S_g\, \rho_g\, C_{ig}]$$

Mass Balance for Water

water i = 1

C_{1o} = Concentration of water in oil phase = 0

(no miscibility between oil and water)

C_{1w} = Concentration of water in aqueous phaSe ≠ 0

C_{1g} = Concentration of water in vapour ≠ 0

(from Partial Pressure)

Diffusion of water gas to water ≠ 0

oil to water = 0

gas to oil = 0

$$\nabla \left(\frac{k\, k_{rw}\, C_{1w}\, \rho_w}{\mu_w} \nabla \Phi_w\right) + \nabla \left(\frac{k\, k_{rg}\, C_{1g}\, \rho_g}{\mu_g} \nabla \Phi_g\right)$$

$$+ \nabla(D_{1gw}\, \rho_g\, \nabla C_{1g}) + m_1^* = \frac{\partial}{\partial t} (\phi\, S_w\, \rho_w\, C_{1w} + \phi\, S_g\, \rho_g\, C_{1g})$$

Other Equations

Surfactant i = 2

$$\nabla \left(\frac{k\, k_{rw}\, C_{2w}\, \rho_w}{\mu_w} \nabla \Phi_w\right) + \nabla \left(\frac{k\, k_{rg}\, C_{2g}\, \rho_g}{\mu_g} \nabla \Phi_g\right)$$

$$+ \nabla (D_{2wg}\, \rho_w\, \nabla C_{2w}) + m_2^* =$$

$$\frac{\partial}{\partial t} (\phi\, S_w\, \rho_w\, C_{2w} + \phi\, S_g\, \rho_g\, C_{2g})$$

Nitrogen $i = 3$

$$\nabla\left(\frac{k\,k_{rg}\,C_{3g}\,\rho_g}{\mu_g}\,\nabla\,\phi_g\right) + m_3^{\,*} = \frac{\partial}{\partial t}\,(\phi\,S_g\,\rho_g\,C_{3g})$$

Oil $i = 4$

$$\nabla\left(\frac{k\,k_{ro}\,C_{4o}\,\rho_o}{\mu_o}\,\nabla\,\phi_o\right) + m_4^{\,*} = \frac{\partial}{\partial t}\,(\phi\,S_o\,\rho_o\,C_{4o})$$

Solution Gas $i = 5$

$$\nabla\left(\frac{k\,k_{ro}\,C_{5o}\,\rho_o}{\mu_o}\,\nabla\,\phi_o\right) + \nabla\left(\frac{k\,k_{rg}\,C_{5g}\,\rho_g}{\mu_g}\,\nabla\,\phi_g\right)$$

$$+\ \nabla(D_{5go}\,\rho_g\,\nabla C_{5g}) + m_5^{\,*} =$$

$$\frac{\partial}{\partial t}\,(\phi\,S_o\,\rho_o\,C_{5o} + \phi\,S_g\,\rho_g\,C_{5g})$$

Energy Balance

Consider the flow of the three phases and the simultaneous conduction and convection of heat through an element of a porous medium as shown in the sketch.

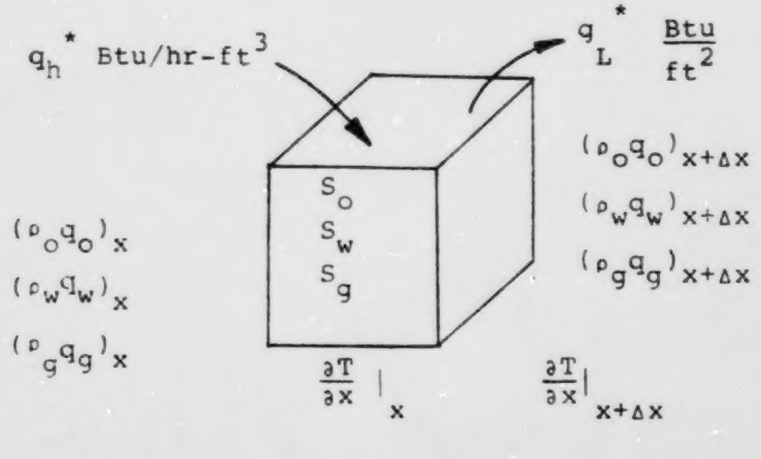

q_h^* Btu/hr-ft^3
q_L^* $\frac{\text{Btu}}{\text{ft}^2}$
$(\rho_o q_o)_{x+\Delta x}$
$(\rho_w q_w)_{x+\Delta x}$
$(\rho_g q_g)_{x+\Delta x}$
S_o
S_w
S_g
$(\rho_o q_o)_x$
$(\rho_w q_w)_x$
$(\rho_g q_g)_x$
$\frac{\partial T}{\partial x}\Big|_x$
$\frac{\partial T}{\partial x}\Big|_{x+\Delta x}$

Net Throughput + Net Change = 0

$$(-k_h\, A\, \frac{\partial T}{\partial x}\,\Big|_{x+\Delta x} \; + [q_w\, \rho_w\, C_w\, \Delta T$$

$$+\, q_o\, \rho_o\, C_o\ \Delta T + q_g\, \rho_g\, C_{1g}\, (h_w + L_v)$$

$$+\, q_g\, \rho_g\, C_{3g}\, C_{N2}\, \Delta T + q_g\, \rho_g\, C_{5g}\, C_{sg}\ \Delta T]_{x+\Delta x}$$

$$+\, q_L^{*} A)\ \ \Delta t$$

$$-(-k_h\, A\, \frac{\partial T}{\partial x}\,\Big|_x \; + \; [q_w\, \rho_w\, C_w\ \Delta T + q_o\, \rho_o\, C_o\ \ \Delta T$$

$$q_g\, \rho_g\, C_{1g}\, (h_w + L_v) + q_g\, \rho_g\, C_{3g}\, C_{N2}\ \ \Delta T$$

$$+\, q_g\, \rho_g\, C_{sg}\, \Delta T]_x \; + q_h^{*}\ (A \Delta x))\ \Delta t$$

$$+(\phi A \Delta x)\ (S_o\, \rho_o\, C_o\, \Delta T \; + \; S_w\, \rho_w\, C_w\ \ \Delta T$$

$$+\, S_g\, \rho_g\, C_{1g}\, h_s \quad S_g\, \rho_g\, C_{3g}\, C_{N2}\, \Delta T\, +$$

$$S_g\, \rho_g\, C_{5g}\, C_{sg}\, \Delta T)\ t + \Delta t$$

$$-\ (\phi A\ \Delta x)\ (S_o\, \rho_o\, C_o\, \Delta T + S_w\, \rho_w\, C_w\ \ \Delta T$$

$$+\, S_g\, \rho_g\, C_{1g}\, h_s + S_g\, \rho_g\, C_{3g}\, C_{N2}\ \ \Delta T$$

$$+\, S_g\, \rho_g\, C_{5g}\, C_{sg}\ \ \Delta T)\ t = 0$$

Let $q_L^{'*}$ = heat loss/unit length of reservoir = $\dfrac{q_L^{*}}{\Delta x}$

$$\nabla\, (k_h \nabla\, T) - \ \nabla (V_w\, \rho_w\, C_w\, \Delta T) - \quad (V_o\, \rho_o\, C_o\, \Delta T)$$

$$-\ \nabla (V_g\, \rho_g\, C_{1g}\, h_s) - \nabla\, (V_g\, \rho_g\, C_{3g}\, C_{N2}\, \Delta T)$$

$$-\ \nabla (V_g\, \rho_g\, C_{5g}\, C_{sg}\, \Delta T) - q_L^{'*} + q_h^{*}$$

$$= \frac{\partial}{\partial t} (\phi \; S_o \; \rho_o \; C_o \; \Delta T) + \frac{\partial}{\partial t} (\phi \; S_w \; \rho_w \; C_w \; \Delta T)$$

$$+ \frac{\partial}{\partial t} (\phi \; S_g \; \rho_g \; C_{1g} \; h_s) + \frac{\partial}{\partial t} (\phi \; S_g \; \rho_g \; C_{3g} \; C_{N2} \; \Delta T)$$

$$+ \frac{\partial}{\partial t} (\phi \; S_g \; \rho_g \; C_{5g} \; C_{sg} \; \Delta T)$$

where $\Delta T = T - T_R$

Formulation of the Problem

Unknowns: ΔT, S_o, S_w, S_g, P_o, P_w, P_g, C_{1g}, C_{2g}, C_{3g}, C_{5g}, C_{4o}, C_{5o}, C_{1w}, C_{2w}

Equations:

Mass balance for i = 1, 2, 3, 4, 5	5
Energy balance	1
$S_o + S_w + S_g = 1$	1
$P_{cow} = P_o - P_w$	1
$P_{cgo} = P_g - P_o$	1
$C_{1g} + C_{2g} + C_{3g} + C_{5g} = 1$	1
$C_{4o} + C_{5o} = 1$	1
$C_{1w} + C_{2w} = 1$	1

Solution Method

The above equations are discretized by means of appropriate finite difference approximations, in particular, fully implicit saturations is unity) and capillary pressure in time. Using the constraint equations (e.g. sum of the relationships, a system of six simultaneous equations in six unknowns: S_o, S_g, P_o, C_{1g}, C_{5o}, C_{2w} is obtained. The fully implicit formulation is more stable than other formulations, and can thus permit the use of a large Δt.

The above six equations are to be solved simultaneously using a direct solution technique. The solution will then be used in a semi-implicit approximation of the temperature equation. An alternative approach under consideration involves the simultaneous solution of all seven equations, although this has certain disadvantages, since the heat loss term comes from still another partial differential equation, written for the adjacent media.

The fully implicit solution will be executed by means of a Newton-Raphson iteration, with the Jacobian calculated analytically. Numerical calculation of derivatives will be considered also, using special techniques, but the conventional explicit approach is much more time-consuming than the analytical.

Current Status

The numerical model has been formulated. A number of enhancements are being incorporated into the equations. The partial differential equations have been derived, as noted above. All difference equations for the non-linear, fully implicit formulation, incorporating Newtonian iteration, have been derived, and are not reproduced here in view of the large volume of mathematical expressions involved. The logic of the solution scheme is being developed, and the coding of the computer program will begin shortly.

8. CONCLUSIONS

1. A low pressure, scaled steamflood model was designed and constructed, and tested for a variety of steamflood runs, and found to be satisfactory for all purposes.
2. Oil viscosity has a considerable influence on the type of steam drive developed. In the case of the Aberfeldy oil (208 mPa-s at 24 C; 1275 mPa-s at 24 C in prototype), the steam zone develops in the upper part of the formation, with steam condensate movement toward the base. In the case of a more viscous oil (9250 mPa-s at 24 C; 13085 mPa-s at 24 C in prototype), the steam zone development is clearly in the upper part of the sand. In the case of the light oil (60 mPa-s at 24 C; 25.6 mPa-s at 23 C in prototype), the steam zone development is closer to a frontal drive.
3. Based upon one run, it was concluded that bottom water has an extremely unfavorable effect on steamflood efficiency, with a cumulative recovery of only 3% for a water/oil zone thickness ratio of 5:1.
4. The steam slug process appears to be an efficient and practically viable recovery technique, with oil recovery of 30.9% of the original oil in place, for a 0.29 pore volume slug of steam, followed by a 1.16 pore volume slug of water.
5. Among the techniques tested thus far, the steam slug process appears to be best suited for the Aberfeldy crude, with a recovery of at least 31% depending on the

volume of the injected slugs.

6. The oil recovery observed for a light oil steamflood was higher than that of the Aberfeldy model, being 35.7% of the original oil in place, after the injection of 1.65 pore volumes of steam. Thus steamflooding may be a viable recovery method for light oils as well, although the flood performance needs to be examined for a variety of operating parameters, in particular, the oil saturation, since such reservoirs would normally be waterflooded first.

NOMENCLATURE

f_{sr} = Steam quality. (dimensionless)

h_{ss} = Enthalpy of saturated steam. (kJ/kg)

h_{wa} = Enthalpy of water. (kJ/kg)

k_m = Permeability in the model. (darcies)

k_p = Permeability in the prototype. (darcies)

k_{hm} = Thermal conductivity in the model. (kW/m·K)

k_{hp} = Thermal conductivity in the prototype. (kW/m·K)

L_m = Length of the model.

L_p = Length of the prototype.

L_v = Latent heat of vapourization. (kJ/kg)

M_m = Heat capacity in the model. (kJ/kg·K)

M_p = Heat capacity in the prototype. (kJ/kg·K)

P_m = Pressure in the model. (MPa or kPa)

P_p = Pressure in the prototype. (MPa)

$(P_p)_m$ = Production pressure in the model. (MPa)

$(P_p)_p$ = Production pressure in the prototype. (MPa)

r = Scaled radius of the well. (inches)

S_g = Saturation of gas. (dimensionless)

S_o = Saturation of oil. (dimensionless)

S_{or} = Residual oil saturation to steam. (dimensionless)

S_w = Saturation of water. (dimensionless)

t_m = Time in the model. (min)

t_p = Time in the prototype. (days)

T_m = Model temperature. (C)

T_p = Prototype temperature. (C)

T_{o_m} = Initial model temperature. (C)

T_{o_p} = Initial prototype temperature. (C)

w = Slit width of scaled well. (inches)

w_a = Mass rate of flow of the aqueous phase.

w_m = Injection rate into the model. (cm^3/min)

w_p = Injection rate into the prototype. (m^3/day)

w_s = Mass rate of flow of superheated steam.

w_{wi} = Total mass rate injected.

$\gamma(L)$ = Length scaling factor. (dimensionless)

$\gamma(\Delta P)$ = Pressure scaling factor. (dimensionless)

ρ = Density. (kg/m^3)

ϕ_m = Porosity in the model. (dimensionless)

ϕ_p = Porosity in the prototype. (dimensionless)

μ = Viscosity. (mPa-s)

REFERENCES

1. "Annual Production Report", Oil and Gas Journal (April 2, 1984), 83-105.

2. Farouq Ali, S.M., "Steam Injection as a Method for Recovering Light Oil Crudes -- The Bradford Steamflood", Paper presented at the 1978 Eastern Regional Meeting of the Society of Petroleum Engineers held in Washington, D.C., November 10, 1978.

3. Farouq Ali, S.M., "Potential of Steamflooding for Recovering Light Oils", Paper presented at the meeting of the Petroleum Society of the Canadian Institute of Mining and Metallurgy held in Banff, Alberta, May 9-11, 1979.

4. Farouq Ali, S. M. and Meldau, R.F.: "Current Steamflood Technology", J.P.T., October 1979, 1332-1342.

5. Blevins, T.R., Duerksen, J.H., Ault, J.W.: "Light Oil Steamflooding -An Emerging Technology," Paper presented at the 1982 SPE/DOE Third Joint Symposium on Enhanced Oil Recovery of the Society of Petroleum Engineers held in Tulsa, Oklahoma, April 4-7,1982.

6. Farouq Ali, S.M.: "Steam Injection Theories--A Unified Approach", Paper presented at the 1982 California Regional Meeting of the SPE held in San Francisco, California (March 24-26, 1982).

7. Willman, B.T., Valleroy, V.V., Runberg, G.W., Cornelius, A.J., and Powers, L.W.: "Laboratory Studies of Oil Recovery by Steam Injection", J. Pet. Tech. (July, 1961, 681-690.

8. Marx, J.W. and Langenheim, R.H.: "Reservoir Heating by Hot Fluid Injection", Trans. AIME, (1959) vol. 216, 312-315.

9. Ozen, A.S. and Farouq Ali, S.M.: "An Investigation of the Recovery of the Bradford Crude by Steam Injection", J.P.T., June 1969, 692-698.

10. Baker, P.E.: "An Experimental Study of Heat Flow in Steamflooding", S.P.E.J., (March 1969) 89-99.

11. Baker, P.E.: "Effect of Pressure and Rate on Steam Zone Development in Steamflooding", Paper presented at SPE-AIME 47th Annual Fall Meeting held in San

Antonio, Texas, Oct. 8-11,1972.

12. El-Saleh, M.M. and Farouq Ali, S.M.: "Oil Recovery by a Water-Driven Steam Slug", SPEJ, (December, 1971), 351-355.

13. Hong, K.C.: "Guidelines for Converting Steamflood to Waterflood", Paper presented at the SPE 1985 California Regional Meeting, held in Bakersfield, California (March 27-29, 1985), 167-179.

14. Ault, J.W., Johnson, W.M., and Kamilos, G.N.: "Conversion of Mature Steamfloods to Low-Quality Steam and/or Hot-Water Injection Projects", Paper presented at the SPE 1985 California Regional Meeting, held in Bakersfield, California (March 27-29, 1985), 149-166.

15. Redford, D.A., Flock, D.L., Peters, E.J., and Lee, J.: "Laboratory Model Flow-Test Systems of In Situ Recovery From Alberta Oil Sands", Annual Meeting of Can. Chem. Soc., Montreal (1976).

16. Flock, D.L. and Lee, J.: "An Experimental Investigation of Steam Displacement of a Medium Gravity Crude Oil", Canadian Institute of Mining and Metallurgy, Special Volume No. 17, 386-394.

17. Farouq Ali, S.M. and Abad, B.: "Bitumen Recovery from Oil Sands, Using Solvents in Conjunction With Steam", J.C.P.T., (July-Sept., 1976).

18. Lee, J.L.: Experimental Investigation of Steamflooding Behavior in an Adiabatic Water-Saturated Core", M.Sc. Thesis, U. of Alberta (1977).

19. Farouq Ali, S.M. and Redford, D.A.: "Physical Modeling of In Situ Recovery Methods for Oil Sands", Canadian Institute of Mining and Metallurgy, Special Volume No. 17, 319-326.

20. Johnstone, R.E. and Thring, N.W.: "Pilot Plants, Models and Scale-Up Methods in Chemical Engineering", McGraw-Hill Book Co., New York (1957).

21. Geertsma, J., Croes, G.A., and Schwarz, N.: "Theory of Dimensionally Scaled Models of Petroleum Reservoirs", Trans. AIME, Vol. 207 (1956) 118-127.

22. Pujol, L. and Boberg, T.C.: "Scaling Accuracy of Laboratory Steamflooding Models", Paper presented at the California Regional Meeting of the Society of Petroleum Engineers held in Bakersfield, Nov. 8-10, 1972. SPE paper #4191.

23. Niko, H. and Troost, P,J,P,M.: "Experimental Investigation of Steam Soaking in a Depletion-Type Reservoir", J.P.T. (Aug., 1971), 1006-1014.

24. Perkins, F.M. and Collins, R.E.: "Scaling Laws for Laboratory Flow Models of Oil Reservoirs", Trans., AIME (1960), vol. 219, 383-385

25. Demetre, G.P., Bentsen, R.G., and Flock, D.L.: "A Multi-Dimensional Approach to Scaled Immiscible Fluid Displacement", JCPT, (July-August, 1982), 49-61.

26. Greenkorn, R.A.: "Flow Models and Scaling Laws for Flow Through Porous Media", Industrial and Engineering Chemistry, (March, 1964) Vol. 56, No. 3, 32-37.

27. Loomis, A.G. and Crowell D.C.: "Theory and Application of Dimensional and Inspectional Analysis to Model Study of Fluid Displacements in Petroleum Reservoirs", Bureau of Mines Report RI6546 (1964).

28. Bentsen, R.G.: "Scaled Fluid-Flow Models With Permeabilities Differing From That of the Prototype", JCPT (July-September, 1976).

29. Rapoport, L.A.: "Scaling Laws for Use in Design and Operation of Water-Oil Flow Models", Trans., AIME (1955), vol. 204, 143-150.

30. Leverett, M.C., Lewis, W.B. and True, M.E.: "Dimensional-Model Studies of Oil-Field Behavior", Trans., AIME (1942), vol. 146, 175-193.

31. Pursley, S.A.: "Experimental Studies of Thermal Recovery Processes", Paper presented at the Heavy Oil Symposium, Maracaibo, Venezuala (1974).

32. Ehrlich, R.: "Laboratory Investigation of Steam Displacement in the Wabasca Grand Rapids A Sand", Paper presented at the Canada-Venezuela Oil Sands Symposium, Edmonton, Alberta, (May 1977), 364-379.

33. Huygen, H.H.A.: "Laboratory Steamfloods in Half of a Five-Spot", Paper presented at the 51st Annual Fall Meeting of the Society of Petroleum Engineers of AIME held in New Orleans, (Oct. 3-6, 1976).

34. Huygen, H.H.A. and Lowry, W.E.: "Steamflooding Wabasca Tar Sand Through The Bottom Water Zone -- Scaled Lab Experiments", Paper presented at the 54th Annual Fall Meeting of the Society of Petroleum Engineers held in Las Vegas, (Sept. 23-26, 1979).

35. Singhal, A.K.: "Physical Model Studies of Inverted Seven-Spot Steamfloods in a Pool Containing a Lloydminster Type Heavy Oil", Petroleum Recovery Institute Research Report RR-38 (November, 1978).

36. Lo, H.Y.: "Laboratory Model Study of Steamflood Oil Recovery", Petroleum Recovery Institute Interim Report, IR-5, (March, 1977).

37. Stegemeier, G.L., Laumbach, D.D., and Volek, C.W.: "Representing Steam Processes With Vacuum Models", Paper presented at the 52nd Annual Fall Technical Conference and Exhibition of the SPE, held in Denver (Oct.9-12, 1977).

38. French M.S. and Howard, R.L.: "The Steamflood Job, Hefner Sho-Vel-Tum", Oil and Gas Journal (July, 1967), Vol 65, No. 29, 64.

39. Afoeju, B.I.: "Conversion of Steam Injection to Waterflood, East Coalings Field", J.P.T. (Nov. 1974), 1227-1232.

40. Hall, A.L. and Bowman, R.W.: "Operation and Performance of the Slocum Thermal Recovery Project , J.P.T. (April 1973), 402-408.

41. Stokes, D.D., Brew, J.R., Whitten, D.G., and Wooden, L.W.,: "Steam Drive as a Supplemental Recovery Process in an Intermediate Viscosity Reservoir, Mount Poso Field, California", Paper presented at the 47th Annual California Regional Meeting of the SPE held at Bakersfield, (April 13-15, 1977).

42. Prats, M.: "Peace River Steam Drive Scaled Model Experiments", 28th Annual Technical Meeting of the Petrol. Soc. of the CIM, CanadaVenezuala Oil Sands Symposium of 1977, Edmonton (May, 1977).

43. Stokes, D.D. and Doscher, T.M.: "Shell Makes a Success of Steamflood at Yorba Linda", Oil and Gas Journal (Sept. 2, 1974), 71-78.

44. Doscher, T.M.: "Scaled Physical Model Studies of the Steam Drive Process", First Annual Report (Sept., 1977 to Sept. 1978), U.S. Department of Energy, Contract DOE/ET/12075-1

45. Yortsos, Y.C.: "Analytical Modeling of Oil Recovery by Steam Injection", Ph.D. Dissertation, California Institute of Technology (1979).

46. Doscher, T.M. and Huang, W.: "Steam-drive Performance

Judged Quickly From Use of Physical Models", Oil and Gas Journal (Oct. 22, 1979), 52-57.

47. Doscher, T.M. and Ghassemi, F.: "The Influence of Oil Viscosity and Thickness on the Steam Drive", JPT (February, 1983), 291-298.

48. Kimber, K. and Farouq Ali, S.M.: Paper in progress.

49. Prats, M.: Comment to the Discussion on Physical Modeling, CIM Special volume no. 17, p397.

50. Kasraie, M. and Farouq Ali, S.M.: "Heavy Oil Recovery in the Presence of Bottom Water", Paper presented at the 35th Annual Technical Meeting of the Petroleum Society of CIM held in Calgary (June 10-13, 1984).

51. Singh, B., Malcolm, J.D., and Heidrick, T.M.: "Injection-Production Strategies for Reservoirs Having a Bottomwater Zone", Paper presented at the SPE 1985 California Regional Meeting, held in Bakersfield (March 27-29, 1985).

52. Coats, K.H., Ramesh, A.B., and Winestock, A.G.: "Numerical Modeling of Thermal Reservoir Behavior", CIM Special Volume No. 17, 399-410.

53. CRC Handbook of Chemistry and Physics, 59 th Edition, page E-16.

54. CRC Handbook of Chemistry and Physics, 59 th Edition, 1978-1979, page F-1.

55. Van Wylen, G.J. and Sonntag, R.J.: Fundamentals of Classical Thermodynamics, Steam Tables.

56. Currie, J.B. and Gregory, A.R.: "Homogeneously Distributed Particles", U.S. Patent 2,808,242 (Oct. 1, 1957).

57. Wygal, R.J.: "Construction of Models that Simulate Oil Reservoirs", SPE Journal, (December, 1963).

APPENDIX A:

Tables of Experimental Data for All Runs.

Table 9: Experimental Data for Run #5

Steamflood in Aberfeldy Model

Type of Oil Used:	Faxam-100 (208 mPa-s at 23 C)
Pore Volume:	14180 cm^3
Porosity of Bead Pack:	33.76 %
Hydrocarbon Pore Volume:	12300 cm^3
Initial Oil Saturation:	86.74 %
Irreducible Water Saturation:	13.26 %
Initial Model Temperature:	2.5 C
Water Feed Flow Rate:	199.6 cm^3/min
Boiler Feed Flow Rate:	27.3 cm^3/min
Total Flow Rate of Steam:	226.9 cm^3/min
Total Volume of Steam Injected:	6320 cm^3 (0.45 PV)
Total Volume of Oil Recovered:	810 cm^3 (6.59 % OOIP)

Table 10: Experimental Data for Run #6

Steamflood in Aberfeldy Model

Type of Oil Used:	Faxam-100 (208 mPa-s at 23 C)
Pore Volume:	13990 cm^3
Porosity of Bead Pack:	33.31 %
Hydrocarbon Pore Volume:	12160 cm^3
Initial Oil Saturation:	84.49 %
Irreducible Water Saturation:	15.51 %
Initial Model Temperature:	1.93 C
Water Feed Flow Rate:	200.2 cm^3/min
Boiler Feed Flow Rate:	27.1 cm^3/min
Total Flow Rate of Steam:	227.3 cm^3/min
Total Volume of Steam Injected:	32710 cm^3 (2.34 PV)
Total Volume of Oil Recovered:	2660 cm^3 (21.89 % OOIP)

Table 11: Experimental Data for Run #7

Steamflood Following Waterflood on Aberfeldy Model

Type of Oil Used:	Faxam-100 (208 mPa-s at 23 C)
Pore Volume:	13040 cm³
Porosity of Bead Pack:	31.04 %
Hydrocarbon Pore Volume:	11420 cm³
Initial Oil Saturation:	90.41 %
Irreducible Water Saturation:	9.59 %
Initial Model Temperature:	3.0 C
Water Feed Flow Rate:	(A) 96.9 cm³/min (B) 93.6 cm³/min (C) 197.7 cm³/min
Boiler Feed Flow Rate:	(A) 0.0 cm³/min (B) 0.0 cm³/min (C) 27.6 cm³/min
Total Flow Rate of Steam:	(A) 96.9 cm³/min (B) 93.6 cm³/min (C) 225.3 cm³/min
Total Volume of Water Injected:	15295 cm³ (1.1729 PV)
Total Volume of Oil Recovered:	2655 cm³ (22.52 % OOIP)

(A) Low Temperature Waterflood

Cumulative Total PV Injected (cm³)	Cumulative Total PV Injected (PV)	Cumulative Oil Produced (cm³)	Cumulative Oil Produced (% OOIP)	Oil/Water Ratio (cm³/cm³)
1610	0.124	1010	8.57	0.6273
3410	0.262	1415	12.00	0.2250
5240	0.402	1755	14.89	0.1858
7085	0.543	1990	16.88	0.1274
8905	0.683	2190	18.58	0.1099
10740	0.824	2305	19.55	0.0627
12505	0.959	2400	20.36	0.0538
14465	1.109	2540	21.54	0.0714
15295	1.173	2655	22.52	0.1386

(B) Room Temperature Waterflood

Cumulative Total PV Injected (cm^3)	Cumulative Total PV Injected (PV)	Cumulative Oil Produced (cm^3)	Cumulative Oil Produced (% OOIP)	Oil-Water Ratio (cm^3/cm^3)
17050	1.308	2740	23.24	0.0484
18910	1.450	2840	24.09	0.0538
20690	1.587	2920	24.77	0.0449
21840	1.675	3120	26.47	0.1739

(C) Steamflood

Cumulative Total PV Injected (cm^3)	Cumulative Total PV Injected (PV)	Cumulative Oil Produced (cm^3)	Cumulative Oil Produced (% OOIP)	Oil/Steam Ratio (cm^3/cm^3)
23750	1.821	3170	26.89	0.0262
25670	1.969	3240	27.48	0.0365
26655	2.044	3285	27.86	0.0457
27635	2.119	3340	28.33	0.0561
29635	2.273	3520	29.86	0.0900
33585	2.576	3720	31.55	0.0506
37385	2.867	3820	32.40	0.0263

Incremental recovery by steam = 5.9% OOIP (8.1% of the waterflood residual oil saturation).

Table 12: Experimental Data for Run #9

Steamflood in Heavy Oil Model

Type of Oil Used:	Heavy Oil (9256.5 mPa-s at 23 C)
Pore Volume:	13800 cm^3
Porosity of Bead Pack:	32.85 %
Hydrocarbon Pore Volume:	12100 cm^3
Initial Oil Saturation:	87.68 %
Irreducible Water Saturation:	12.32 %
Initial Model Temperature:	4.03 C
Water Feed Flow Rate:	199.0 cm^3/min
Boiler Feed Flow Rate:	29.8 cm^3/min
Total Flow Rate of Steam:	228.8 cm^3/min
Total Volume of Steam Injected:	14000 cm^3 (1.01 PV)
Total Volume of Oil Recovered:	200.0 cm^3 (1.65 % OOIP)

Only 200 cc of oil was produced after injecting 14000 cc of steam, thus the run was terminated.

Table 13: Experimental Data for Run #10

Steamflood in Aberfeldy Model

Type of Oil Used: Faxam-100 (208 mPa-s At 24 C)
Pore Volume: 12700 cm^3
Porosity of Bead Pack: 30.23 %
Hydrocarbon Pore Volume: 11680 cm^3
Initial Oil Saturation: 92.00 %
Irreducible Water Saturation: 8.00 %
Initial Model Temperature: 4.07 C
Water Feed Flow Rate: 199.8 cm^3/min
Boiler Feed Flow Rate: 30.3 cm^3/min
Total Flow Rate of Steam: 230.1 cm^3/min
Total Volume of Steam Injected: 26850 cm^3 (2.114 PV)
Total Volume of Oil Recovered: 3677 cm^3 (31.48 % OOIP)

Cumulative Total PV Injected (cm^3)	Cumulative Total PV Injected (PV)	Cumulative Oil Produced (cm^3)	Cumulative Oil Produced (%OOIP)	Oil/Steam Ratio (cm^3/cm^3)
1100	0.087	540	4.62	0.4909
2830	0.223	895	7.66	0.2052
4280	0.337	1245	10.66	0.2414
6085	0.479	1690	14.47	0.2465
7575	0.596	1897	16.24	0.1389
9265	0.730	2027	17.35	0.0769
10760	0.847	2234	19.13	0.1385
12550	0.988	2399	20.54	0.0922
14240	1.212	2624	22.47	0.1331
16050	1.264	2749	23.54	0.0691
17745	1.397	2859	24.48	0.0649
19535	1.538	2998	25.67	0.0776
21335	1.680	3162	27.07	0.0911
23135	1.822	3304	28.29	0.0789
24030	1.892	3381	28.95	0.0860
24950	1.965	3422	29.30	0.0446
26850	2.114	3677	31.48	0.1342

Table 14: Experimental Data for Run #12

Steamflood in Light Oil Prototype

Type of Oil Used:	MCT-10 (60 mPa-s at 23 C)
Pore Volume:	14050 cm^3
Porosity of Bead Pack:	33.45 %
Hydrocarbon Pore Volume:	12535 cm^3
Initial Oil Saturation:	89.22 %
Irreducible Water Saturation:	10.78 %
Initial Model Temperature:	3.0 C
Water Feed Flow Rate:	199.3 cm^3/min
Boiler Feed Flow Rate:	30.1 cm^3/min
Total Flow Rate of Steam:	229.4 cm^3/min
Total Volume of Steam Injected:	20170 cm^3 (1.4356 PV)
Total Volume of Oil Recovered:	4130 cm^3 (32.95 % OOIP)

Cumulative Total PV Injected (cm^3)	**Cumulative Total PV Injected (PV)**	**Cumulative Oil Produced (cm^3)**	**Cumulative Oil Produced (%OOIP)**	**Oil/Steam Ratio (cm^3/cm^3)**
920	0.066	870	6.94	0.9457
2770	0.197	1520	12.13	0.3514
4460	0.317	2305	18.39	0.4645
6280	0.447	2595	20.70	0.1593
7995	0.569	2875	22.94	0.1633
9885	0.704	3185	25.41	0.1640
11695	0.832	3355	26.77	0.0939
13465	0.958	3545	28.28	0.1073
15275	1.087	3725	29.72	0.0945
17035	1.213	3875	30.91	0.0852
18835	1.341	4035	32.19	0.0889
20170	1.436	4130	32.95	0.0712

Table 15: Experimental Data for Run #13

Steamflood in Light Oil Prototype

Type of Oil Used:	MCT-10 (60 mPa-s at 23 C)
Pore Volume:	12660 cm^3
Porosity of Bead Pack:	30.14 %
Hydrocarbon Pore Volume:	11670 cm^3
Initial Oil Saturation:	92.18 %
Irreducible Water Saturation:	7.82 %
Initial Model Temperature:	3.0 C
Water Feed Flow Rate:	199.3 cm^3/min
Boiler Feed Flow Rate:	30.1 cm^3/min
Total Flow Rate of Steam:	229.4 cm^3/min
Total Volume of Steam Injected:	20920 cm^3 (1.6524 PV)
Total Volume of Oil Recovered:	4145 cm^3 (35.52 % OOIP)

Cumulative Total PV Injected (cm^3)	**Cumulative Total PV Injected (PV)**	**Cumulative Oil Produced (cm^3)**	**Cumulative Oil Produced (%OOIP)**	**Oil/Steam Ratio (cm^3/cm^3)**
1870	0.148	1345	11.53	0.7193
3800	0.300	1780	15.25	0.2254
5710	0.451	2210	18.94	0.2251
7450	0.588	2525	21.64	0.1810
9345	0.738	2820	24.16	0.1557
11275	0.891	3145	26.95	0.1684
13225	1.045	3415	29.26	0.1385
15155	1.197	3630	31.11	0.1114
17105	1.351	3800	32.56	0.0872
19060	1.506	3985	34.15	0.0946
20920	1.652	4145	35.52	0.0860

Table 16: Experimental Data for Run #15

Steamflood in Aberfeldy Model with Bottom Water

Type of Oil Used:	Faxam-100 (208 mPa-s at 23 C)
Pore Volume Oil Zone:	13136 cm³
Porosity of Bead Pack:	35.92 %
Hydrocarbon Pore Volume:	11520 cm³
Initial Oil Saturation:	87.70 %
Irreducible Water Saturation:	12.30 %
Initial Model Temperature:	3.0 C
Thickness of Water Layer:	0.4252 Inches
Water Feed Flow Rate:	199.5 cm³/min
Boiler Feed Flow Rate:	29.1 cm³/min
Total Flow Rate of Steam:	228.6 cm³/min
Total Volume of Steam Injected:	15895 cm³ (1.210 PV)
Total Volume of Oil Recovered:	355 cm³ (3.08 % OOIP)

Cumulative Total PV Injected (cm³)	Cumulative Total PV Injected (PV)	Cumulative Oil Produced (cm³)	Cumulative Oil Produced (%OOIP)	Oil/Steam Ratio (cm³/cm³)
1930	0.147	25	0.22	0.0130
3610	0.275	45	0.39	0.0119
5250	0.400	65	0.56	0.0122
7010	0.534	90	0.78	0.0142
8745	0.666	110	0.95	0.0115
10585	0.806	155	1.35	0.0245
12320	0.938	190	1.65	0.0202
14085	1.072	245	2.13	0.0312
15895	1.210	355	3.08	0.0608

Table 17: Experimental Data for Run #17

Slug Run on Aberfeldy Model

Type of Oil Used: Faxam-100 (208 mPa-s at 23 C)
Pore Volume Oil Zone: 13820 cm^3
Porosity of Bead Pack: 32.90 %
Hydrocarbon Pore Volume: 12800 cm^3
Initial Oil Saturation: 92.62 %
Irreducible Water Saturation: 7.38 %
Initial Model Temperature: 3.0 C
Water Feed Flow Rate: 198.7 cm^3/min
Boiler Feed Flow Rate: 30.4 cm^3/min
Total Flow Rate of Steam: 229.1 cm^3/min
Flow Rate of Water Slug: 198.7 cm^3/min
Total Volume of Steam Injected: 14250 cm^3 (1.031 PV)
Total Volume of Oil Recovered: 3100 cm^3 (24.22 % OOIP)

Cumulative Total PV Injected (cm^3)	Cumulative Total PV Injected (PV)	Cumulative Oil Produced (cm^3)	Cumulative Oil Produced (%OOIP)	Oil/Steam Ratio (cm^3/cm^3)
1910	0.138	1610	12.58	0.8429
3790	0.274	2070	16.17	0.2447
	COLD	WATER	SLUG	
5670	0.410	2390	18.67	0.1702
7470	0.541	2590	20.23	0.1111
9320	0.674	2765	21.60	0.0946
11220	0.812	2925	22.85	0.0842
13100	0.948	3045	23.79	0.0638
14250	1.031	3100	24.22	0.0478

Table 18: Experimental Data for Run #18

Slug Run on Aberfeldy Model

Type of Oil Used:	Faxam-100 (208 mPa-s at 23 C)
Pore Volume Oil Zone:	13880 cm³
Porosity of Bead Pack:	33.04 %
Hydrocarbon Pore Volume:	12770 cm³
Initial Oil Saturation:	92.00 %
Irreducible Water Saturation:	8.00 %
Initial Model Temperature:	3.0 C
Water Feed Flow Rate:	199.3 cm³/min
Boiler Feed Flow Rate:	30.1 cm³/min
Total Flow Rate of Steam:	229.4 cm³/min
Flow Rate of Water Slug:	199.3 cm³/min
Total Volume of Steam Injected:	20040 cm³ (1.444 PV)
Total Volume of Oil Recovered:	3940 cm³ (30.85 % OOIP)

Cumulative Total PV Injected (cm³)	**Cumulative Total PV Injected (PV)**	**Cumulative Oil Produced (cm³)**	**Cumulative Oil Produced (%OOIP)**	**Oil/Steam Ratio (cm³/cm³)**
1920	0.138	1490	11.67	0.7760
4000	0.288	2660	20.83	0.5625
	COLD	WATER	SLUG	
5890	0.424	3035	23.77	0.1984
8040	0.579	3265	25.57	0.1070
9950	0.717	3450	27.02	0.0969
12175	0.877	3595	28.15	0.0652
14215	1.024	3720	29.13	0.0613
16080	1.159	3805	29.80	0.0456
18060	1.301	3875	30.34	0.0354
20040	1.444	3940	30.85	0.0328

Table 19: Experimental Data for Run #19

Slug Run on Aberfeldy Model

Type of Oil Used:	Faxam-100 (208 mPa-s at 23 C)
Pore Volume Oil Zone:	13970 cm^3
Porosity of Bead Pack:	33.26 %
Hydrocarbon Pore Volume:	12785 cm^3
Initial Oil Saturation:	91.52 %
Irreducible Water Saturation:	8.48 %
Initial Model Temperature:	3.0 C
Water Feed Flow Rate:	199.8 cm^3/min
Boiler Feed Flow Rate:	29.4 cm^3/min
Total Flow Rate of Steam:	229.2 cm^3/min
Flow Rate of Water Slug:	199.8 cm^3/min
Total Volume of Steam Injected:	21800 cm^3 (1.560 PV)
Total Volume of Oil Recovered:	3845 cm^3 (30.07 % OOIP)

Cumulative Total PV Injected (cm^3)	Cumulative Total PV Injected (PV)	Cumulative Oil Produced (cm^3)	Cumulative Oil Produced (%OOIP)	Oil/Steam Ratio (cm^3/cm^3)
1905	0.136	1115	8.72	0.5853
4080	0.292	2135	16.70	0.4690
	COLD	WATER	SLUG	
5970	0.427	2535	19.83	0.2116
8030	0.575	2840	22.21	0.1481
9990	0.715	3070	24.01	0.1173
11980	0.858	3260	25.50	0.0955
13845	0.991	3395	26.55	0.0724
15940	1.141	3515	27.49	0.0573
17780	1.273	3655	28.60	0.0761
19860	1.422	3755	29.37	0.0481
21800	1.560	3845	30.07	0.0464

Table 20: Experimental Data for Run #22

Hot Waterflood on Aberfeldy Model

Type of Oil Used: Faxam-100 (208 mPa-s at 23 C)
Pore Volume Oil Zone: 14310 cm^3
Porosity of Bead Pack: 34.07 %
Hydrocarbon Pore Volume: 11600 cm^3
Initial Oil Saturation: 81.06 %
Irreducible Water Saturation: 18.94 %
Initial Model Temperature: 3.0 C
Water Feed Flow Rate: 199.3 cm^3/min
Boiler Feed Flow Rate: 30.9 cm^3/min
Total Flow Rate of Steam: 230.2 cm^3/min
Total Volume of Steam Injected: 19377 cm^3 (1.354 PV)
Total Volume of Oil Recovered: 3317 cm^3 (28.59 % OOIP)

Cumulative Total PV Injected (cm^3)	Cumulative Total PV Injected (PV)	Cumulative Oil Produced (cm^3)	Cumulative Oil Produced (%OOIP)	Oil/Steam Ratio (cm^3/cm^3)
1950	0.136	1310	11.29	0.6718
3900	0.273	1640	14.14	0.1692
5961	0.417	1891	16.30	0.1218
7891	0.551	2101	18.11	0.1088
9851	0.688	2281	19.66	0.0918
11641	0.813	2651	22.85	0.2067
13401	0.936	2821	24.32	0.0966
15291	1.069	3021	26.04	0.1058
17437	1.219	3187	27.47	0.0774
19377	1.354	3317	28.59	0.0670

APPENDIX B:

Experimental Results Presented in Graphical Form.

FIGURE 6: TEMPERATURE PROFILE FOR
RUN 4: CONT. STEAMFLOOD ON WATER SATURATED MODEL

0.25 Pore Volumes Steam Injected

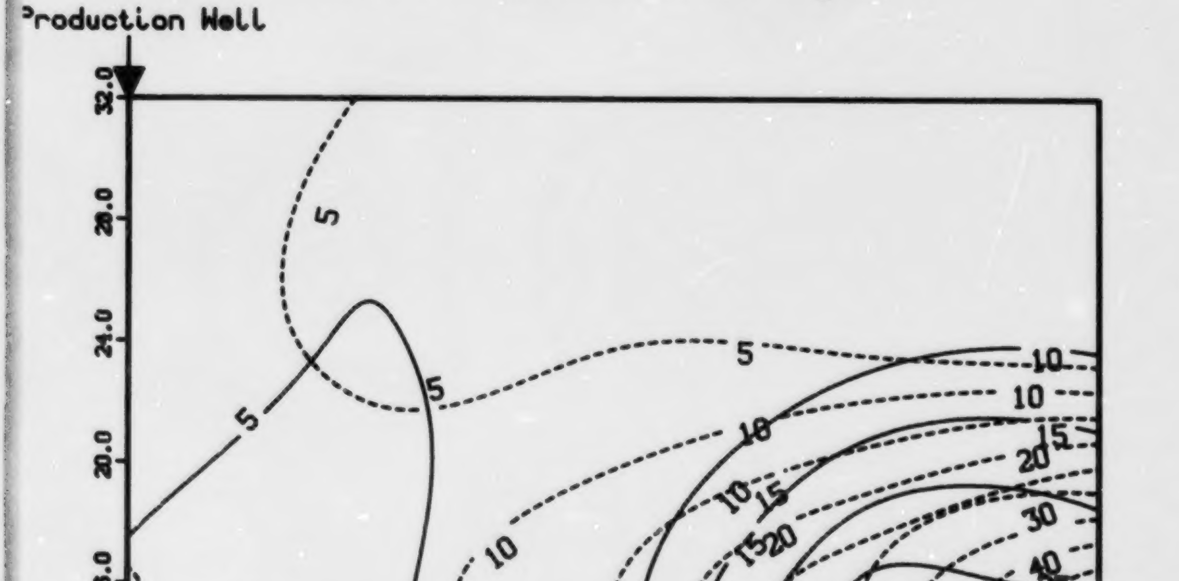

FIGURE 7: TEMPERATURE PROFILE FOR
RUN 4: CONT. STEAMFLOOD ON WATER SATURATED MODEL
0.50 Pore Volumes Steam Injected

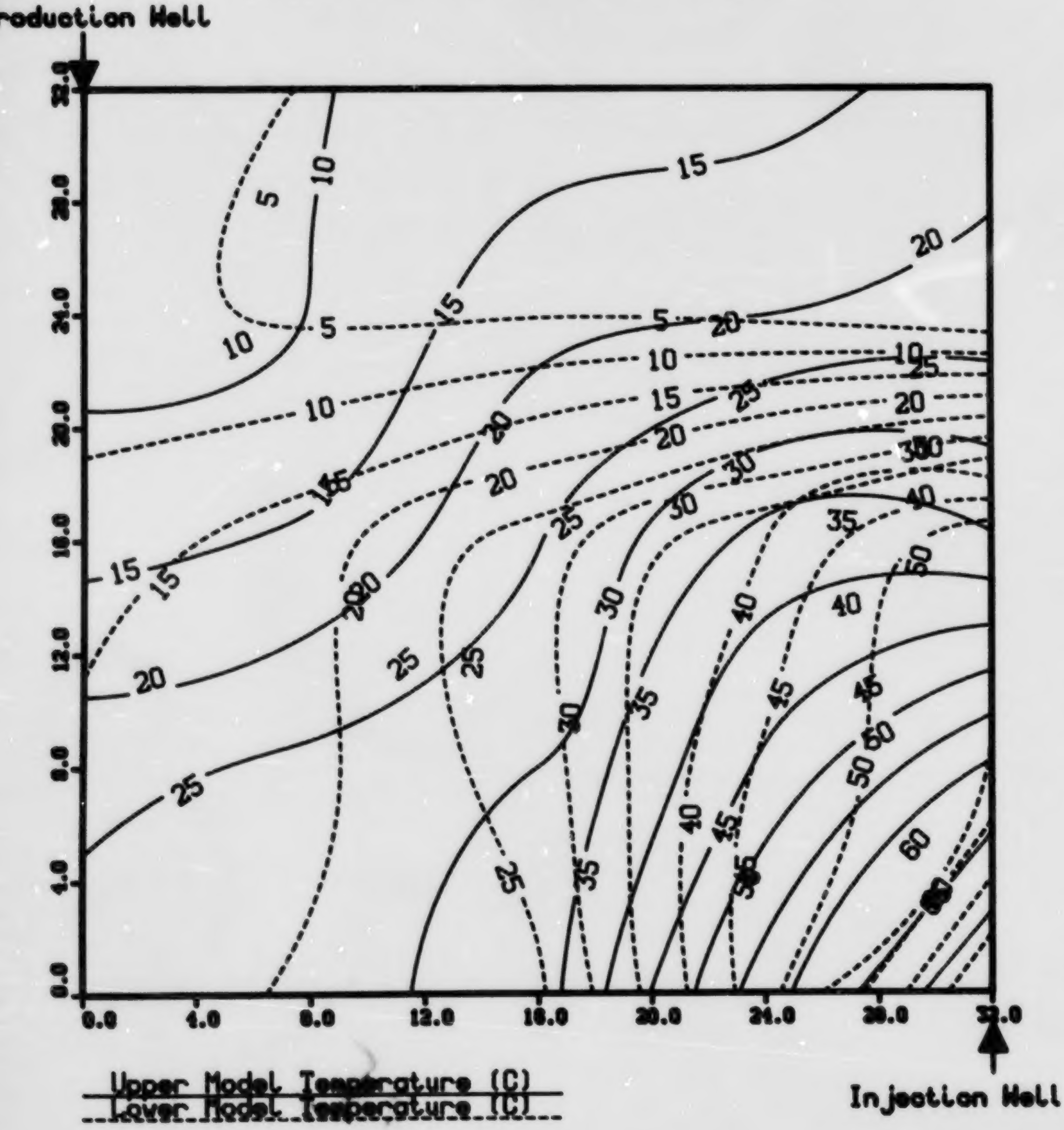

FIGURE 8: TEMPERATURE PROFILE FOR
RUN 4: CONT. STEAMFLOOD ON WATER SATURATED MODEL

0.75 Pore Volumes Steam Injected

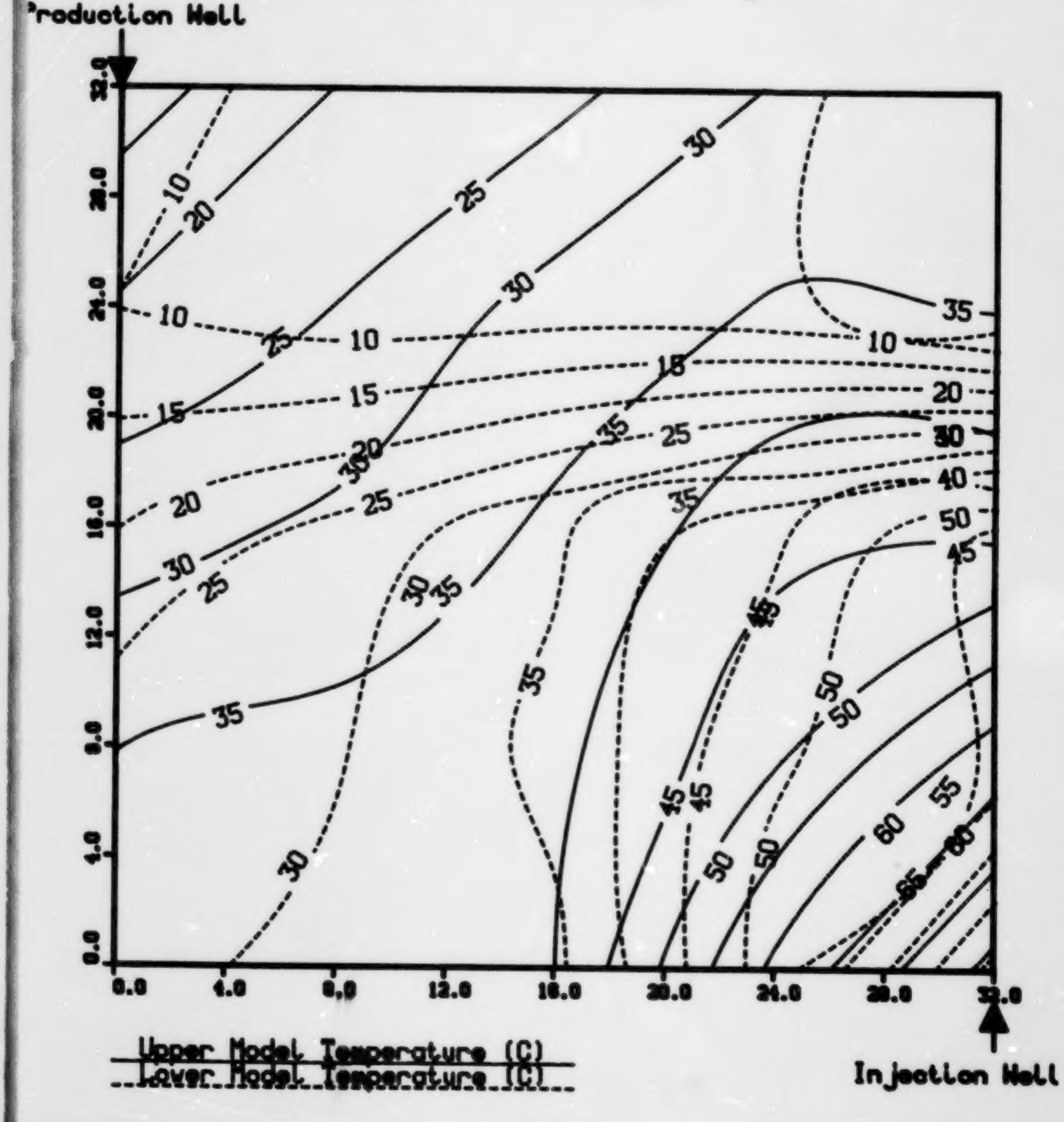

FIGURE 9: TEMPERATURE PROFILE FOR RUN 4: CONT. STEAMFLOOD ON WATER SATURATED MODEL

1.00 Pore Volumes Steam Injected

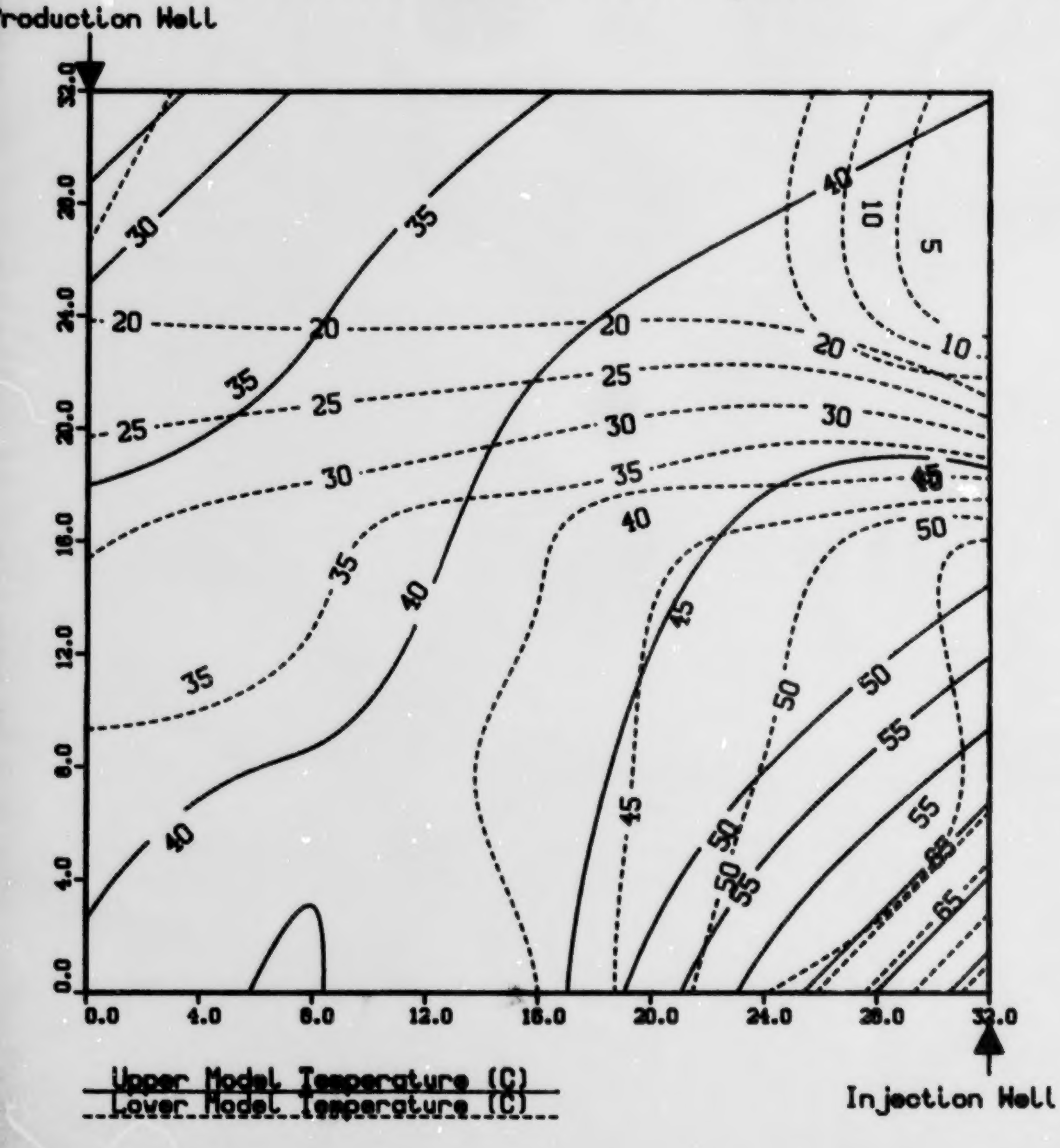

Continuous Steamflood in Aberfeldy Model.

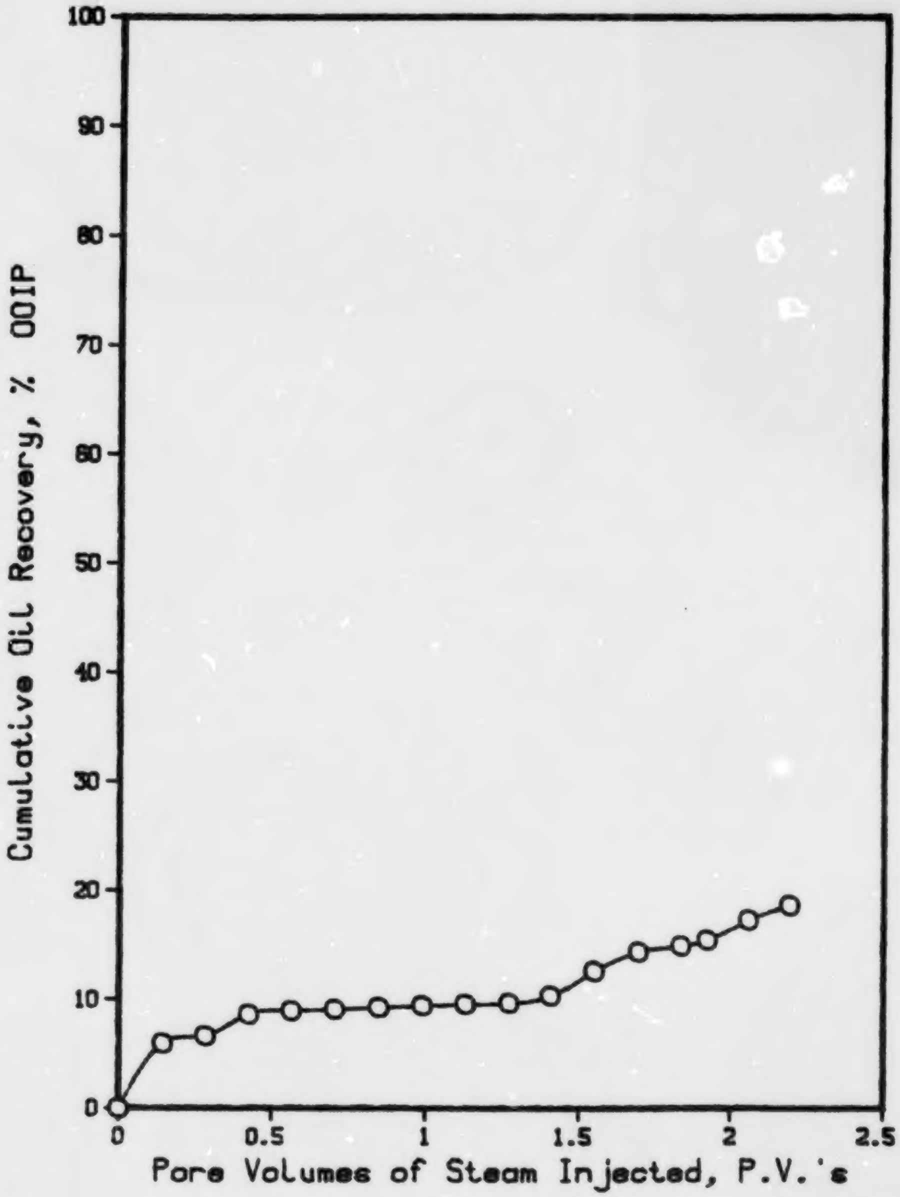

Figure 10. Run 6, Cumulative Recovery vs. PV Injected.

FIGURE 11: TEMPERATURE PROFILE FOR
RUN 6: CONTINUOUS STEAMFLOOD ON ABERFELDY MODEL

0.25 Pore Volumes Steam Injected

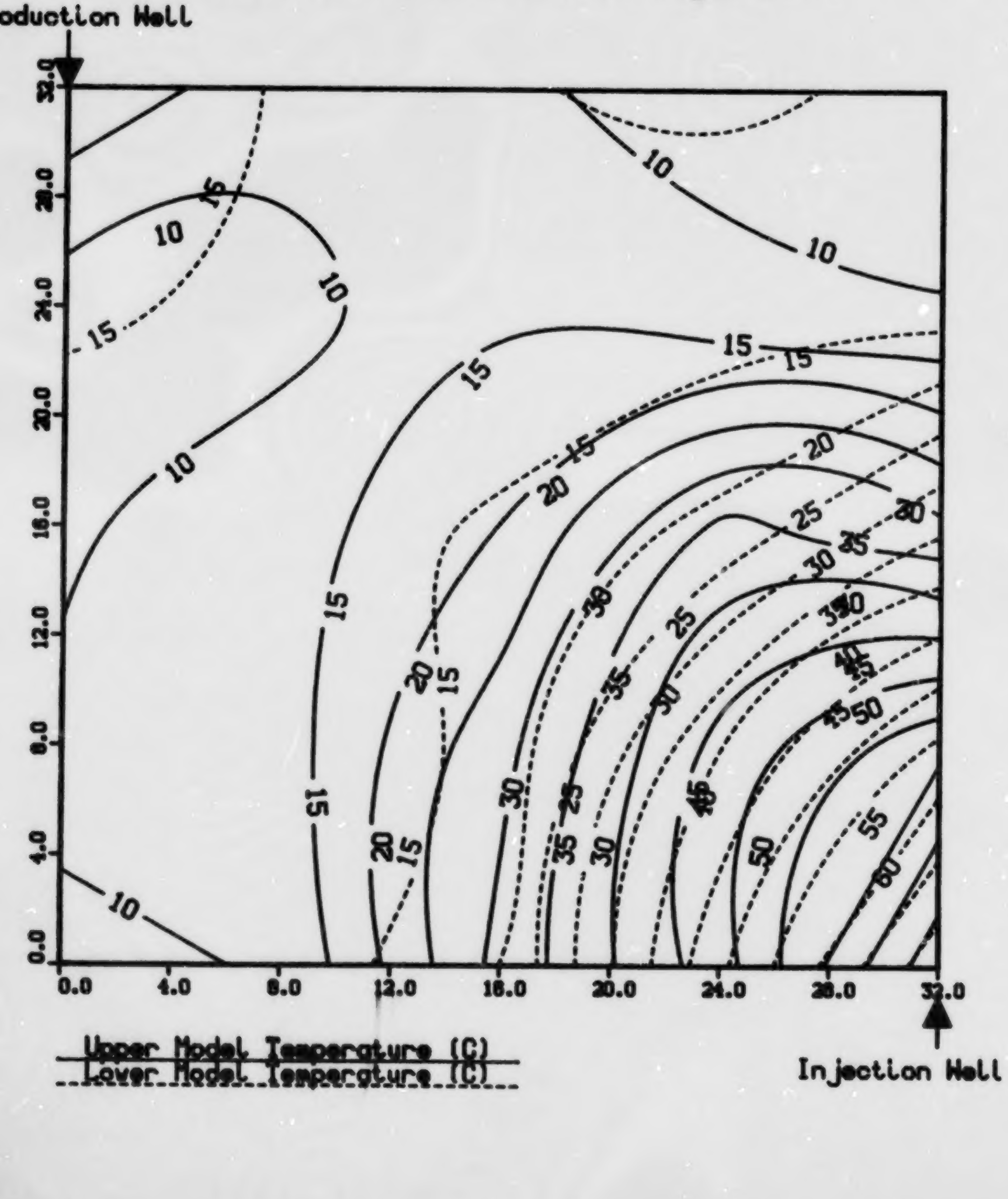

FIGURE 12: TEMPERATURE PROFILE FOR
RUN 6: CONTINUOUS STEAMFLOOD ON ABERFELDY MODEL

0.50 Pore Volumes Steam Injected

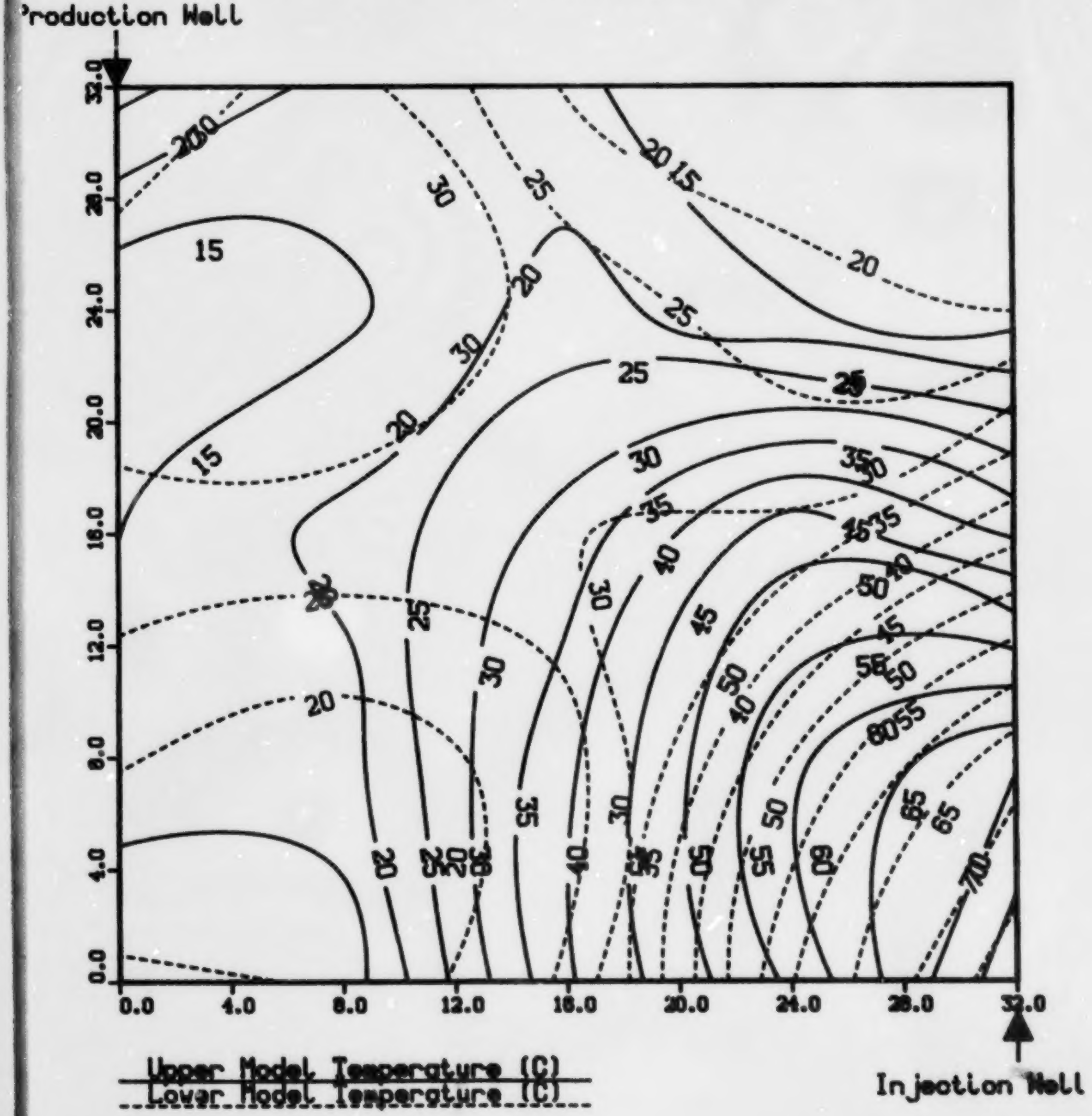

FIGURE 13: TEMPERATURE PROFILE FOR RUN 6: CONTINUOUS STEAMFLOOD ON ABERFELDY MODEL

0.75 Pore Volumes Steam Injected

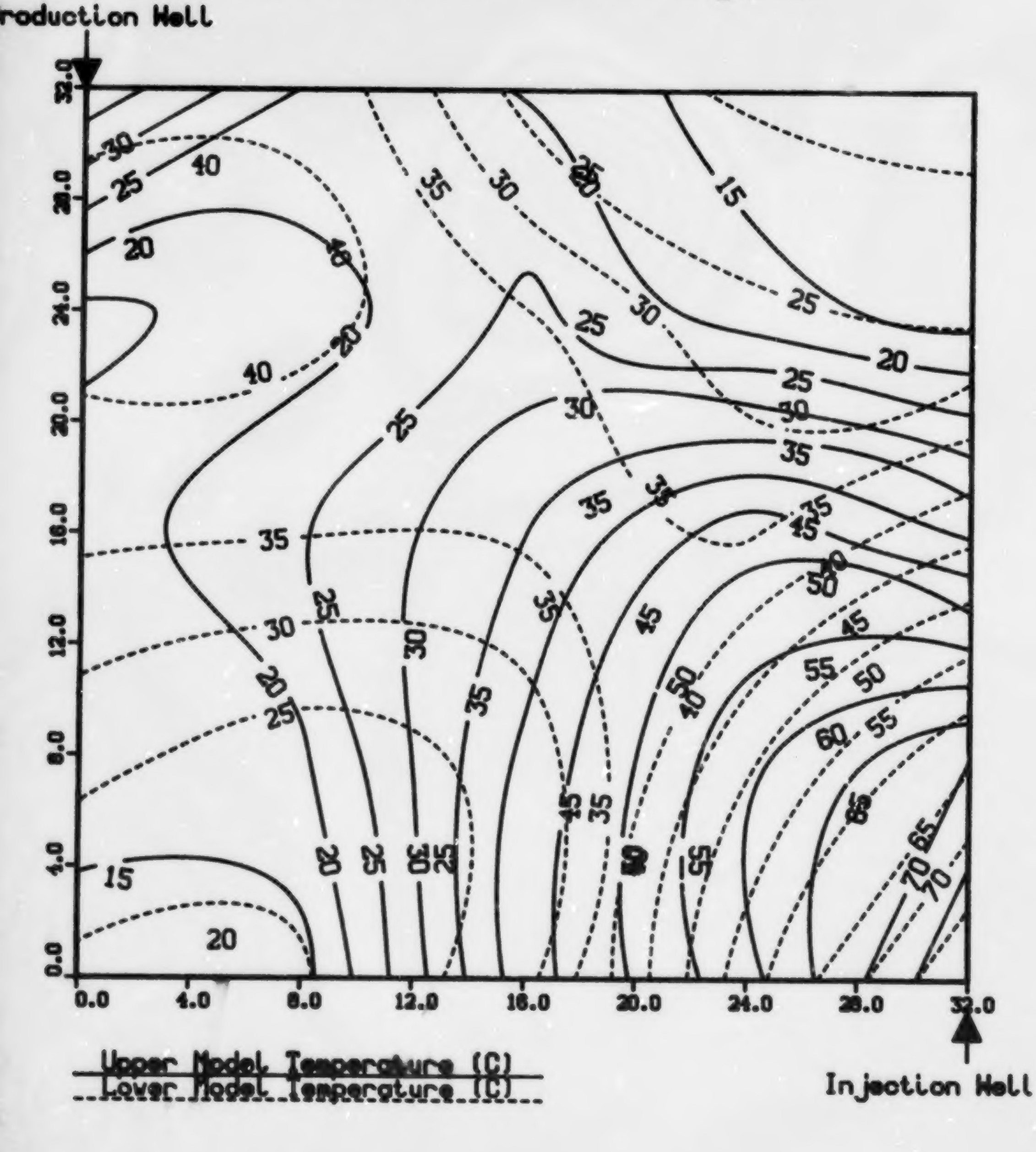

FIGURE 14: TEMPERATURE PROFILE FOR RUN 6: CONTINUOUS STEAMFLOOD ON ABERFELDY MODEL

1.0 Pore Volume Steam Injected

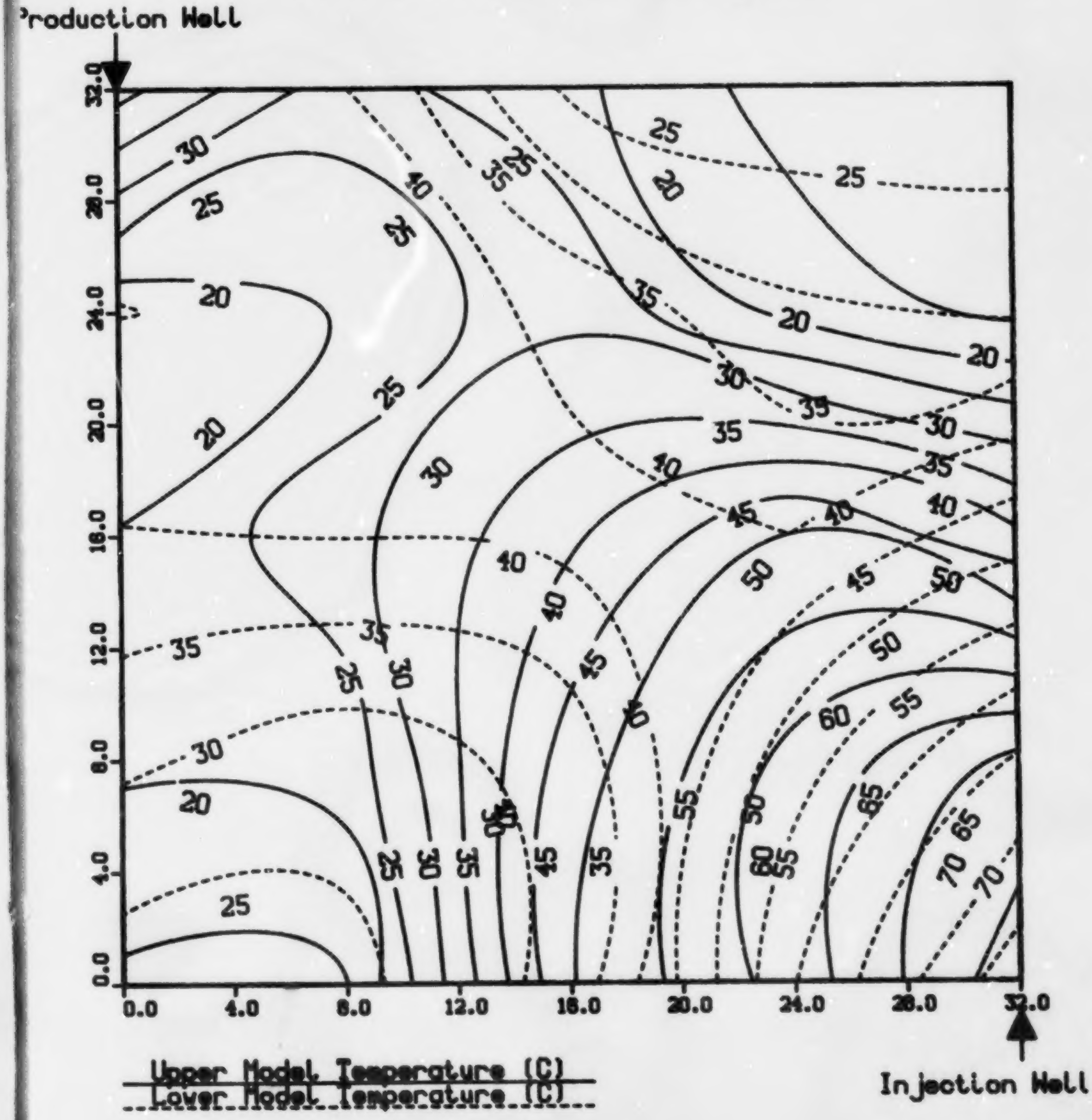

Continuous Steamflood in Aberfeldy Model.

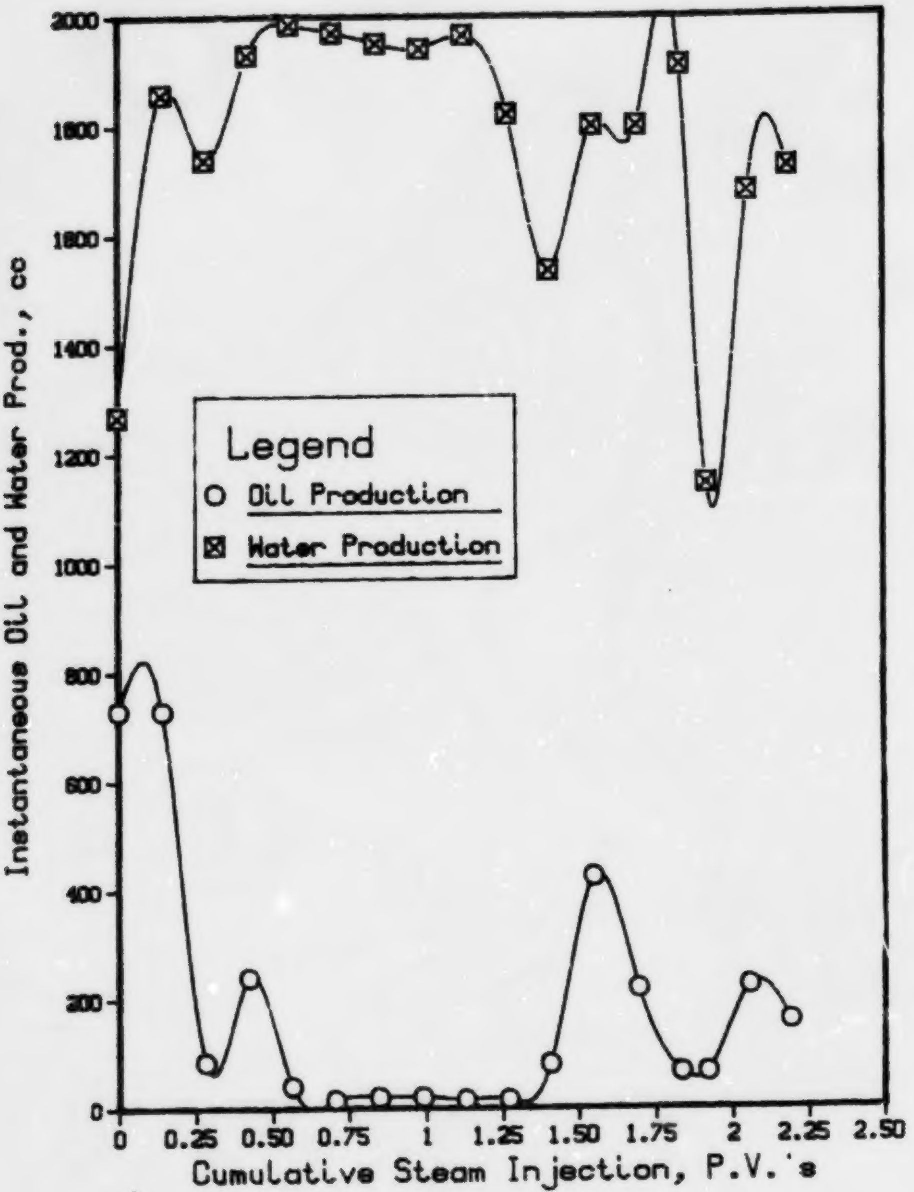

Figure 15. Run 6, Instantaneous Oil and Water Production vs. Cumulative Injection.

FIGURE 16: TEMPERATURE PROFILE FOR RUN 7C: STEAMFLOOD ON ABERFELDY MODEL AFTER W.F.

0.25 Pore Volumes Steam Injected

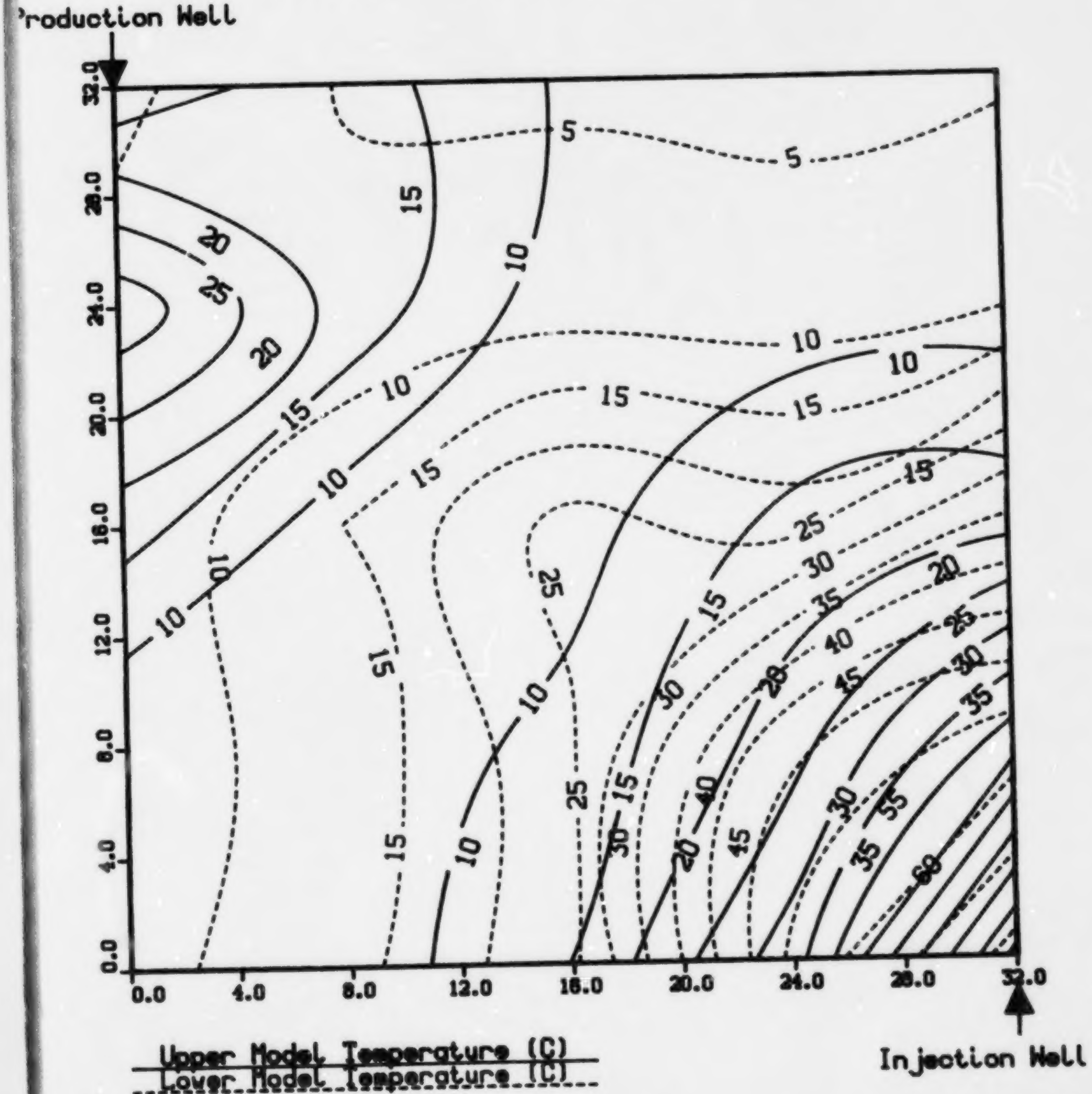

FIGURE 17: TEMPERATURE PROFILE FOR
RUN 7C: STEAMFLOOD ON ABERFELDY MODEL AFTER W.F.

0.50 Pore Volumes Steam Injected

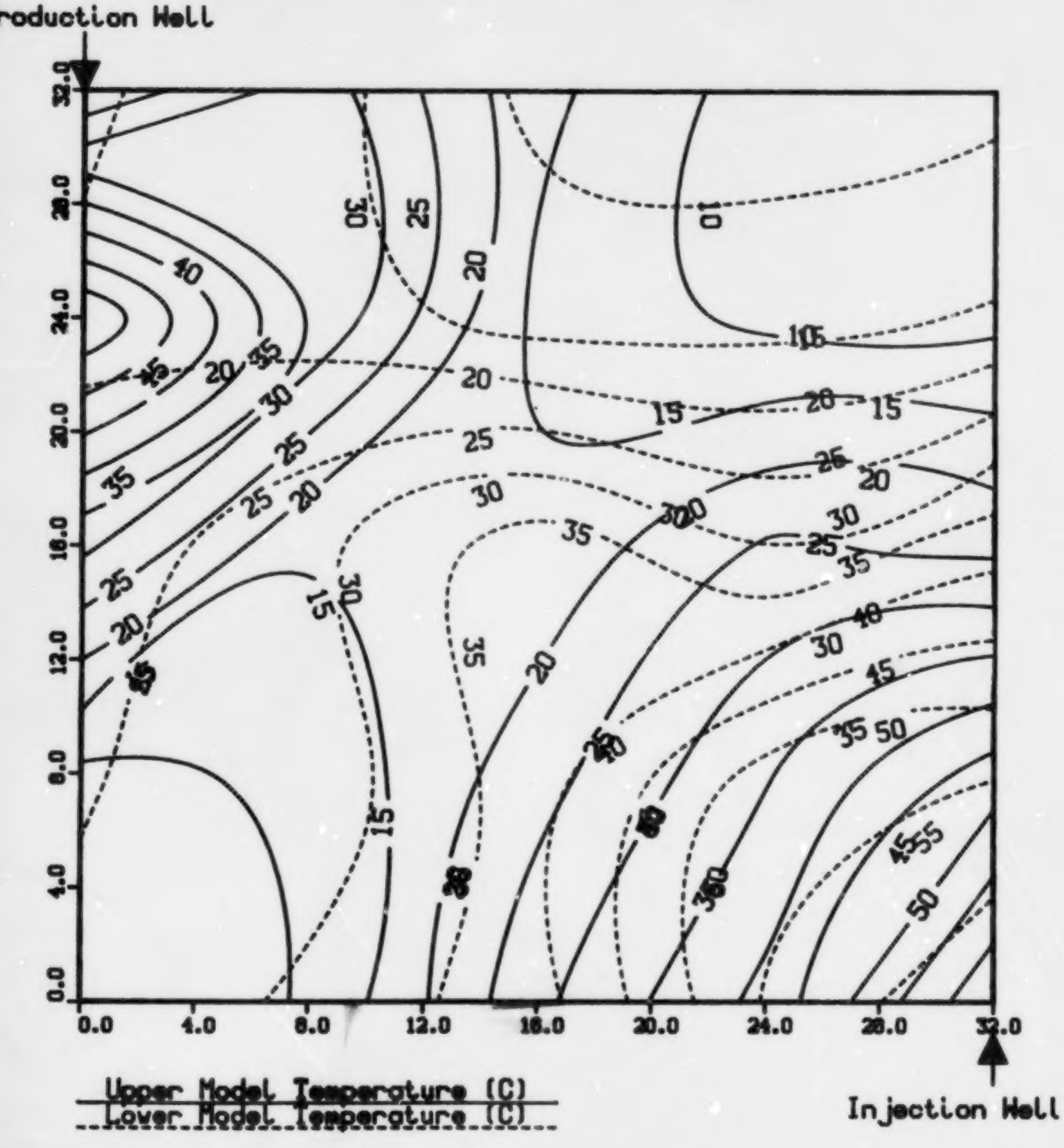

FIGURE 18: TEMPERATURE PROFILE FOR
RUN 7C: STEAMFLOOD ON ABERFELDY MODEL AFTER W.F.

0.75 Pore Volumes Steam Injected

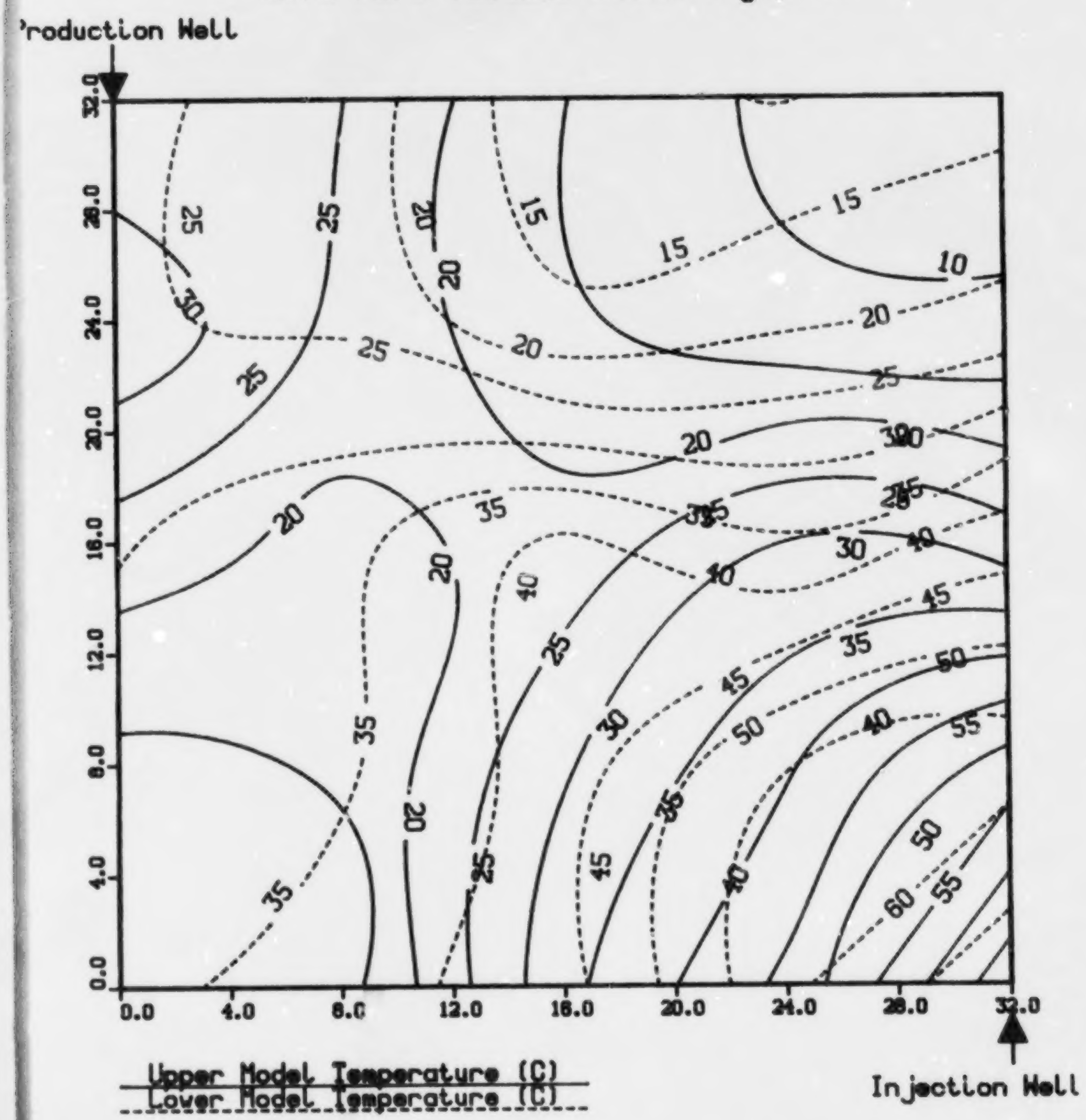

FIGURE 19: TEMPERATURE PROFILE FOR
RUN 7C: STEAMFLOOD ON ABERFELDY MODEL AFTER W.F.
1.00 Pore Volumes Steam Injected

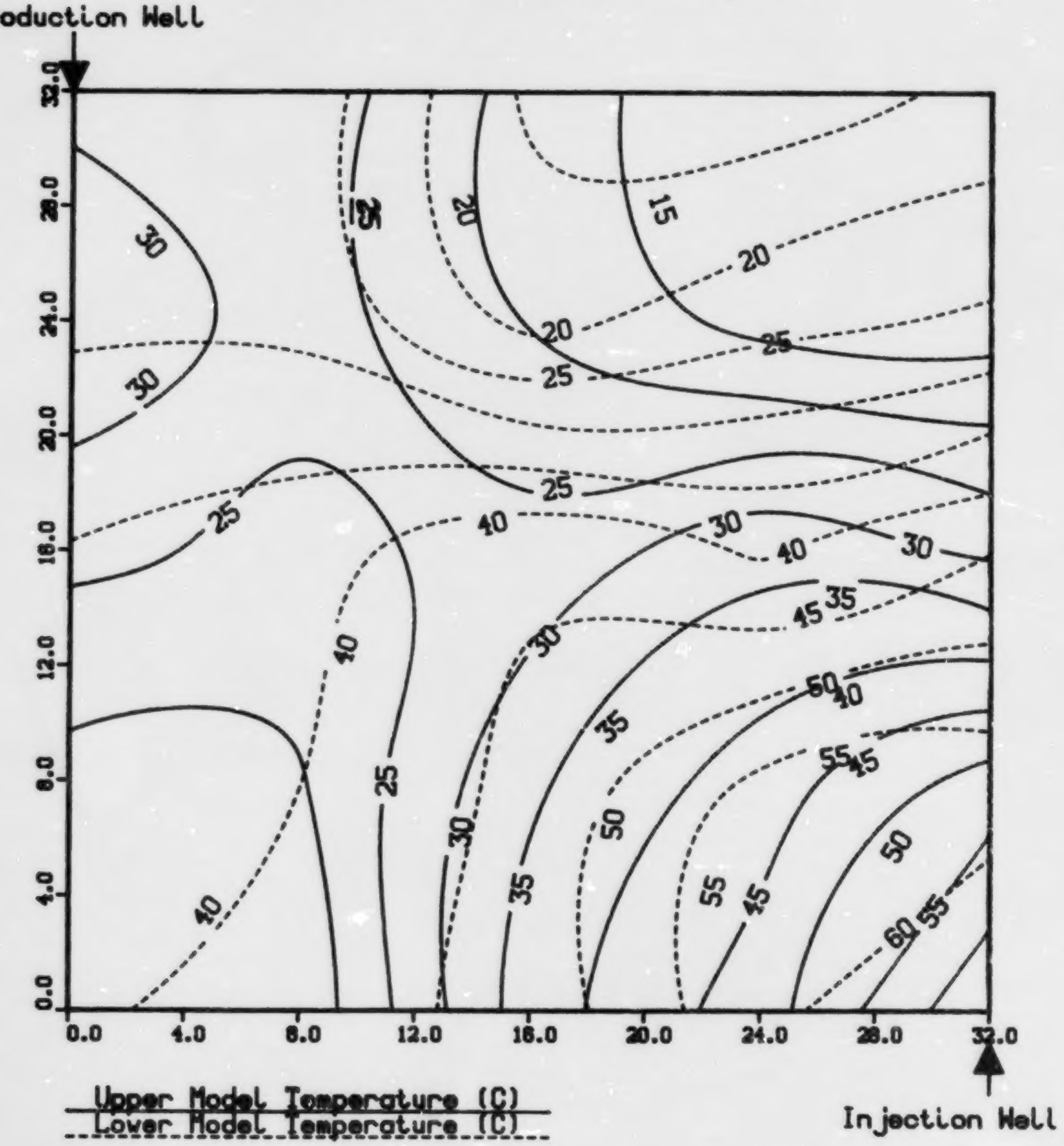

Steamflood Following Waterflood in Aberfeldy Model.

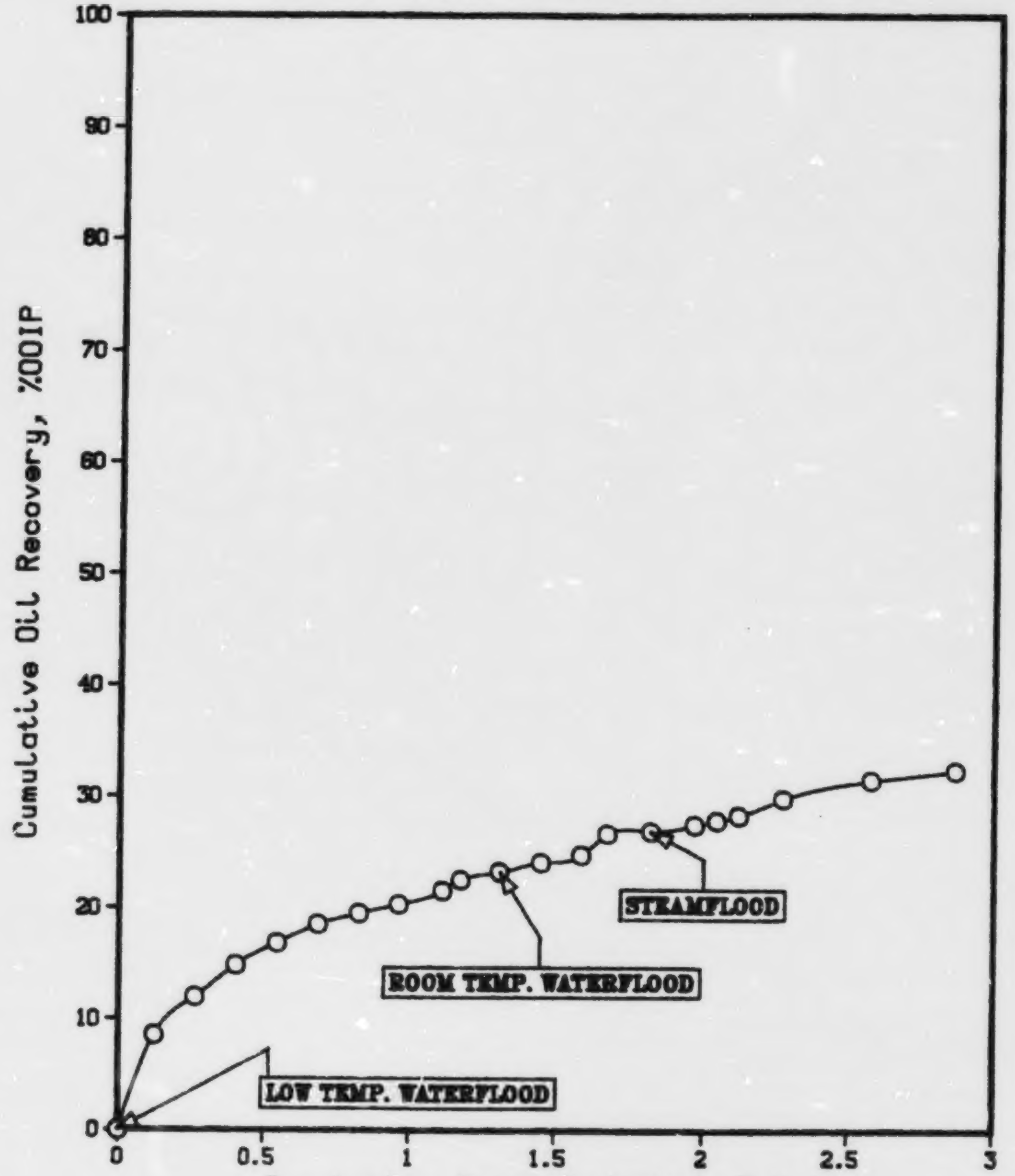

Figure 20. Run 7, Cumulative Recovery vs. PV Injected.

Steamflood Following Waterflood in Aberfeldy Model.

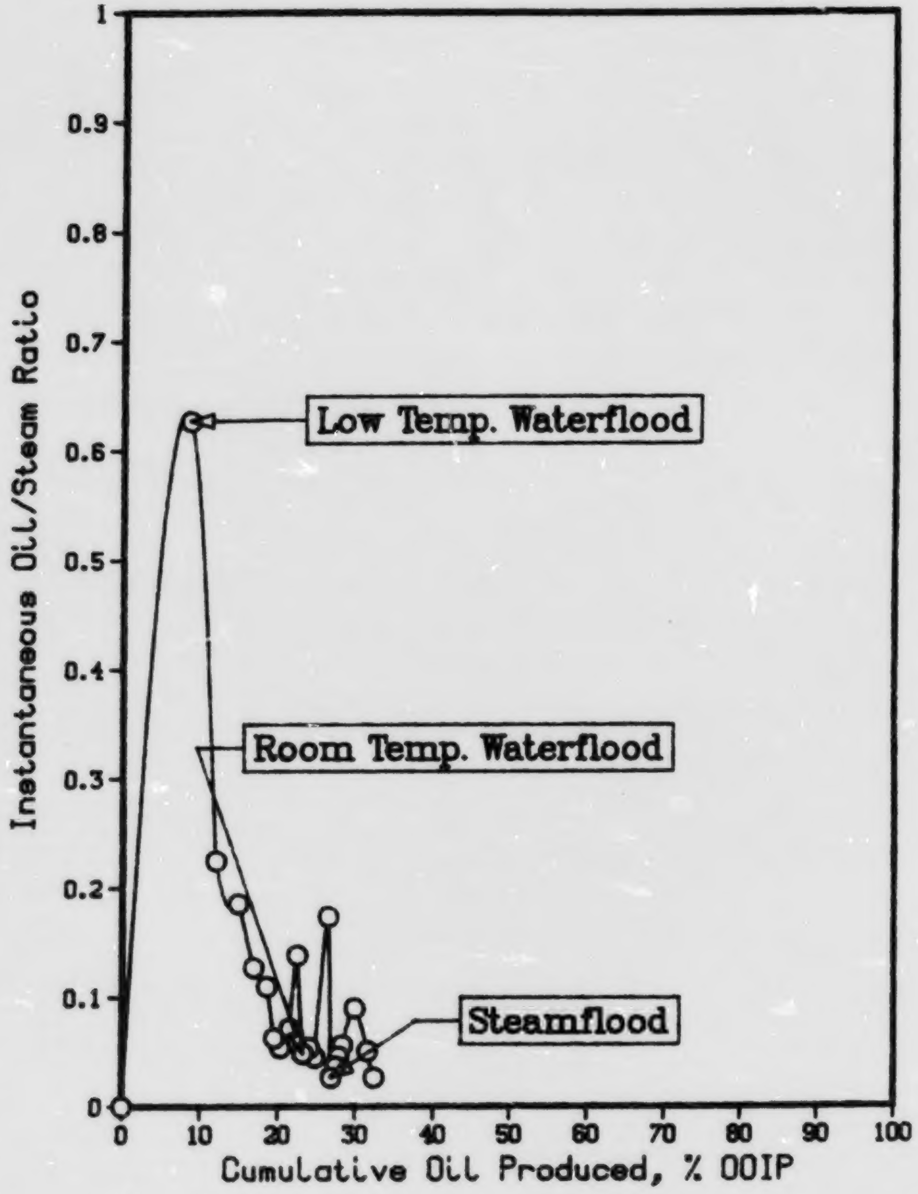

Figure 21. Run 7, Instantaneous Oil/Steam Ratio vs. Cumulative Oil Production.

Steamflood Following Waterflood in Aberfeldy Model.

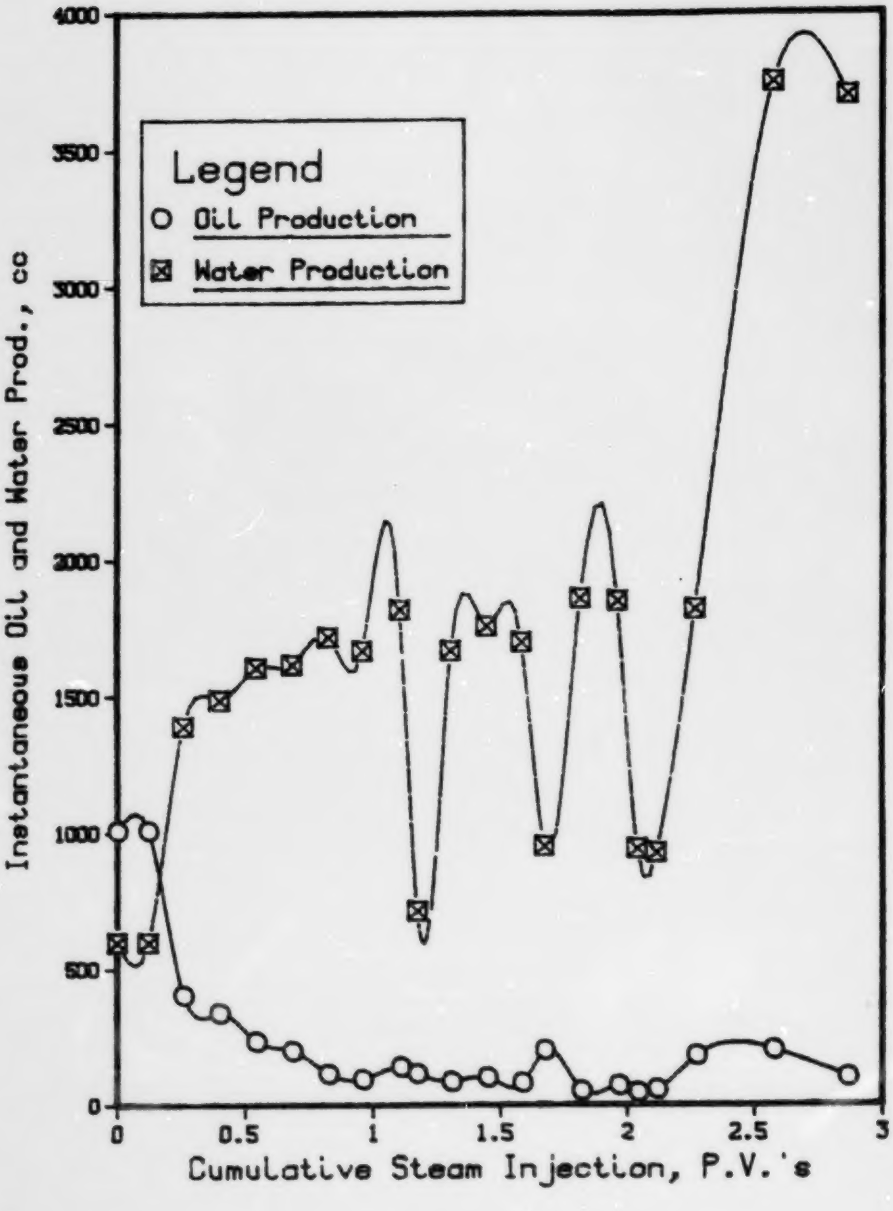

Figure 22. Run 7, Instantaneous Oil and Water Production vs. Cumulative Injection.

FIGURE 23: TEMPERATURE PROFILE FOR RUN 10: CONTINUOUS STEAMFLOOD ON ABERFELDY MODEL

0.25 Pore Volumes Steam Injected

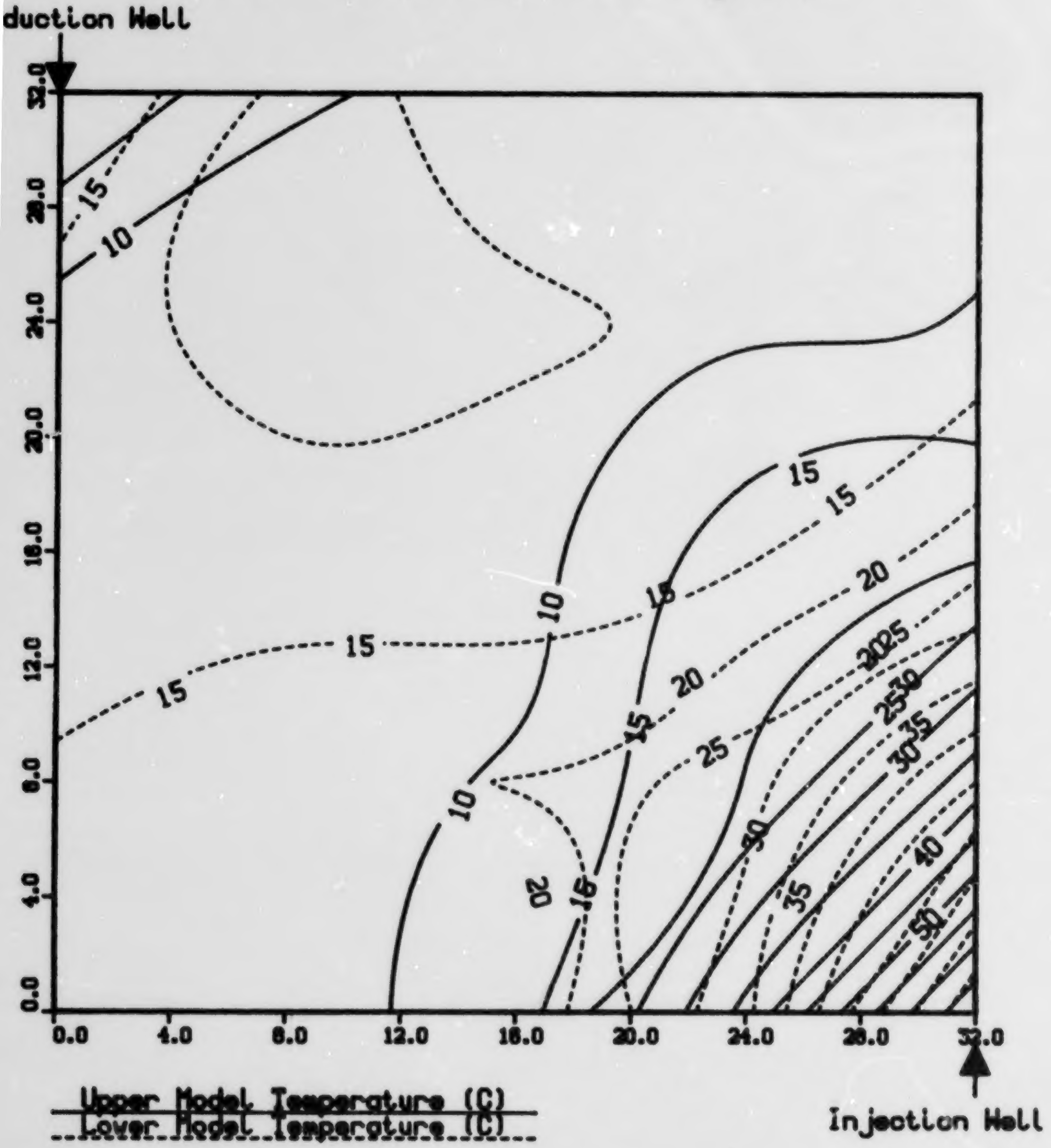

FIGURE 24: TEMPERATURE PROFILE FOR
RUN 10: CONTINUOUS STEAMFLOOD ON ABERFELDY MODEL

0.50 Pore Volumes Steam Injected

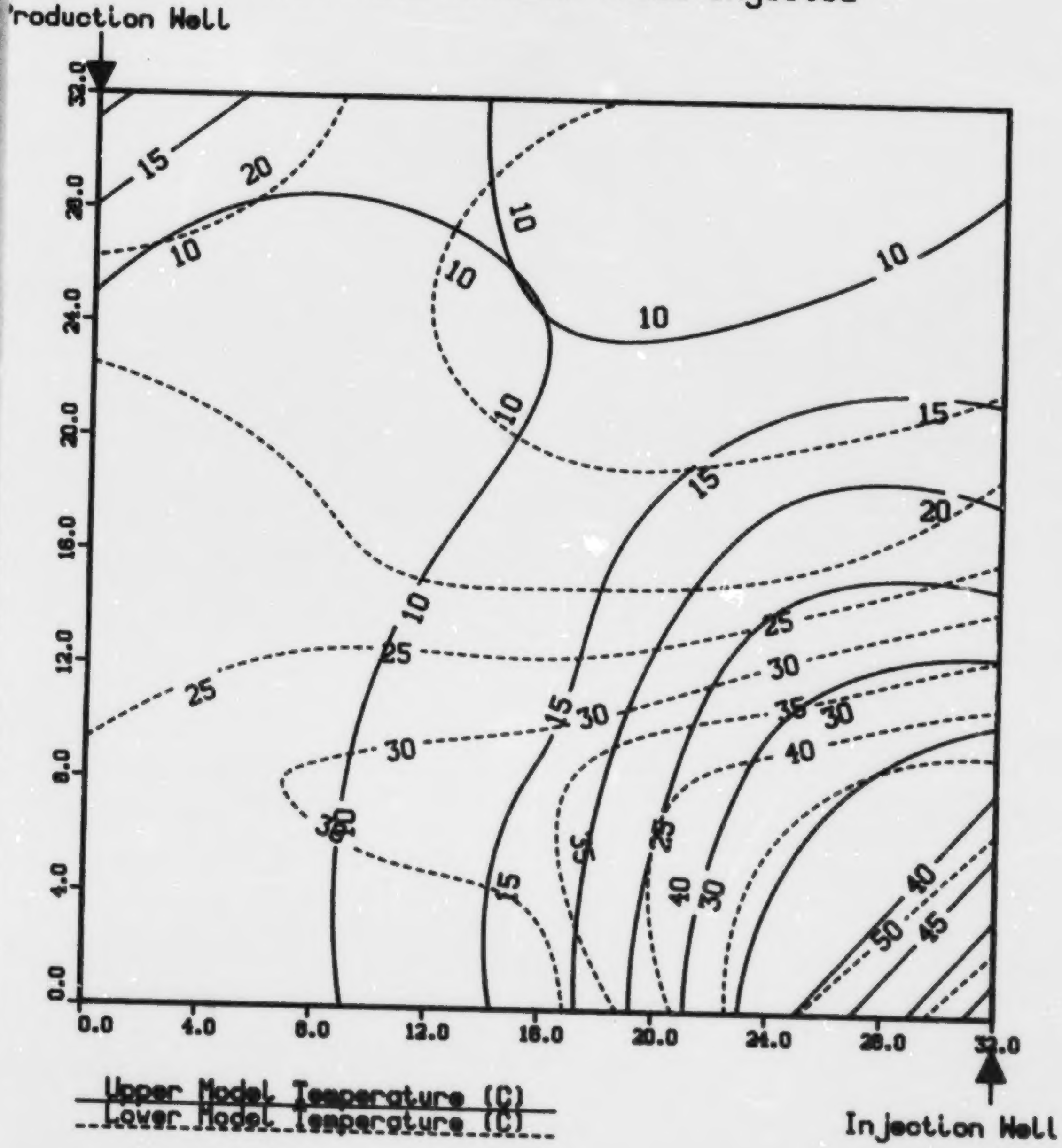

FIGURE 25: TEMPERATURE PROFILE FOR RUN 10: CONTINUOUS STEAMFLOOD ON ABERFELDY MODEL

0.75 Pore Volumes Steam Injected

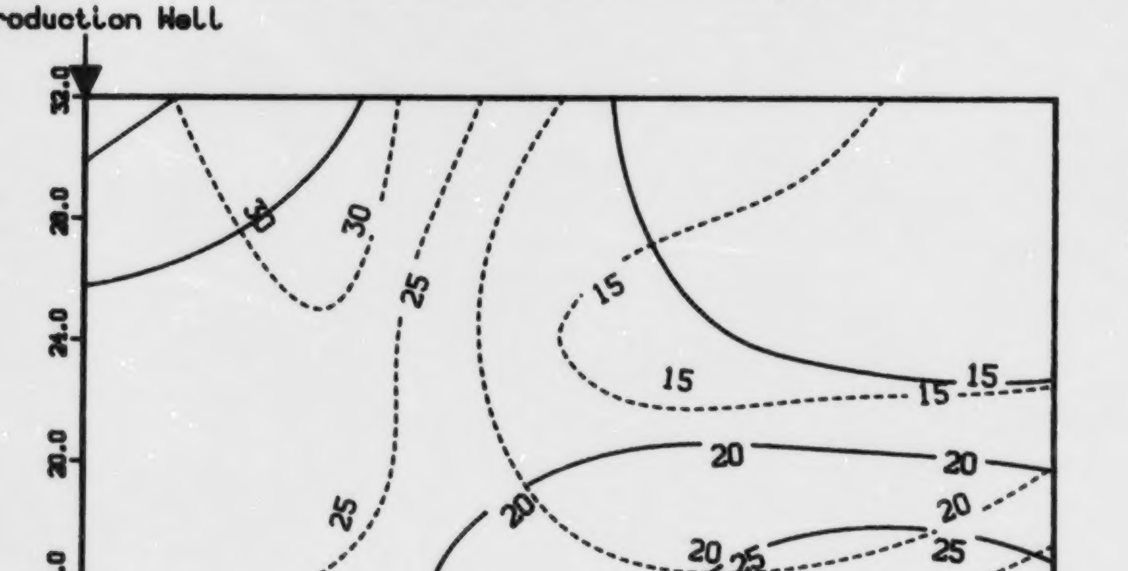

FIGURE 26: TEMPERATURE PROFILE FOR
RUN 10: CONTINUOUS STEAMFLOOD ON ABERFELDY MODEL

1.00 Pore Volumes Steam Injected

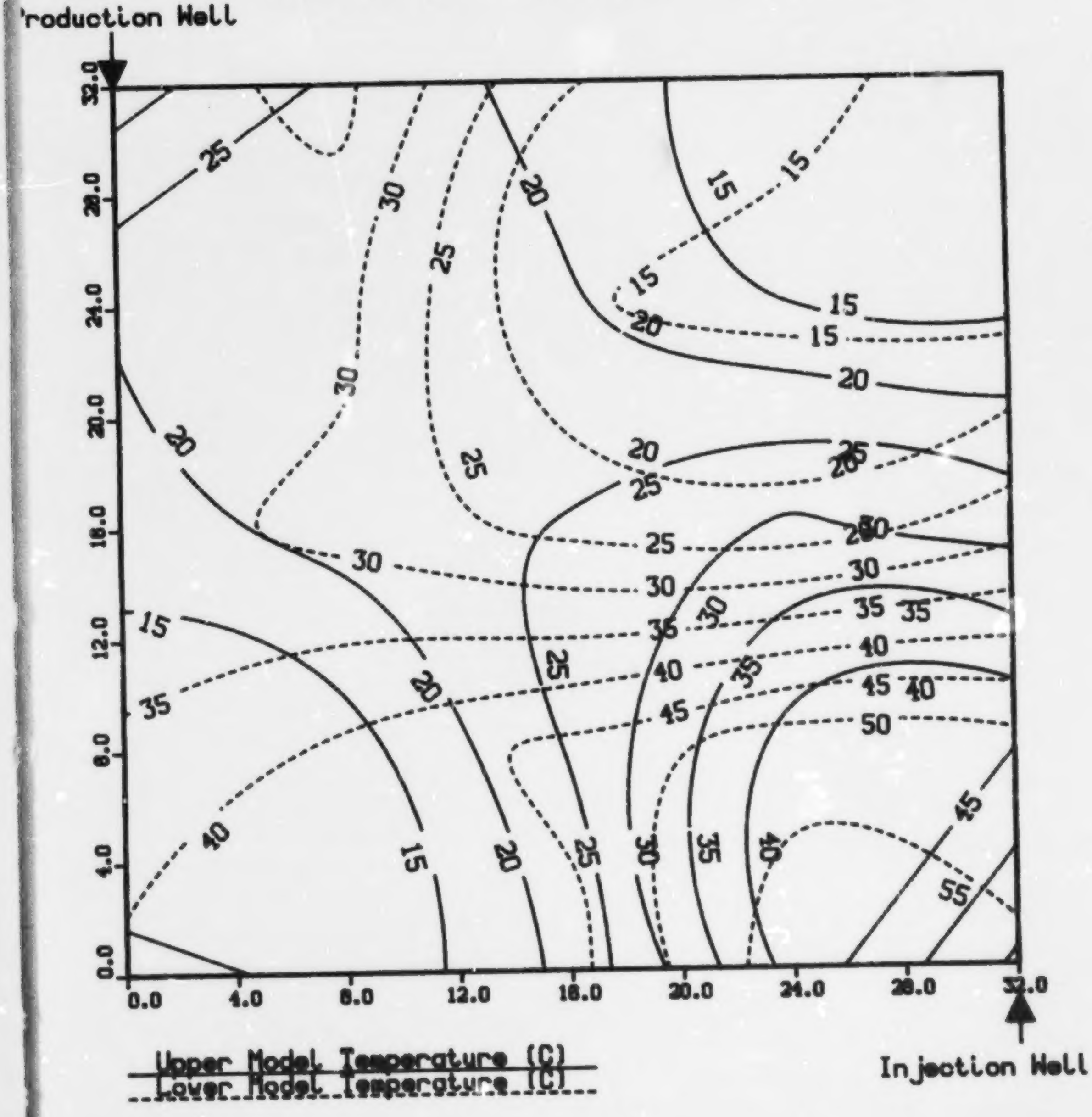

Continuous Steamflood in Aberfeldy Model.

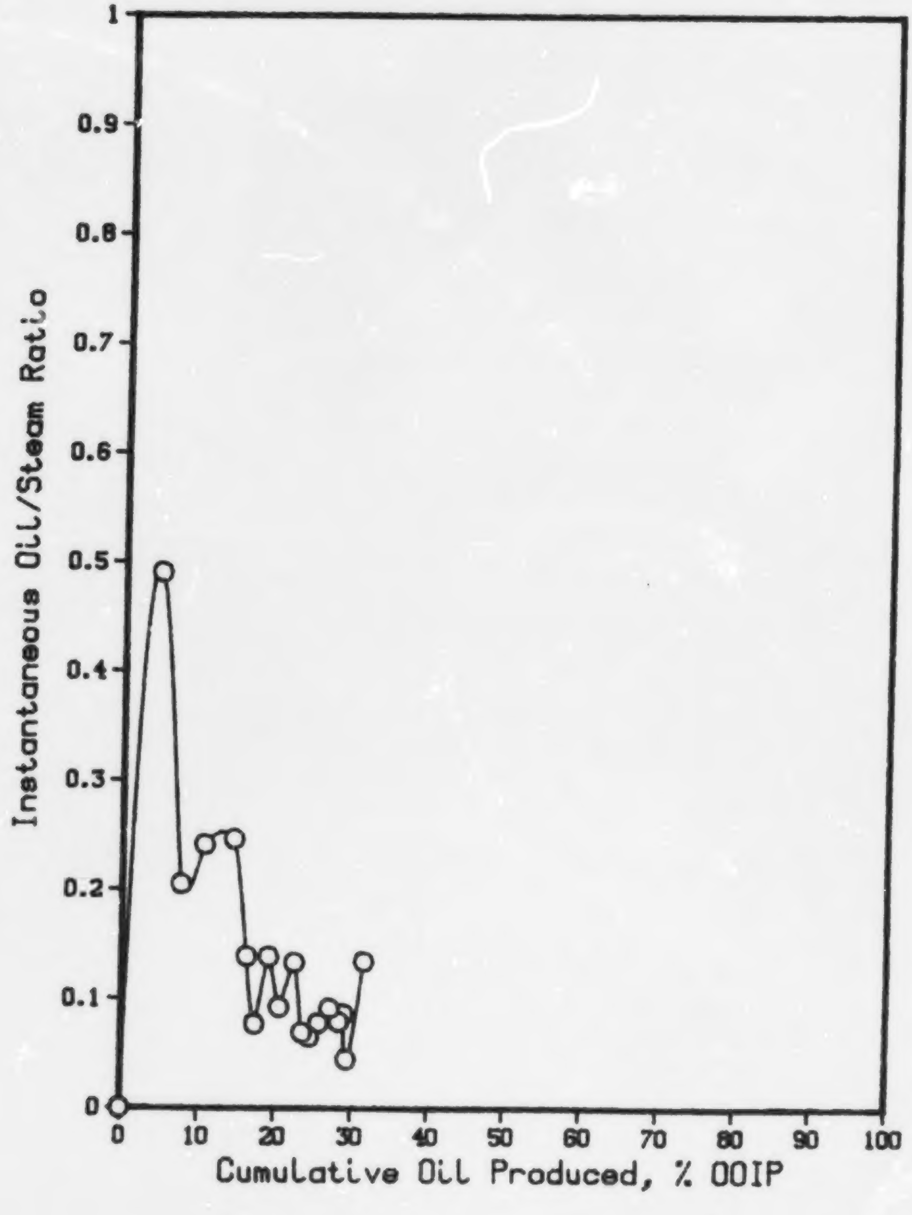

Figure 27. Run 10, Instantaneous Oil/Steam Ratio vs. Cumulative Oil Production.

Continuous Steamflood in Aberfeldy Model.

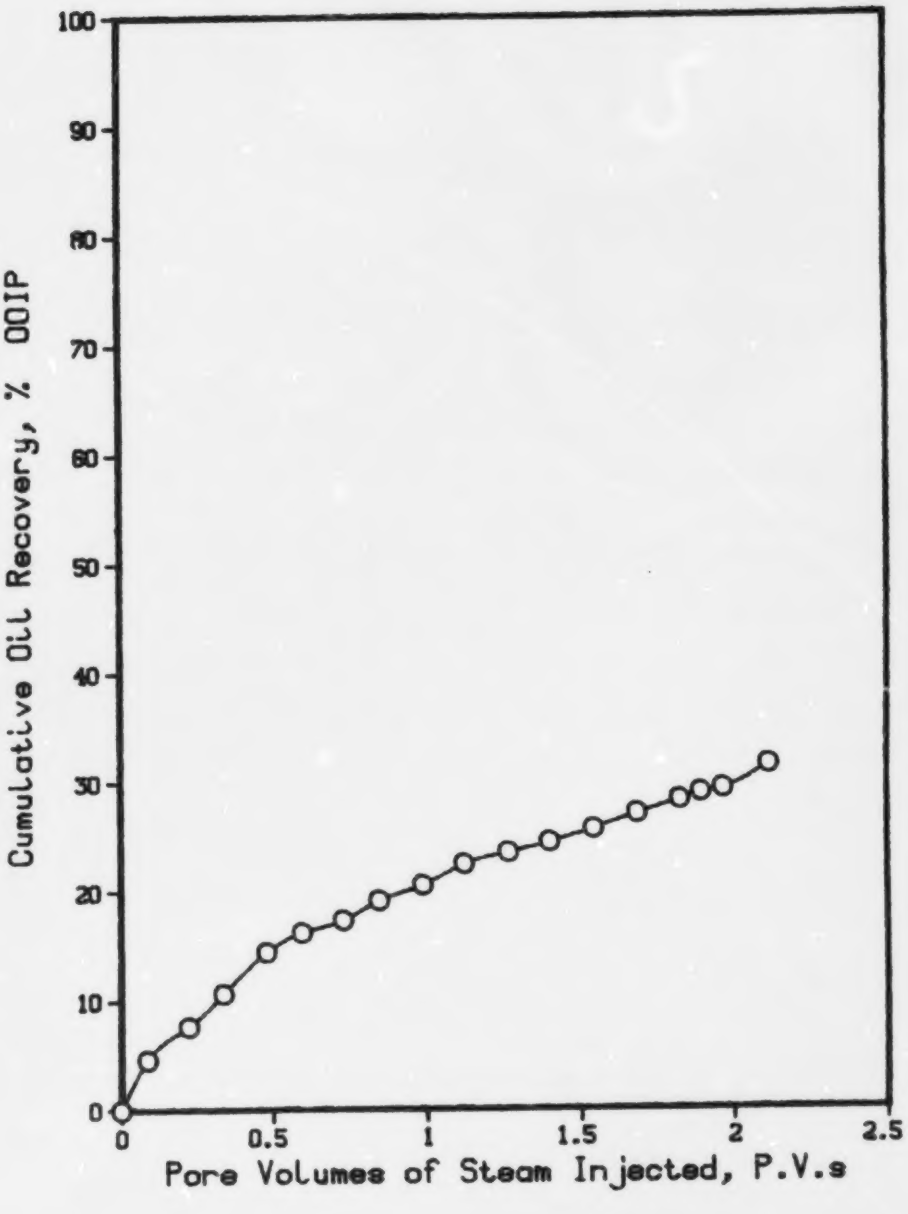

Figure 28. Run 10, Cumulative Recovery vs. Pore Volumes Steam Injected.

Continuous Steamflood in Aberfeldy Model.

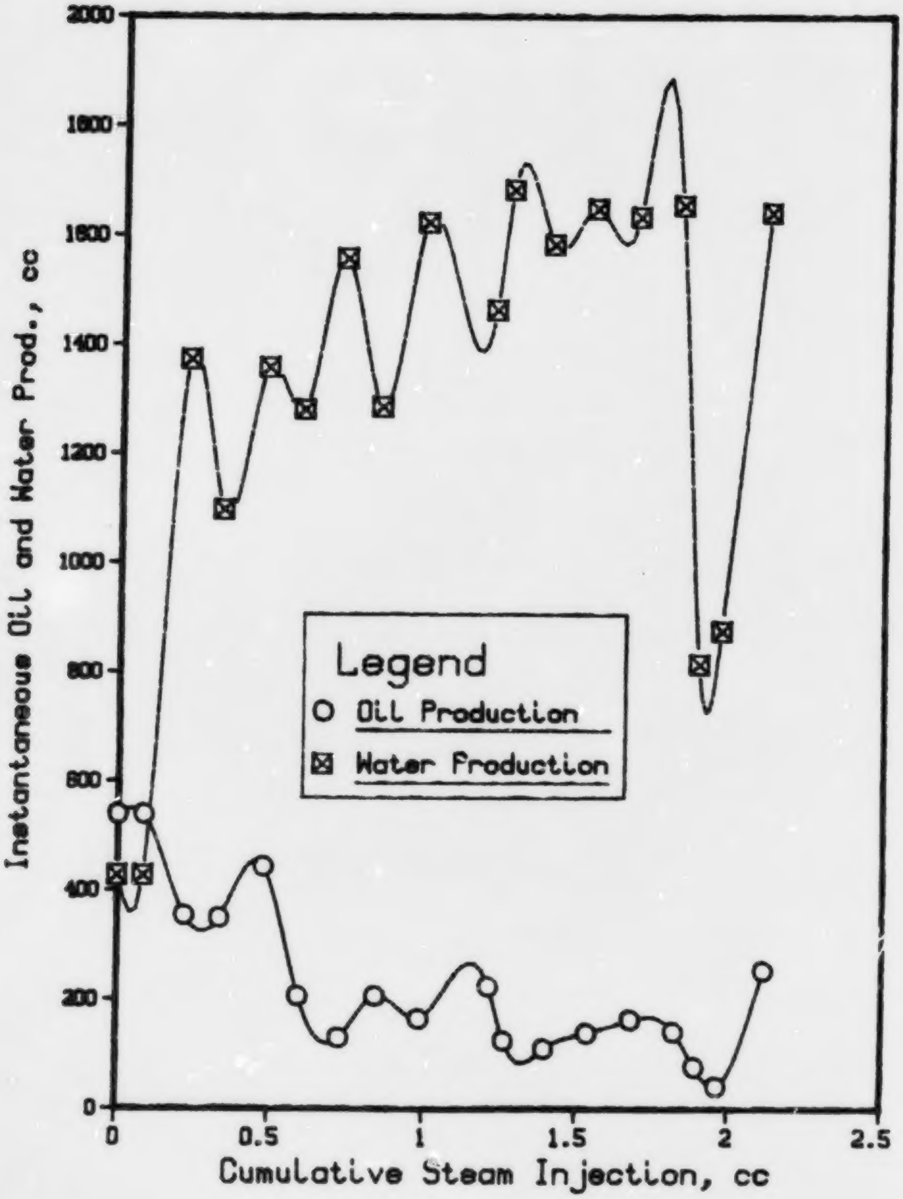

Figure 29. Run 10, Instantaneous Oil and Water Production vs. Cumulative Injection.

Two Continuous Steamfloods in Aberfeldy Model.

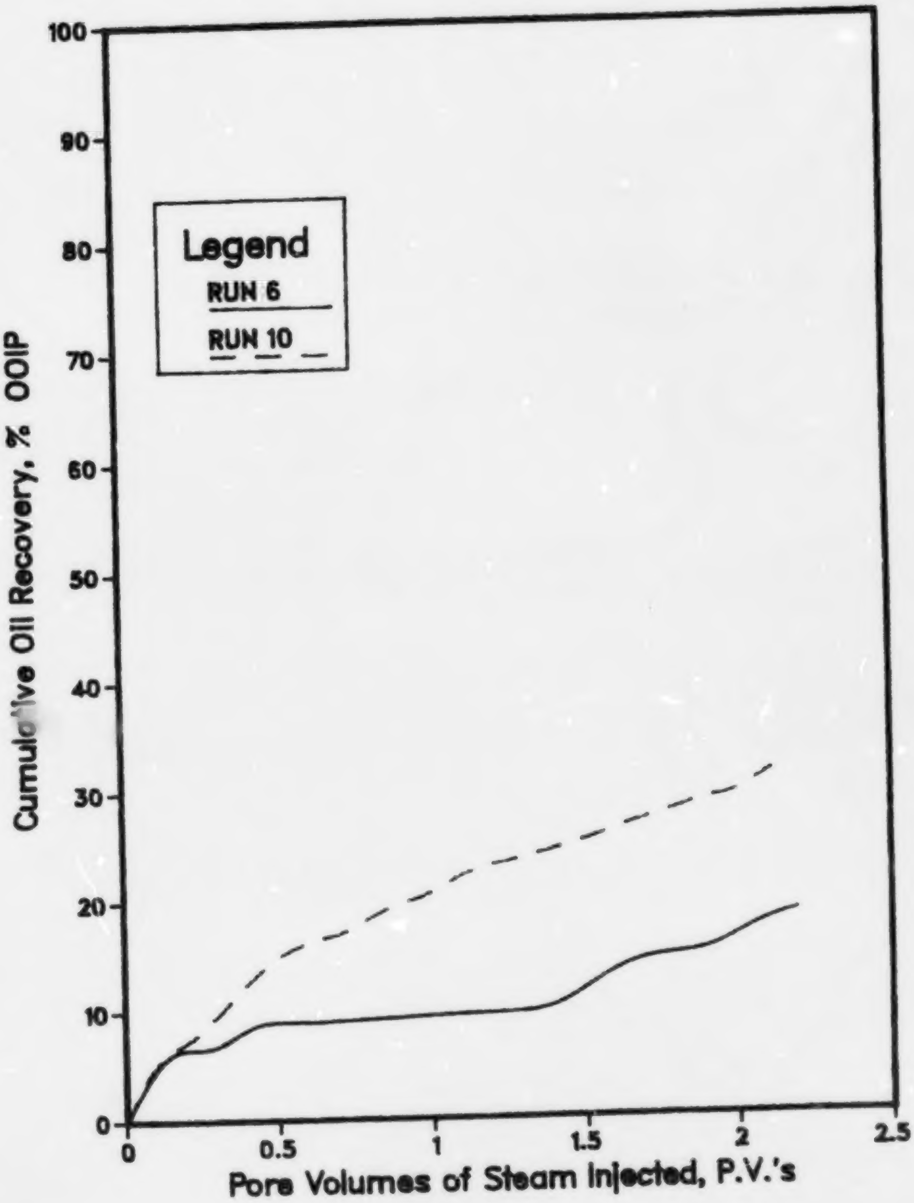

Figure 30. Comparison of the Recovery Response of Run 6 and Run 10.

FIGURE 31: TEMPERATURE PROFILE FOR
RUN 9: CONTINUOUS STEAMFLOOD ON HEAVY OIL MODEL

0.50 Pore Volumes Steam Injected

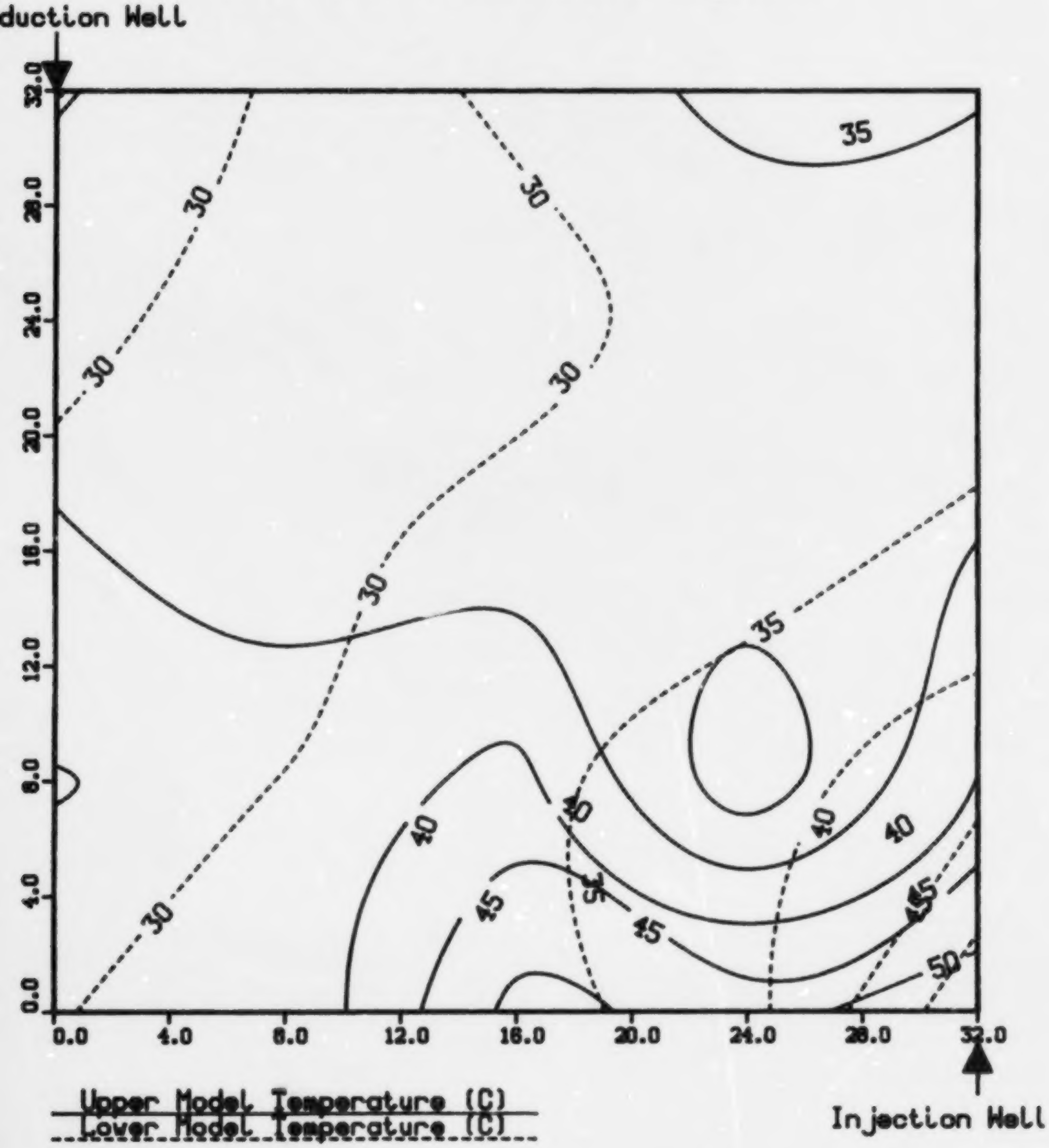

FIGURE 32: TEMPERATURE PROFILE FOR
RUN 9: CONTINUOUS STEAMFLOOD ON HEAVY OIL MODEL

1.00 Pore Volumes Steam Injected

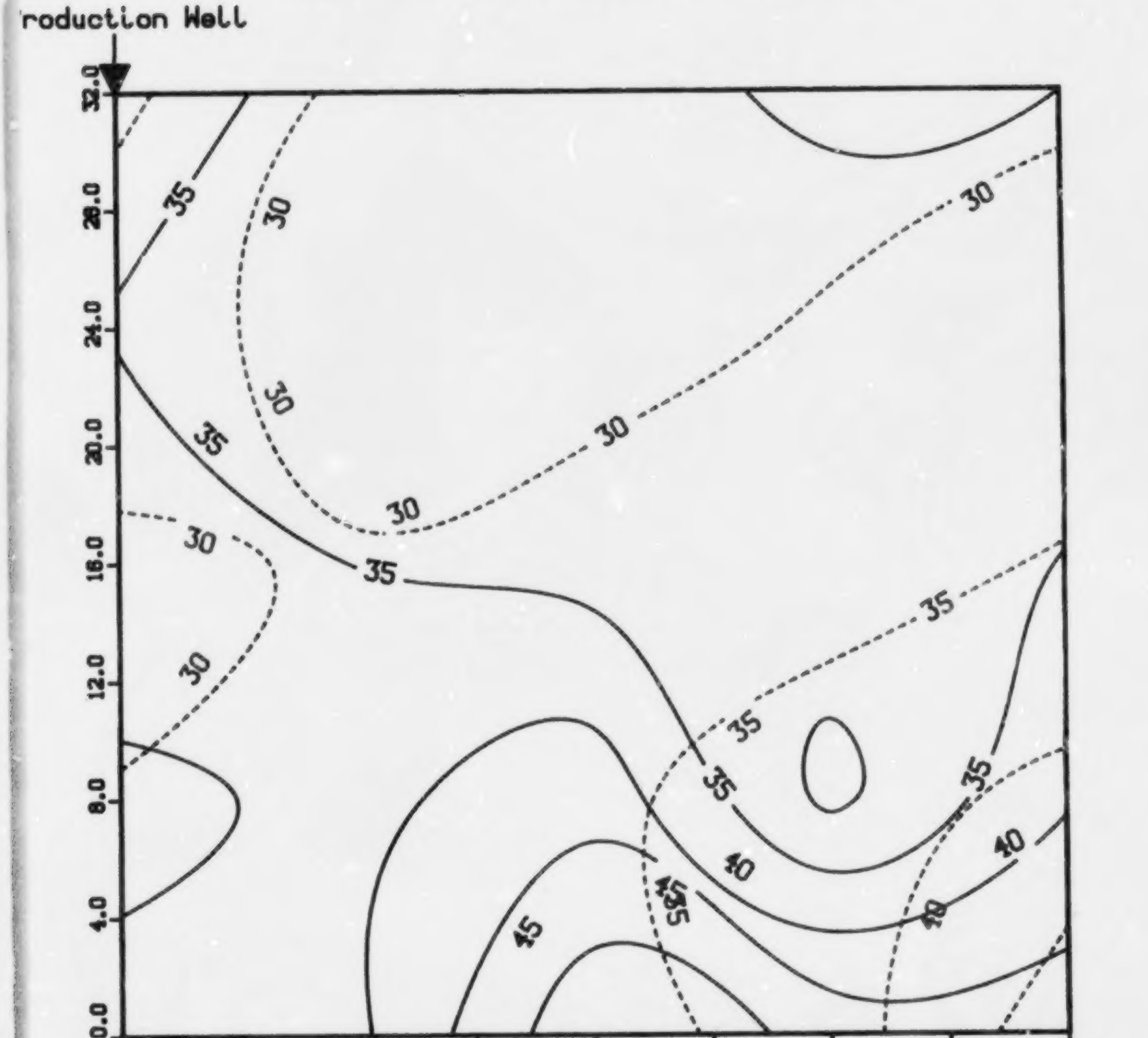

FIGURE 33: TEMPERATURE PROFILE FOR RUN 12: CONTINUOUS STEAMFLOOD ON LIGHT OIL MODEL

0.25 Pore Volumes Steam Injected

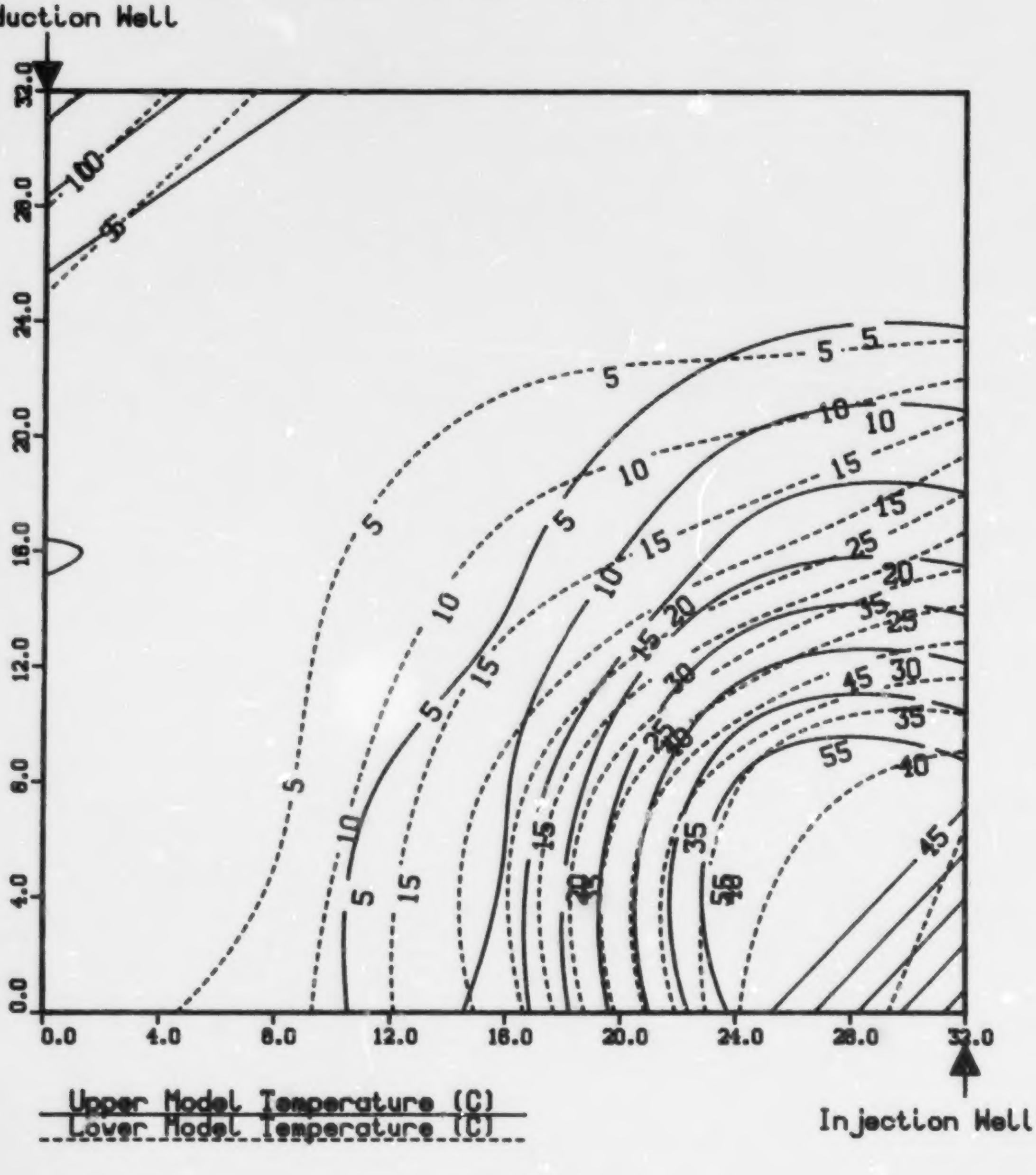

FIGURE 34: TEMPERATURE PROFILE FOR RUN 12: CONTINUOUS STEAMFLOOD ON LIGHT OIL MODEL

0.50 Pore Volumes Steam Injected

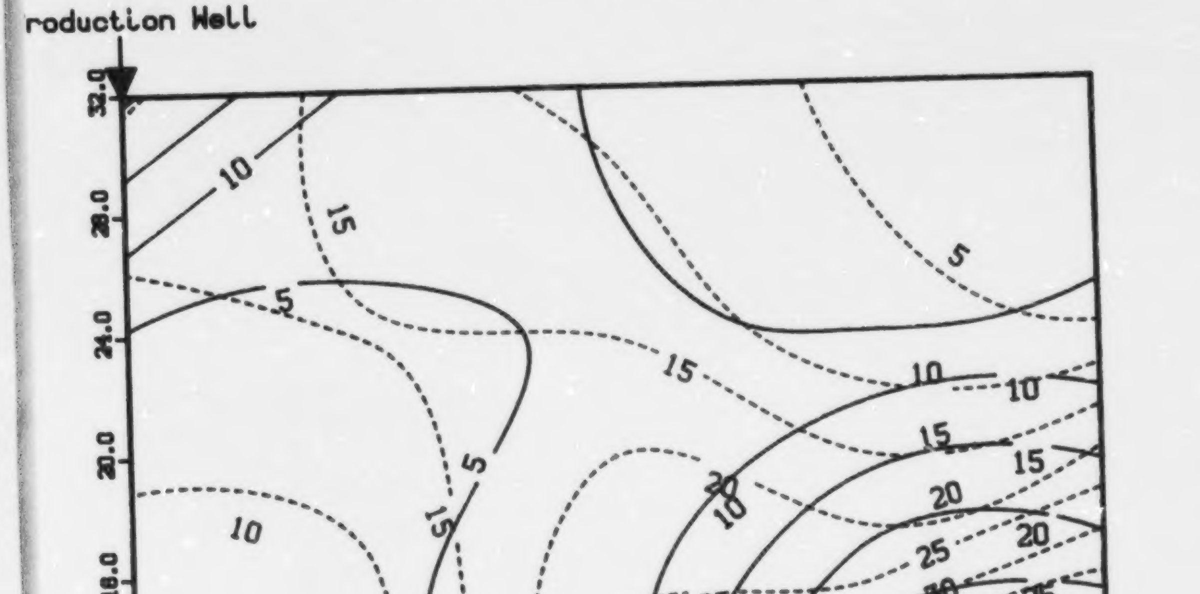

FIGURE 35: TEMPERATURE PROFILE FOR
RUN 12: CONTINUOUS STEAMFLOOD ON LIGHT OIL MODEL

0.75 Pore Volumes Steam Injected

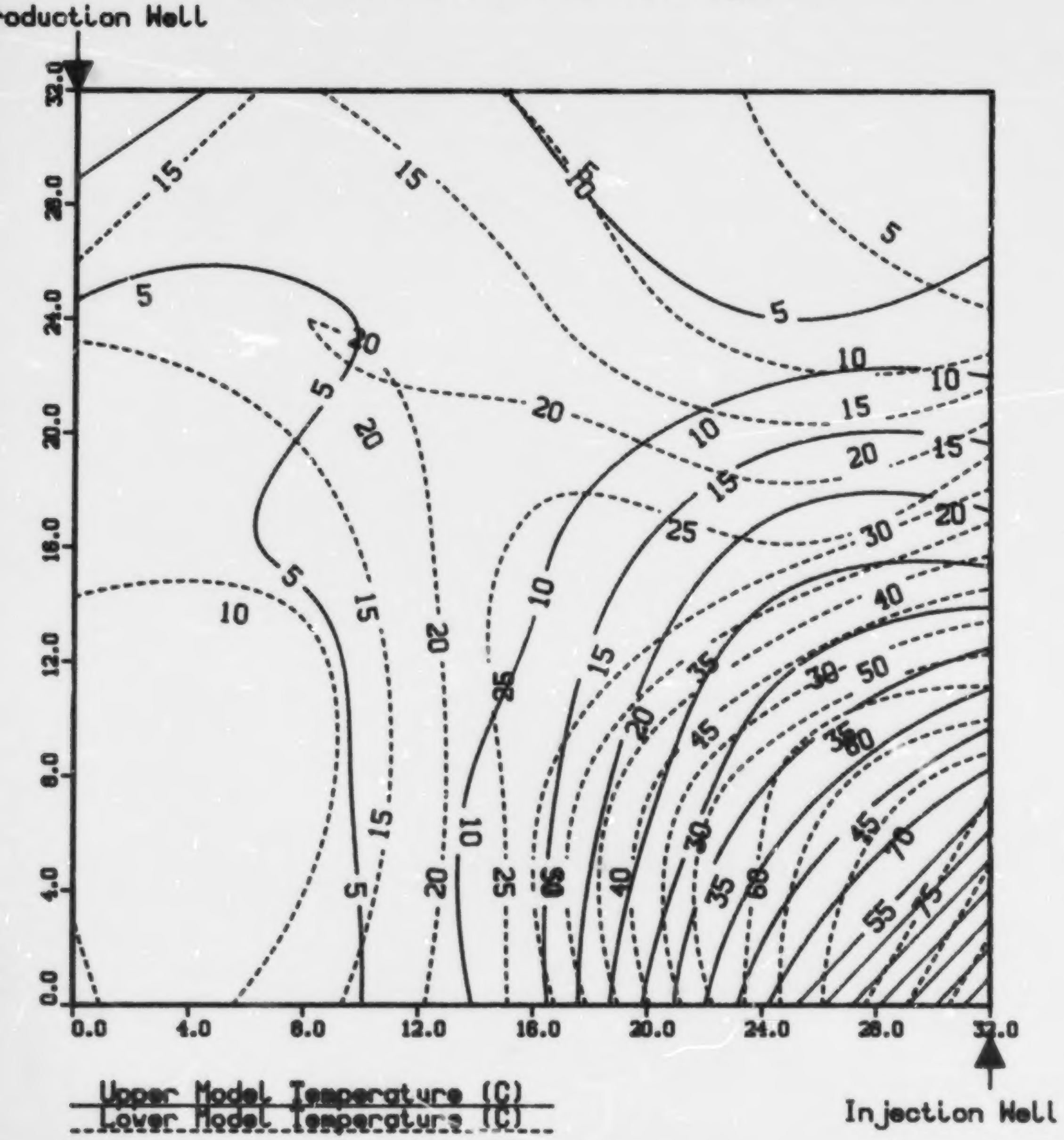

FIGURE 36: TEMPERATURE PROFILE FOR
RUN 12: CONTINUOUS STEAMFLOOD ON LIGHT OIL MODEL

1.00 Pore Volumes Steam Injected

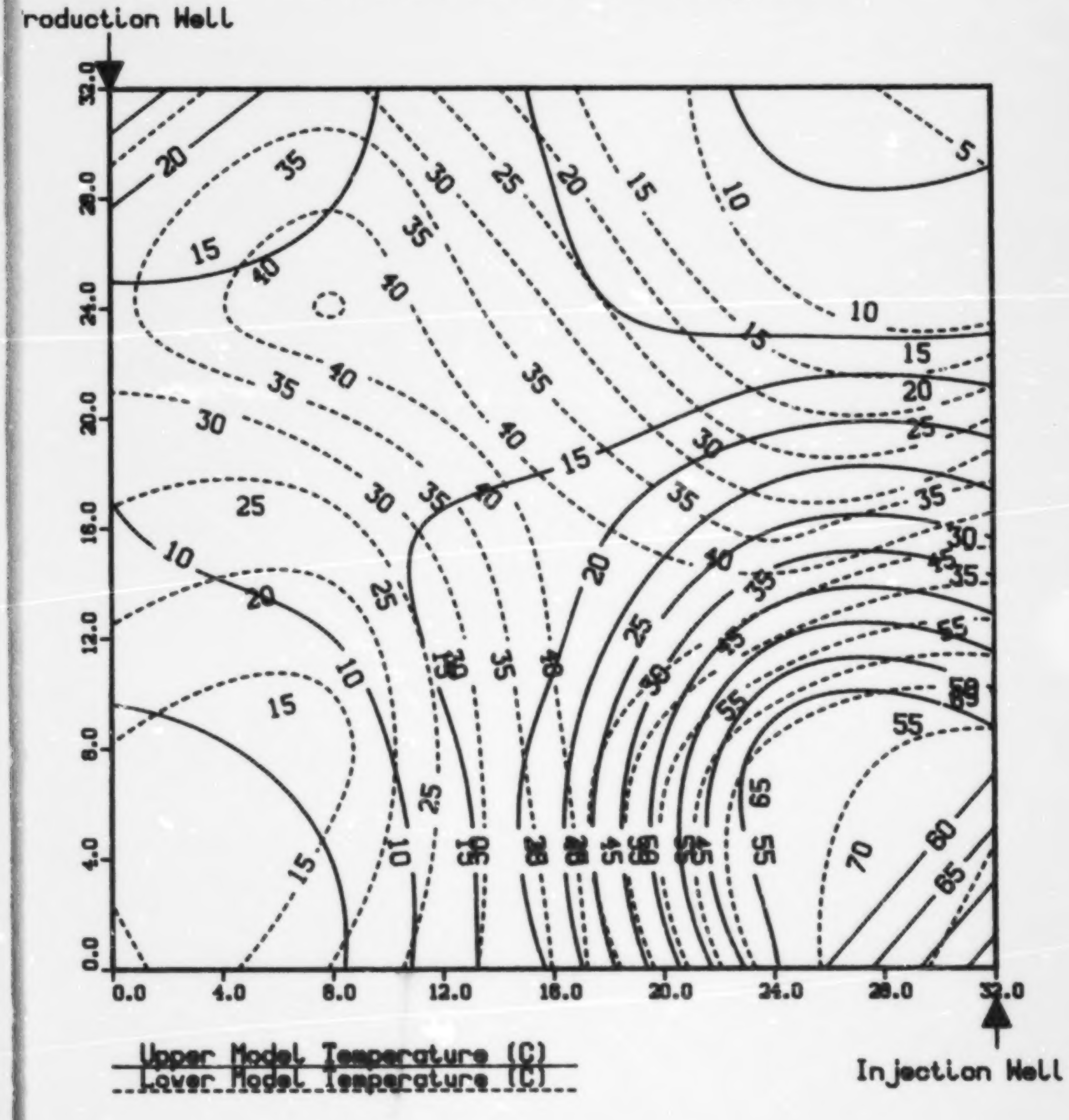

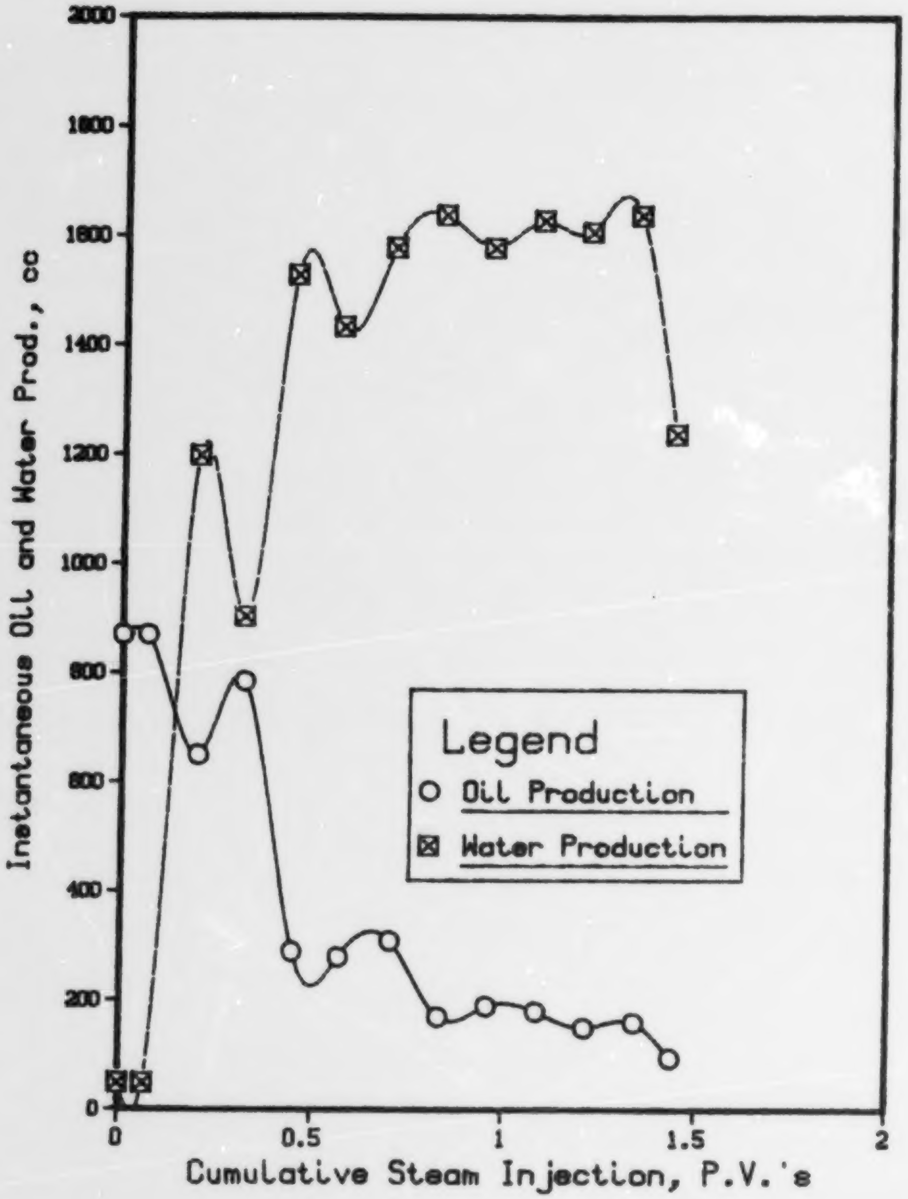
Continuous Steamflood in Light Oil Model,
Production Well Completed Over Lower Half.

Figure 37. Run 12, Instantaneous Oil and Water Production vs. Cumulative Injection.

Continuous Steamflood in Light Oil Model,
Production Well Completed Over Lower Half.

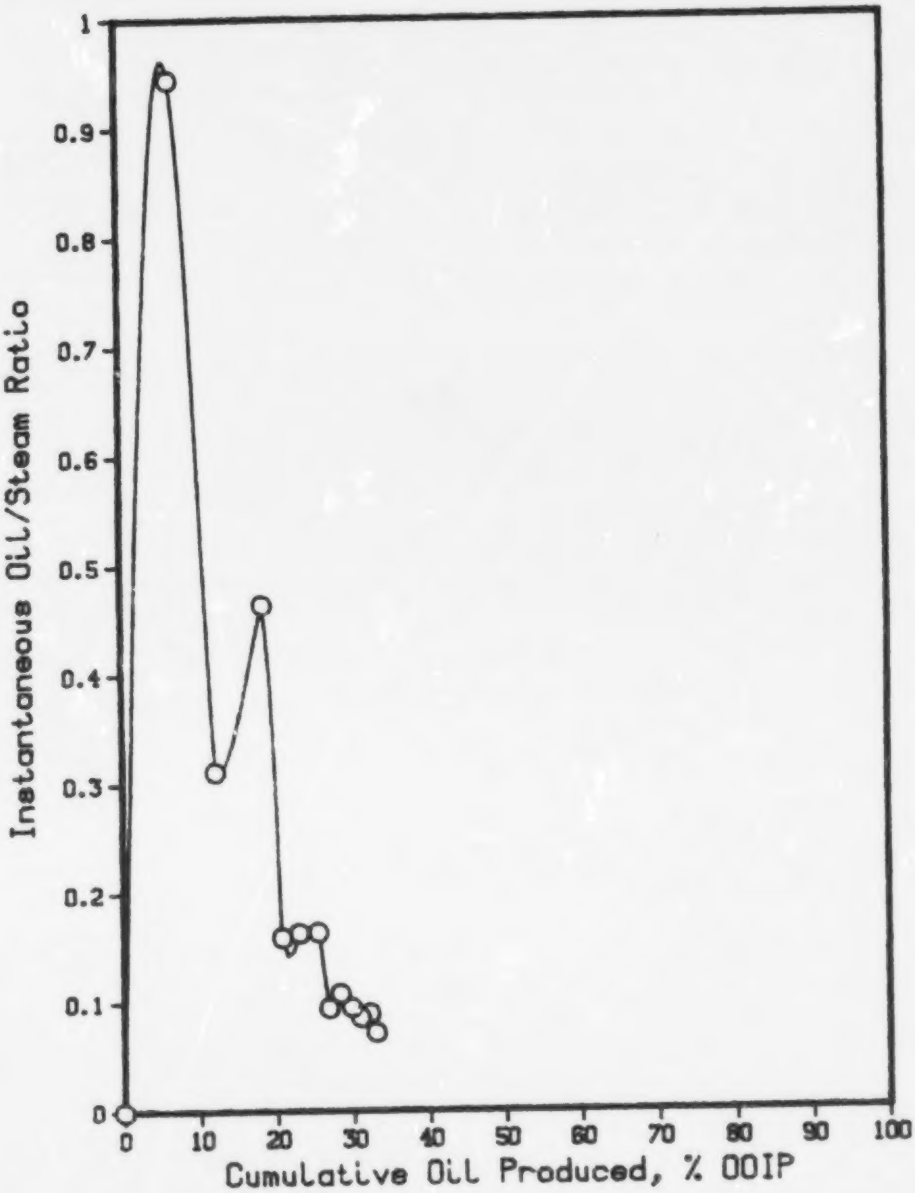

Figure 38. Run 12, Instantaneous Oil-Steam Ratio vs. Cumulative Oil Production.

FIGURE 39: TEMPERATURE PROFILE FOR
RUN 13: CONTINUOUS STEAMFLOOD ON LIGHT OIL MODEL

0.25 Pore Volumes Steam Injected

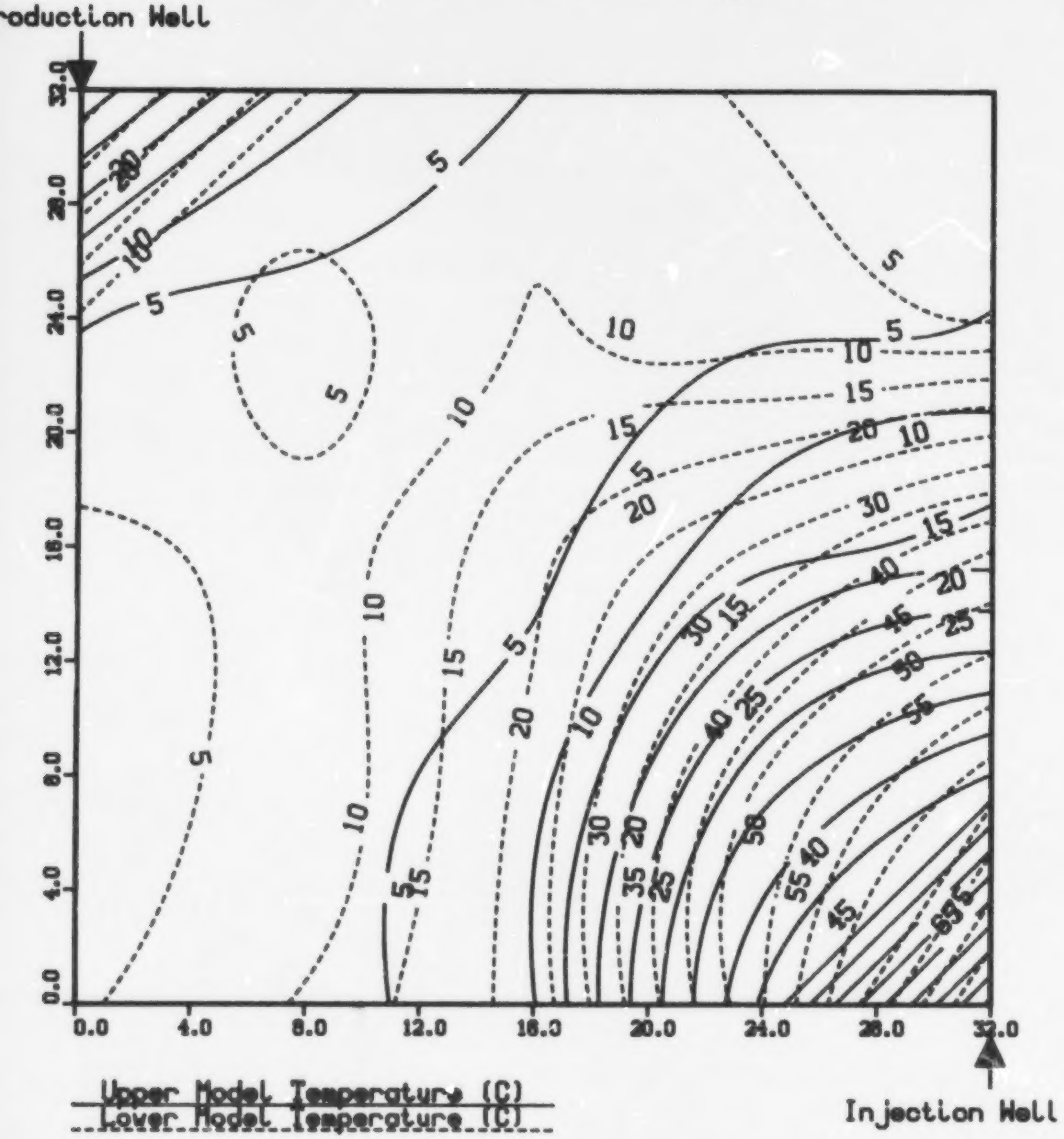

FIGURE 40: TEMPERATURE PROFILE FOR RUN 13: CONTINUOUS STEAMFLOOD ON LIGHT OIL MODEL

0.50 Pore Volumes Steam Injected

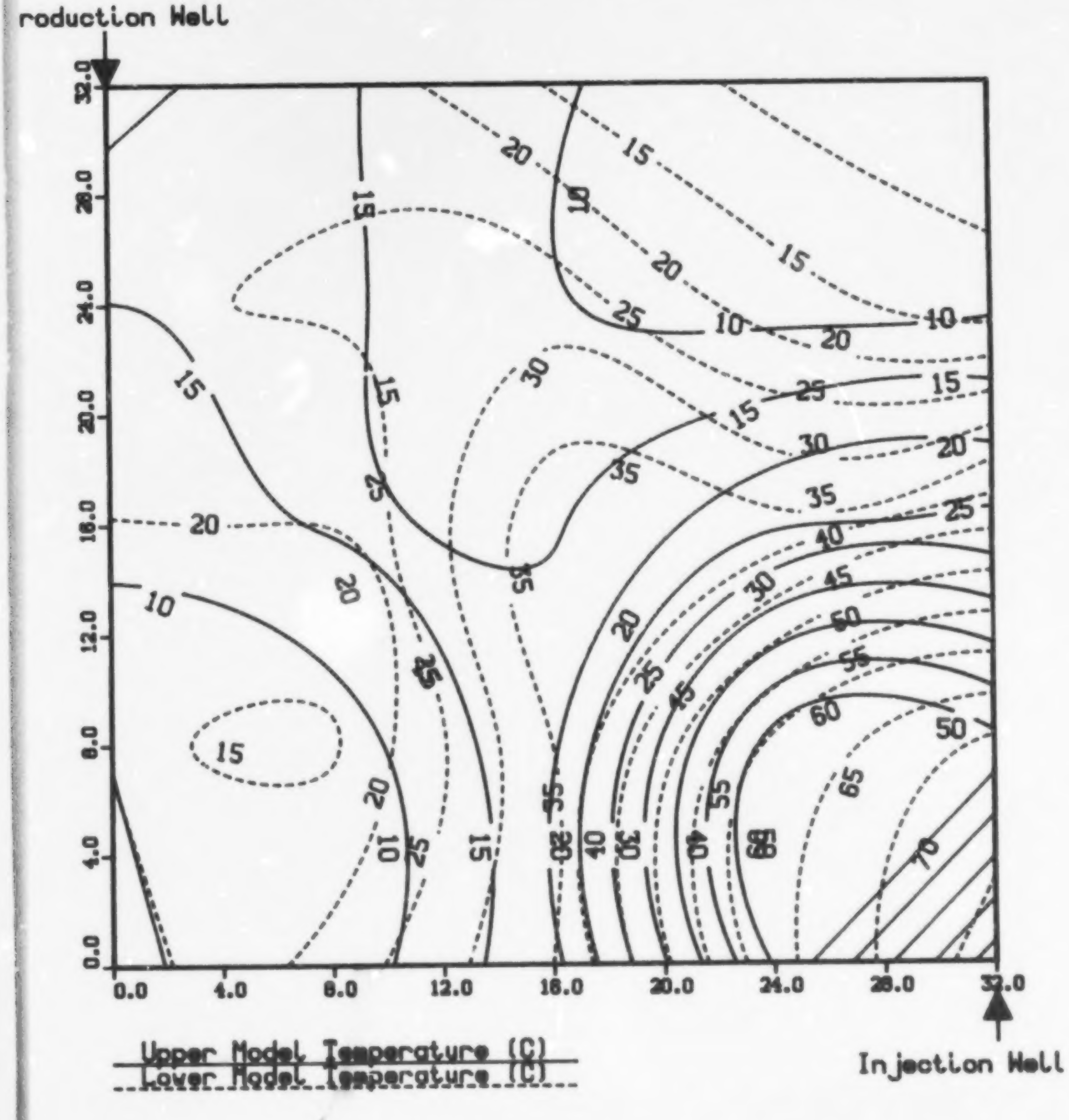

FIGURE 41: TEMPERATURE PROFILE FOR
RUN 13: CONTINUOUS STEAMFLOOD ON LIGHT OIL MODEL

0.75 Pore Volumes Steam Injected

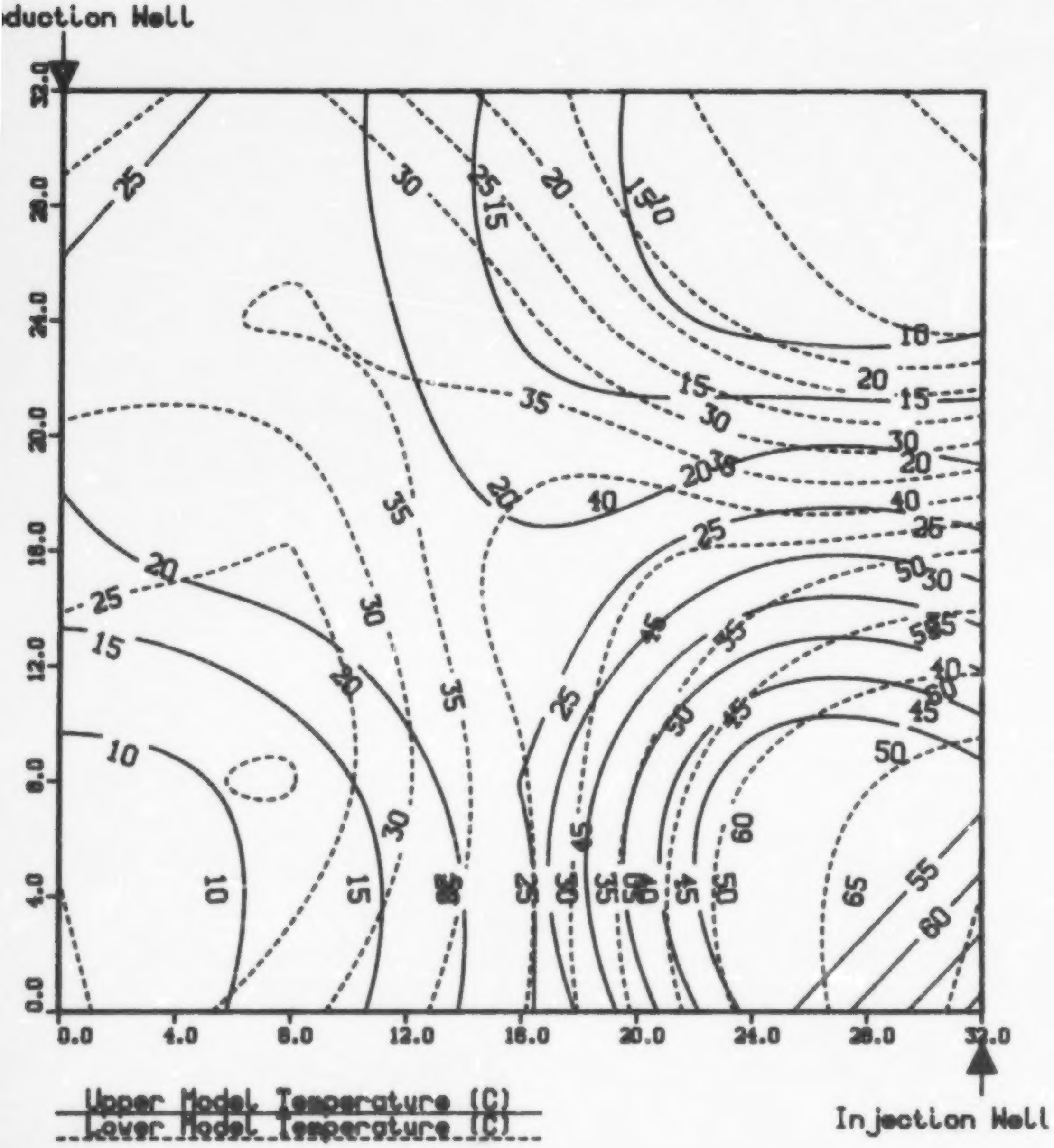

FIGURE 42: TEMPERATURE PROFILE FOR
RUN 13: CONTINUOUS STEAMFLOOD ON LIGHT OIL MODEL

1.00 Pore Volumes Steam Injected

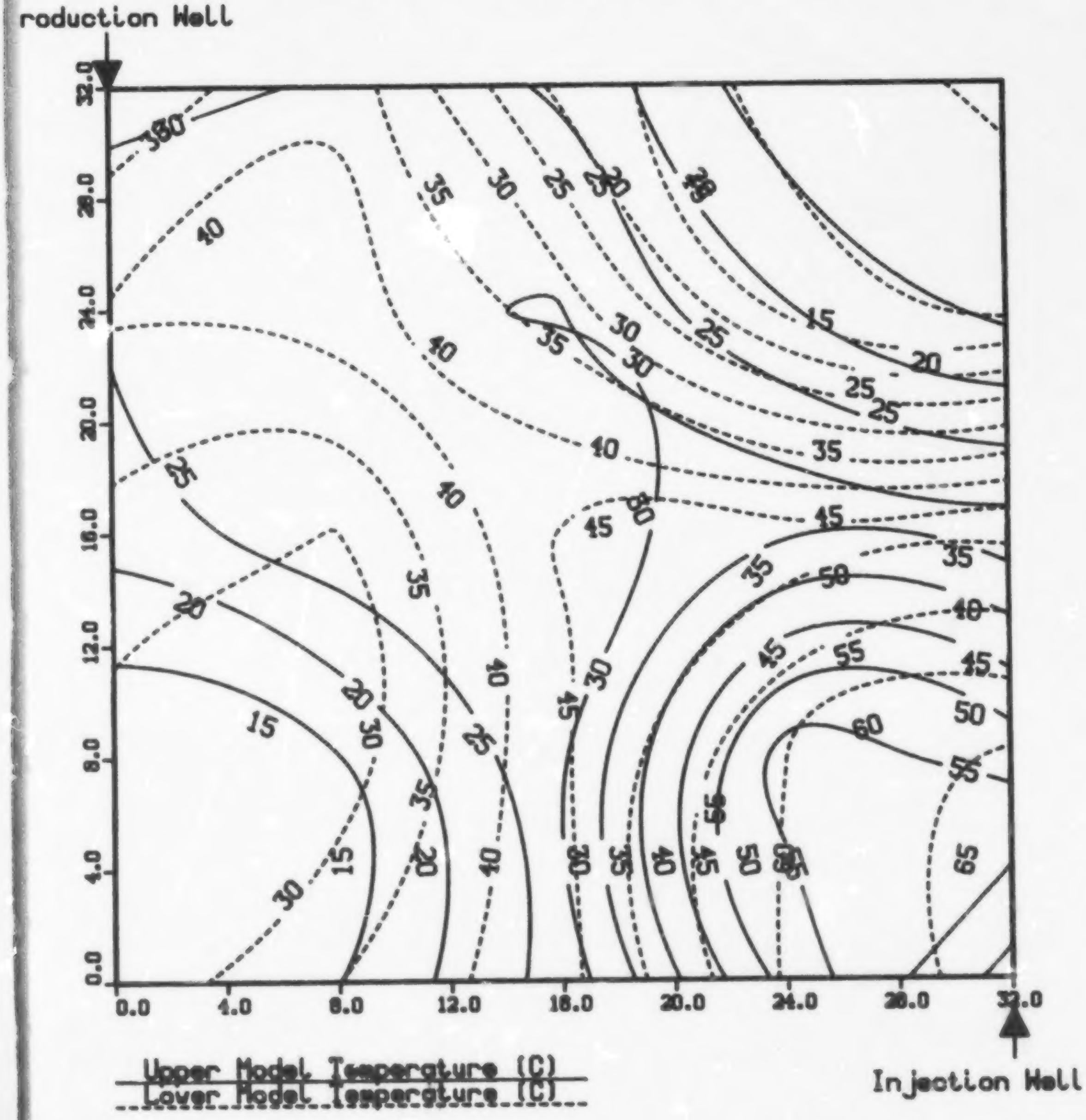

Continuous Steamflood in Light Oil Model,
Production Well Completed Over Upper Half.

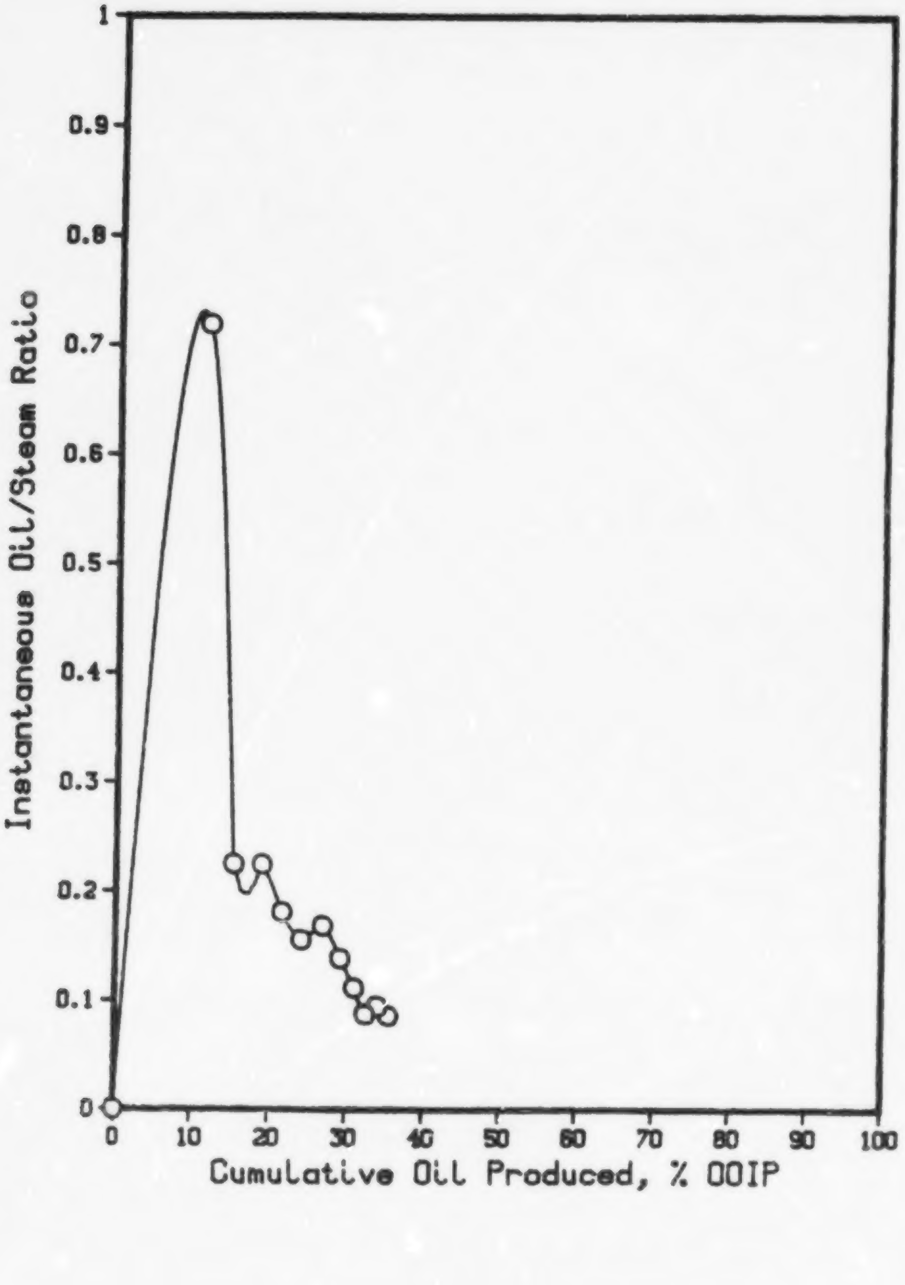

Figure 43. Run 13, Instantaneous Oil-Steam Ratio vs. Cumulative Oil Production.

Continuous Steamflood in Light Oil Model,
Production Well Completed Over Upper Half.

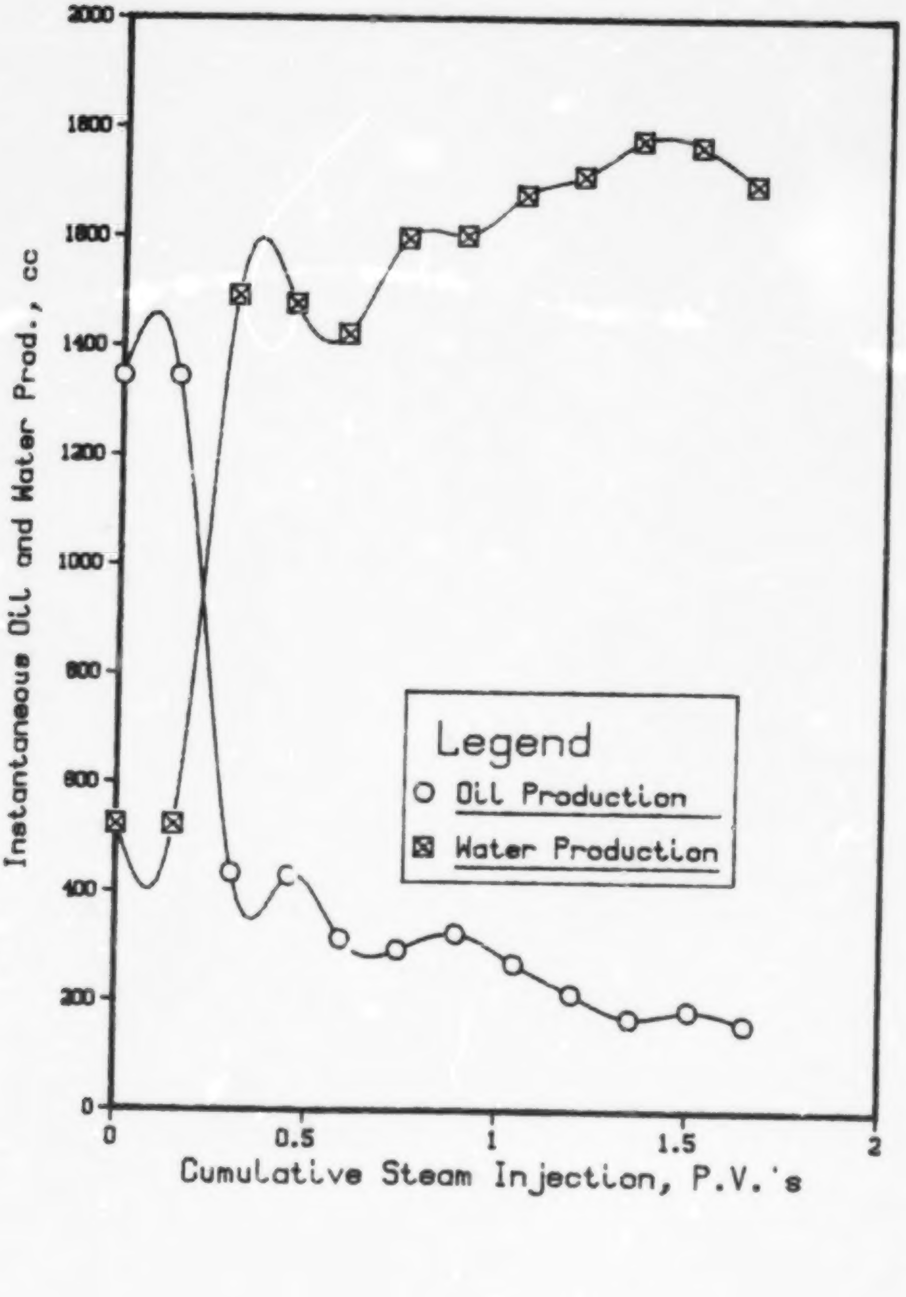

Figure 44. Run 13, Instantaneous Oil and Water Production vs. Cumulative Injection.

Two Steamfloods in Light Oil Models.

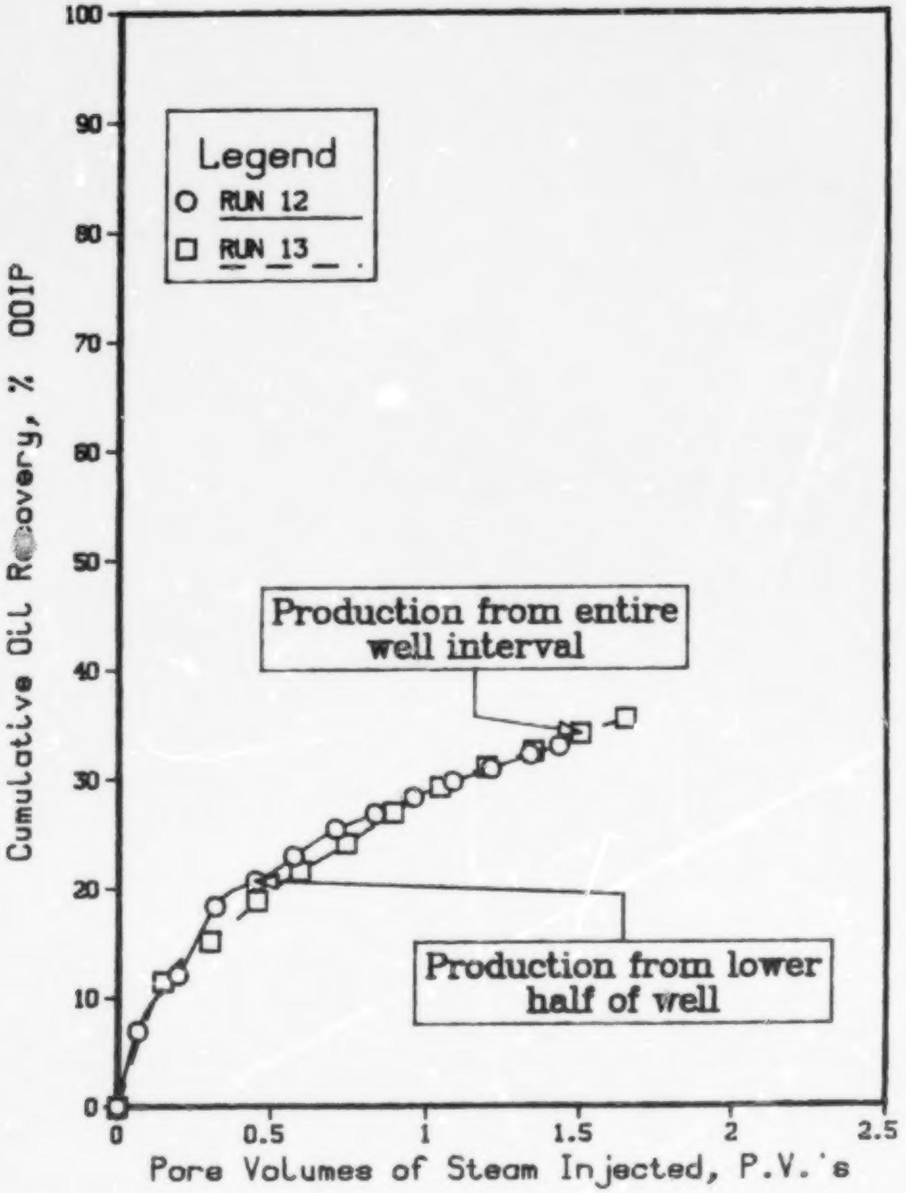

Figure 45. Comparison of the Steamflood Recovery Response of Run 12 and Run 13.

FIGURE 46: TEMPERATURE PROFILE FOR
RUN 15: CONT. STEAMFLOOD ON BOTTOM WATER MODEL

0.25 Pore Volumes Steam Injected

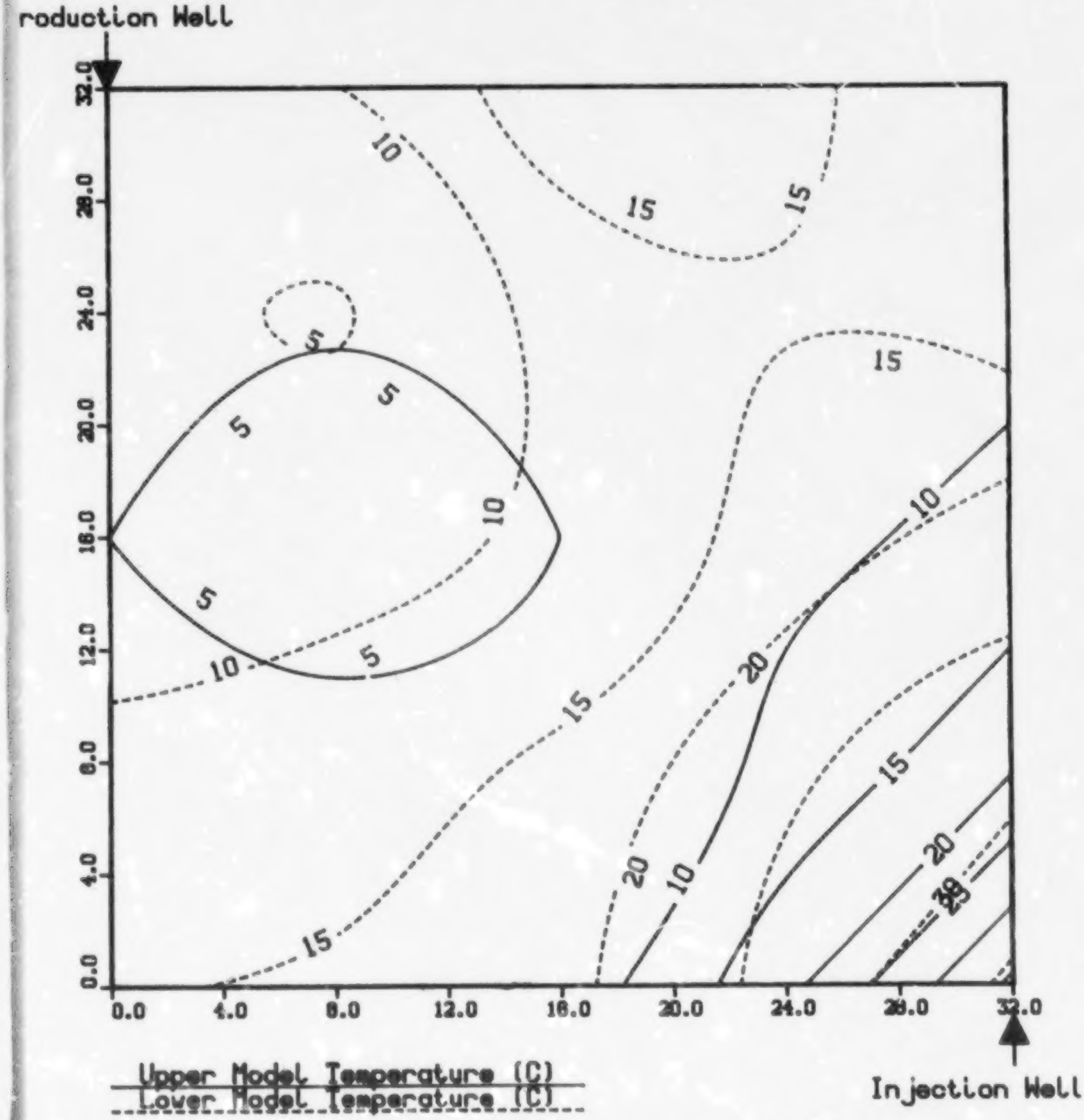

FIGURE 47: TEMPERATURE PROFILE FOR RUN 15: CONT. STEAMFLOOD ON BOTTOM WATER MODEL

0.50 Pore Volumes Steam Injected

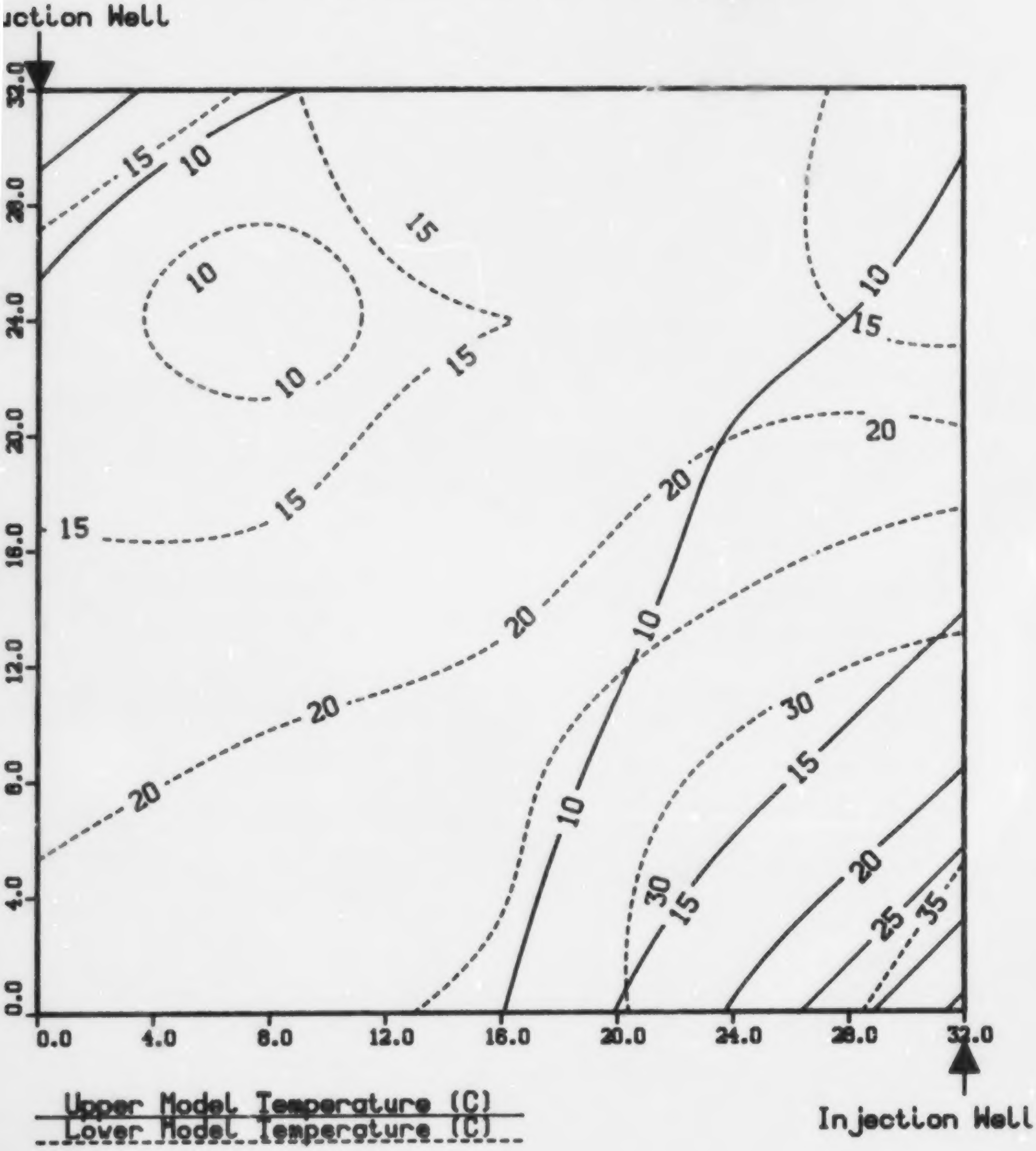

FIGURE 48: TEMPERATURE PROFILE FOR RUN 15: CONT. STEAMFLOOD ON BOTTOM WATER MODEL

0.75 Pore Volumes Steam Injected

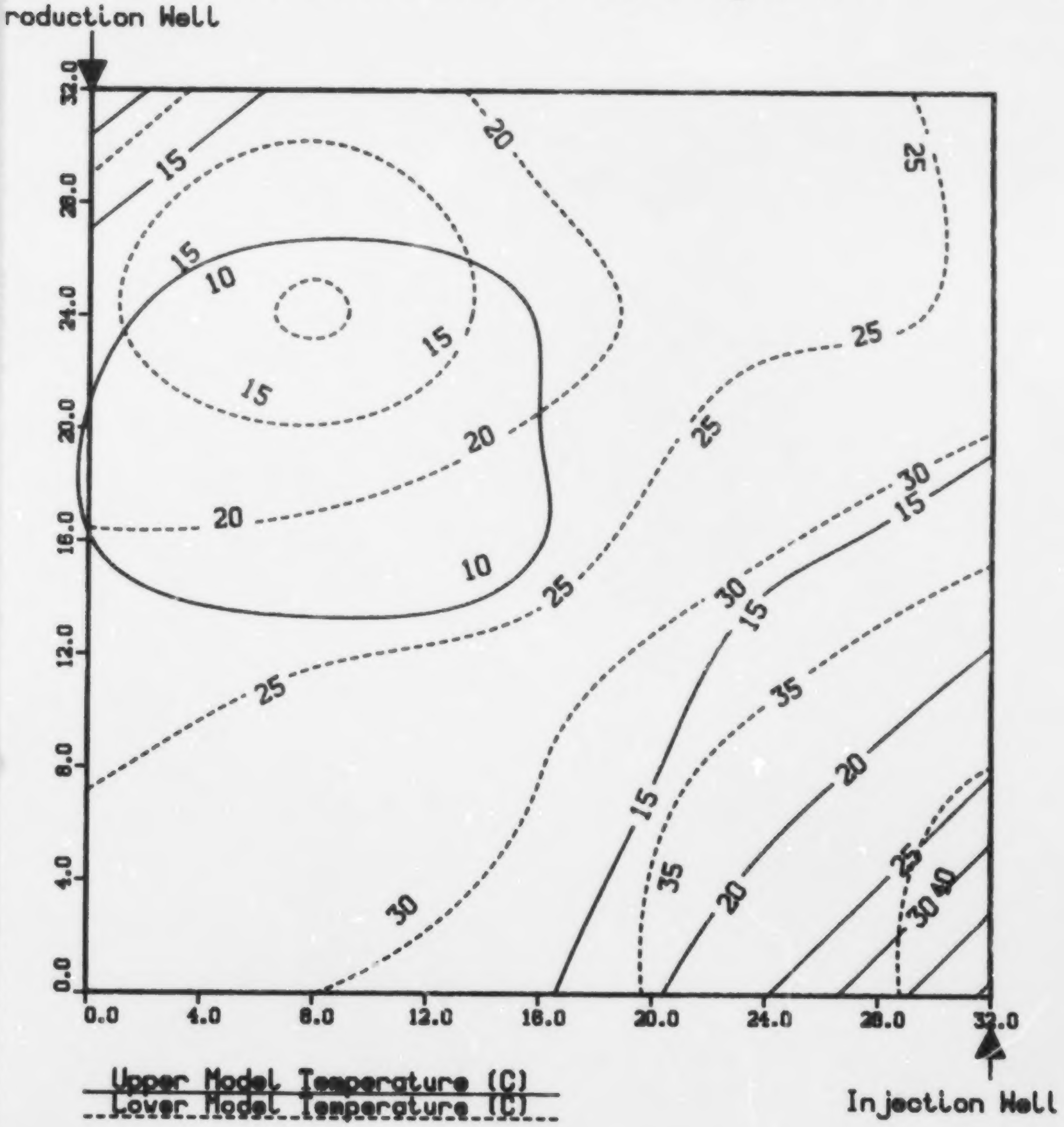

FIGURE 49: TEMPERATURE PROFILE FOR RUN 15: CONT. STEAMFLOOD ON BOTTOM WATER MODEL

1.00 Pore Volumes Steam Injected

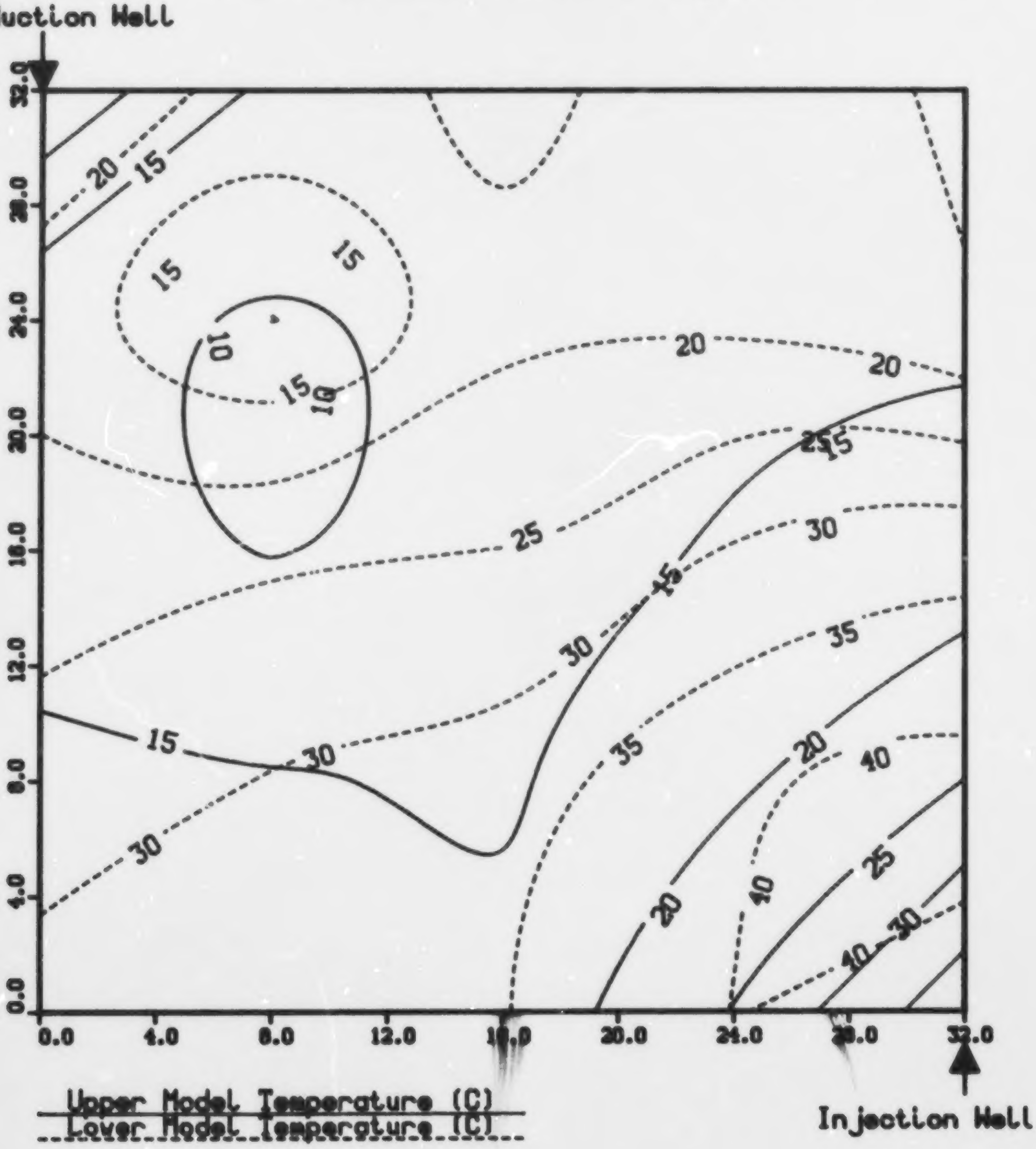

Continuous Steamflood in a Bottom Water Aberfeldy Model.

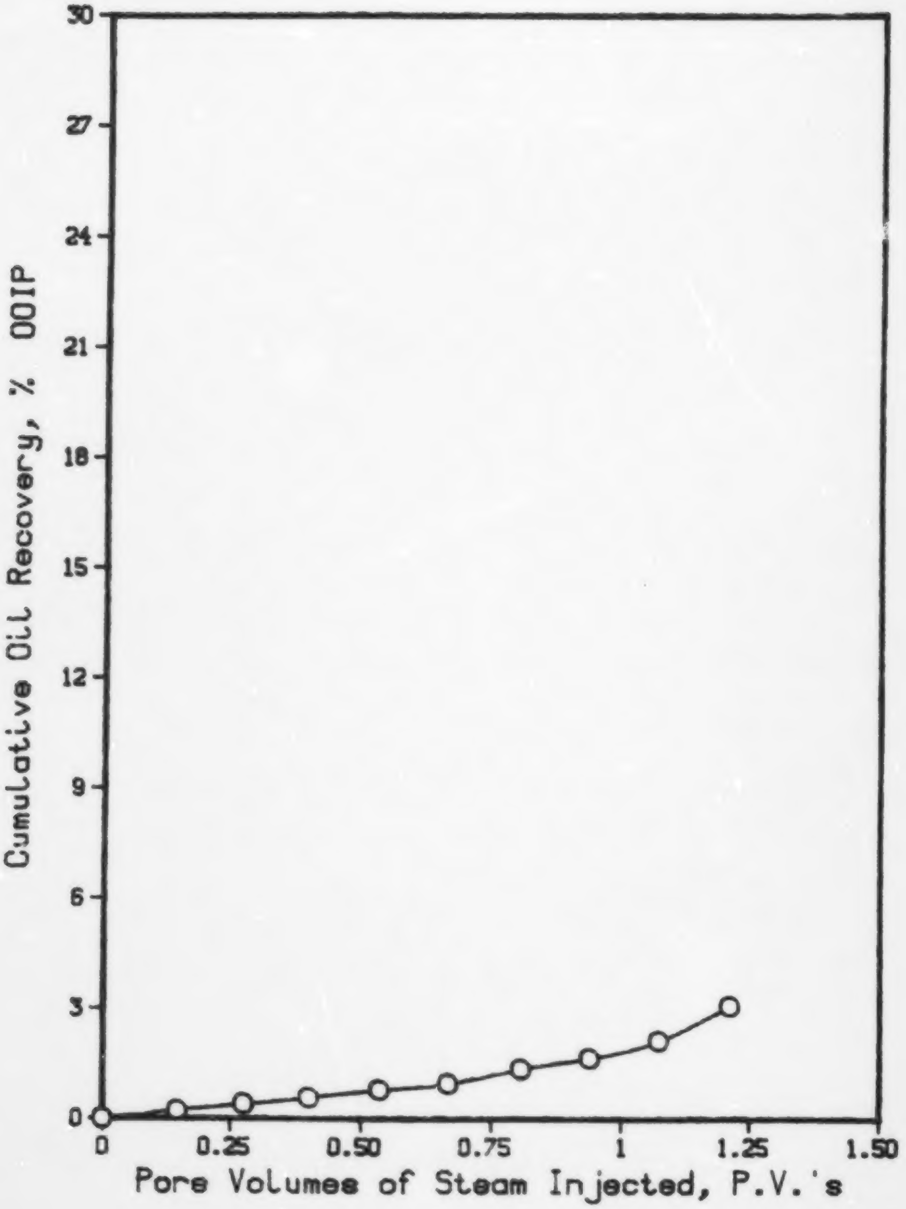

Figure 50. Run 15, Cumulative Oil Recovery vs. PV Steam Injected.

Continuous Steamflood in a Bottom Water Aberfeldy Model.

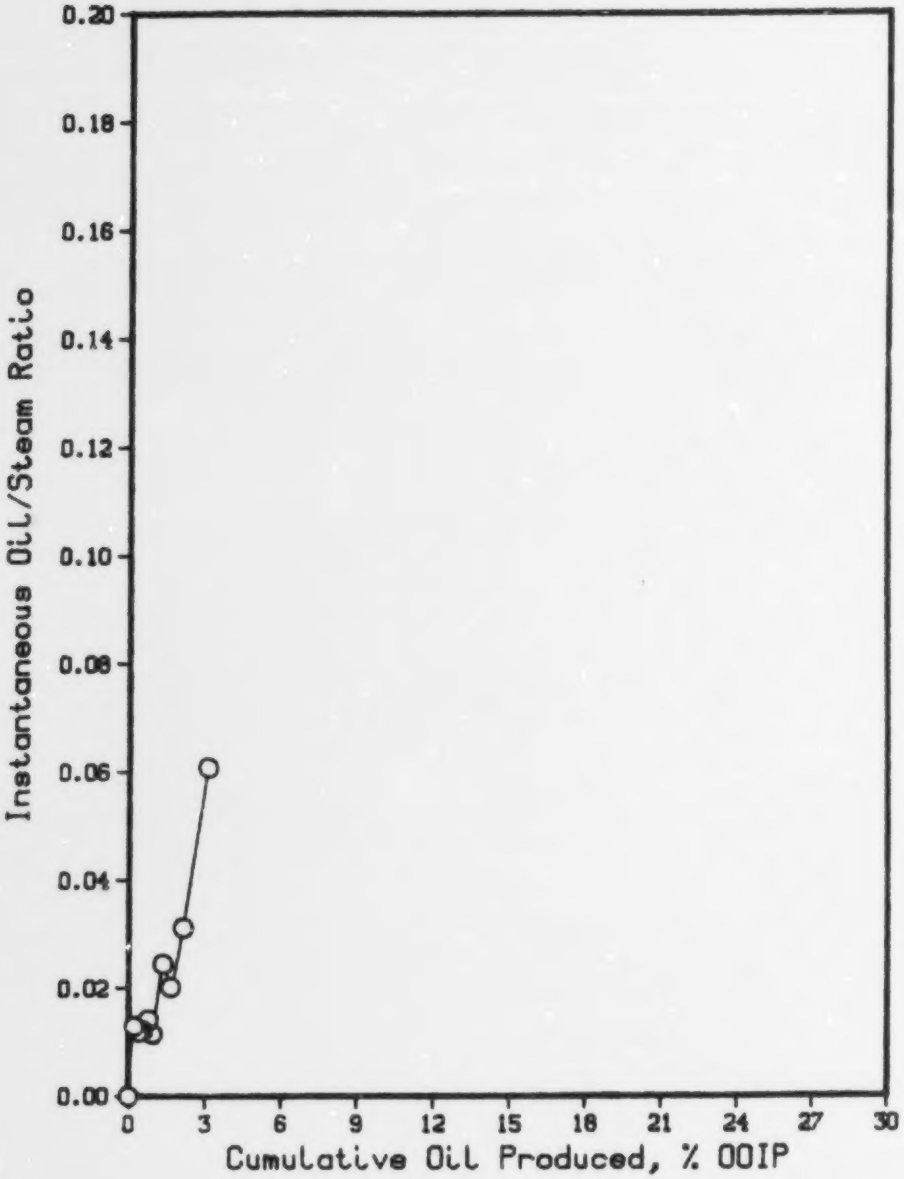

Figure 51. Run 15, Instantaneous Oil-Steam Ratio vs. Cumulative Oil Production.

Continuous Steamflood in a Bottom Water Aberfeldy Model.

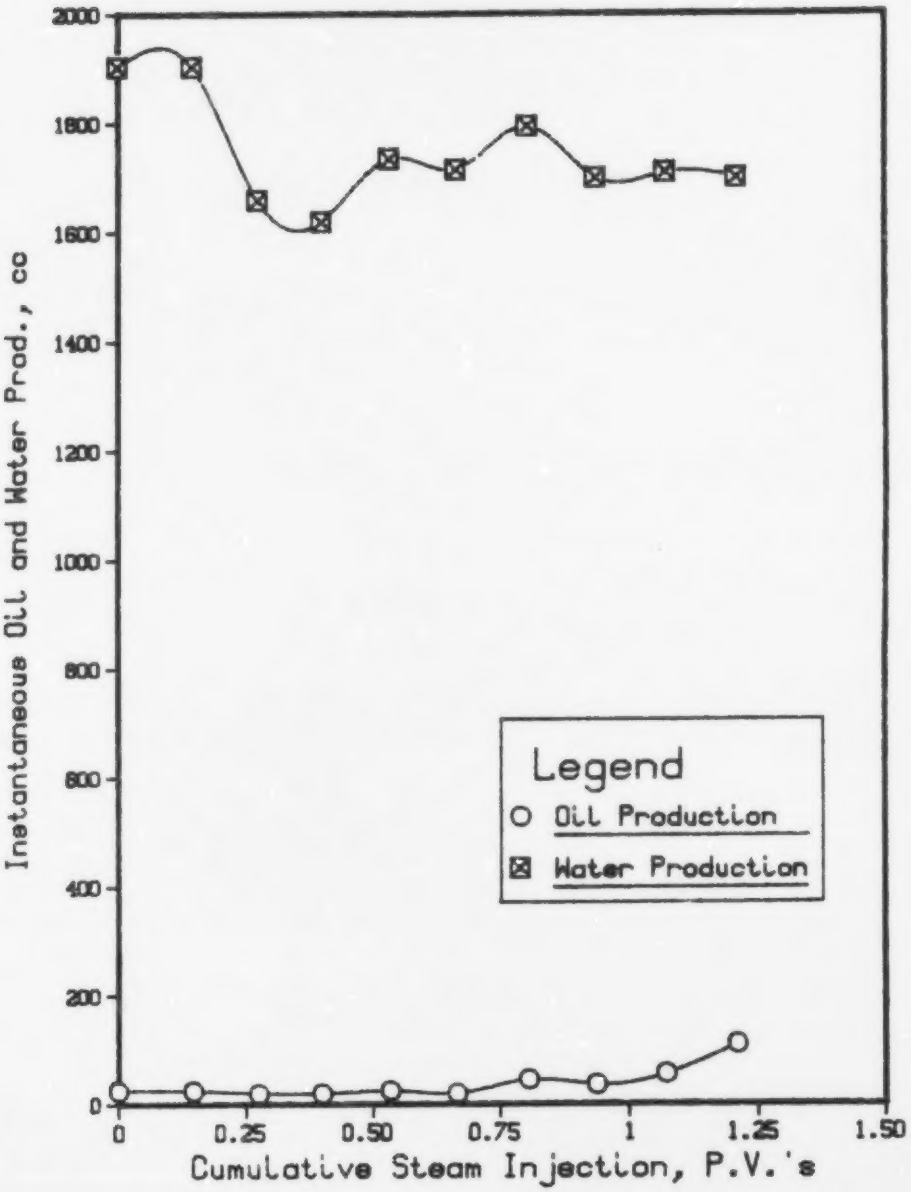

Figure 52. Run 15, Instantaneous Oil and Water Production vs. Cumulative Injection.

FIGURE 53: TEMPERATURE PROFILE FOR
RUN 17: COLD WATER SLUG RUN ON ABERFELDY MODEL

0.25 Pores Volumes Steam Injected

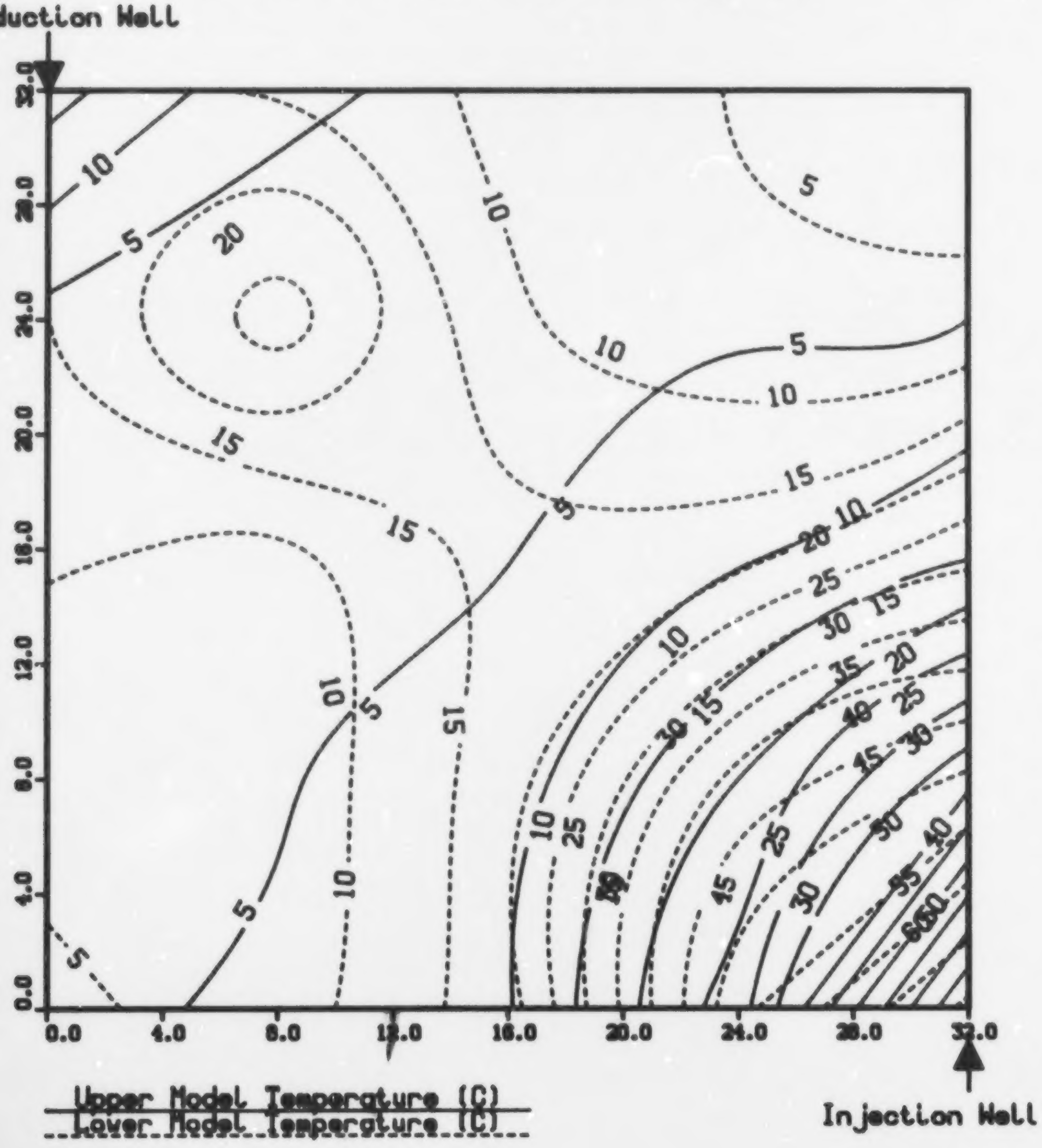

FIGURE 54: TEMPERATURE PROFILE FOR
RUN 17: COLD WATER SLUG RUN ON ABERFELDY MODEL

Start of Cold Water Slug (0.31 p.v.s)

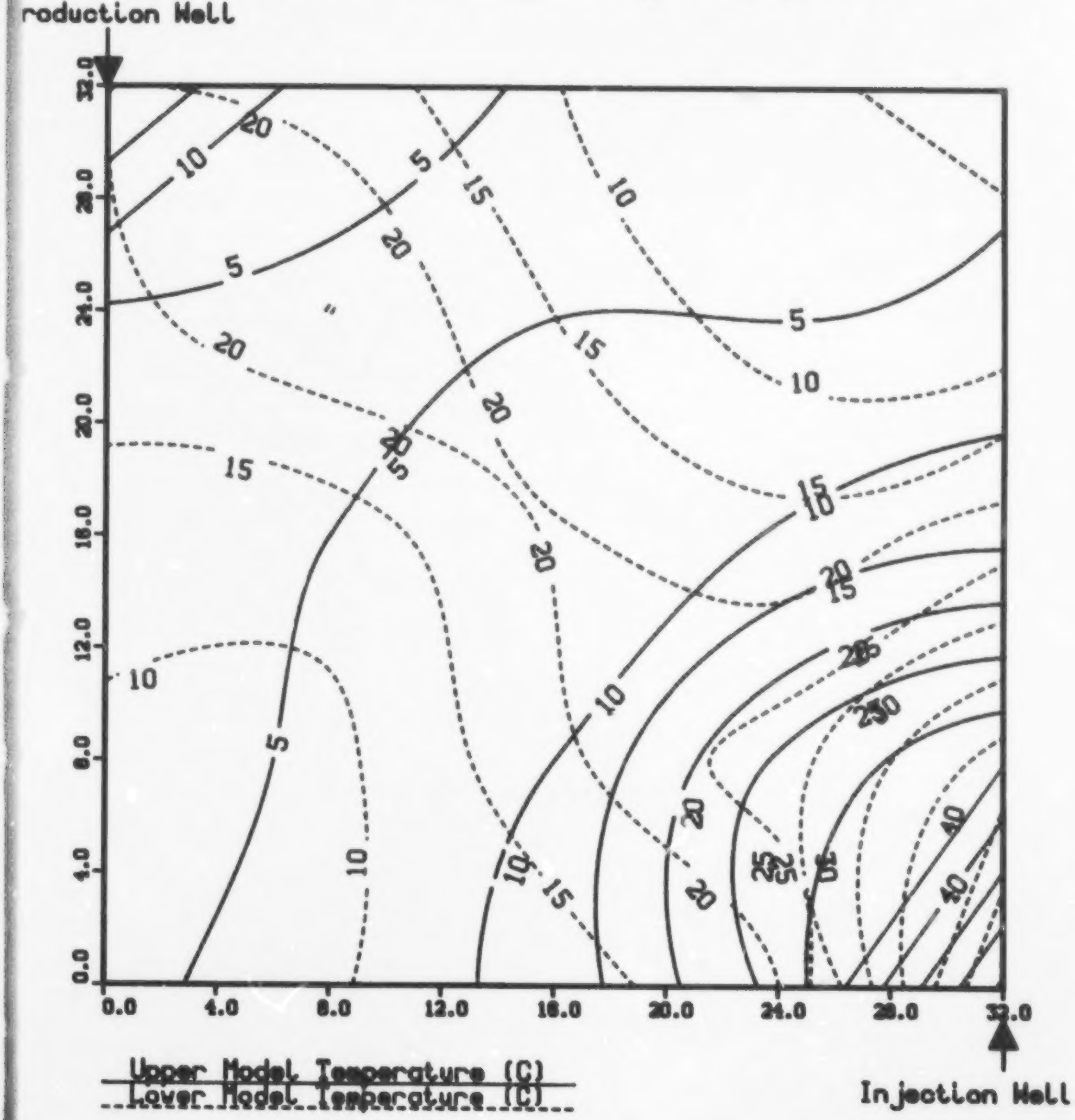

FIGURE 55: TEMPERATURE PROFILE FOR RUN 17: COLD WATER SLUG RUN ON ABERFELDY MODEL

0.50 Pore Volumes Steam Injected

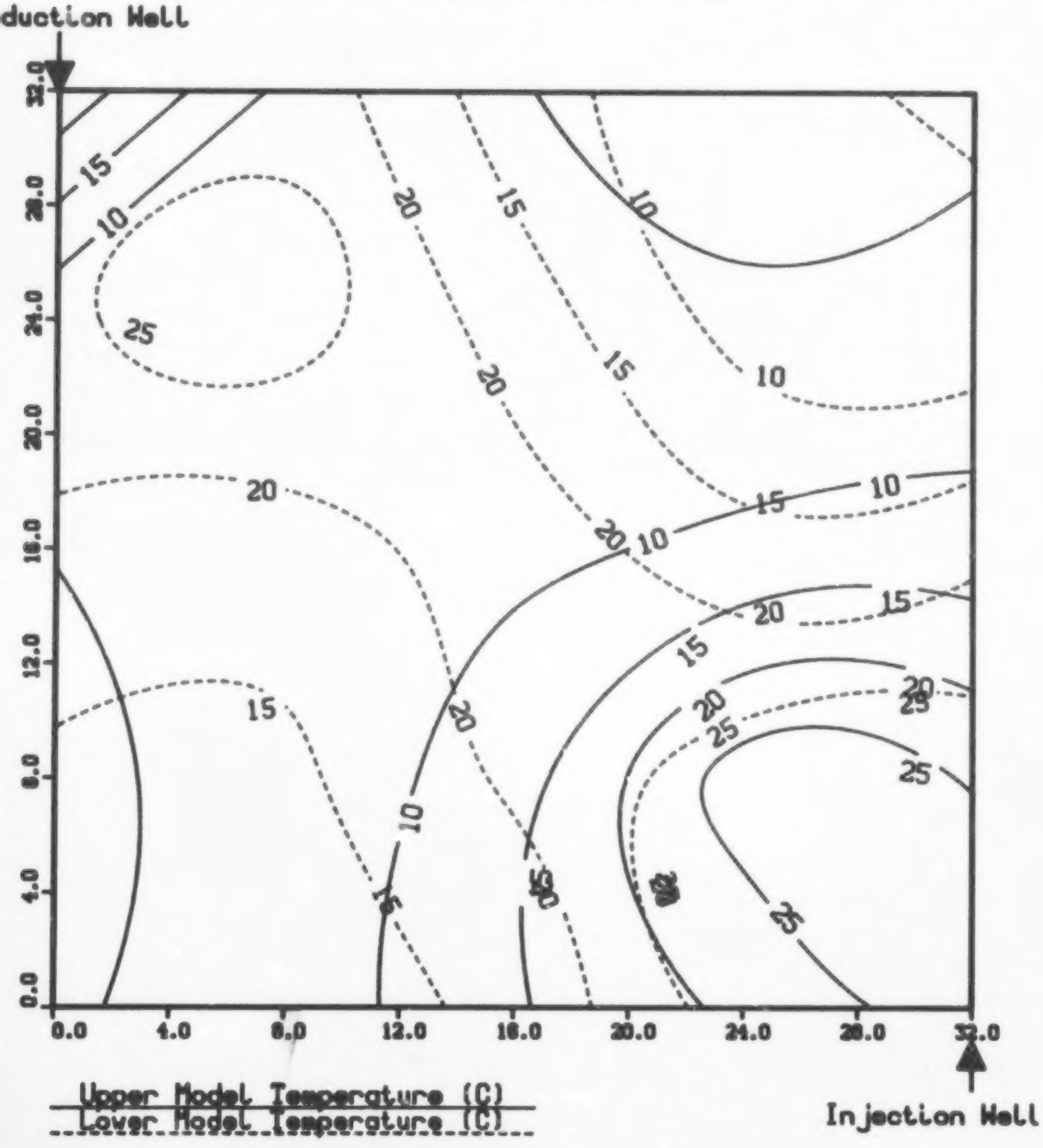

FIGURE 56: TEMPERATURE PROFILE FOR RUN 17: COLD WATER SLUG RUN ON ABERFELDY MODEL

0.75 Pore Volumes Steam Injected

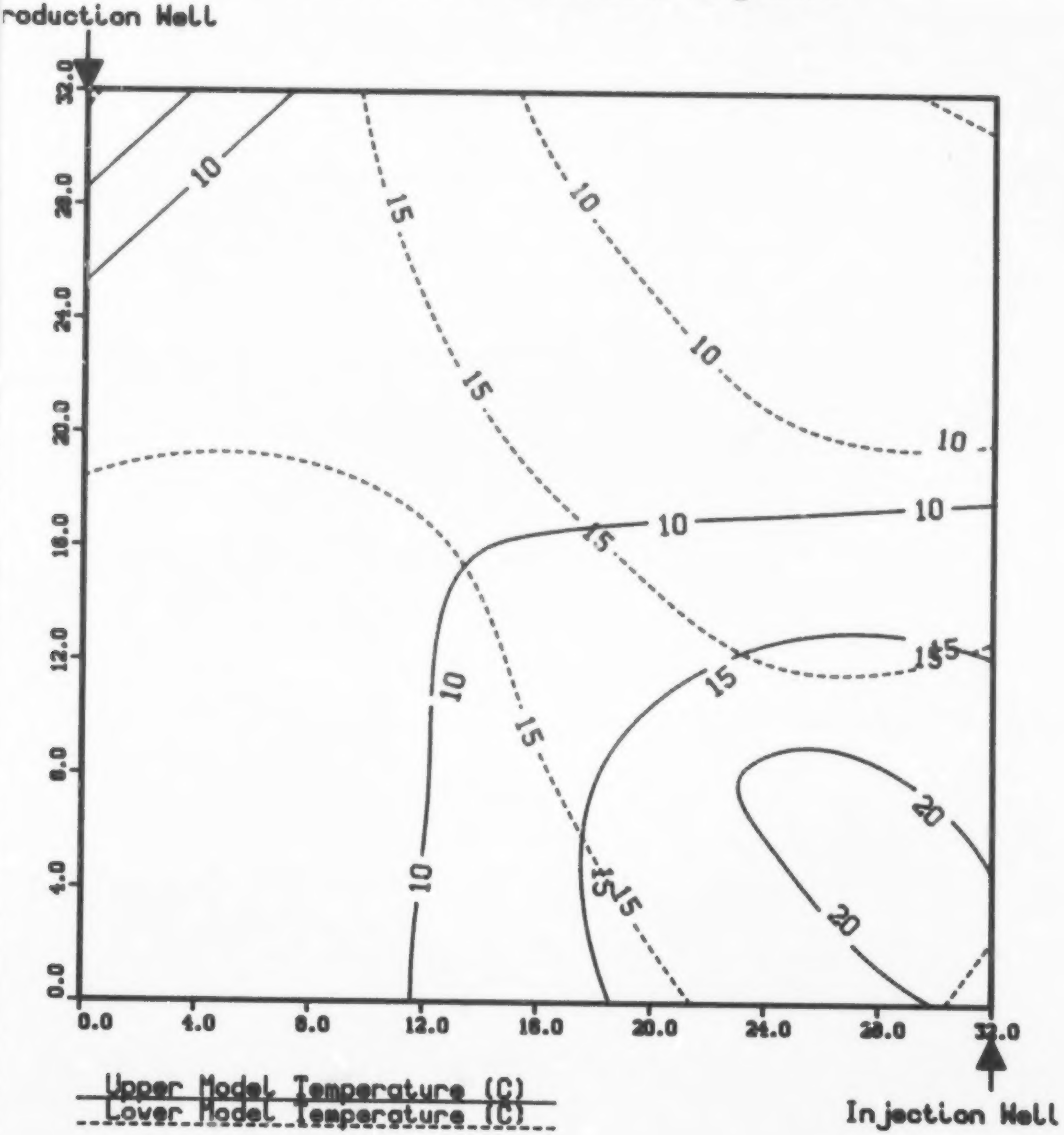

FIGURE 57: TEMPERATURE PROFILE FOR
RUN 17: COLD WATER SLUG RUN ON ABERFELDY MODEL

1.00 Pore Volumes Steam Injected

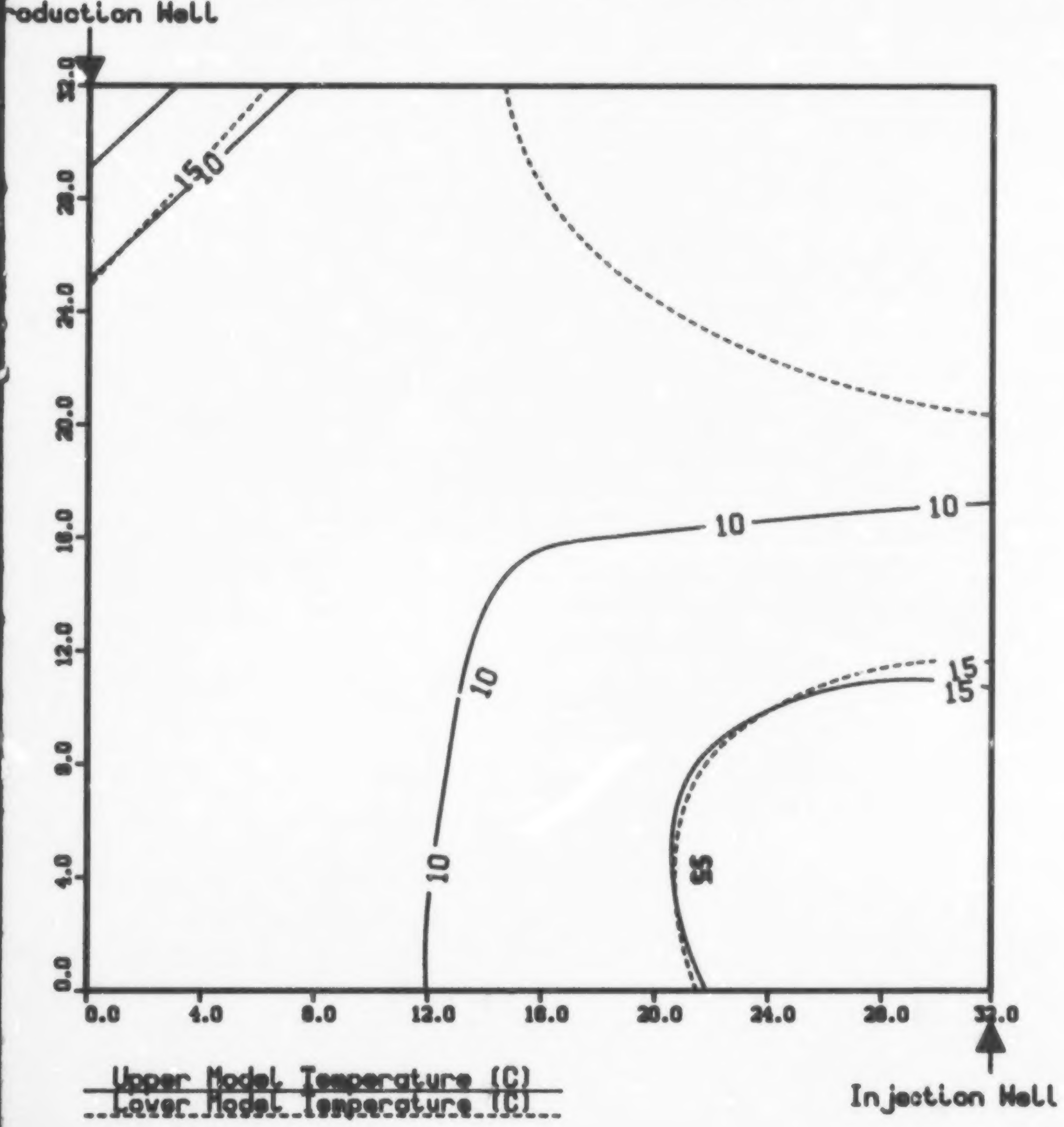

Steam Slug Run in Aberfeldy Model.

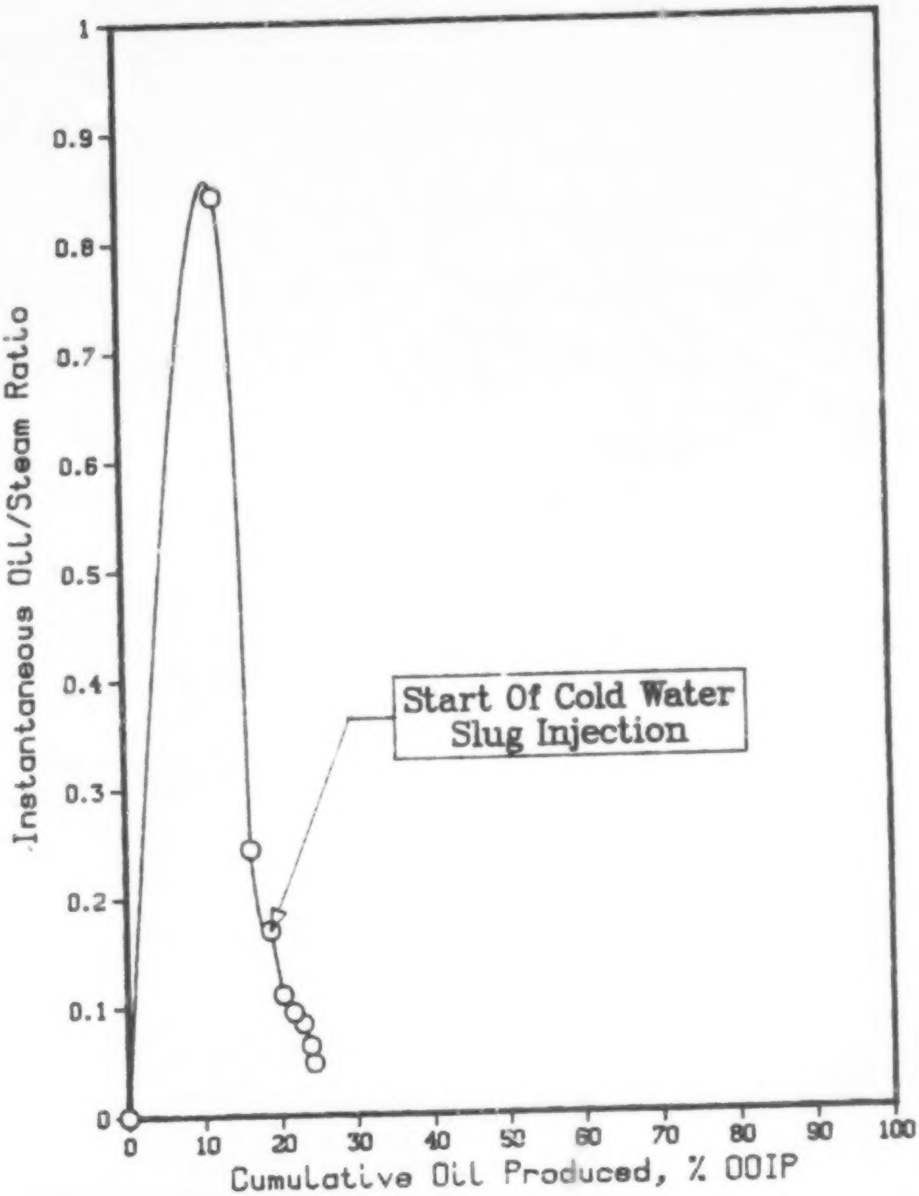

Figure 58. Run 17, Instantaneous Oil-Steam Ratio vs. Cumulative Oil Production.

Steam Slug Run in Aberfeldy Model.

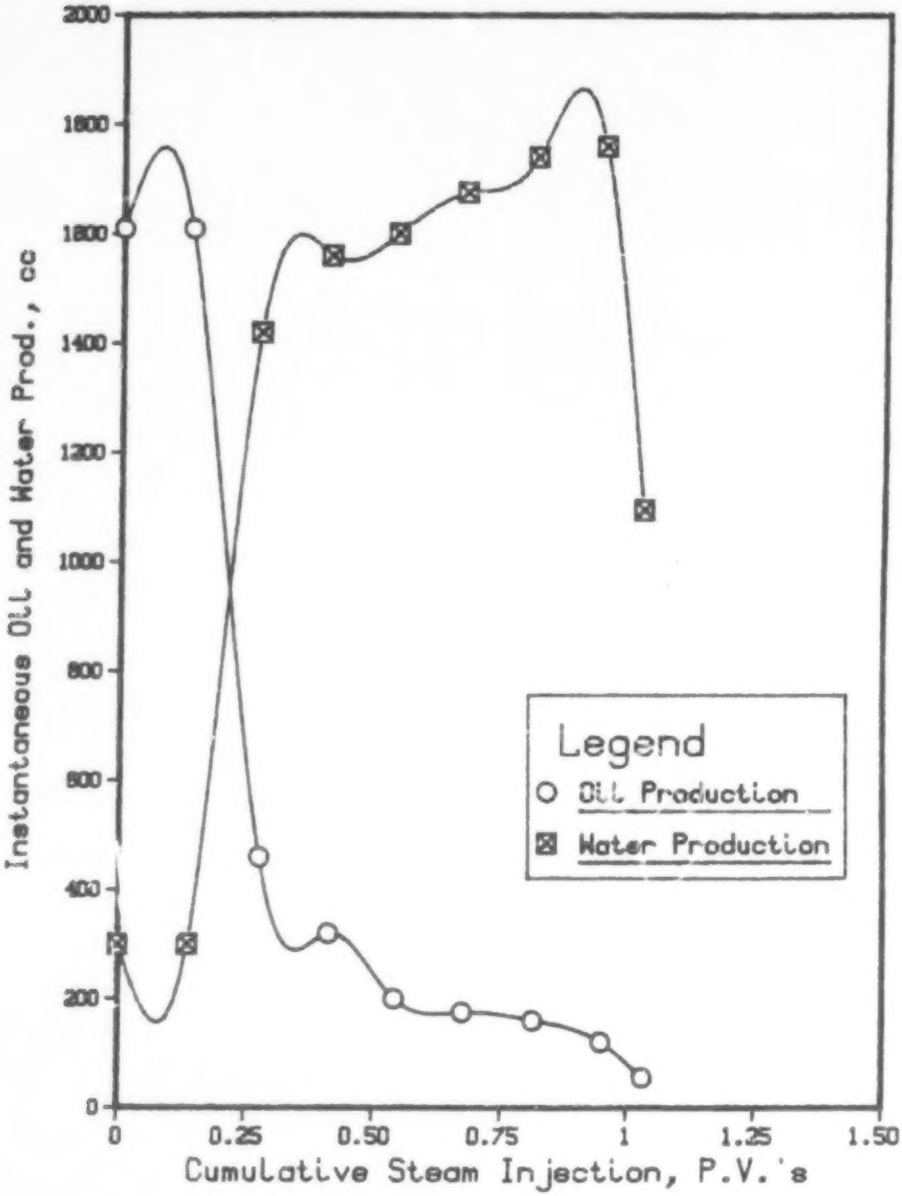

Figure 59. Run 17, Instantaneous Oil and Water Production vs. Cumulative Injection.

FIGURE 60: TEMPERATURE PROFILE FOR RUN 18: COLD WATER SLUG RUN ON ABERFELDY MODEL

0.25 Pore Volumes Steam Injected

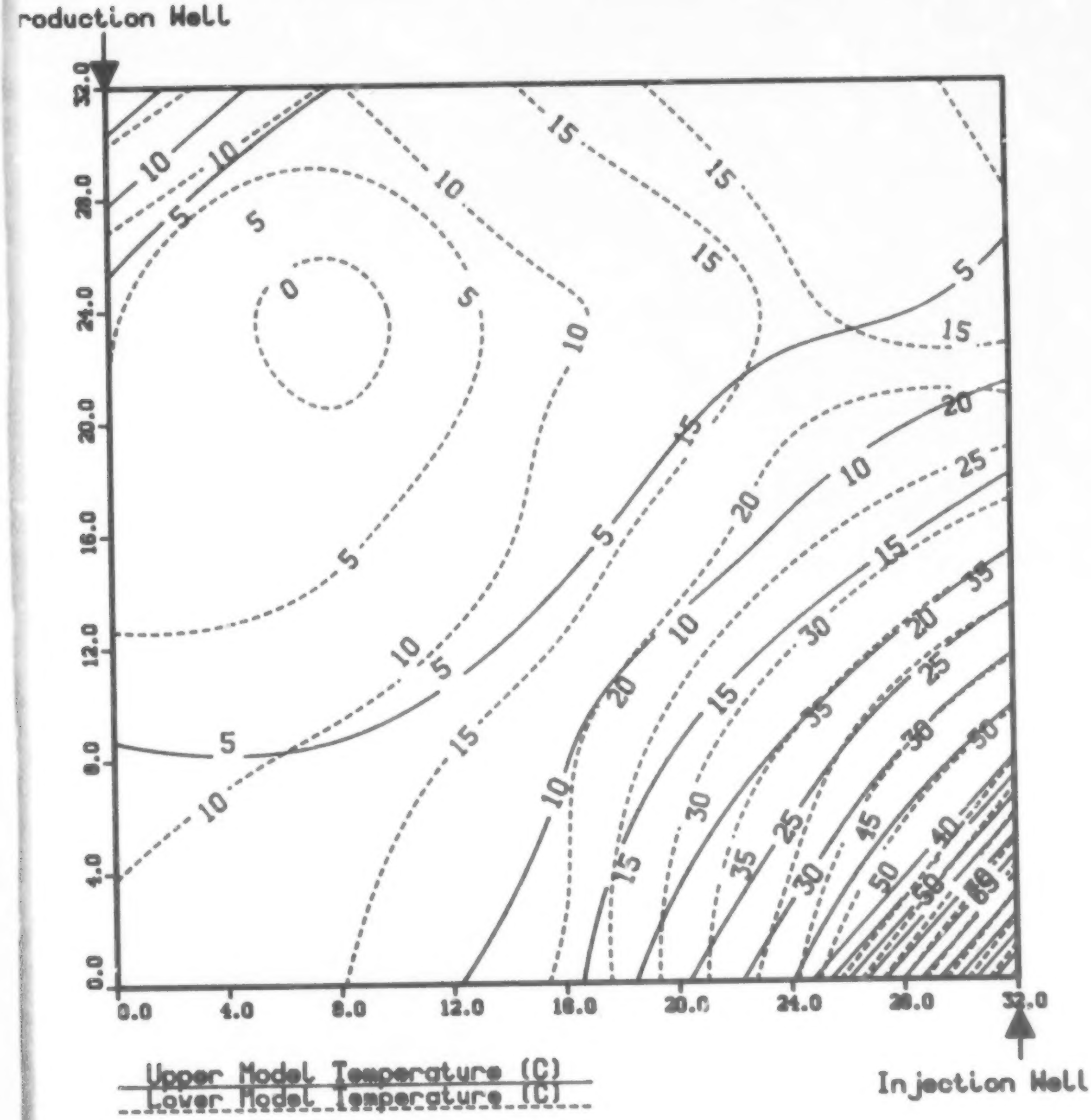

FIGURE 61: TEMPERATURE PROFILE FOR
RUN 18: COLD WATER SLUG RUN ON ABERFELDY MODEL

Start of Cold Water Slug (0.30 p.v.s)

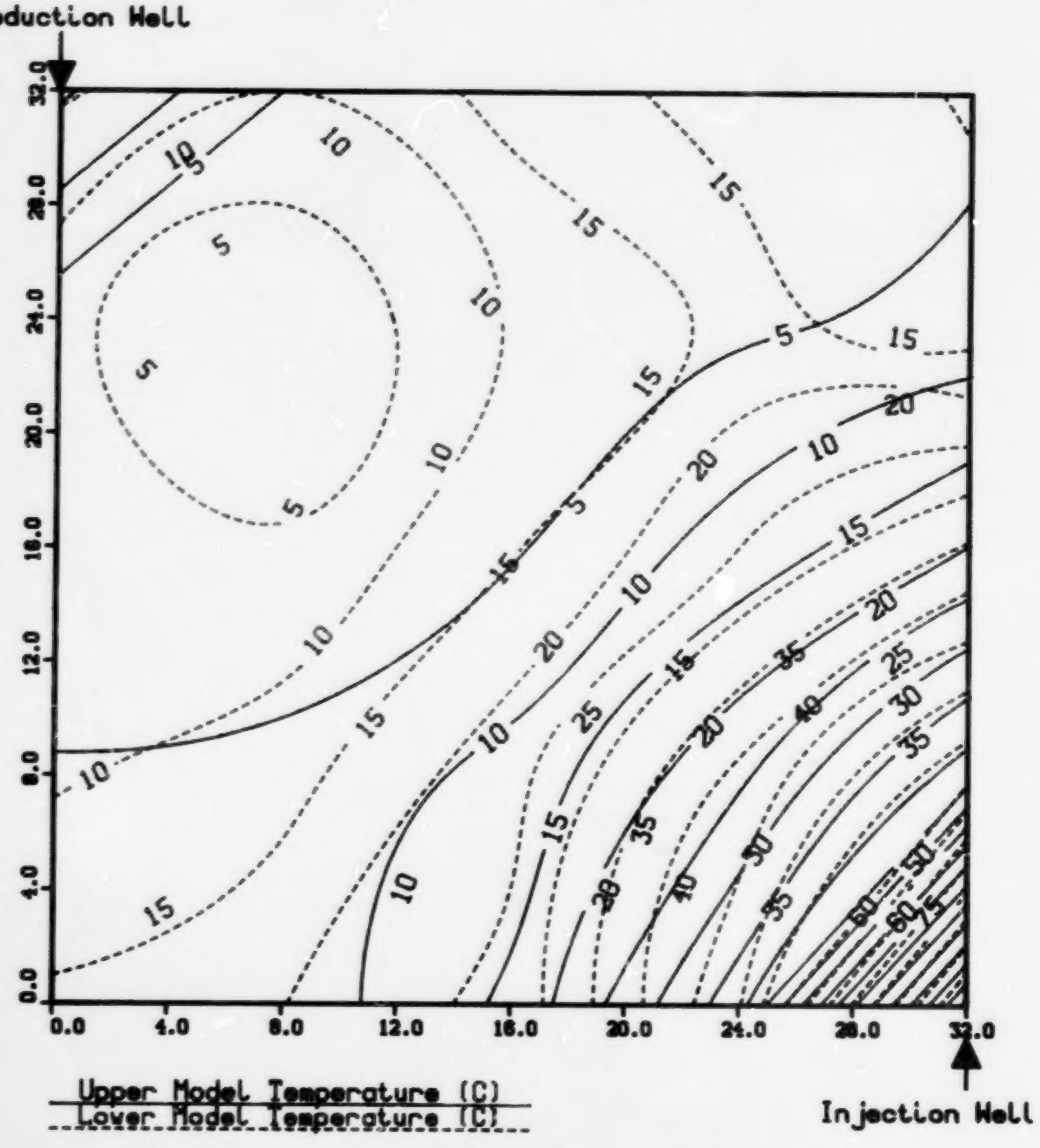

FIGURE 62: TEMPERATURE PROFILE FOR
RUN 18: COLD WATER SLUG RUN ON ABERFELDY MODEL

0.50 Pore Volumes Steam Injected

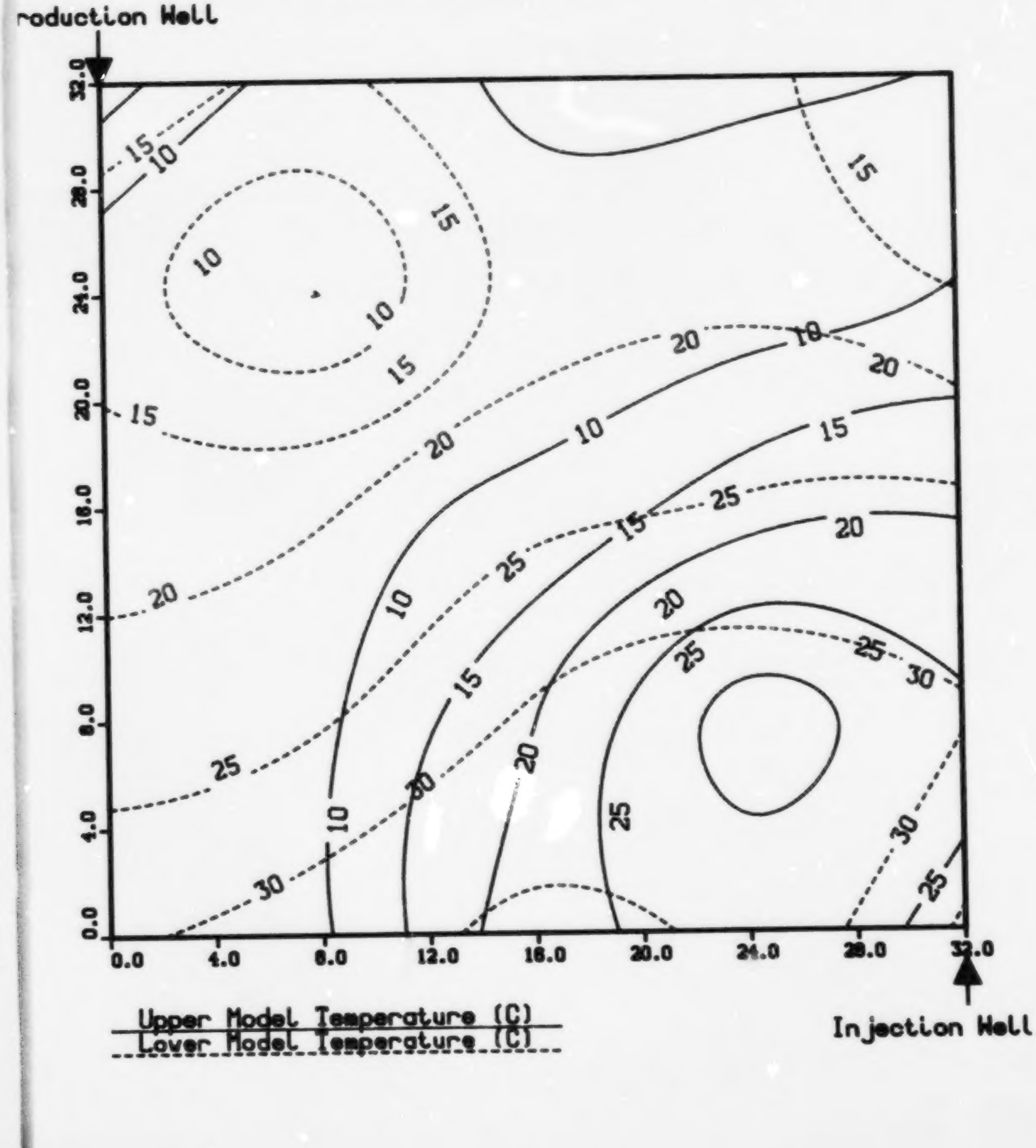

FIGURE 63: TEMPERATURE PROFILE FOR
RUN 18: COLD WATER SLUG RUN ON ABERFELDY MODEL

0.75 Pore Volumes Steam Injected

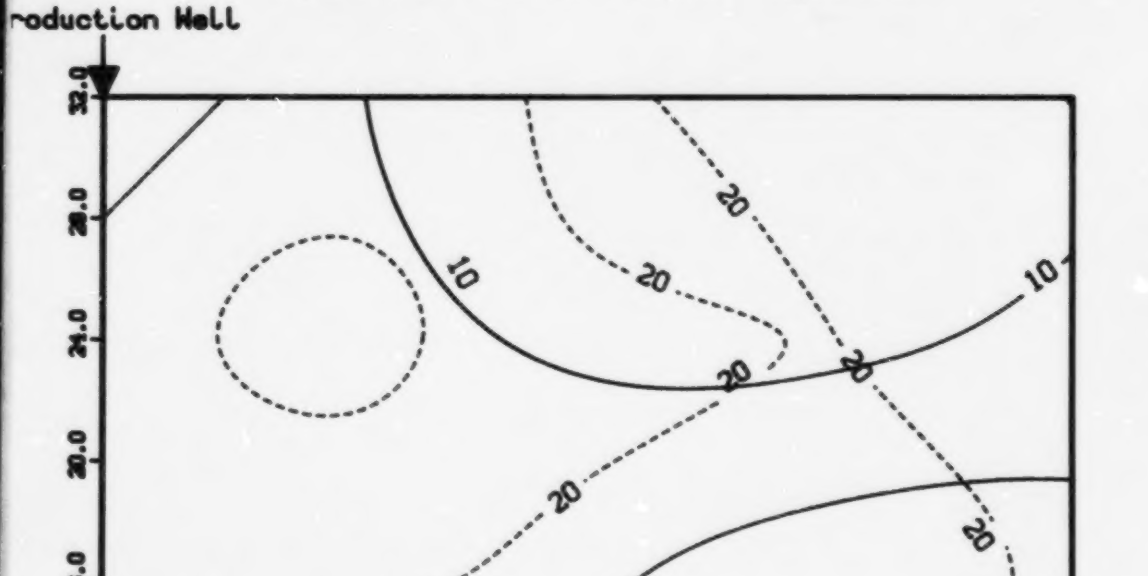

FIGURE 64: TEMPERATURE PROFILE FOR RUN 18: COLD WATER SLUG RUN ON ABERFELDY MODEL

1.00 Pore Volumes Steam Injected

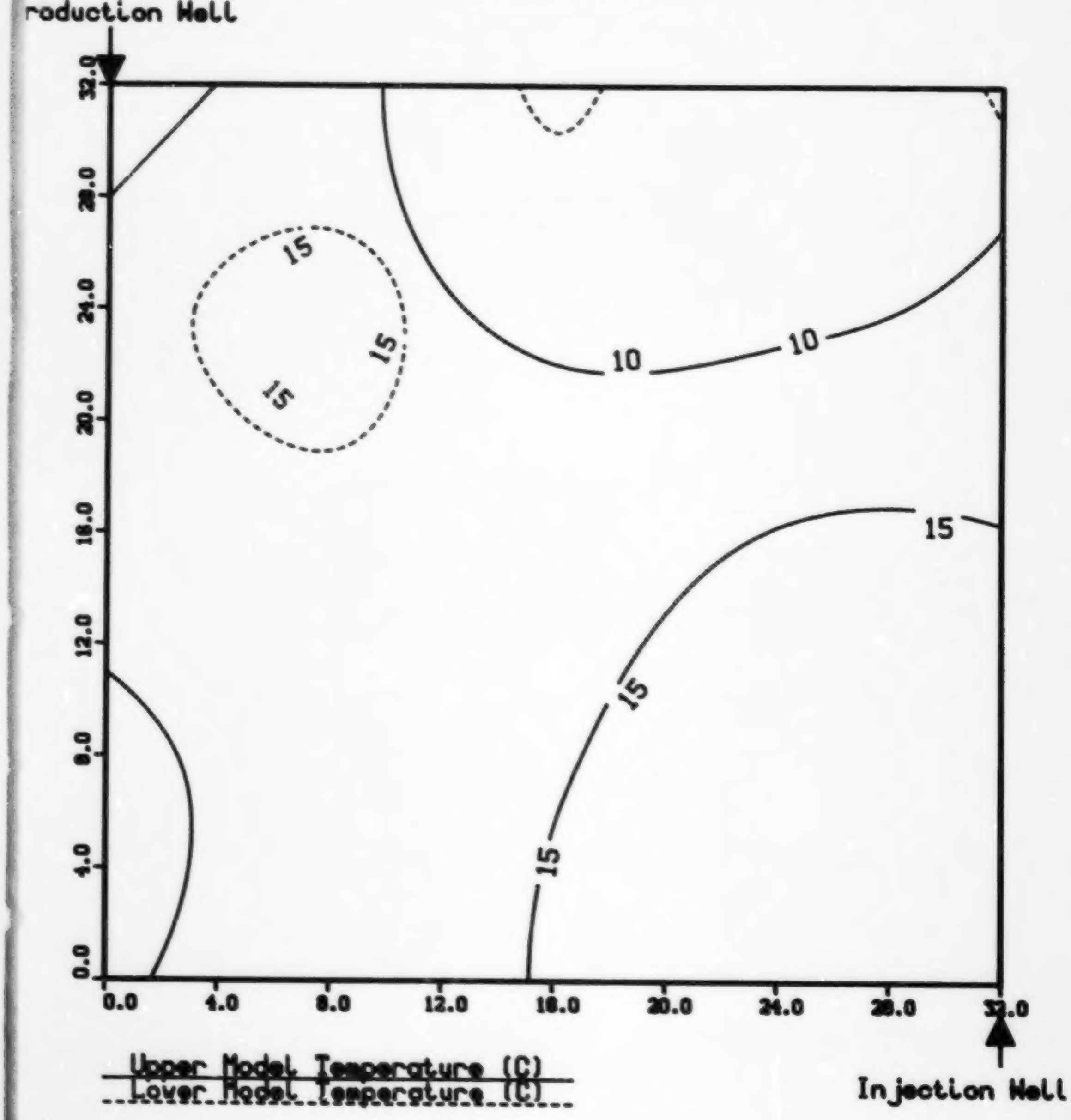

FIGURE 65: TEMPERATURE PROFILE FOR
RUN 18: COLD WATER SLUG RUN ON ABERFELDY MODEL

1.25 Pore Volumes Steam Injected

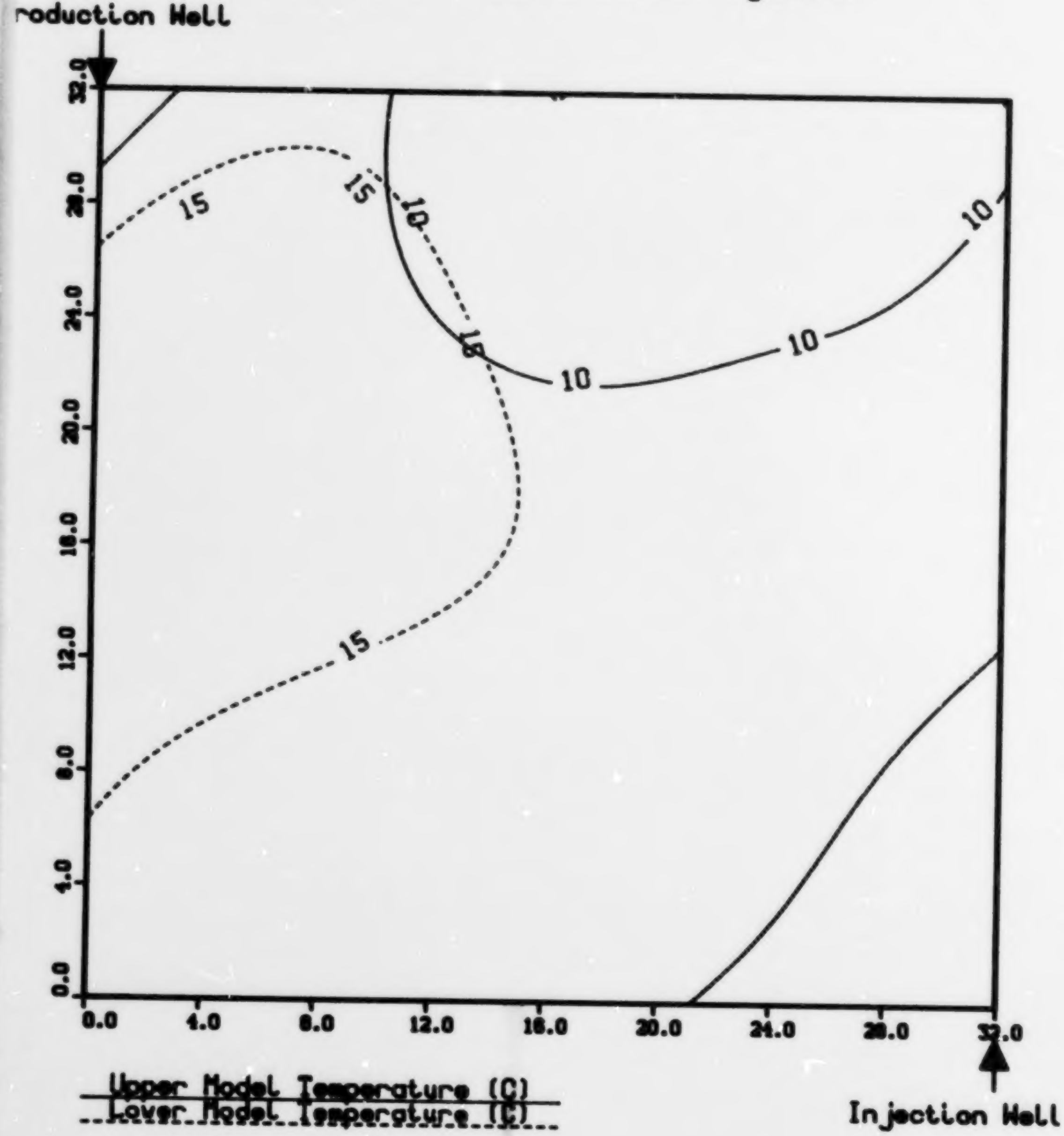

Steam Slug Run in Aberfeldy Model.

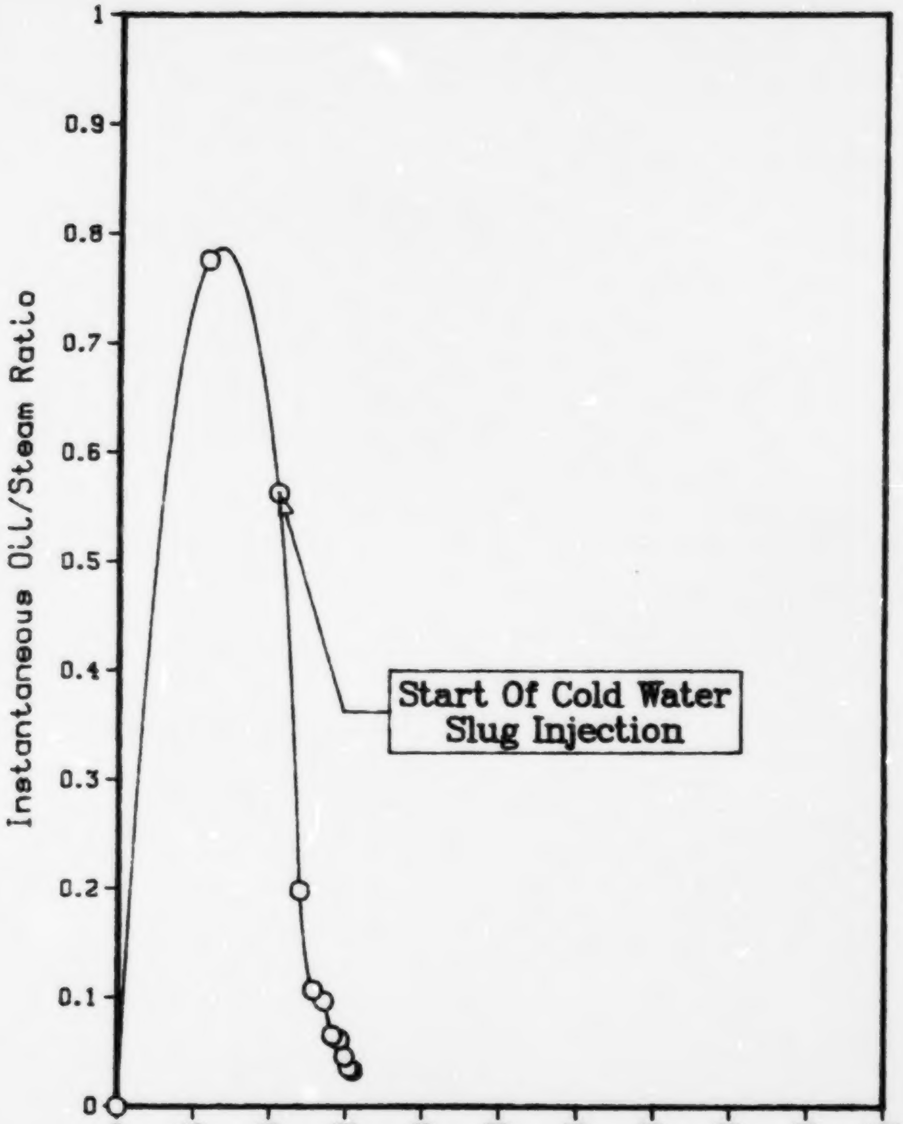

Figure 66. Run 18, Instantaneous Oil-Steam Ratio vs. Cumulative Oil Production.

Steam Slug Run in Aberfeldy Model.

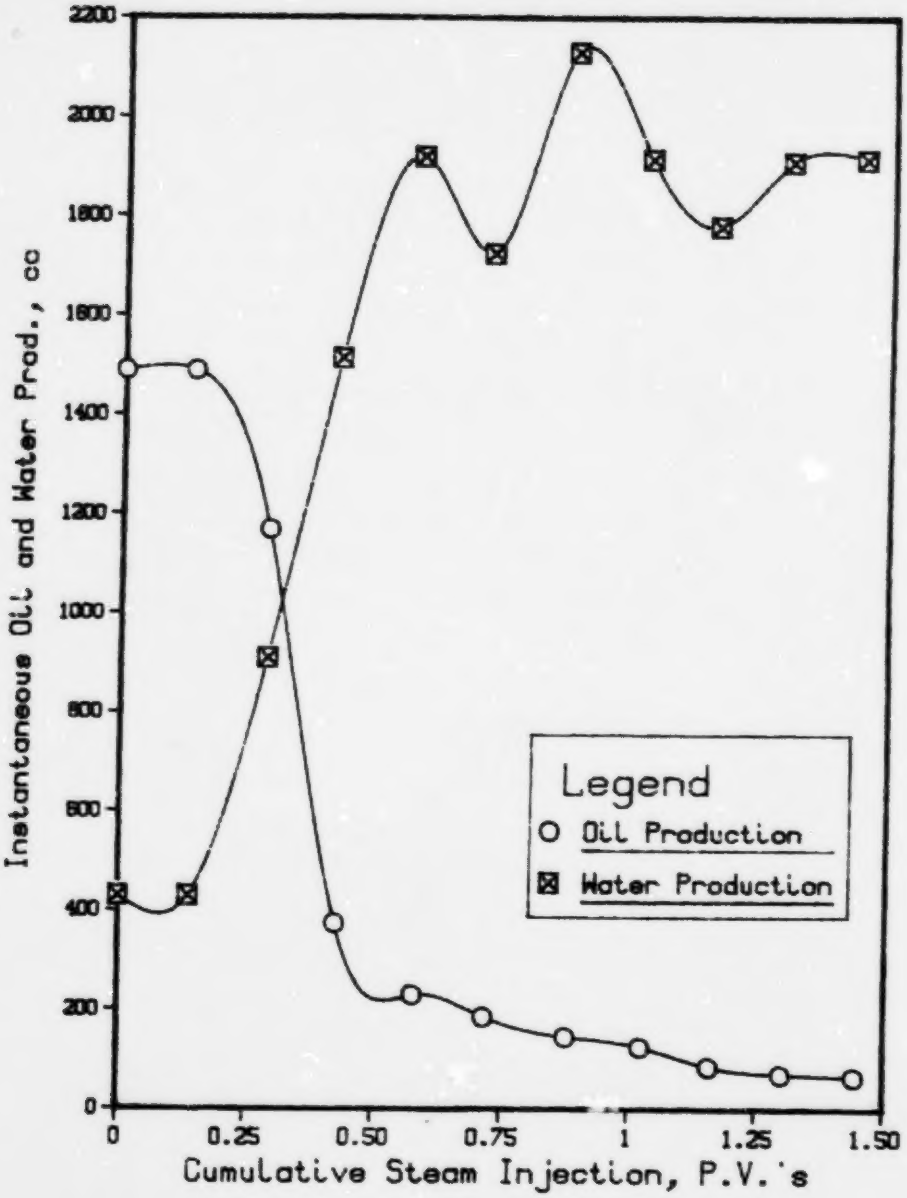

Figure 67. Run 18, Instantaneous Oil and Water Production vs. Cumulative Injection.

FIGURE 68: TEMPERATURE PROFILE FOR
RUN 19: COLD WATER SLUG RUN ON ABERFELDY MODEL

0.25 Pore Volumes Steam Injected

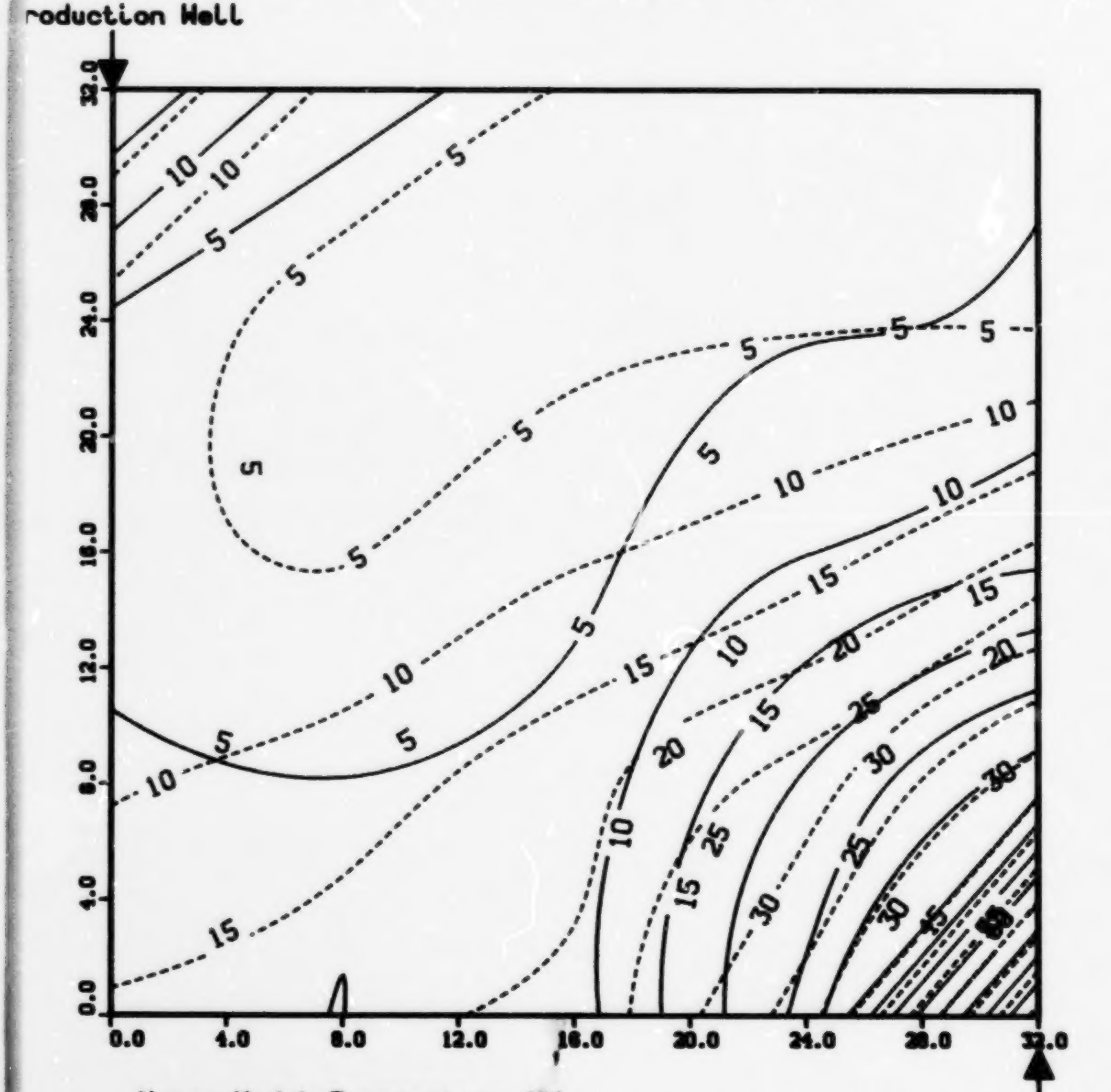

FIGURE 69: TEMPERATURE PROFILE FOR
RUN 19: COLD WATER SLUG RUN ON ABERFELDY MODEL
Start of Cold Water Slug (0.28 p.v.s)

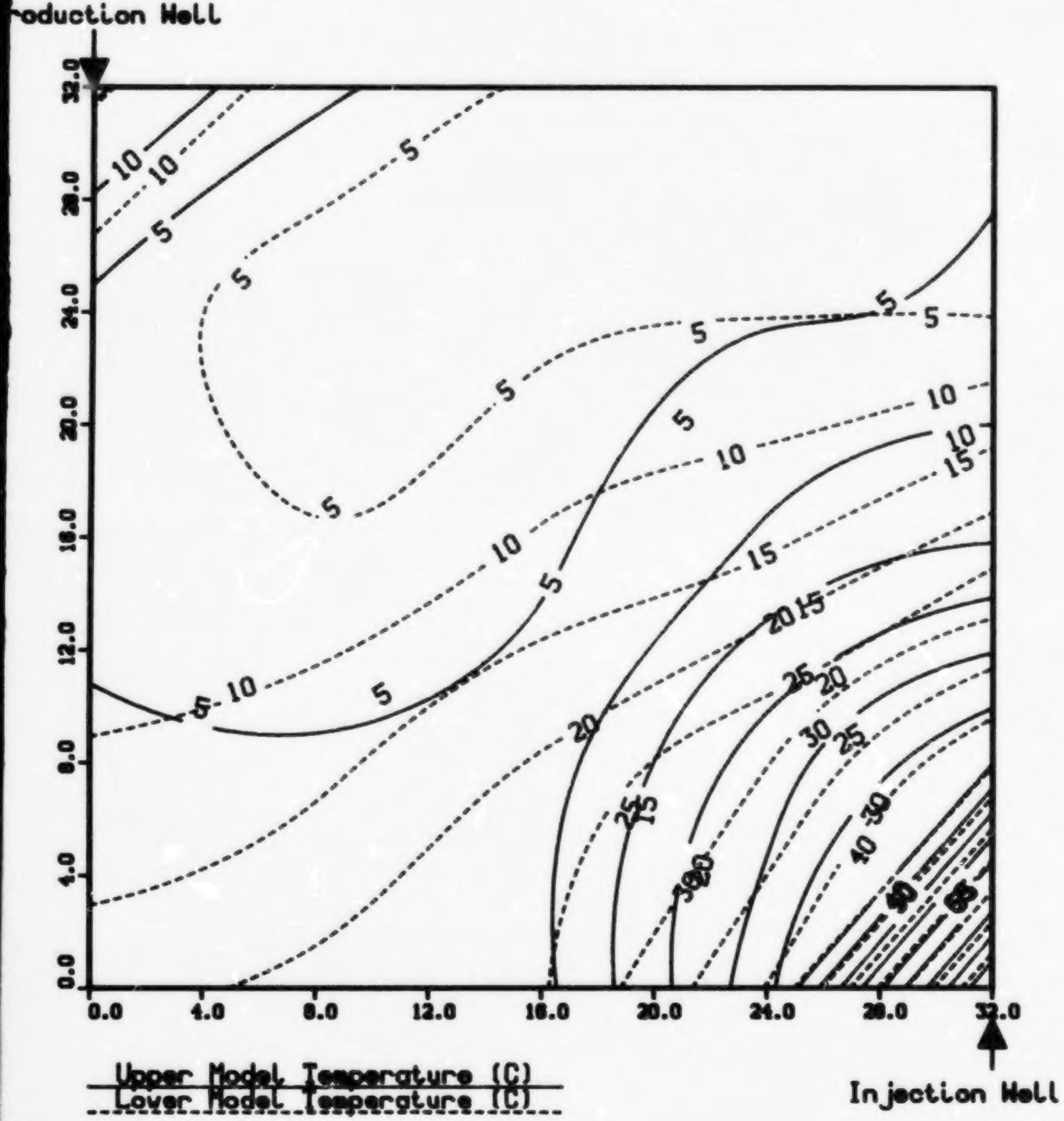

FIGURE 70: TEMPERATURE PROFILE FOR RUN 19: COLD WATER SLUG RUN ON ABERFELDY MODEL

0.50 Pore Volumes Steam Injected

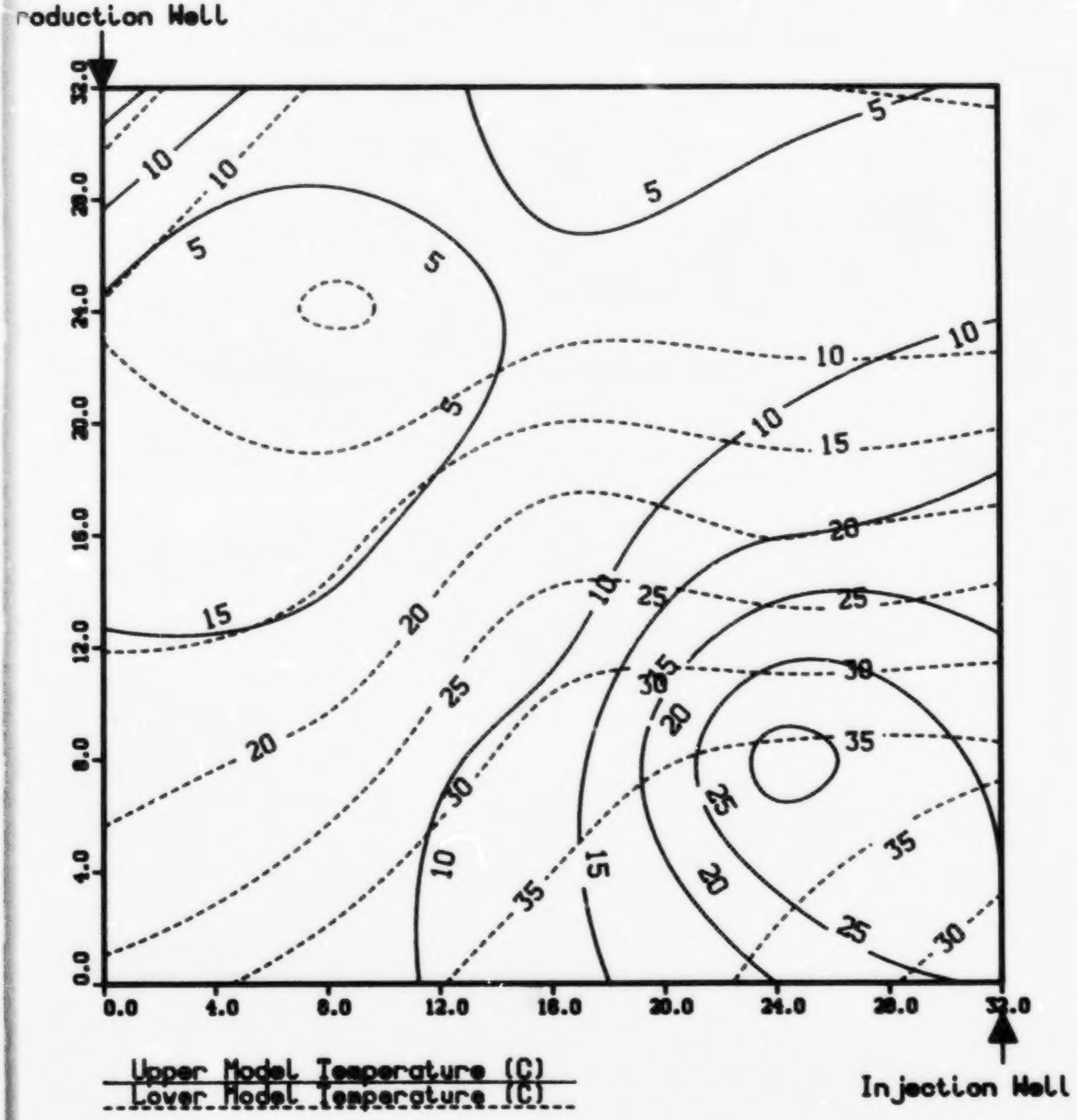

FIGURE 71: TEMPERATURE PROFILE FOR
RUN 19: COLD WATER SLUG RUN ON ABERFELDY MODEL

0.75 Pore Volumes Steam Injected

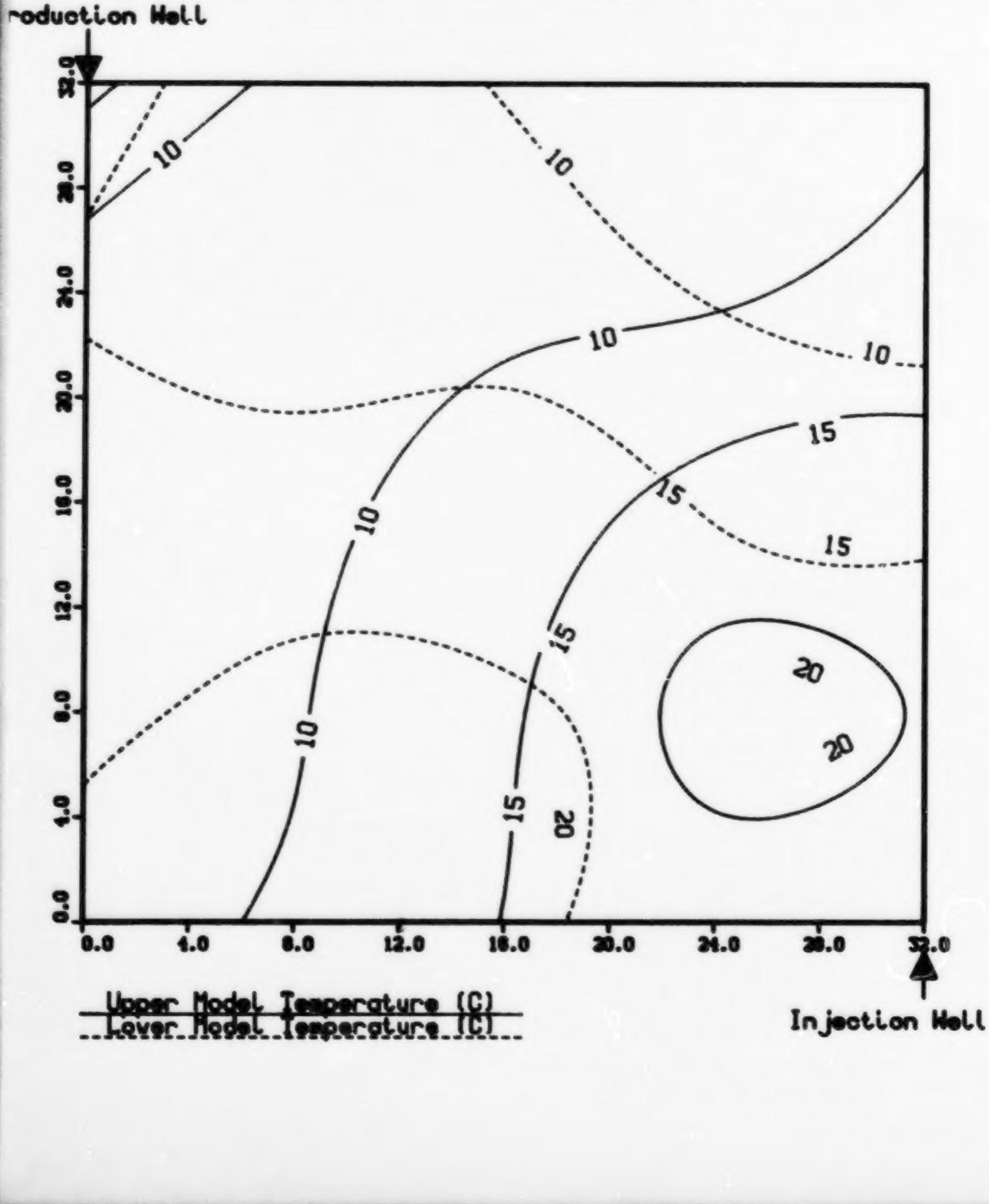

FIGURE 72: TEMPERATURE PROFILE FOR
RUN 19: COLD WATER SLUG RUN ON ABERFELDY MODEL

1.00 Pore Volumes Steam Injected

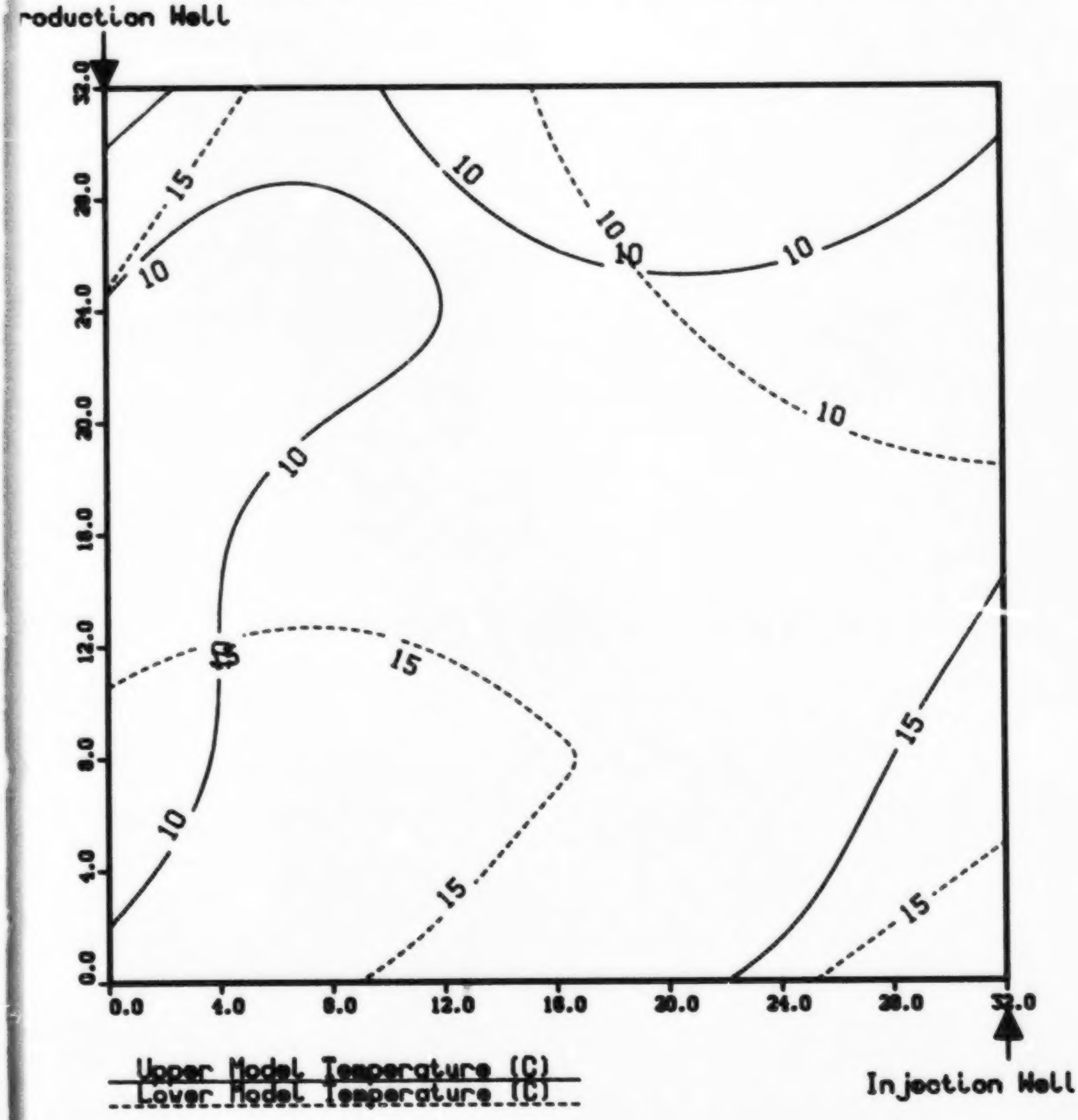

FIGURE 73: TEMPERATURE PROFILE FOR RUN 19: COLD WATER SLUG RUN ON ABERFELDY MODEL

1.25 Pore Volumes Steam Injected

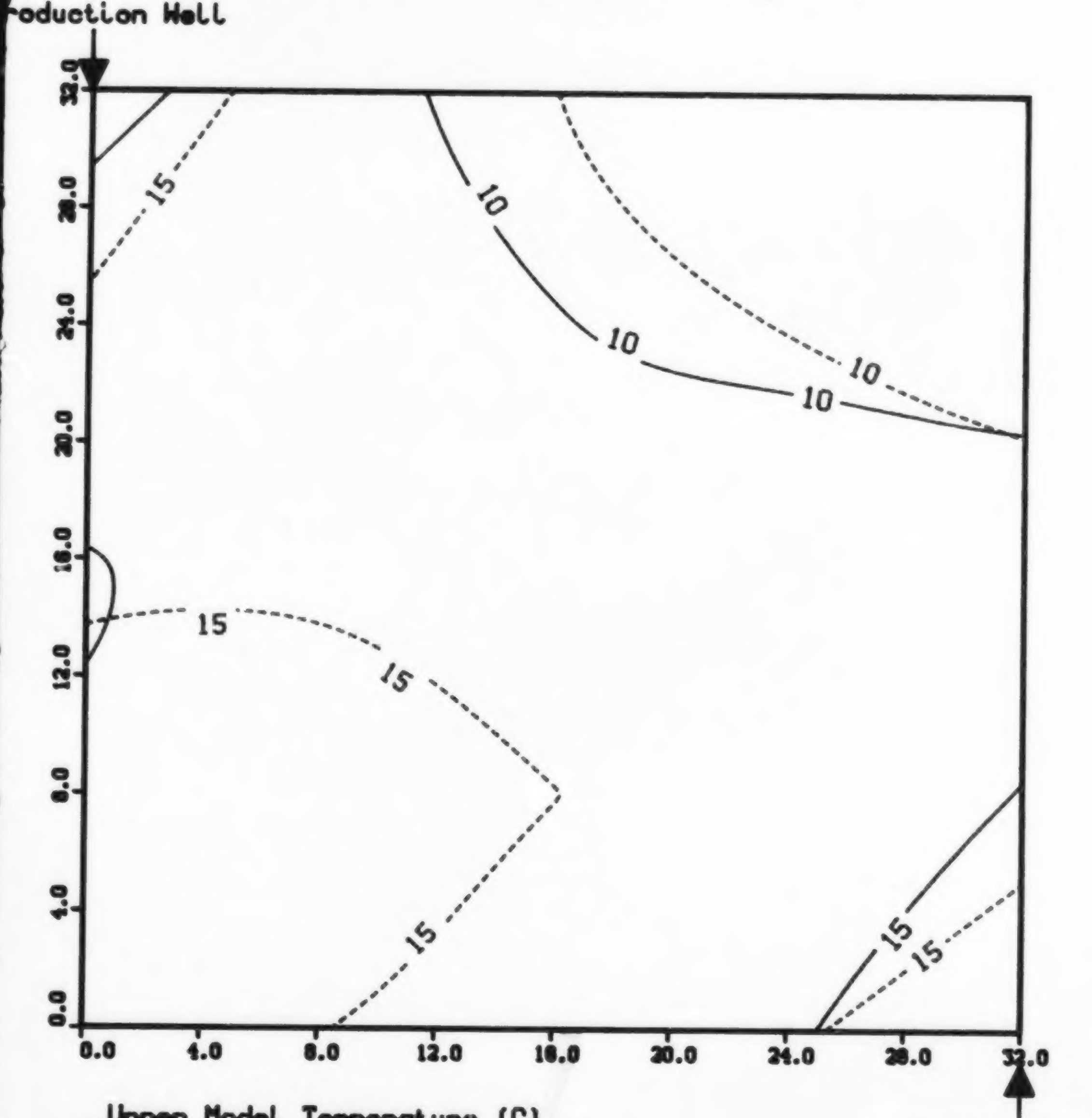

Steam Slug Run in Aberfeldy Model.

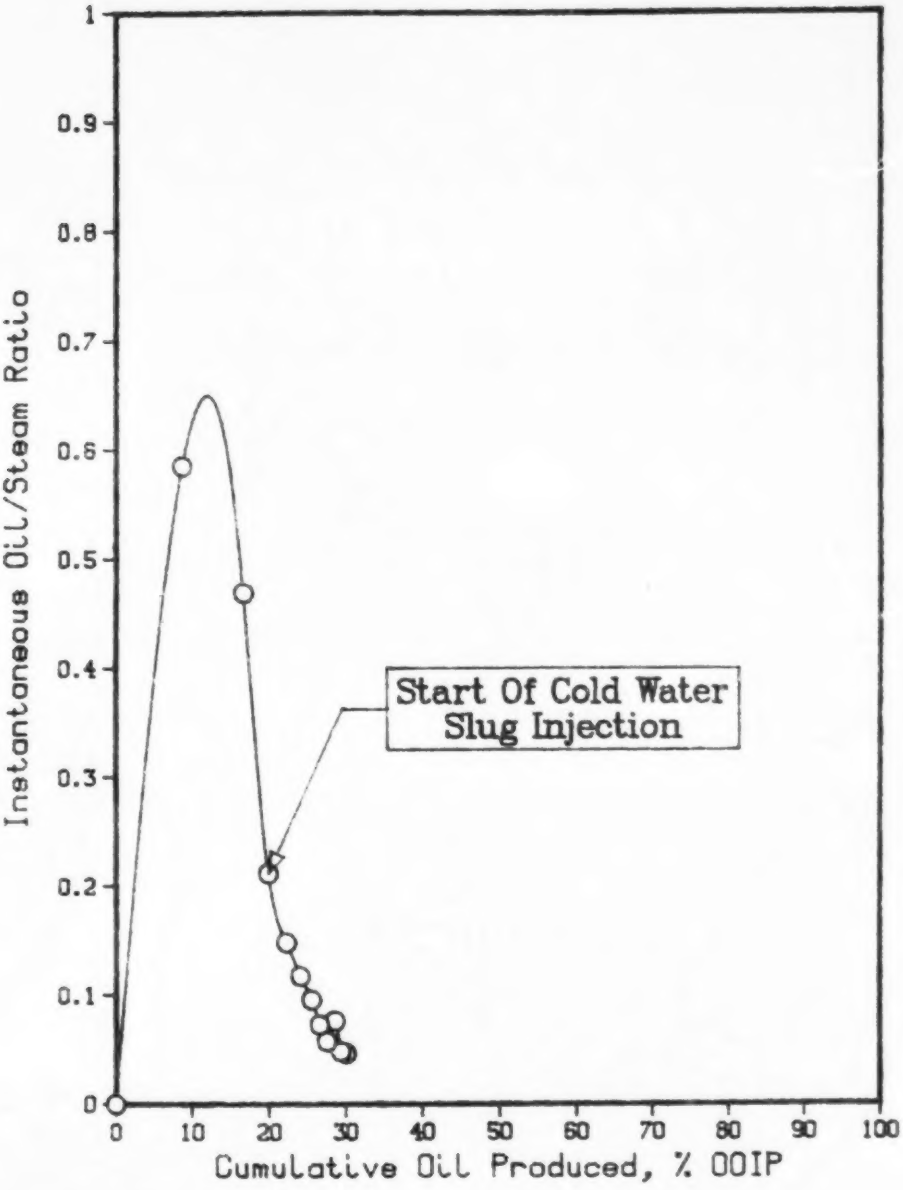

Figure 74. Run 19, Instantaneous Oil-Steam Ratio vs. Cumulative Oil Production.

Steam Slug Run in Aberfeldy Model.

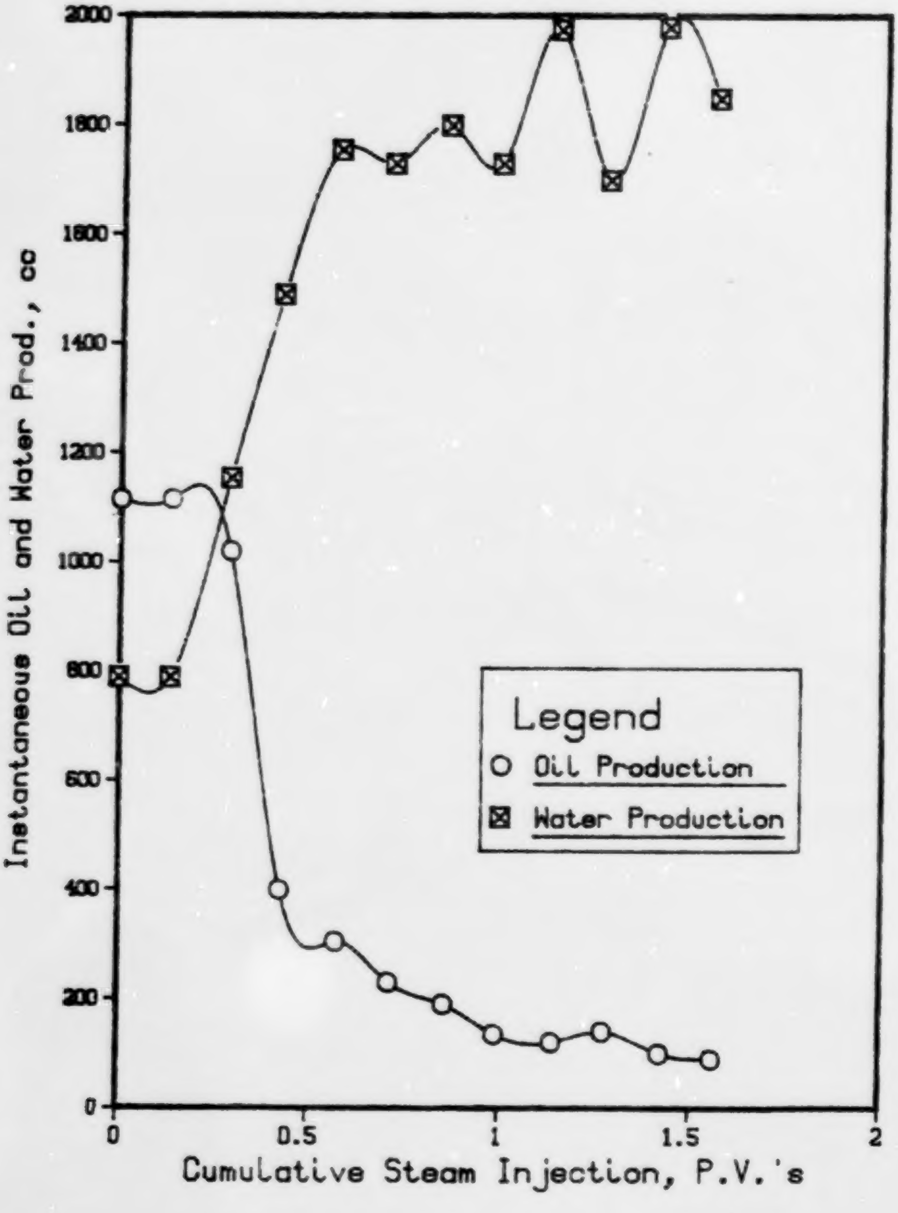

Figure 75. Run 19, Instantaneous Oil and Water Production vs. Cumulative Injection.

Three Slug Runs on Aberfeldy Model.

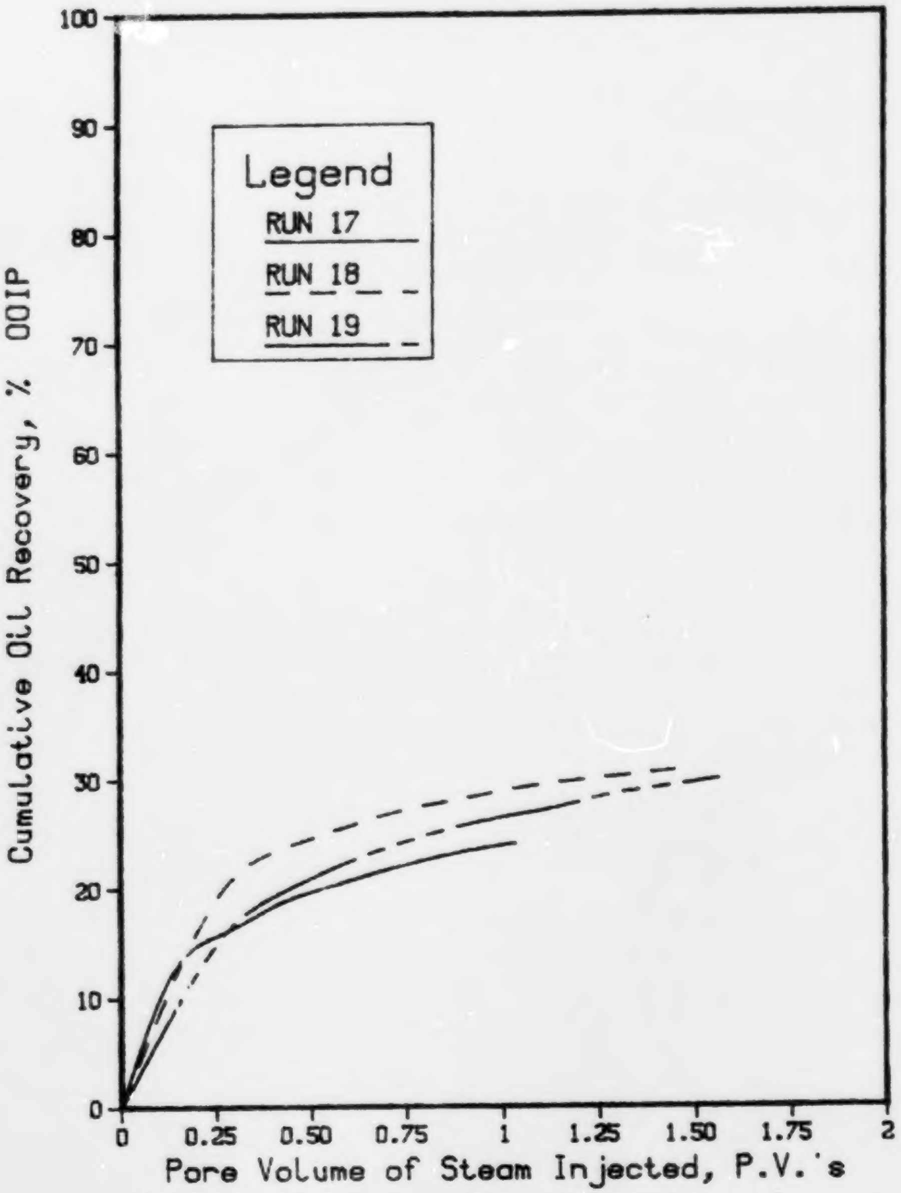

Figure 76. Comparison of the Recovery Responses of Runs 17, 18, and 19.

FIGURE 77: TEMPERATURE PROFILE FOR
RUN 22: HOT WATER SLUG RUN ON ABERFELDY MODEL

0.25 Pore Volumes Steam Injected

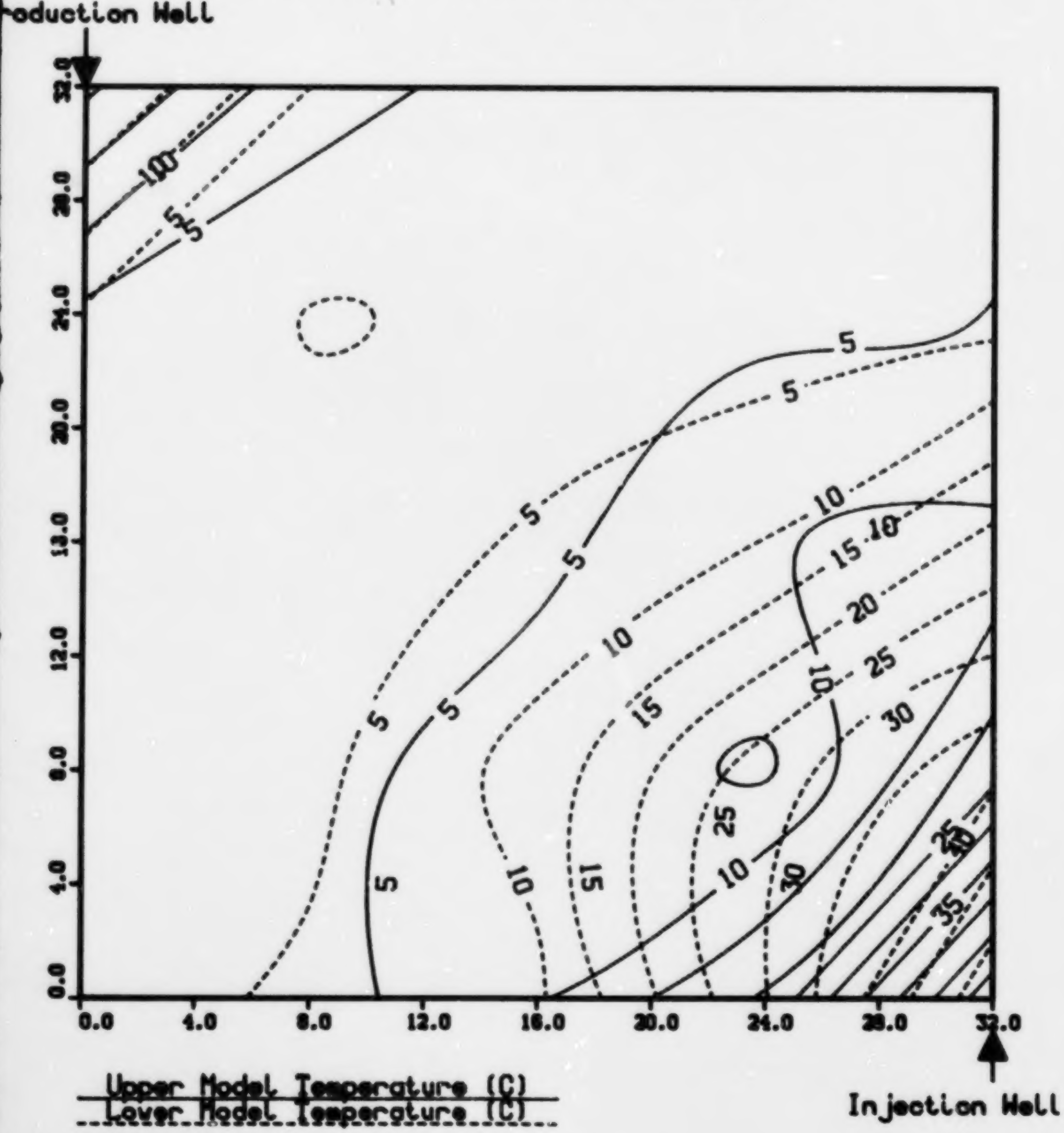

FIGURE 78: TEMPERATURE PROFILE FOR RUN 22: HOT WATER SLUG RUN ON ABERFELDY MODEL

0.50 Pore Volumes Steam Injected

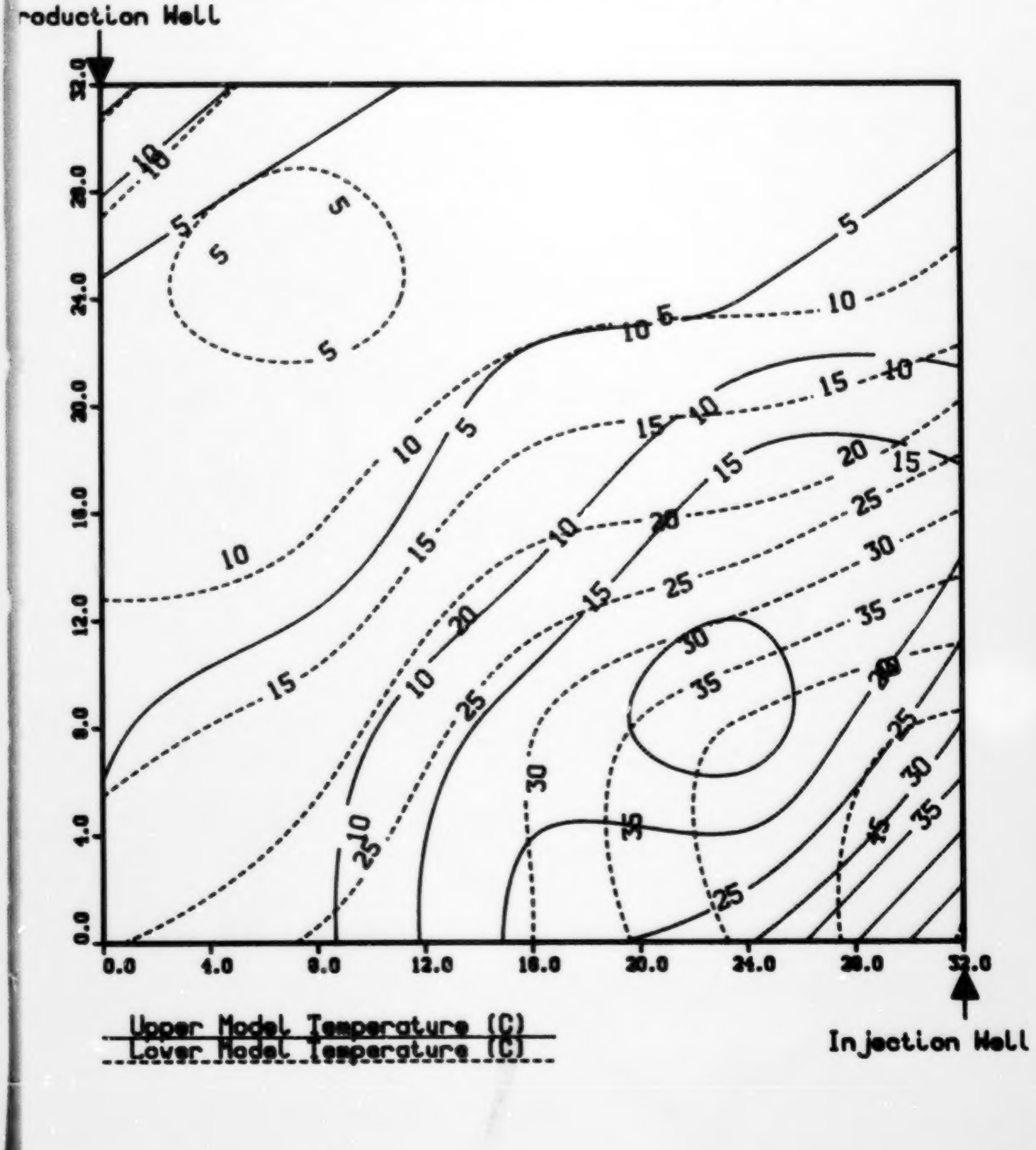

FIGURE 79: TEMPERATURE PROFILE FOR
RUN 22: HOT WATER SLUG RUN ON ABERFELDY MODEL

0.75 Pore Volumes Steam Injected

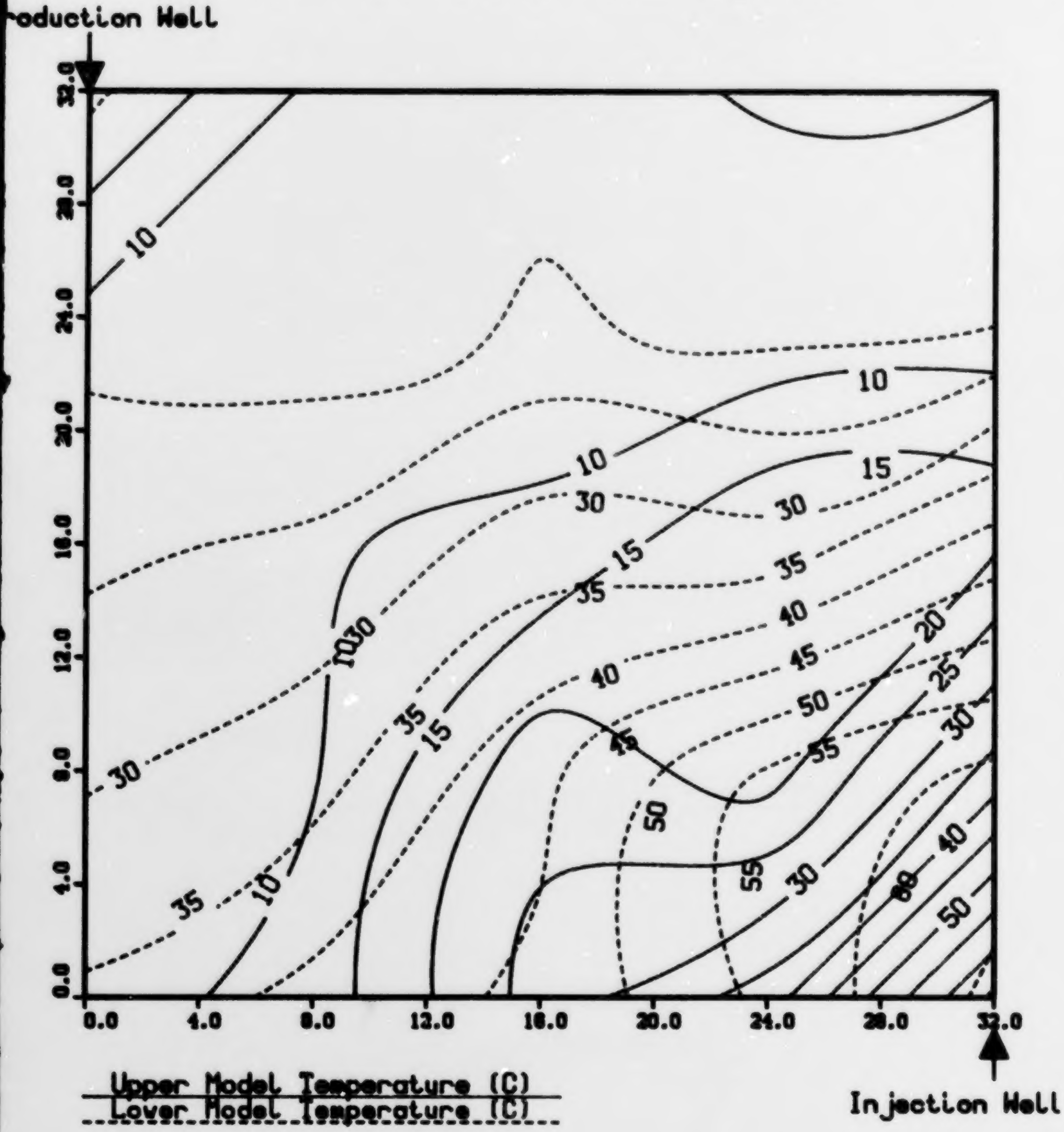

FIGURE 80: TEMPERATURE PROFILE FOR RUN 22: HOT WATER SLUG RUN ON ABERFELDY MODEL

1.00 Pore Volumes Steam Injected

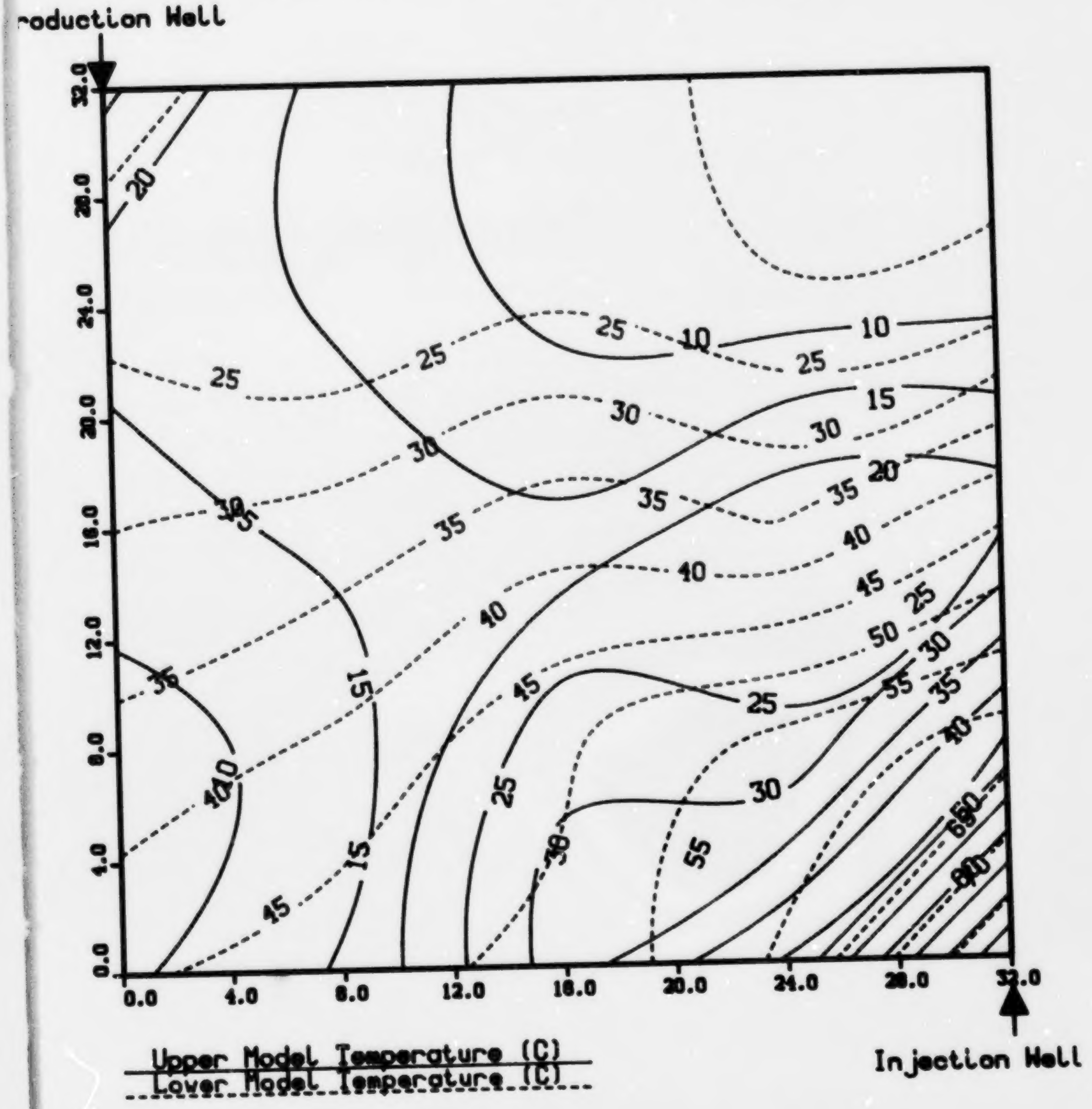

Hot Water Slug Run in Aberfeldy Model.

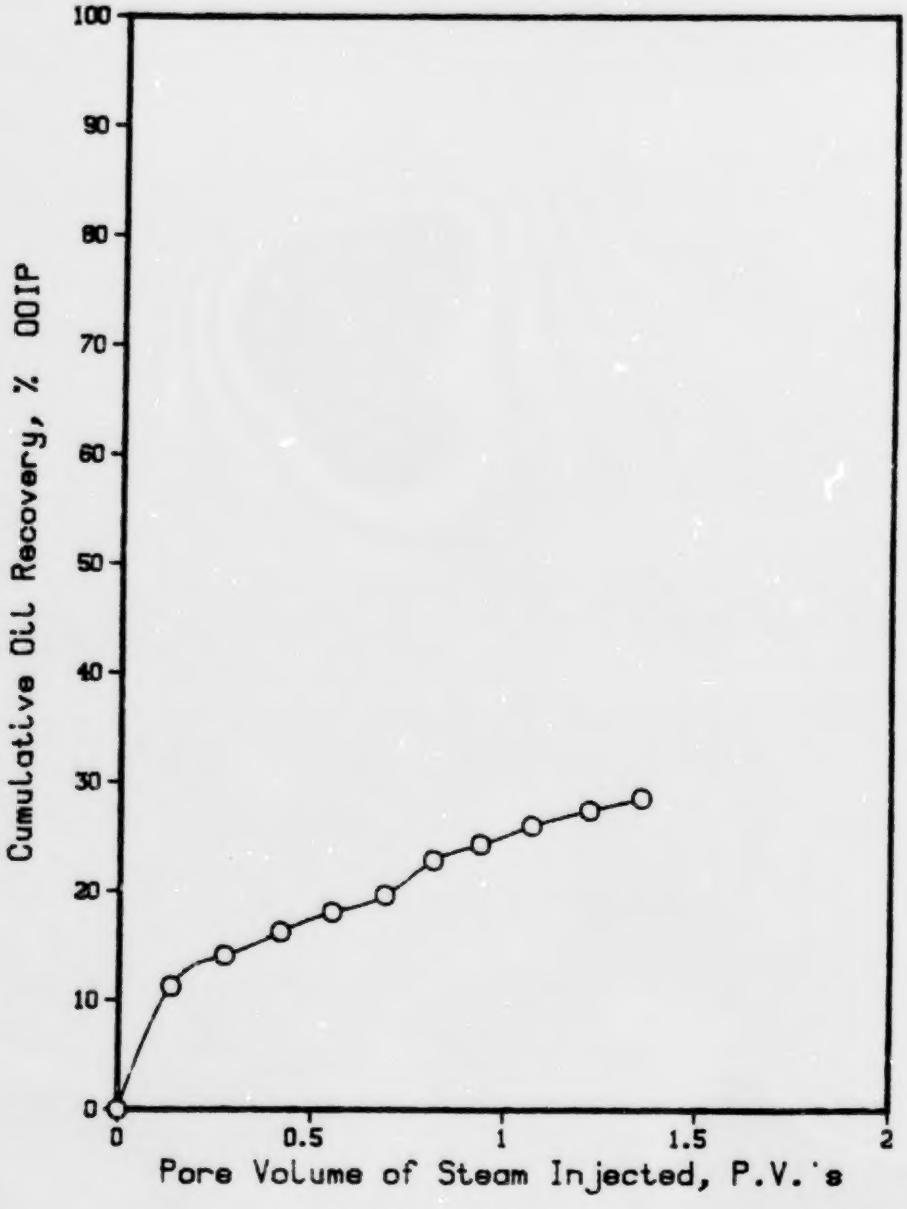

Figure 81. Run 22, Cumulative Oil Recovery vs. PV Injected.

Hot Water Slug Run in Aberfeldy Model.

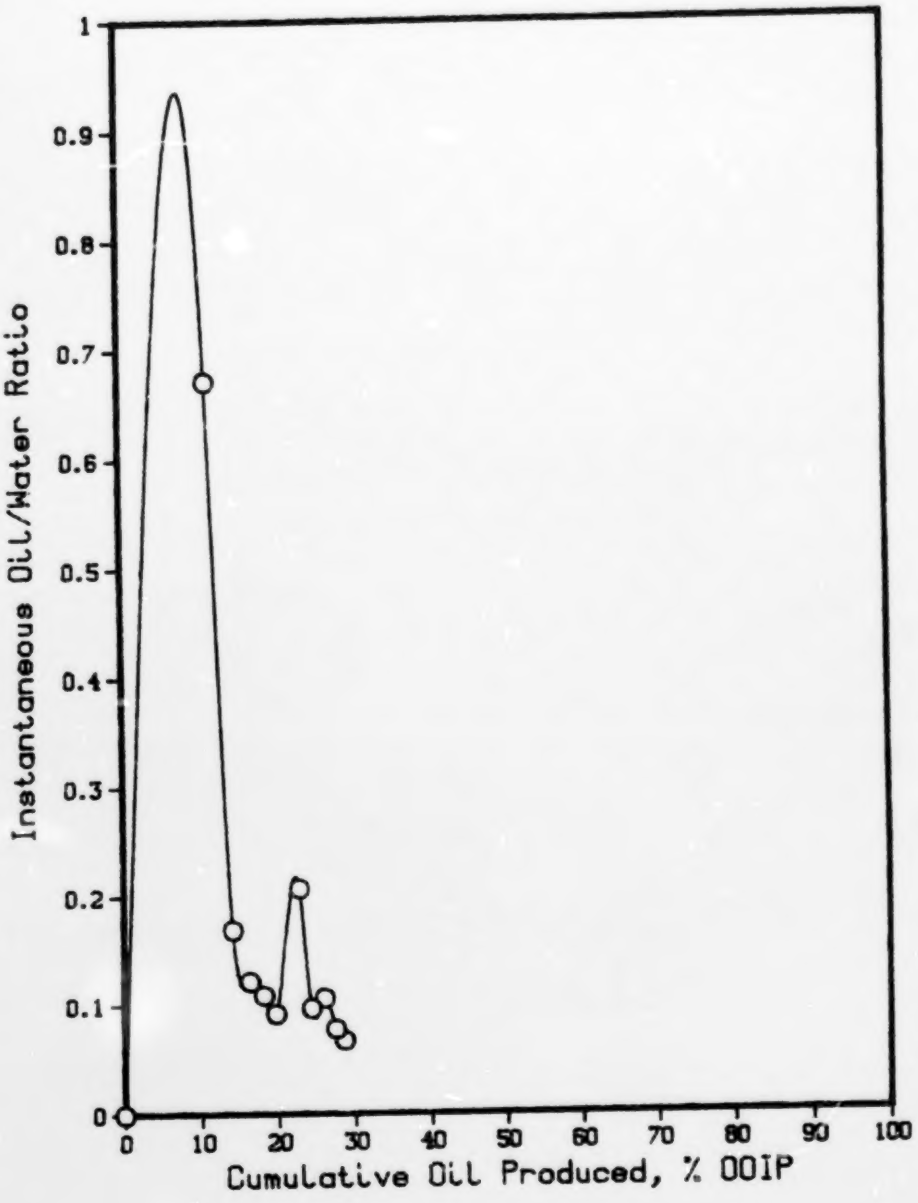

Figure 82. Run 22, Instantaneous Oil-Steam Ratio vs. Cumulative Oil Production.

Hot Water Slug Run in Aberfeldy Model.

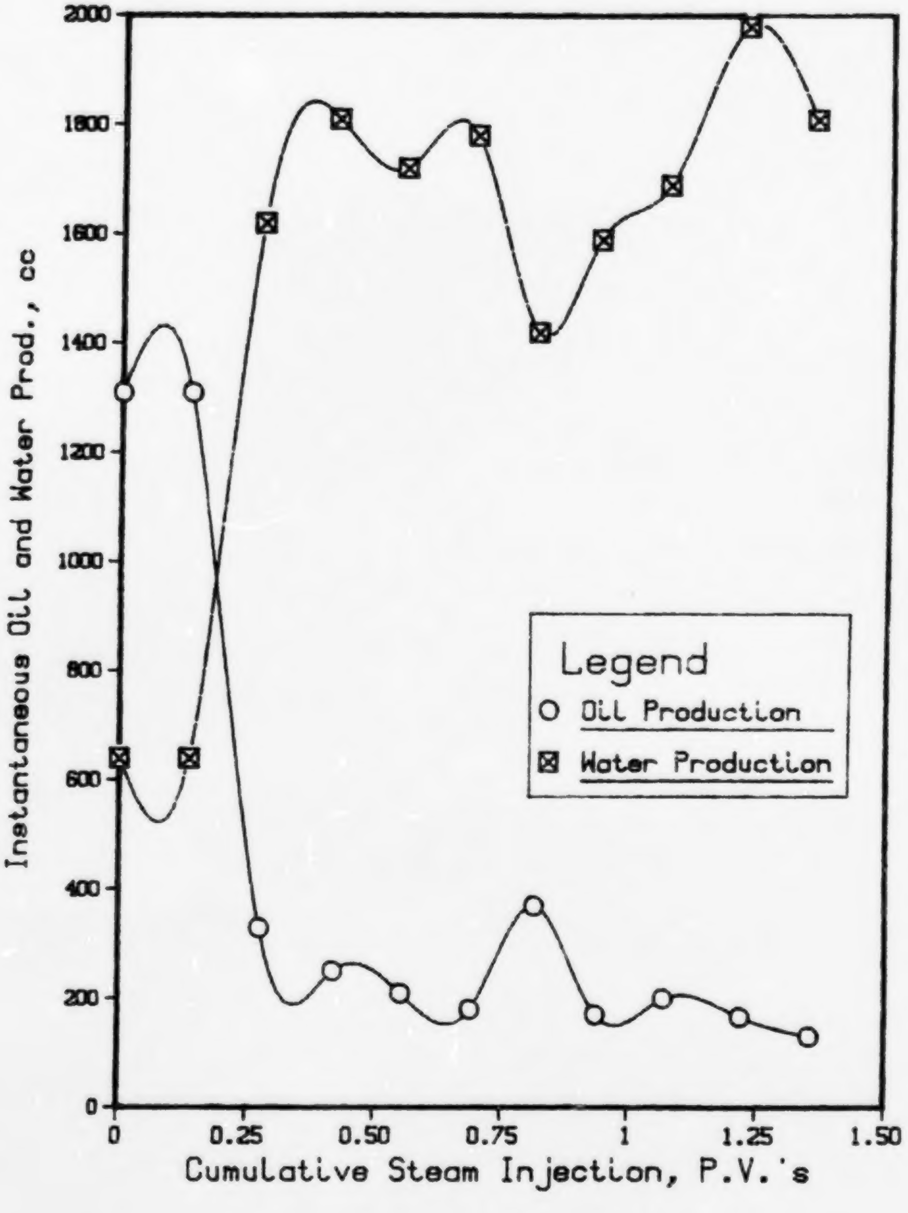

Figure 83. Run 22, Instantaneous Oil and Water Production vs. Cumulative Injection.

APPENDIX C:

Papers Presented.

3ème COLLOQUE EUROPEEN SUR L'AMELIORATION DE LA RECUPERATION DU PETROLE
3° CONVEGNO EUROPEO SUL MIGLIORAMENTO DELLE TECNICHE DI RECUPERO DEL PETROLIO
Roma, 16-18 Aprile 1985

PROCEEDINGS
ACTES
ATTI

1

FLUID FLOW IN POROUS MEDIA
ECOULEMENT DES FLUIDES DANS LES MILIEUX POREUX

WATERFLOODING AND IMMISCIBLE GAS INJECTION
INJECTION D'EAU ET DE GAZ NON MISCIBLE

THERMAL PROCESSES
PROCEDES THERMIQUES

Organization/Organisation/Organizzazione: Agip S.p.A.
Co-sponsors: Elf Italiana - Montedison - Shell Italia - Snia BPD

APPLICATION OF THERMAL RECOVERY TECHNIQUES TO MARGINAL RESERVOIRS

MAHNAZ KASRAIE, S.M. FAROUQ ALI
University of Alberta
Edmonton, Alberta, Canada

ABSTRACT

With the depletion of the more prolific heavy oil reservoirs, attention is being directed to less favourable, or "marginal" reservoirs, which are characterized by bottom water, gas cap, thin formations, extra-heavy oil, deep formations, or fissured rocks. This paper presents simulations, laboratory, and field results for the application of thermal processes to such marginal reservoirs, and offers operational guidelines.

RESUME

Considérant l'état d'épuisement des plus prolifiques nappes d'huile lourde, il y a un regain d'intérêt dans l'exploitation des nappes moins avantageuses, dites "marginales", characterisées par une nappe d'eau sousjacente, la présence d'une nappe de gaz, une huile extra-lourde, et par des formations à grande profondeur ou fissurées. Cet article présente des résultats de simulations numériques, d'experiences de laboratoire et industrielles, concernant l'application de procédés thermiques à de telles nappes marginales, et suggère des modes d'exploitation.

1. INTRODUCTION

Thermal processes - steam injection, and to a lesser extent, in situ combustion - have been remarkably successful for heavy oil recovery, and currently account for nearly 90% of the total enhanced oil production. Many heavy oil reservoirs in Canada, the U.S., and other countries are unsuitable for the application of conventional thermal methods for technical and/or economic reasons. For example, in Cold Lake, Alberta, only one out of five types of reservoirs is suitable for thermal recovery(1). This paper discusses the application of thermal techniques to "marginal" heavy oil reservoirs. Such reservoirs are defined to have one or more of the following characteristics: thin formation (less than 6 m), bottom water present, gas cap present, depths greater than 900 m, low oil saturation (less than 50% pv), fissures, or very high viscosity (over 10 Pa·s).

The authors attempt to present laboratory data, simulation results, their own as well as those of other investigators, and field results, where available. Also considered are the National Petroleum Council's application criteria for the current as well as the expected advanced technology(2).

2. MARGINAL RESERVOIRS

As the more favourable heavy oil reservoirs are increasingly exploited by thermal methods, attention is being directed toward less favourable, or marginal reservoirs. Such heavy oil reservoirs contain vast amounts of oil, but currently offer little economic incentive. These reservoirs are classified as follows:

2.1 Bottom Water

In these formations, a water sand occurs below the oil sand, in communication with it. It can be part of an aquifer, part of a transition zone, or simply a zone of high water saturation. The permeability of the water layer may vary greatly from that of the oil zone, if clays are present. The thickness of bottom water can be a metre or so, to many metres, and would determine the extent of success of a thermal process.

2.2 Gas Cap

A gas cap is here defined as a high gas saturation zone, or a desaturated zone, near the top of a heavy oil sand. Occasionally small discontinuous gas caps occur in heavy oil formations.

2.3 Deep Heavy Oil Formations

Heavy oil reservoirs that are deeper than the current depth limit of about 900 m could be considered to be marginal. To-date, there is no economic success reported for deeper projects. Such reservoirs occur in California, Texas, the Middle East, Argentina, etc. Similarly, offshore heavy oil reservoirs could also be considered marginal depending on the rock and fluid characteristics.

2.4 Extra-Heavy Oil Formations

Oil viscosities in excess of several thousand mPa·s present special problems, since injectivity would be low even if the permeability is high. Injection at acceptable rates would frequently entail parting.

2.5 Thin Formations

In Saskatchewan, some 80% of the heavy oil occurs in formations less than 4 m thick. Application of thermal processes to such formations would normally cause prohibitive heat loss.

2.6 Fissured Heavy Oil Formations

Occasionally, heavy oil occurs in carbonates that are extensively fissured and faulted. Application of thermal processes to such formations is problematic in view of the great variation of conductivity in different directions.

We shall now consider each type of reservoir in greater detail, first discussing the mechanistic features of each recovery process, followed by model, simulation, and field results, where applicable.

3. BOTTOM WATER

3.1 Cyclic Steam Simulation

The performance of cyclic steam stimulation under bottom water conditions would depend on the water zone-to-oil zone thickness ratio, oil viscosity, vertical permeability, and steam injection rate and volume. In the case of a highly viscous oil (over 10 Pa·s), the injected steam would channel into the water sand either by creating a path, or more likely, by formation parting. The mobilized oil is displaced into the water zone. When the well is put on production, some oil and a large volume of steam and water are produced. The extent of oil production would depend upon how much of the oil zone is heated before steam short-circuits into the water sand. This in turn depends on the oil zone thickness, steam injectivity, and any redeeming features, such as reduced permeability of the water sand, or presence of a small gas saturation in the oil zone. Oil production would tend to improve in subsequent cycles.

3.2 Steamflooding

The variables mentioned previously determine the efficiency of a steamflood also under bottom water conditions. The water zone-to-oil zone thickness ratio is particularly important. In most cases, steam would advance in the oil zone to a limited extent, then shortcircuiting into the water. Thereafter it would flow in the water zone, heating the oil zone above by conduction, later supplemented by convection, as steam rises into the oil zone. Time is an important factor in this process because heating of the oil zone is slow. Large volumes of water and steam would be produced during this period, if unrestricted An advantage of a bottom water sand is the ability to inject steam in a very high viscosity oil formation, which would not accept steam at satisfactory rates.

3.3 In Situ Combustion

The injected air would partially support the firefront in the oil zone. But the bulk of air would flow in the water layer. Since air is the nonwetting phase, it would tend to flow in the upper part of the water sand, in a desaturated capillary-gravity zone. As a result, the performance would be relatively independent of the water zone thickness. The air flowing in the water zone would re-enter the oil zone near the producers, thereby leading to possible spontaneous ignition, and formation of secondary combustion surfaces around the producers. On the whole, high producing well temperatures and high air-oil ratios would be expected.

3.4 Numerical Simulation

Numerical simulations of cyclic steaming in the presence of bottom water have been carried out by the authors(3) and others(e.g. 4,5). The authors found that for bottom water thickness-to-oil zone thickness ratios of about 0.2, the oil-steam ratio may be in the acceptable range (0.1 to 0.2 m^3/m^3). Beyond that, it drops rapidly. For a ratio of 1.0, very little oil is produced. These numbers were for a 50 Pa·s oil, and would vary with the aforementioned operating parameters. Figure 1 shows the oil-steam ratio as a function of the said ratio for a 10 Pa·s oil for steam slugs of 1590 m^3 (10,000 bbls) and 4770 m^3 (30,000 bbls). It appears that for thin water zones the smaller slug is more effective. A small slug would tend to create a heated zone rather than channelling directly into the water zone. Figure 2 shows the effect of oil viscosity for the same slug size. It is seen that the performance is somewhat better for the lower viscosity oil, but the adverse effect of bottom water is present in both

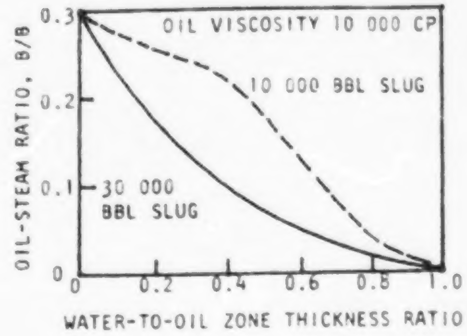

FIGURE 1

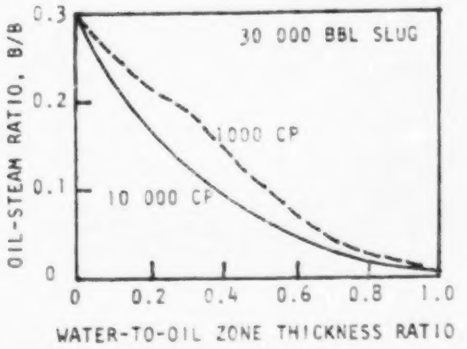

FIGURE 2

cases. Saturation and temperature distributions obtained in the simulations clearly show the steam channelling and oil migration into the water zone. The above results are for the first cycle. In subsequent cycles, performance improves somewhat due to conduction heating of the oil sand.

Numerical simulations of steamflooding in the presence of bottom water are relatively easy to carry out. Figure 3 shows the oil-steam ratio vs. cumulative steam injection for a 50 Pa·s oil in a 15 m (50 ft) sand with 3 m (10 ft) of water. It is seen that the oil-steam ratio tends to increase at first, decreasing later.

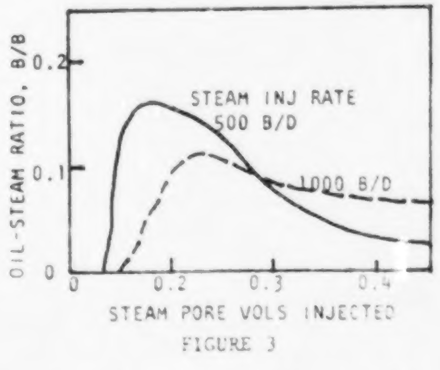

FIGURE 3

Also there is a strong rate dependence. Saturations and temperatures show steam mainly flowing through the water zone, with heating of the overlying oil, much of which gravitates into the water zone, from where it is driven by hot water. At later times steam segregates by gravity in the oil zone as well, which then has a competing effect on the water zone. Much depends on the water zone thickness: for a water sand equal in thickness to the oil sand, recovery was virtually nil.

Many numerical simulations of bottom water steaming and pressure cycling were carried out for the design of the Peace River project in Alberta(6). Crookston, Culham, and Chen(7) cite one example of a bottom water steamflood.

Numerical simulation of in situ combustion is still subject to grid size and other limitations. Farouq Ali, employing a three-phase in situ combustion simulator, showed channelling of air into the bottom water zone, spontaneous ignition near the producer, and high air-oil ratios(15). Results for similar studies for two reservoirs in Alberta and Saskatchewan are shown in Figure 4. The upper two curves are for a 100 mPa·s oil, while the bottom curve is for a 2700 mPa·s oil (Eyehill, Sask.). It is seen that the air-oil ratio increases with an increase in the air injection rate, as well as the bottom water thickness. For a given set of conditions, results were less sensitive to bottom water thickness.

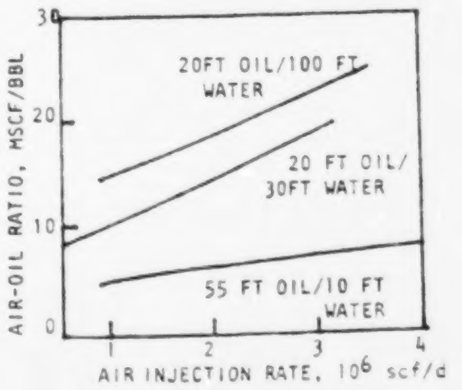

FIGURE 4

3.5 Laboratory Experimentation

Several laboratory studies of bottom water steamfloods have been reported. Pursley(8) employed a scaled model to simulate a 0.5 ha pattern, with a 43 m sand, 15% of it being water, and 100 Pa·s oil. Recovery upon the injection of one pore volume of steam was 36%. Steam was found to override, and thus contact a large proportion of the oil. The water layer was helpful in achieving injectivity. Heating at the base of the oil sand and vertical permeability were the key factors.

Ehrlich(9) and Huygen and Lowry(10) investigated the recovery of a 5 kPa·s bitumen, with bottom water present. It was found that the heated bitumen was swept into the water zone by the condensate. As Ehrlich notes, once the water zone is preheated, it cannot be plugged off, and must be saturated with oil by gravity flow before steam will advance into the oil zone. As a result, some of the oil is left in the water zone, and the resulting oil-steam ratio is low, varying from 0.041 to 0.175 in the experiments.

Stegemeier, Laumbach and Volek(11), Prats(5), and Doscher and Huang(12) have reported the use of low pressure scaled models for bottom water steamfloods. Prats(5) reported experimental results for Peace River conditions (200 Pa·s oil), with water-to-oil zone thickness ratios of 0.50, 0.25, and 0.10. The "water" zone contained 55-65% oil. The operational strategy consisted in injecting steam into the water zone, pressurize, and then blow down to raise the temperature of the overlying oil zone, and to conduct controlled steam drives, with the aim of limiting steam production. It is interesting to note that in each case of bottom water, a different operating policy proved to be optimal. In all cases, oil-steam ratios were between 0.2 and 0.3.

Stegemeier et al(11) carried out experiments to simulate the Mt. Poso field, which has a water drive, and developed a successful operating strategy for an otherwise marginal steamflood prospect.

Doscher and Huang(12) studied the effect of a 15% water zone on a steamflood. They found that as the steam injection rate was increased, oil production was delayed and the oil-steam ratio dropped. At long times, gravity segregation of steam also occurred.

In a series of experimental studies, Farouq Ali and Abad and Snyder(13, 14) simulated bottom water by means of a high permeability sand placed at the base of a vertical tar sand pack. Steam zone growth was initially at the base of the sand, advancing upward, eventually heating the entire sand, with recovery of almost 50%.

Few laboratory studies of in situ combustion in the presence of bottom water seem to have been reported. A notable example is the work of Garon, Geisbrecht and Lowry(16) in scaled models, using a 5 kPa·s bitumen. When there was no communication between the oil and water layers, the combustion zone advanced near the base of the oil zone, following steam preheating of the water layer. In addition to a fire front advancing in the direction of air flow, a second slowly moving front was observed moving in the perpendicular direction. When the oil and water layers were in communication, the sweep was good, but the air-oil ratio was much higher (3600 vs. 2300 m^3/m^3). Recovery was 11-12% in both cases.

3.6 Field Experience: Steam Injection

Several cyclic steaming projects have been conducted in Alberta and Saskatchewan with varying amounts of underlying bottom water. Results have not been reported, but it seems that bottom water thicknesses in excess of a few metres greatly reduced the oil-steam ratio. An interesting example of a successful project is Murphy's Lindbergh project. Here the formation thickness is 15-20 m, with varying amounts of bottom water, on the order of 3 m. Oil viscosity is about 50 kPa·s. As many as eight cycles have been conducted with oil-steam ratios averaging 0.25, close to the predicted value of 0.3.

Cyclic steaming is known to be successful in several other projects where the bottom water sand was separated by a discontinuous shale break.

Table I lists several steamfloods conducted in the presence of bottom water. In the Slocum and Peace River projects, steam is injected into the water sand. The Peace River recovery process is unique in that it combines cyclic steam stimulation, pressure cycling and steamflooding, showing how to make a success out of a seemingly unfavourable situation. All injectors and producers are first steam stimulated, for one to three cycles, using 8 to 12 x 10^3 m^3 of steam per cycle. Following this, the reservoir is pressurized, and then blown down over a three year period. A significant feature of the formation (25.4 m) is the thin water zone (2 m), which contains a high oil saturation (54% vs. 72-88% in the oil zone). Recovery-to-date has been 17%, with 55% expected.

3.7 Field Experience: In Situ Combustion

Table II lists several in situ combustion projects, where bottom water was present. In S.E. Paul's Valley project, the air-oil ratio was low in spite of a high oil viscosity. Air was injected below the oil-water contact to promote a peripheral drive. The presence of high permeability channels gave rise to a variety of operating problems leading to failure(20).

In the Carlyle Pool fireflood, air was injected into the water zone. The combustion

TABLE I

Steamfloods

Field	Depth m	Oil Zone m	Water Zone m	Porosity %	Perm. darcy	°API	Oil Satn. %	Viscosity Pa·s(°C)	Res. Press. kPa	Pattern Size ha	Steam Inj.Rate m³/day	Oil-Steam Ratio m³/m³	Oil Rec. %	Ref
Slocum, TX	160	13	3	38	4	19	63	1.3(11)	700	2.5	400	0.17	32	17
Smackover, AK	610	5	?	36	5	19	80	0.08(43)	35-70	10	490	0.24	52	18
Peace R., AB	550	25	3	28	0.4-1.6	9	77	200(16)	3700	3	160-320	0.25	55	6
Mt. Poso, CA	550	17	WD	33	20	16	58	0.28(43)	700	.	3200 (tot.)	0.22	60	19

TABLE II

Firefloods

Field	Depth m	Oil Zone m	Water Zone m	Porosity %	Perm. darcy	°API	Oil Satn. %	Viscosity Pa·s(°C)	Res. Press. kPa	Pattern Size ha	Air/Wat Inj.Rate m³/day	Air-Oil Ratio m³/m³	Oil Rec. %	Ref	Notes
St Pauls, OK	130	30	15	24	2	10	80	8(43)	13000	4	50000,0	1070	10	20	A
Carlyle, KS	260	12	34	25	0.25	19	45	0.7(23)	1600	1	20000,16	7660	8.6	21	B
N.Tisdale, WY	284	15	4	24	1	21	65	0.18(23)	2000	.	25000,0	4450	14	22	C
CaddoPine, LA	300	9	30	37	0.6	21	53	0.11(32)	450	.	29000,60			23	D
Eyehill, SASK	750	16	3	14	6	14	86	2.7 (27)	5100	8	29000,0				E
Suffield, AB	910	18	9	25	1	13	75	0.17(32)	10500	.	17000,40			.	F
Pearl L., AB	180	70	3	32	1.5	8	75	1000(11)		12					[illegible]

Notes: A. Water drive, expected recovery less than 5%.

B. Combustion occurred 13 ft. below air injection well, in water sand. Three pilots; only Riggs Pilot data is given.

C. Also 15 ft. transition zone. Water injected upon termination of air injection.

D. In first eight months total oil production was 2000 bbls, total air injection 147 MMscf. Lab values of AOR were 7,200 scf/bbl (wet) and 10,100 scf/bbl (dry), and recovery of 85 to 90%. Water injection not started as yet.

E. 9 injectors and 16 producers, 9 20-acre patterns. Current oil production rate for project 500 B/D.

F. Water injection not started as yet.

G. 16 injectors and 10 producers, total pattern area given.

front essentially propagated in the water zone, which contained 5-15% oil(21).

In the N. Tisdale fireflood, the bottom water thickness was small, and it was part of the transition zone. On the whole, the performance was good although the air-oil ratios were high(22).

The Caddo Pine Is. fireflood had a water zone four times as thick as the oil zone. Initially, water did not seem to cause air channelling. Later, operating problems led to the project termination(23).

Other examples of bottom water firefloods are given in Table III. The early response of the Eyehill project is good, although the possibility of air channelling remains in this high permeability reservoir. The Suffield test has not shown oil production response as yet(24) and the Kearl Lake fireflood has been terminated. Raisbeck(25) reported combustion initiation at the oil-water contact, in order to develop an upward moving fire front.

3.8 Possible Operating Strategies

Cyclic steam stimulation in the presence of bottom water should aim at preventing steam flow into the water zone (unless it is very thin). Possible solutions are: use of small steam slugs, increasing in subsequent cycles, creating a gas saturation in the upper part of the formation to promote steam flow there, carbon dioxide injection prior to steam, use of horizontal wells in order to minimize injection pressures, use of solvents to open up injection paths in the oil zone, and formation fracturing to create a horizontal fracture for steam emplacement. (The FAST Process: Britton et al(26)). None of these techniques is inexpensive; the specific geology and economics would determine the success of cyclic steaming in bottom water situations.

Steamflooding in the presence of bottom water has been shown to be economically feasible, provided that the water zone is relatively thin. Apart from the pressure cycling strategy of the Peace River project, any technique for creating a barrier at the oil-water contact would help. High temperature polymers, foams, and additives may help. However, a successful project would have to rely on a carefully thought-out long-term injection/production strategy.

In situ combustion appears to be less unattractive for bottom water situations, being relatively insensitive to the water zone thickness. Injection of surfactant into the water layer to create foam barriers may help. Again the operating strategy is important in this case also.

4. GAS CAP

4.1 Cyclic Steam Stimulation

When a gas saturation is present, steam will tend to flow into such a high conductivity zone, and combined with gravity segregation of steam, a steam zone would be formed in the upper part of the formation. The flow of oil in the production phase of the cycle would depend on the roles of gravity and pressure; if gravity flow is significant, as it is likely to be in desaturated formations, its role would be decreased in view of top heating. On the whole, the production performance would be inferior to that in the absence of gas.

4.2 Steamflooding

A gas saturation may be rather effective in a steamflood if the vertical permeability is high to promote gravity flow. In such an instance, it may be possible to spread steam over the entire formation, and develop a downward drive. This would be particularly useful in thin formations, where a frontal drive may lead to excessive heat loss. Special techniques would be needed to minimize steam production.

4.3 In Situ Combustion

A gas zone in a combustion drive would lead to channelling of the injected air. If there is some oil saturation in the gas zone, a fast-moving combustion front will form, and arrive at the producers, causing excessive channelling thereafter. On the other hand, if the vertical permeability is high and the air flux is high enough, it may be possible to develop a downward moving firefront.

4.4 Numerical Simulation and Lab Experimentation

Gottfried(27) simulated in situ combustion in an oil sand with a clean porous zone above. It was concluded that fuel deposition occurred from the oil zone into the clean zone. Limited experimental studies supported this behaviour.

Khelil(28) carried out a numerical and laboratory investigation of combustion in a segregated system. Figure 5 shows the calculated isotherms after five days of burning. It is seen that a secondary, fast-moving firefront forms in the gas cap, with early breakthrough. Migration of oil into the gas cap, with accompanying high temperature peaks, was also noted.

Numerical simulations of cyclic steaming or steamflooding in the presence of a gas saturation, are routinely done. An extensive study of cyclic steaming in the presence of a gas zone was reported by

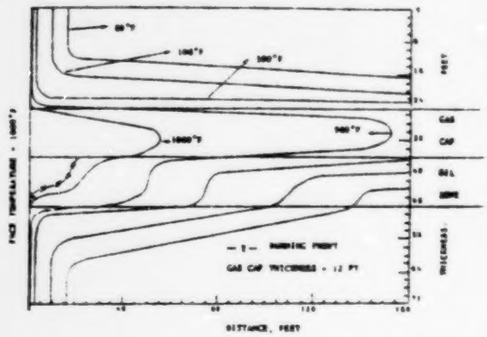

FIGURE 5

Bowen and Patel(4). The gas zone (20% of oil zone) was found to lower oil recovery by 30% in the absence of gas. Also, there was rate dependence, so that the recovery decreased by 15% when the production rate was halved. Perforating the well near the base improved performance.

4.5 Field Experience

In California, a gas saturation frequently occurs in the depleted, low pressure formations. Cyclic steaming under such conditions has performed well. An example in the Yorba Linda field(29). Steamflooding in such formations can help develop a downward drive under some conditions. An outstanding example of such a drive is the San Ardo field, where the recovery is close to 80%.

There are few examples of in situ combustion in the presence of a gas zone. One instance in which it was eventually possible to conduct a downward combustion drive is that of the Tulare formation in the S. Belridge field in California(31). Under most conditions it would be difficult to maintain a high enough air flux over a large area.

5. THIN FORMATIONS

Many heavy oil formations are less than 6 m thick, which is currently considered to be the minimum for the application of steamflooding. In situ combustion, though better suited for thin formations, must operate on a large spacing for economic reasons. Thus the application of thermal processes to thin formations is problematic. Numerical simulations bring out these limitations. Experimental studies of steamfloods in a thin formation were reported by Ghassemi and Doscher(32). It was shown that if a steam zone can be formed to blanket the formation, a downward drive could be initiated, so that heat losses would be much smaller than in a frontal drive. Recently, Doscher and El-Arabi(33) described a field test in a formation 5 to 6 m thick. Steam was injected at a high rate to permit breakthrough, following which a downward steam drive was attempted. The early results of the test were said to be encouraging.

Thin formations could be good prospects for partially quenched combustion, if this process could be better controlled, and some of its shortcomings eliminated. Steam slugs, driven by water, with a suitable buffer in between, may alse be feasible. Table III shows NPC's Implemented and Advanced Technolgoy (1995) thermal recovery screening criteria, taken from the paper by King, Blevins, and Britton(34). It is to be noted that even with advanced technology, the minimum formation thickness for steam injection is about 5 m (15 ft).

Thermal Recovery Screening Criteria

	Steam Injection		In Situ Combustion	
	Implemented Technology	Advanced Technology	Implemented Technology	Advanced Technology
Depth (ft)	≤ 3,000	5,000	11,500	-
Net Pay (ft)	≥ 20	15	≥ 20	≥ 10
Porosity*	≥ 0.20	0.15	0.20	≥ 0.15
Oil Saturation x Porosity	≥ 0.10	≥ 0.08	0.08	≥ 0.08
Permeability (md)	≥ 250	≥ 10	35	≥ 10
Oil Gravity (°API)	10 to 36	-	10 to 35	-
Oil Viscosity (cp)	≤ 15,000	-	≤ 5,000	≤ 5,000
Transmissibility (md-ft/cp)	≥ 5	-	≥ 5	-
Current Reservoir Pressure (psia)	≤ 1,500	≤ 2,000	2,000	≤ 4,000

---

* Ignored if oil saturation x porosity criteria are satisfied.

TABLE III

6. EXTRA-HEAVY OIL FORMATIONS

Tar sands, and formations containing oils with viscosities of 100 to 1000 Pa·s pose special problems. Although the absolute permeability is high, injectivity is nil to very low. Thus steam (or air) must be injected at pressures in excess of fracture pressures, leading to a series of problems, which render a pattern drive ineffective. Simulations of steam injection under frac pressures are difficult, and must consider formation stresses and strains, in addition to a suitable fracture theory(35).

Field experience with cyclic steaming in Cold Lake under frac pressures is extensive (e.g. see Ref. 36). This process has been developed to a point where recoveries of up to 20% can be attained. On the other hand, little success has been achieved in conversion to steamfloods. Possibly a pressure cycling type process would be feasible in the long run after the formation has been sufficiently heated.

In situ combustion under air injection at frac pressures has been largely unsuccessful. An outstanding example is the Gregoire Lake project in Athabasca(37). Smaller field tests, such as the one in Utah(38) have had some success. It seems that such a process is workable at small spacings only.

The aforementioned FAST technology(26) and horizontal wells (Butler et al(39)) hold promise for extra-heavy oil formations, if economics can justify them.

7. DEEP HEAVY OIL FORMATIONS

Table III shows that the current depth limit on steam injection is about 900 m (3000 ft). At the advanced stage is may increase to 1500 m. Currently, no successful steam projects operating below 900 m are known. The same is true of firefloods. On the other hand, injection of steam with additives, in particular gases, holds considerable promise, since high pressures would then be attainable at relatively low temperatures. High pressure water injection also appears to have certain benefits. Development of super-insulated tubings, high temperature packers, and downhole steam generators may make it possible to run commercial operations at depths of 1500 m. A this point, however, economics of such operations do not look favourable.

8. FISSURED HEAVY OIL FORMATIONS

Some of the largest heavy oil accumulations (e.g. Grosmont in Alberta) occurs in carbonates, which may be fissured or have other typical heterogeneities. Application of thermal processes to such formations is often problematic. Numerical simulation or physical modelling is equally difficult, since the nature of heterogeneities is not known, nor is fracture modelling any easier. Thus much reliance must be placed on field-testing. Figures 6 and 7 show temperature distributions for steamflooding in the presence of fractures (10 darcies vs. matrix permeability of 25 md), computed by Dr. B. Abad(40). It is seen that whereas the effect of fractures is clearly seen at 3 years (Fig. 6), it is barely perceptible after 12 years (Fig. 7). It is questionable whether steam injection over such a long period would be economical. Similar simulation studies by Nolan et al(41) show that steamflooding in thick fissured carbonate formations may be viable. The thermal efficiency of the process can be considerably increased by some form of heat scavenging.

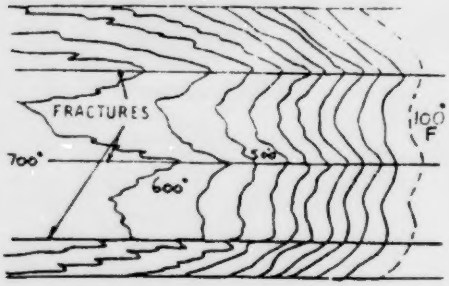

FIGURE 6

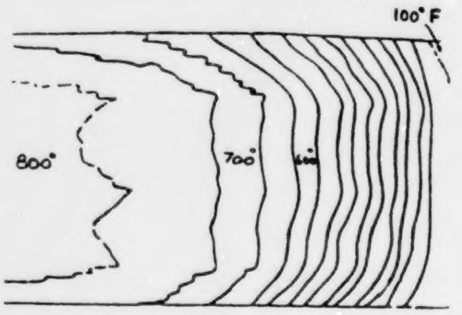

FIGURE 7

Few field tests of steam injection in fissured rocks have been reported. Sahuquet and Ferrier(42) described a steamflood pilot in the Lacq Superior field, in France. The project was largely successful, but the well response had little correlation with directional permeabilities. Cordell(43) reported a steamflood pilot with three producers 60 m apart, and a central injector, in Grosmont. All three thermal processes were tested with limited success.

In situ combustion simulation studies of Schulte and de Vries(44) show that the process may be feasible in fissured rocks if the fracture spacing is about one metre.

On the whole, fissured formations appear to be good prospects for steamflooding, if a pressure cycling type process is used, together with a means for increasing the overall thermal efficiency of the process. At the same time, judicious application of blocking agents such as foams may increase recovery efficiency.

9. CONCLUSIONS

Based upon numerical simulations, lab experimentation, and field experience, it can be said that in some instances, marginal heavy oil formations, with bottom water, can be successfully exploited by steamflooding, and to a lesser extent by in situ combustion. The performance of cyclic steaming would depend strongly on the specific conditions. Where a gas cap is present, a modified steam drive has a chance of success. Formations containing extra-heavy oil may be amenable to new technologies, although cyclic steam stimulation at frac pressures seems to be a workable process. Fissured heavy oil formations, thin formations, and deep sands are starting to look promising, but their commercial exploitation by thermal processes is well in the future.

ACKNOWLEDGMENTS

The authors wish to thank Mr. Robert F. Meldau for many information discussions. Thanks are expressed to Mr. D.K. Faurschou and EMR/CANMET/ERL, Ottawa, for supporting this research.

REFERENCES

1. Towson, D.E.: "Importance of Reservoir Description in Evaluating In Situ Recovery Methods for Cold Lake Heavy Oil - Part II: In Situ Application", J. Can. Pet. Tech. (Jan.-Mar. 1977).

2. National Petroleum Council: Enhanced Oil Reocvery (June 1984).

3. Kasraie, M., and Farouq Ali, S.M.: "Effect of Bottom Water and Gas Cap on Steam Injection Response", Paper SPE 13039, presented at the 59th Annual Fall Meeting of Soc. Pet. Engrs., Houston, Sept. 16-19, '84.

4. Bowen, W.B., and Patel, C.: "Use of a Numerical Simulator as an Aid to the Optimization of Steam Stimulation in a Typical 15° API Heavy Oil Reservoir", Paper 82-33-38, presented at the 33rd Annual Tech. Meeting of the Pet. Soc. of CIM, Calgary, June 6-9, 1982.

5. Prats, M.: "Peace River Steam Drive Scaled Model Experiments", Oil Sands of Canada - Venezuela (1977) 346-363.

6. Shell Canada Resources: Peace River Expansion Project - Application to ERCB, Calgary, Vol. 1, (1984).

7. Crookston, R.B., Culham, W.E., and Chen, W.H.: "A Numerical Simulation Model for Thermal Recovery Processes", Soc. Pet. Eng. J. (Feb. 1979), 37-58.

8. Pursley, S.A.: "Experimental Studies of Thermal Recovery Processes", Proc. of Heavy Oil Symp., Maracaibo (1974).

9. Ehrlich, R.: "Laboratory Investigation of Steam Displacement in the Wabasca Grand Rapids "A" Sand", Oil Sands of Canada - Venezuela, CIM (1977), 364-379.

10. Huygen, H.H.A., and Lowry, W.E., Jr.: "Steamflooding Wabasca Tar Sand Through the Bottom Water Zone - Scaled Lab Experiments", Paper SPE 8398, presented at the 54th Annual Fall Meeting of SPE, Las Vegas, Sept. 23-26, 1979.

11. Stegemeier, G.L. et al: "Representing Steam Processes With Vacuum Models", SPEJ. (June 1980), 151-174.

12. Doscher, T.M., and Huang, W.: "Steam Drive Performance Judged Quickly for Use of Physical Models", Oil & Gas J. (Oct. 22, 1979), 52-57.

13. Farouq Ali, S.M., and Abad, B.: "Bitumen Recovery from Oil Sands, Using GCOS Synthetic Crude in Conjunction With Steam", J. Can. Pet. Tech. (July-Sept. 1976), 1-11.

14. Farouq Ali, S.M., and Snyder, S.G.: "Miscible-Thermal Methods Applied to a Two-Dimensional, Vertical Tar Sand Pack, With Restricted Fluid Entry", J. Can. Pet. Tech. (1974).

15. Farouq Ali, S.M.: "Multiphase, Multidimensional Simulation of In Situ Combustion", Paper SPE 6896, presented at the 52nd Annual Fall Meeting of SPE, Denver, Oct. 9-12, 1977.

16. Garon, A.M., Geisbrecht, R.A., and Lowry, W.E.: "Scaled Model Experiments of Fireflooding in Tar Sands", Paper SPE 9449, presented at the 55th Annual Fall Meeting of SPE, Dallas, Sept. 21-24, 1980.

17. Hall, A.L., and Bowman, R.W.: "Operation and Performance of the Slocum Thermal Recovery Project", J. Pet. Tech. (April 1973), 402-408.

18. Smith, R.W., Bertuzzi, A.F., Templeton, E.E., and Clampitt, R.L.: "Recovery of Oil by Steam Injection in the Smackover Field, Arkansas", Paper SPE 3779, presented at the Improved Oil Rec. Symp., Tulsa, April 16-19, 1972.

19. O'Dell, P.M., and Rogers, W.L.: "Use of Numerical Simulation to Improve Thermal Recovery Performance in the Mt. Poso Field, California", Paper SPE 7078, presented at the 5th Symp. on Improved Oil Rec., Tulsa, April 16-19, 1978.

20. Elkins, L.F., Morton, D., and Blackwell, W.A.: "Experimetal Fireflood in a Very Viscous Oil-Unconsolidated Sand Reservoir, S.E. Pauls Valley Field, Oklahoma", Paper SPE 4086, presented at the 47th Annual Fall Meeting of SPE, San Antonia, Texas, Oct. 8-11, 1972.

21. Elkins, L.F., Skov, A.M., Martin, P.J., and Lutton, D.R.: "Experimental Fireflood - Carlyle Field, Kansas", Paper SPE 5014, presented at the 40th Annual Fall Meeting of SPE, Houston, Oct. 6-9, 1974.

22. Martin, W.L., Alexander, J.D., Dew, J.N., and Tynan, J.W.: "Thermal Recovery at North Tisdale Field, Wyoming", J. Pet. Tech. (May 1972), 606-616.

23. Horne, J.S., Bousaid, I.S., Dore, T.L., and Smith, L.B.: "Initiation of an In Situ Combustion Project in a Thin Oil Column Underlain by Water", Paper SPE 10248, presented at the 56th Annual Fall Meeting of SPE, San Antonio, Texas, Oct. 5-7, 1981.

24. (Anon.): "Southeast Alberta Fireflood is Way Behind Schedule", Enhanced Rec. Week, (1982).

25. Raisbeck, J.M.: "Combustion Initiation at the Bottom Water-Oil Sands Interface", Paper 79-30-15, presented at the 30th Annual Meeting of Pet. Soc. of CIM, Banff, May 8-11, 1979.

26. Britton, M.W., Martin, W.L., Leibrecht, R.J., and Harmon, R.A.: "The Street Ranch Pilot Test of Fracture-Assisted Steamflood Technology", SPE Fape 10707, presented at the Calif. Regional Meeting, San Francisco, March 1982.

27. Gottfried, B.Sc.: "Some Theoretical Aspects of Underground Combustion in Segregated Oil Reservoirs", Soc. Pet. Eng. J., (Sept. 1966), 281-291.

28. Khelil, C.: "A Study of In Situ Combustion in a Segregated System", Paper SPE 2519, presented at the 44th Annual Fall Meeting of the SPE, Denver, Sept. 28 - Oct. 1, 1969.

29. Stokes, D.D., and Doscher, T.M.: "Shell Makes a Success of Steamflood at Yorba Linda", Oil & Gas J., (Sept. 2, 1974), 71-78.

30. Traverse, E.F., Deibert, A.D., and Sustek, A.J.: "San Ardo Field - Case History of a Successful Steam Flood", presented at the AIChE Spring National Meeting, Anaheim, 1982.

31. Gates, C.F., Jung, K.D., and Surface, R.A.: "In-Situ Combustion in the Tulare Formation, South Belridge Field, Kern County, California", Paper SPE 6554, presented at the Calif. Regional Meeting of SPE, Bakersfield, April 13-15, 1977.

32. Ghassemi, F.: "Steam Drive - Its Extension to Thin Oil Sands...", Ph.D. Thesis, U. of S. Calif. (Aug. 1981).

33. Doscher, T.M., and El-Arabi, M.A.: "Steamflooding Strategy for Thin Sands", Paper SPE 11679, presented at the Calif. Regional Meeting, Ventura, Mar. 23-25, 1983.

34. King, J.E., Blevins, T.R., and Britton, M.W.: "The National Petroleum Council EOR Study: Thermal Processes", Paper SPE 13242, presented at the 59th Annual Fall Meeting of Soc. Pet. Engrs., Sept. 16-19, 1984.

35. Farouq Ali, S.M., and Blunschi, J.: "Cyclic Steam Stimulation With Formation Parting", Paper 83-84-45, presented at 34th Annual Meeting of Pet. Soc. of CIM, Banff, May 10-13, 1983.

36. Buckles, R.S.: "Steam Stimulation Heavy Oil Recovery at Cold Lake, Alberta", SPE 7994, presented at Calif. Regional Meeting of SPE, Ventura (April 1979).

37. Marchesin, L.A.: "Gregoire Lake Block 1 Pilot, 1976-1981," Paper 82-33-62, presented at the 33rd Annual Tech. Meeting of Pet. Soc. of CIM, Calgary, Jun. 6-9, 1982.

38. Terwilliger, P.M.: "Fireflood in a Shallow Tar Sand", CIM (1982).

39. Butler, R.M., McNab, G.S., and Lo, H.Y.: "Theoretical Studies on the Gravity Drainage of Heavy Oil During In-Situ Steam Heating", presented at the 29th Can. Chem. Eng. Conf., Sarnia, Ont., Oct. 1-3, 1979.

40. Abad, B.: Private Communication, January 1981.

41. Nolan, J.B., Ehrlich, R., and Crookston, R.B.: "Applicability of Steamflooding for Carbonate Reservoirs", Paper SPE 8821, presented at the First Joint SPE/DOE Symp. on EOR, Tulsa, April 1980.

42. Sahuquet, B.C., and Ferrier, J.J.: "Steam Drive Pilot in a Fractured Carbonated Reservoir Lacq Superieur Field", SPE Paper 9453, presented at the 55th Annual Meeting of Soc. of Pet. Engrs., Dallas, Sept. 1980.

43. Cordell, G.M.: "Reservoir Simulation of a Grosmont Carbonate Pilot", presented at the AOSTRA Seminar, Calgary, June 1982.

44. Schulte, W.M., and de Vries, S.: "In Situ Combustion in Naturally Fractured Heavy Oil Reservors", SPE/DOE Paper 10723, presented at the SPE/DOE Third Symp. on EOR, Tulsa, April 1982.

PETROLEUM SOCIETY OF CIM PAPER NO. 84-35-122

THIS IS A PREPRINT – SUBJECT TO CORRECTION

HEAVY OIL RECOVERY IN THE PRESENCE OF BOTTOM WATER

M. Kasraie and S.M. Farouq Ali,
University of Alberta

PUBLICATION RIGHTS RESERVED
THIS PAPER IS TO BE PRESENTED AT THE 35th ANNUAL TECHNICAL MEETING OF THE PETROLEUM SOCIETY OF CIM HELD JOINTLY WITH THE CANADIAN ASSOCIATION OF DRILLING ENGINEERS IN CALGARY, JUNE 10 - 13, 1984. DISCUSSION OF THIS PAPER IS INVITED. SUCH DISCUSSION MAY BE PRESENTED AT THE TECHNICAL MEETING AND WILL BE CONSIDERED FOR PUBLICATION IN CIM JOURNALS IF FILED IN WRITING WITH THE TECHNICAL PROGRAM CHAIRMAN PRIOR TO THE CONCLUSION OF THE MEETING.

ABSTRACT

Many heavy oil formations in Alberta and Saskatchewan have underlying water sands. Thermal recovery applications under such conditions depend strongly on the extent of bottom water, oil viscosity, vertical permeability, oil saturation, and fluid injection rate.

This paper discusses in situ combustion, cyclic steam stimulation, and steamflooding under bottom water conditions, from the mechanistic standpoint, with field examples cited to illustrate the expected performance. While the emphasis is on thermal processes, selected non-thermal techniques are also considered in a qualitative sense. It is seen that although bottom water is undesirable in most instances, it may serve the purpose of providing initial injectivity in very viscous oil formations.

The major portion of the paper is devoted to a discussion of field case histories where thermal recovery methods (in situ combustion, cyclic and continuous steam injection) were applied in bottom water formations. The results are described to derive general conclusions. Firefloods under bottom water conditions seem to have been largely unsuccessful in that air-oil ratios were above the marginal value of 2 700 sm^3/sm^3, although the extent of bottom water was less critical than in steam injection. Cyclic steam stimulation performed poorly in the reported field tests, except in one case where the bottom water was less than one-fifth of the oil zone thickness. Steamfloods under bottom water conditions are few and far between, but in selected instances they performed more favourably because of the careful prior choice of the operating conditions.

INTRODUCTION

Many heavy oil formations in Alberta and Saskatchewan are characterized by a water-saturated sand directly below the oil zone and often in communication with it. The water sand may be merely a high water saturation zone, or a transition zone. In the following, "bottom water" will refer to all these situations. The extent of bottom water would vary from reservoir to reservoir. It may be thin sand, a few metres in thickness, or it may be an aquifer

In any oil recovery process, the presence of bottom water is likely to have a detrimental effect on oil recovery. The injected fluid -air, steam, solvent, etc.- will have a tendency to migrate into the low resistance water sand, resulting in poor displacement and sweep efficiencies. The magnitude of such channelling will depend on a variety of factors, notably oil viscosity, relative water sand thickness, injection rate, oil saturation in the water sand, if any, and vertical permeability. The latter factor is of considerable importance, for even a limited barrier would drastically reduce the channelling tendency. Thus any shale breaks, silt zones, or other heterogeneities at the base of the oil sand would serve to improve the oil recovery performance.

The above simplified picure is complicated by the flow of heat from the water zone into the oil sand, if a hot fluid is injected. If air is the injected fluid, the situation may be even more complex. It is quite likely that in the case of a limited water sand, a thermal recovery process could be designed around the water zone, even utilizing it under certain conditions, as a means of initial injectivity.

As far as can be ascertained, field tests of non-thermal oil recovery under bottom water conditions have not been conducted. It is conjectured that there is even less likelihood of success with such methods.

This paper discusses the mechanistic features of the major thermal recovery techniques in the presence of bottom water, based upon laboratory and field performance as well as numerical simulation studies. Following that, field test results are briefly outlined. It should be noted that bottom water heavy oil reservoirs are commonplace in Alberta and Saskatchewan. As such, they merit considerable research effort to devise means for the successful application of various enhanced oil recovery techniques. Experimental and theoretical research in this direction is underway at the University of Alberta.

PRINCIPAL MECHANISTIC FEATURES OF THERMAL PROCESSES UNDER BOTTOM WATER

In Situ Combustion

Figure 1 illustrates the overall behaviour of a fireflood in the presence of bottom water. An important factor is oil viscosity. Assuming that the oil is highly viscous (e.g. 1000 mPa.s), the injected air, initially constrained to penetrate the oil zone, where a firefront has been initiated, would tend to migrate into the underlying water zone, where the flow resistance is much lower. The lower density of air would counteract this tendency to a limited extent. If there is any oil saturation in the water sand, the air may initiate a second, fast moving, firefront in the water sand, which would tend to starve the main front. Alternatively, the main front may migrate into the water sand. Even if there is no secondary front, the amount of air channelling into the water sand would vary with time: it would decrease if the main front is moving at a reasonable velocity. Such a situation may obtain in the case of a relatively low viscosity oil. If the oil viscosity is high, the main front may become extinct because of low rate of advance due to channelling of air. The air flowing in the water sand will eventually re-enter the oil zone, and thence into the producers. This may lead to spontaneous ignition in this region; thus a stationary combustion front may cause the producers to become hot well before the arrival of the main firefront. This has the beneficial effect of productivity stimulation, which is outweighed by the added mechanical problems of hot well operation, corrosion, high water production rates, early in the life of the flood. Measures such as air injection near the top of the sand, and completing the producers in the water sand have met with little success.

An important feature of in situ combustion in the presence of bottom water consists in that the extent of air channelling is relatively independent of the water sand thickness. The injected air would tend to form a gravity-capillary zone near the base of the oil sand, which would serve as the path for the major portion of the air. This concept was first suggested by E.R. Abernethy and A.F. Balasch (1), and has since been verified by simulation, and appears to occur in the field as well. This implies that in the case of very thick water zones, in situ combustion may be less inefficient than steamflooding. However, the air-oil ratios may still be very high - and uneconomical.

Theoretically, it may be possible to ignite the oil sand areally, by air injection into the oil zone, so that the combustion front moves upwards. However, in actual practice it is unlikely that either the front could be created without discontinuities in it, or the air flux would be high enough to support combustion. Such a process may be feasible over short well spacings.

Cyclic Steam Stimulation

Figure 2 illustrates two situations where steam is injected into an oil sand, with a (i)thin, and (ii)thick water sand below it. Assuming that a large slug of steam is injected in the two cases, and that there are no vertical flow barriers, in the first case of a thin water sand, a certain portion of the injected steam will penetrate the oil zone (depending on oil viscosity), while the balance will enter the water sand. The latter being thin, the steam zone would extend to a considerable distance away from the well. Half of the heat lost will enter the oil zone. The overall behaviour will be such that the oil production response during the first cycle would be mediocre, but in subsequent cycles it would tend to improve, because of oil mobilization away from the wellbore. In later cycles, water production would increase sharply because of water coning from the water zone becoming increasingly dominant with time. Under such conditions, the second or third cycle may produce the most oil, while the other cycles may not be as productive. Field test results seem to exhibit such performance.

In the second case, where the water sand is thick, the injected steam would mainly enter the water zone. Again oil viscosity would be a decisive factor. The water sand would act as a heat sink in that very little heat would be transmitted to the oil zone above. With many cycles, there will be heating of the oil sand, because the steam in the water sand will tend to stay near the top, viz. the base of the oil zone. The overall performance will be poor: very large volumes of water and small volumes of oil will be produced. The oil-steam ratios under such conditions may be well below 0.1, but they would tend to improve slightly in later cycles. On the whole, cyclic steam stimulation in the presence of thick bottom water sands is likely to be uneconomical, as a number of filed tests show. There may be some possibility of improving performance, as discussed in the last part of this paper.

Steamflooding

Figure 3 illustrates steamflooding in the presence of a water sand. If the oil viscosity is high, the injected steam will tend to migrate into the water zone, which has much higher conductivity. If the water sand is thin, much of the heat will be transferred into the oil zone above. Initially such transfer will be largely by conduction. As oil is mobilized and gravitates into the water zone, steam will increasingly rise into the oil zone, and the heating process will become more efficient. After a long enough time, the oil viscosity will be lowered sufficiently so that it may be possible to conduct the oil zone flood successfully. Time is an important factor, because heating of the oil zone will be slow. It is also evident that if the water sand is thick, even prolonged steam injection would result in limited heating of the oil zone. Also, in a process of the type described, large volumes of water would be produced; consequently some flow restriction may be necessary.

An important aspect of the steamflood process outlined above is that a thin bottom water sand may permit a steamflood in very viscous oils. An example of this type is the Peace River pilot of Shell Canada. The bottom water sand fulfills the function of a communication path at the base of the sand, e.g. horizontal fractures, as used by Shell in their 1962-64 caustic-steamfloods in Athabasca, and Continental's FAST process.

It is noteworthy that if the oil viscosity is not too high, gravity segregation of steam would develop in the oil zone, and the increased steam conductivity would compete with the high conductivity of steam in the water sand. Even under these conditions water production rates would be high.

The above observations are qualitative, but they largely agree with field performance. The authors are conducting laboratory experiments as well as numerical simulations for the case of steam injection, results of which will be presented in a forthcoming paper(2). Even there one can only derive generalizations in view of the large number of process variables and complexity.

MECHANISM OF NON-THERMAL RECOVERY PROCESSES UNDER BOTTOM WATER CONDITIONS

It is instructive to consider the performance of non-thermal heavy oil recovery methods when bottom water is present. Such methods include: solvent flooding, polymer floods, various chemical and caustic floods and gas-based processes, such as inert gas injection and immiscible carbon dioxide floods. In all cases, the injected fluid would tend to flow more readily in the water zone, especially if it is miscible with water (e.g. chemical floods, carbon dioxide). In the case of polymers, the polymer mobility will decrease in the water zone, and the injected fluid will tend to flow more into the oil zone. Solvents too will channel into the water sand; the part entering into the oil layer will be subject to viscous fingering. Non-soluble gases may perform in a manner similar to that noted above for in situ combustion. A recent paper by Alikhan and Farouq Ali(3) noted the lack of success with non-thermal methods applied to heavy oils, based upon field experience. It is rather unlikely that such methods would perform any better under the less favourable conditions as presented by the presence of bottom water.

FIELD EXPERIENCE WITH IN SITU COMBUSTION IN THE PRESENCE OF BOTTOM WATER

Several in situ combustion projects have been reported where there was a water sand in communication with the oil zone above. In the following the salient aspects of these tests are reviewed. Table 1 lists the more important data for the same. It should be noted that the water sand thicknesses vary widely as does also the oil viscosity at reservoir conditions.

S.E. Paul's Valley

Elkins, Morton, and Blackwell(4) described the results for the S.E. Pauls Valley fireflood in Oklahoma (Test#1 in Table 1). This is a relatively deep (1 310m) reservoir, with an oil zone 30 m thick, and a water sand over 15 m thick. The reservoir is characterized by what the authors call "wormholes". The reservoir permeability was 12-30 darcys, and it produced many thousands of tons of sand. There was other positive proof of severe air channelling. Air was injected below the oil-water contact, with the intention of developing a peripheral fireflood. During the air injectivity test, the oxygen concentration in the produced gas was less than 3%, carbon dioxide less than 1%. Air injection rate during the fireflood was 200-300 Mcf/day, at a rather high pressure (3000 psi). Carbon dioxide breakthrough occurred within two days after ignition. The firefront moved 660 ft in less than two months. Oil production rate increased from 100-170 B/D to 400 B/D, with an average of 310 B/D, but little carbon dioxide was produced. The air-oil ratio was low (6000 scf/bbl), however, a variety of mechanical problems due to wormholes made the operation uneconomical. It appears that in this field test the very high formation permeability counteracted the air channelling in the water leg. The air-oil ratio was unexpectedly low for this type of reservoir. On the other hand, it seems that combustion was limited, as evidenced by the lack of carbon dioxide.

Carlyle Pool, Kansas

Three firefloods were reported for the Carlyle pool in Kansas by Elkins et al (5). The 12-15 m oil sand is underlain by 30-40 m of water. A lime streak occurs near the water sand. The third pilot was the most significant of the three. Wells were drilled through the streak, and air was injected into the water zone. Burning was in a 10ft interval with lower than the average oil saturation of 5-15%. Many production well stimulation methods were tested, with reverse combustion used as a last resort. Tight emulsions with the consistency of peanut butter were produced. Spontaneous ignition occurred within 8-10 months near the air injector.

North Tisdale field, Wyoming

Martin et al (6) have described the performance of the North Tisdale field, in Wyoming, which has a 15 m thick oil zone and 4 m of water and 5 m of transition zone. It was noted that the presence of bottom water was not detrimental. Breakthrough of gas occurred the same day air injection was started. Fig. 4 depicts a cross-section of the formation with temperature profiles. It is seen that there is little evidence of air channelling into the water sand. It was reported that some loss of oil to the water zone occurred in at least one well. Peak oil production was 250 B/D, with an average of 88.4 B/D - approximately three times the previous rate. Water was injected upon the termination of air injection, which yielded 9% more oil. Vertical sweep was 27%. It is possible that the transition zone restricted air channelling into the bottom water.

Caddo Pine Island Field, Louisiana

An interesting case of bottom water fireflooding is the Caddo Pine Island field, in Lousiana, reported by Horne et al (7)(#4 in Table 1). Here the oil zone thickness is approximately 9 m, while the water zone is some 30 m thick. The authors note that there was no evidence of air bypassing. Air injection was slowly increased from 300 to 1000 Mscf/day "to help reduce viscous fingering of air". A number of factors may explain the lack of adverse effects of the bottom water zone: low vertical permeability or a thick transition zone, or possibly the tendency of the air to channel into the water zone was balanced by air override, in case a gas saturation was present in this relatively light oil (112 mPa.s) formation. This project has been terminated, and there is some indication that the air-oil ratios later increased to high levels.

Other

Table 1 summarizes the data for the Eyehill, Suffield, and Kearl Lake field tests. The most notable example is the Eyehill fireflood, consisting of nine five-spots, with the bottom water thickness increasing from west to east. High air-oil ratios (of the order of 30,000 scf/bbl) were predicted for this fireflood. However, after four years of operation there is still no increase in the air-oil ratios to that level. The oil production is about 500 B/D. The Suffield test has not shown oil production response as yet (8), and the Kearl Lake project has been terminated.

Raisbeck (9) has reported an experiment where combustion was successfully initiated at the bottom water-oil sand interface in Wabasca, Alberta. The combustion scheme is illustrated in Fig. 5, with an upward moving firefront. The formation was substantially preheated (200 to 400°F level) by steam stimulation prior to combustion initiation, in view of the very high oil viscosity, being on the order of 10^6 mPa.s.

FIELD EXPERIENCE WITH STEAM INJECTION IN THE PRESENCE OF BOTTOM WATER

Cyclic Steam Stimulation

Several cyclic steam stimulation projects have been conducted in Alberta and Saskatchewan in heavy oil formations with varying amounts of underlying bottom water. The results are not available at this time, but it can be said that when the bottom water sand was over one-fifth the oil sand thickness, steam largely entered the water leg, and oil production was virtually nil. Large steam slugs are likely to aggravate the situation. An interesting example of a commercially successful cyclic steam stimulation project in the presence of bottom water is Murphy's Lindbergh project. Here the formation thickess is 15-20 m, with varying amounts of bottom water, on the order of 3 m. Oil viscosity is approximately 50 000 mPa.s. As many as eight cycles have been conducted, with oil-steam ratios averaging 0.25, close to the predicted value of 0.3. The predictions took into account the flow of steam into the bottom water, and the mechanisms discussed in the first part of this paper.

There are at least two instances in which cyclic steam stimulation was successful in spite of considerably thick water legs. The chief reason was that a discontinuous shale break was present, and offered resistance to the flow of steam into the water zone. The process may not be as effective when these projects are converted to steamfloods.

Steamfloods

Relatively few steamfloods have been reported where bottom water was present. A number of planned floods in Alberta have water zones of varying thicknesses. A well-known steamflood, where both bottom water and a gas cap are present is the Smackover flood in Arkansas, which is operated at below atmospheric pressure (10). It is possible that the gas cap counteracts the channelling of steam into bottom water. Figure 6 shows a cross-section of the formation and the temperatures: it is seen that more of the steam tends to migrate into the gas cap than into the bottom water zone. This project has been in operation since 1965, and has been economically successful.

The Slocum project in Texas (#8 in Table 1) is the first instance where steam was injected into the water sand, relying on the heating of the overlying oil by conduction, and later convection. In other respects, the project was run as a conventional steamflood. It was noted (11) that in spite of high oil recovery, the large volumes of steam needed reduced the project profitability. Later, selective steam stimulation was susbstituted for steam drive in the field. A fireflood was also conducted in this reservoir without success.

It is evident that a conventional steamflood may not be efficient under bottom water conditions. The operating policy chosen for the Peace River pilot (#10 in Table 1) recognizes this. Prats (12) describes the modified steam injection process being employed for this very high viscosity oil reservoir (200 000 mPa.s). The process consists in pressurizing the bottom "water" zone (oil saturation 45%), producing some oil, then blowing down the water zone, and conducting a steam drive in the oil zone, so that the overall process is akin to a large scale steam soak. Based upon current performance, an oil-steam ratio of 0.25 bbl oil/bbl steam and a recovery of 50% is expected. The project is designed to inject 14,600 B/D of 100% quality steam to produce 3,500 B/D of bitumen.

A unique steamflood, where a water drive is present is the Mt. Poso project (#11 in Table 1). Use of scaled models (13) and numerical simulation (14) permitted the development of an injection-production strategy, which minimized the detrimental effects of water influx. The steamflood is conducted on a line drive basis, with injection points shifted from downdip locations to updip, with the oil driven into preheated downdip area. As a result there is little loss of steam to the downdip aquifer.

CONCLUSIONS

The interaction of bottom water with a thermal process is complex, and it is not possible to offer generalizations that would be applicable to a specific reservoir. The most important factor is the presence of barriers, which would serve to restrict the migration of the injected fluid into the water leg. The following observations are derived based upon the above discussion:

1. A thin bottom water zone may not be excessively detrimental in cyclic steam stimulation. A water leg thicker than about one-fifth the oil zone thickness may make the process uneconomical.
2. It is possible to conduct a steamflood in the presence of bottom water, although thick water zones would delay the steamflood response and reduce the profitability of the process.
3. Where the bottom water zone is relatively thick, in situ combustion offers a less unattractive choice. In such an instance, air-oil ratios would be high, but relatively independent of the water zone thickness.

ACKNOWLEDGMENT

The authors wish to thank Mr. D.K. Faurschou and EMR/CANMET/ERL, Ottawa, for supporting this research.

REFERENCES

1. Balasch, A.F., anf E.R. Abernethy: Private Communication (1978).
2. Kasraie, M., and Farouq Ali, S.M.: "Effect of Bottom Water and Gas Cap on Steam Injection Response", to be preented at the 59th Annual Fall Meeting of Soc. of Pet. Engrs., Houston, September 16-19, 1984.

3. Alikhan, A.A., and Farouq Ali, S.M.: "Current Status of Non-Thermal Heavy Oil Recovery", presented at the Rocky Mtn. Meeting, Salt Lake City, 1983.

4. Elkins, L.F., Morton, D., and Blackwell, W.A.: "Experimental Fireflood in a Very Viscous Oil - Unconsolidated Sand Reservoir, S.E. Pauls Valley Field, Okla.", Paper SPE 4086, presented at the 47th Annual Fall Meeting of Soc. of Pet. Engrs, San Antonio, Oct. 8-11, 1972.

5. Elkins, L.F., Skov, A.M., Martin, P.J., and Lutton, D.R.: "Experimental Fireflood - Carlyle Field, Kansas", Paper SPE 5014, presented at the 49th Annual Fall Meetin of Soc. of Pet. Engrs., Houston, Oct. 6-9, 1974.

6. Martin, W.L., Alexander, J.D., Dew, J.N. and Tynan, J.W.: "Thermal Recovery at North Tisdale Field, Wyoming", J. Pet. Tech. (May 1972) 606-616.

7. Horne, J.S., Bousaid, I.S., Dore, T.L., and Smith, L.B.: "Initiation of an In Situ Combustion Project in a Thin Oil Column Underlain by Water", Paper SPE 10248, presented at the 56th Annual Fall Meeting of Soc. of Pet. Engrs., San Antonio, Oct. 5-7, 1981.

8. (Anon.): "Southeast Alberta Fireflood is Way Behind Schedule", Enhanced Rec. Week (1982).

9. Raisbeck, J.M.: "Combustion Initiation at the Bottom Water-Oil Sands Interface", Paper 79-30-15, presented at the 30th Annual Tech. Meeting of Pet. Soc. of CIM Banff, May 8-11, 1979.

10. Smith, R.V., Bertuzzi, A.F., Templeton, E.E., and Clampitt, R.L.: "Recovery of Oil by Steam Injection in the Smackover Field', Paper SPE 3779, presented at the Improved Oil Rec. Symp., Tulsa, April 16-19, 1972.

11. Hall, A.I., and Bowman, R.W.: "Operation and Performance of the Slocum Thermal Recovery Project", J. Pet. Tech. (April 1973) 402-408.

12. Prats, M.: "Peace River Steam Drive Scaled Model Experiments", Oil Sands of Canada-Venezuela (1977) 346-363.

13. Stegemeier, G.L., Laumbach, D.D., and Volek, C.W.: "Representing Steam Processes With Vacuum Models", Soc. Pet.Eng.J. (1978).

14. O'Dell, P.M., and Rogers, W.L.: "Use of Numerical Simulation to Improve Thermal Recovery Performance in the Mt. Poso Field, Calif.", Paper SPE 7078, presente at Improved Oil Rec. Symp., Tulsa, April 16-19, 1978.

TABLE 1

Reported Field Projects With Bottom Water Present

Firefloods

		Depth ft.	Oil Zone Thickness, ft	Water Zone Thickness, ft.	Porosity %	Permeability md	°API	Oil Satn. %	Oil Viscosity cp(°F)	Res. Pressure psig	Pattern Size acres	Air/Wat Inj MScf/D B/D	Air-Oil Ratio Scf/bbl	Oil Recovery %	Reference	Notes
1	SE Pauls Valley, Okla.	4300	100	>50	23.5	878-2505	10	30	8000(110°)	1850	10	1727/0	6,000	10	4	A
2	Carlyle, Kansas	860	34-45	100-125	25	2500	19	40-49	700(74°)	230	2.5	700/99	43,000	8.6	5	B
3	N.Tisdale, Wyo.	933	50	12	24.5	1034	21	64.6	175(73°)	290	10	900/0	25,000	14	6	C
4	Caddo Pine Is.,La.	1000	29	100	36.9	603	21	52.8	112(89°)	65	5	1000/380	Note D	Note D	7	D
5	Eyehill, Sask.	2460	52	10	34	6000	14	84	2700(81°)	730	20	1000/-	-	-	-	E
6	Suffield, Alta.	3000	60	30	25	1090	13	75	170(90°)	1500	5	600/250	-	-	8	F
7	Kearl Lake, Alta.	590	233	10	32	1500	8	75	10^6(52°)	-	28	-	-	-	-	G

Steamfloods

		Depth ft.	Oil Zone Thickness, ft	Water Zone Thickness, ft.	Porosity %	Permeability md	°API	Oil Satn. %	Oil Viscosity cp(°F)	Res. Pressure psig	Pattern Size acres	Steam Inj. Rate, B/D	Oil-Steam Ratio, B/B	Oil Recovery %	Reference	Notes
8	Slocum, Texas	535	44	10	38	4000	19	63	1300(52°)	100	6	2500 (total)	0.17	52	11	
9	Smackover, Ark.	2000	15	?	36	5000	19	80	75(110°)	5-10	22	3090	0.24	52	10	
10	Peace River, Alta.	1800	81	9	25-31	440-1650	9	77	200,000(60°)	530	7	1000-2000	0.25	40-70	12	
11	Mt. Poso, Calif.	1800	55	WD	33	20,000	16	58	280(110°)	100	-	20,000 (total)	0.22	60	14	

Notes:

A. Water drive, expected recovery less than 5%.

B. Combustion occurred 13 ft. below air injection well, in water sand. Three pilots; only Riggs Pilot data is given.

C. Also 15 ft. transition zone. Water injected upon termination of air injection.

D. In first eight months total oil production was 2000 bbls, total air injection 147 MMscf. Lab values of AOR were 7,200 scf/bbl (wet) and 10,100 scf/bbl (dry), and recovery of 85 to 90%. Water injection not started as yet.

E. 9 injectors and 16 producers, 9 20-acre patterns. Current oil production rate for project 500 B/D.

F. Water injection not started as yet.

G. 16 injectors and 10 producers, total pattern area given.

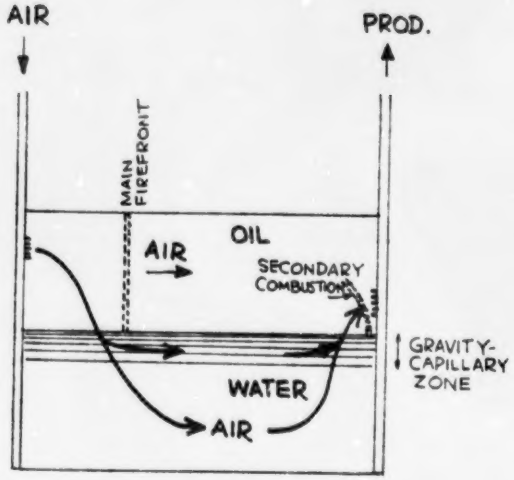
AIR
PROD.
MAIN FIREFRONT
OIL
AIR
SECONDARY COMBUSTION
GRAVITY-CAPILLARY ZONE
WATER
AIR

Fig. 1 - In situ combustion in the presence of bottom water.

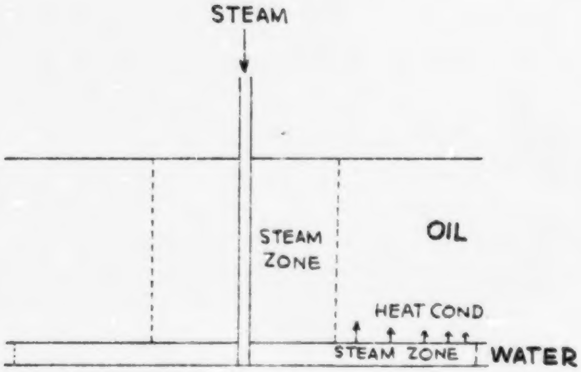
STEAM
STEAM ZONE
OIL
HEAT COND
STEAM ZONE
WATER

Fig. 2(i) - Cyclic steam stimulation in the presence of a thin bottom water zone.

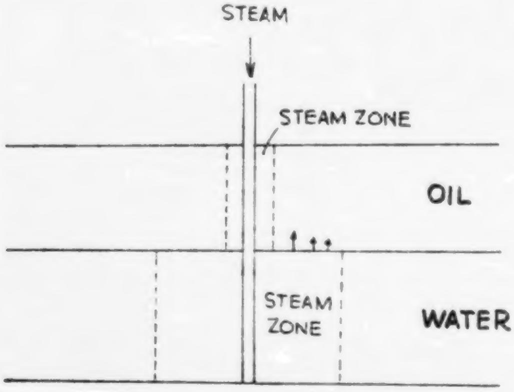
STEAM
STEAM ZONE
OIL
STEAM ZONE
WATER

Fig. 2(ii) - Cyclic steam stimulation in the presence of a thick bottom water zone.

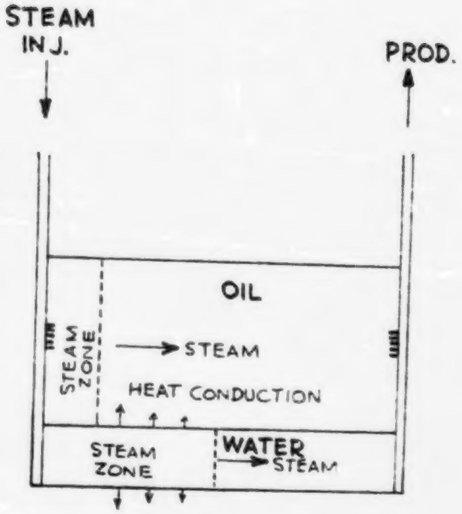
STEAM INJ.
PROD.
OIL
STEAM ZONE
STEAM
HEAT CONDUCTION
STEAM ZONE
WATER
STEAM

Fig. 3 - Steamflooding in the presence of bottom water.

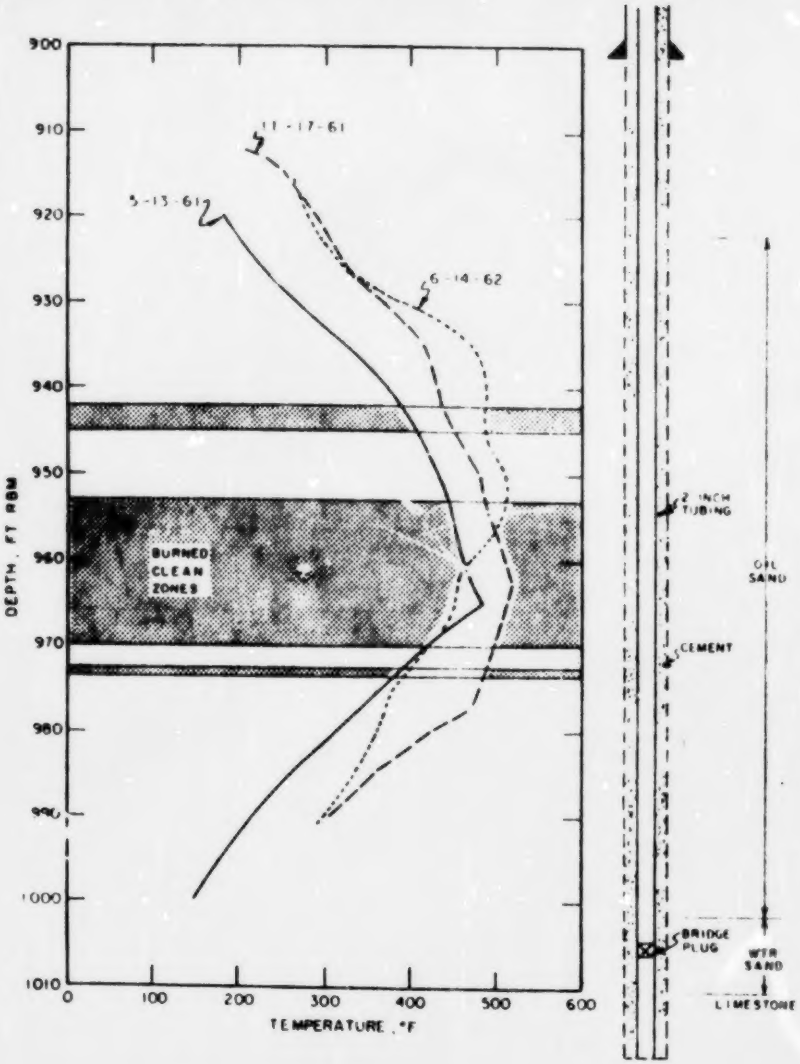

Fig. 4 - Well completion and temperature survey in the N. Tisdale combustion project (Ref.6).

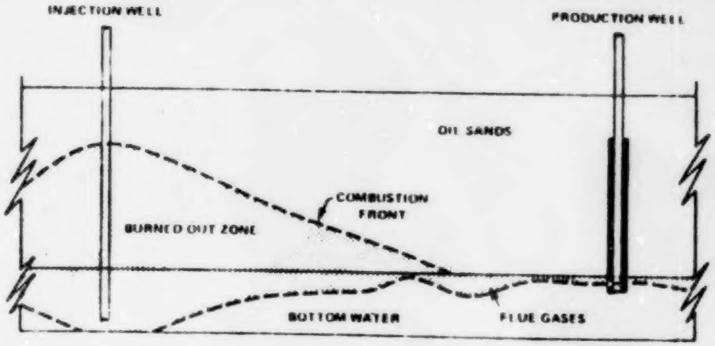
INJECTION WELL
PRODUCTION WELL
OIL SANDS
COMBUSTION FRONT
BURNED OUT ZONE
BOTTOM WATER
FLUE GASES

Fig. 5 - Combustion initiation at the oil-water interface in Wabasca. (Ref. 9).

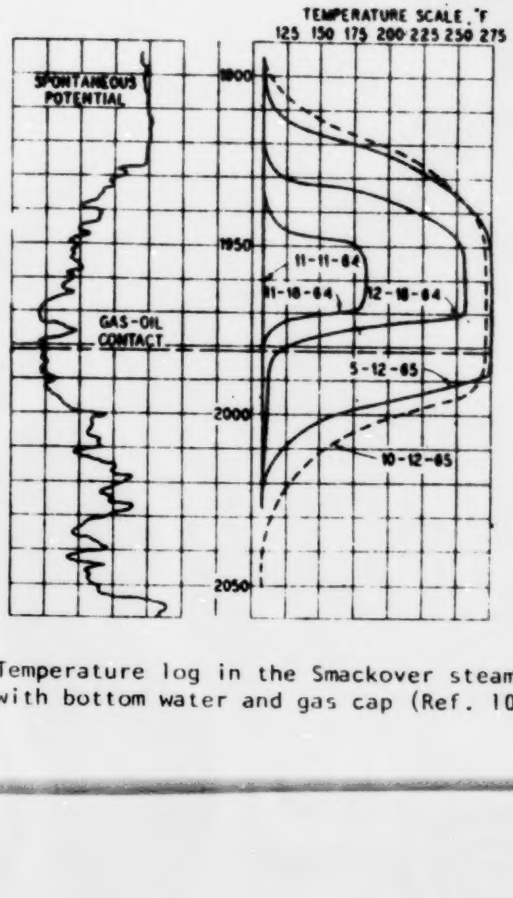

Fig. 6 - Temperature log in the Smackover steamflood with bottom water and gas cap (Ref. 10).